GABA Regulation of Stomatal Function in *Arabidopsis thaliana*

Xueying Feng

A dissertation submitted for the degree of

Doctor of Philosophy

School of Agriculture, Food and Wine

Faculty of Sciences

The University of Adelaide

2021

THE UNIVERSITY of ADELAIDE

Thesis declaration

I certify that this work contains no material which has been accepted for the award of any other degree or diploma in my name in any university or other tertiary institution and, to the best of my knowledge and belief, contains no material previously published or written by another person, except where due reference has been made in the text. In addition, I certify that no part of this work will, in the future, be used in a submission in my name for any other degree or diploma in any university or other tertiary institution without the prior approval of the University of Adelaide and where applicable, any partner institution responsible for the joint award of this degree.

I give permission for the digital version of my thesis to be made available on the web, via the University's digital research repository, the Library Search and also through web search engines, unless permission has been granted by the University to restrict access for a period of time.

I acknowledge the support I have received for my research through the provision of an Australian Government Research Training Program Scholarship.

Acknowledgement

I have gained a lot in many ways through the journey of my PhD project, and for that I would like to thank my superb supervisors Matthew Gilliham and Bo Xu (Weasley). Much appreciation to Matt for the opportunity and the intriguing project here in the laboratory, for the patience and freedom for me to exploring the project, and for the enlightening discussion when I am confused. I am also grateful to Weasley for the expertise he has been showing as a tutor, the inspiration with professionalism, and particularly for being awesome and considerate ever since.

I am also appreciated for the joint research scholarships from China Scholarship Council and the University of Adelaide, and the financial support from Matt during my whole project.

My sincere thanks to the many people who have helped me throughout this project. While there are too many to thank individually, I would particularly like to acknowledge Rakesh David, Stefanie Wege, h and Philip Brewer for the brilliant suggestions and informative conversations, and Wendy Sullivan and Rebecca Vandeleur for their professional supports.

My great appreciation to Fengli and Nina for the precious friendship, which supports me a lot through the journey. We've grown so much separately and thanks for not growing apart. Thanks to the beloved Pt and Jinchen for the grateful friendship, the love and care and the beautiful memories we've built in Adelaide. Also, cheers to Jiaen, Long and Julian for their encouragement and the joyful time with foods and hiking, and to all my PhD fellas for the delightful memories.

Last but not least, I owe a debt of gratitude to my family. Thanks to my mom who motivates me to chase, and to my dad who's my rock no matter what. And from the bottom of my heart to my dearest grandpa, 丁正山, I love you and you will always be in my heart.

Table of Content

List of figures

List of abbreviation

%	percentage
±	plus-minus
±-ABA	racemic mixture of ABA
°C	degrees Celsius
3’	Three prime, of nucleic acid sequence
5'	Five prime, of nucleic acid sequence
AAP3	amino acid/auxin transporter
ABA	abscisic acid
ABA-GE	ABA glucosyl ester
AKG	2-Ketoglutamate
ALMT	Aluminium-Activated Malate Transporters
Arg	Arginine
Asp	Aspartate
bp	base pair
BR	Brassinolide
Ca^{2+}	calcium
Ca^{2+}/CaM	Calcium /Calmodulin Complex
CBL	Calcineurin B-Like protein
CCA1	Circadian Clock associated-1
CDS	Coding DNA sequence
CIPK	CBL-Interacting Protein Kinase
CK	Cytokine
CPK	Calcium-dependent protein kinases
Cys	Cysteine
DPA	dihydrophaseic acid
Em	membrane potential
ET	Ethylene
F	filial generation
FW	Fresh weight
GA	Gibberellin
GABA	γ-Aminobutyric Acid
GABAP	GABA permease
GABA-T	GABA-Transaminase
GABP	GABA permease
GAD	Glutamate Decarboxylase
GAT1	GABA Transporter 1
GB	glycine Betaine
GDH	Glutamate Dehydrogenase
Glu	Glutamate
GSH	Glutathione
IAA	Auxin
JA	Jasmonic acid
K^{+}	potassium

KAT1	potassium imports by potassium channel protein
LHY	Late Elongated Hypocotyl
M^-	anions exports executed by transports
m^{-2} s^{-1}	per square meter per second
Mal^{2-}	malate
MES	2-(N-morpholino) ethanesulfonic acid
mg	milligram
mM	millimolar
mm	millimeter
MPK	mitogen-activated protein kinase
NO_3^-	nitrate
OGDC	A-Ketoglutarate Dehydrogenase
OMT	AKG transporter
OST1	Open Stomata 1
PCR	polymerase chain reaction
Pi	protein phosphorylation
PP2C	type 2C protein phosphatases
Pro	proline
ProTs	Proline transporters
PUT	Putrescine
PYR/PYL/RCAR	Pyrabactin Resistance/ Pyrabactin Resistance-Like/Regulatory Components of The ABA Receptor
qPCR	quantative PCR
QUAC	quick anion channel
SA	Salicylic acid
SCS	Succinyl-Coa Synthetase
SE	Standard error
SLAC	slow anion channel
SlCAT9	cationic amino acid transporter
SnRK2	class III SNF-1-related protein kinase
SO_4^{2-}	sulphate
SSA	Succinic Semi-Aldehyde
SSADH	SSA Dehydrogenase
T	transgenic generation
TOC1	Timing of Cab2 Expression1
w/v	Weigh to volume
α-AA	α-Amino Acid
β-Ala	β-Alanine
δ-ALA	δ- aminolevulinic acid
µm	micrometer
µM	micromolar
ω-AFA	ω - aminiofatty acid

Abstract

Water scarcity limits crop yield. This is in part because of a reduction in plant photosynthetic capacity due to a trade-off between water loss through transpiration and CO_2 intake, which is ordinarily optimised through the opening and closing of stomata, micropores located on the surface of aerial part of plants. Stomatal pores are delineated by pairs of guard cells and stomatal movement is driven by osmolarity changes within guard cells compared to the surrounding cells, which is regulated by an elaborate network of transporters and signalling pathways.

GABA (γ-aminobutyric acid) is a non-proteinogenic amino acid in plants, which is mainly synthesised from glutamate catalysed by Glutamate Decarboxylase (GAD) in the cytosol. There are 5 *GAD* genes (*GAD1-5*) identified in *Arabidopsis thaliana*, with *GAD1* and *GAD2* the most abundant transcripts. GABA has long been speculated as a signalling molecule in plants, with reports connecting GABA synthesis or metabolism to physiological phenotypes, such as accumulation of biomass, pollen tube elongation and tolerance to stress. The recent discovery that Aluminium-activated Malate transporters (ALMTs) may act as GABA receptors has identified a potential mechanism by which GABA affects membrane potential and can act as a signal in plants. A number of ALMTs are involved in stomatal movement, so here, we use stomatal guard cells as a model system to further investigate whether GABA acts as a signalling molecule in plants through the manipulation of GABA metabolism and *ALMT* expression in *Arabidopsis*.

Initial findings within this thesis were that ablation of *GAD2*, the predominant *GAD* in leaves, led to significantly reduced endogenous GABA in leaves and enlarged stomatal pores, decreased water use efficiency, increased drought sensitivity and reduced sensitivity to

abscisic acid (ABA) induced stomatal closing; these were restored to wildtype levels by reintroduction of *GAD2* into leaves targeted exclusively into guard cells. Endogenous concentrations of GABA appeared to be negatively associated with stomatal opening in an ALMT9 dependent manner, which is a tonoplast localised anion transporter. These initial findings are the first clear genetic demonstration that GABA signalling can occur *in planta*.

The impact of the other *GADs* on GABA signalling processes within stomata were further studied by employing the higher order *gad1/2/4/5* knockout mutant, which has further reduced GABA production. Surprisingly, the quadruple mutant did not mimic the stomatal phenotype of *gad2*, instead it resembled WT in stomatal aperture, stomatal conductance and drought tolerance. However, when *GAD2* was expressed in the quadruple mutant background it elevated stomatal conductance to near *gad2* levels. We hypothesised that the divergent phenotypes of *gad2* and *gad1/2/4/5* were due to varied traits of *GADs* homologues, which may result in diverse GABA distribution tissue-wise and thus alter plants response to GABA. This was further explored on other higher order mutants generated from crossing the parental *gad2-1* with *gad1/2/4/5*, comparing to phenotypes of single mutants of *gad1*, *gad2* and *gad4*. The F_1 *gad2-1* x *gad1/2/4/5* plants mimicked the genotype of *gad2-1.* The filial generation has elevated stomatal conductance which consistent with the mutation of *GAD2* being causation of more opened stomata. Stomatal conductance and aperture measurements on F_2 and F_3 plants suggests a synergistic effect of *GAD* homologues in mediating GABA signalling of stomatal movement. Our results indicate that knockout of both *GAD4* and *GAD5* contributes to the divergent phenotypes of *gad2* and *gad1/2/4/5*. We were also able to show that GABA at a non-stressed concentration (0.5 mM) increases stomatal aperture during opening assays of WT in contrast to when GABA is applied at a stress level of GABA (2 mM) which limits opening.

Increased opening due to 0.5 mM GABA was absent in several *GAD(s)* mutant plants, which again suggested an altered cellular homeostasis caused by various mutations in *GADs*. Finally, results from epidermal strip assays with pharmacological treatment of GABA and/or ABA suggests *GAD1* and *GAD4* are required for the full response to ABA for inhibition of stomatal opening.

In summary, this thesis demonstrates that the GABA-ALMT9 interaction mediates a pathway by which GABA signalling occurs in the stomata of *Arabidopsis*. However, it also reveals a complexity in GABA regulation of stomatal movement where it is not a simple linear dose-response relationship and, rather it involves cross talk that is likely to involve multiple *GAD* homologues.

Chapter I General introduction and literature review

General introduction

Land plants are shielded by a hydrophobic cuticle layer on the aerial surfaces of plants, which affords some protection to plants from the challenges of the terrestrial environment, such as desiccation (Domínguez et al. 2017). In order to maintain photosynthesis for growth, plants need to take in CO_2 from the surrounding atmosphere. Meanwhile, water is transpired from plants to support cell expansion and nutrient uptake. Water loss mainly occurs through stomata, which are micropores surrounded by pairs of guard cells on the aerial surfaces of plants (Matthews et al. 2017). To balance the trade-off between carbon gain and water loss, plants finely mediate stomata movement, opening and closing, through hierarchies of endogenous signal pathways, involving plant hormones, ions and metabolites (Singh et al. 2017, Qu et al. 2019, Lawson and Matthews 2020, Hsu et al. 2021). Such delicate modulation occurs in response to environmental stimuli, such as changes in light and humidity (Driesen et al. 2020, Matthews et al. 2020). Therefore, stomatal movement is not only required for higher plants to grow, but also contributes to the water and carbon recycling of the global ecosystem and has significant impact on climate (Beerling and Franks 2010, Nicotra et al. 2010, Zhu et al. 2016, Lemordant et al. 2018).

Global warming has been projected to be a continuing climate challenge for the coming century (Tokarska et al. 2020). The increase in global surface temperature is predicted to lead to a general increase in land water vapor and ultimately reduce humidity in both soil and the atmosphere around the continental region (Huang et al. 2017, Vicente-Serrano et al. 2018, Al‐Ghussain and Energy 2019). Drought stress reduces plant growth and

contributes to a reduction in agricultural productivity (Eziz et al. 2017, Sehgal et al. 2018). Such impact occurs despite intricate stress responses of plants at the transcriptomic and proteomic level, mediated by cascades of signalling networks (Kaur and Asthir 2017, Fàbregas and Fernie 2019).

Abscisic acid (ABA) is a plant hormone, which involved in diverse aspects of physiological process, among which its role in drought tolerance has long been studied (Ali et al. 2020, Takahashi et al. 2020). It is well-known for its function in induction of stomatal closure by targeting both transcriptional reprogramming and osmolarity regulation (Vishwakarma et al. 2017, Kumar et al. 2019, Hsu et al. 2021). In guard cells, ABA synthesis is both autonomous within guard cells and can occur via long distance signals, which enable plants to finely modulate gas exchange to a changing environment (Bauer et al. 2013). Core ABA signalling reduces guard cells turgor by activating transport activity of QUick Anion Channels (QUACs) and SLow Anion Channels (SLACs), which exclude anions from guard cells during stomatal closing (Dreyer et al. 2012, Cotelle and Leonhardt 2019). Anion transport depolarises membrane potential to active potassium outward transporters, and ultimately leads to water loss from guard cells (Hosy et al. 2003).

γ-Aminobutyric acid (GABA) is a non-proteinogenic amino acid found widely across the kingdom of life, which in plants was initially discovered from potato tuber (Elliott and Jasper 1959). In plants, GABA can accumulate markedly and rapidly under varied stresses, and it has long been speculated to be a plant signalling molecule (Bouche and Fromm 2004, Bown and Shelp 2016, 2020). Research conducted during the past decades has connected changes in GABA metabolism to plant transcriptome responses, redox and pH balance, mitogen-activated protein kinase (MAPK) cascades, C/N balance, Ca^{2+} signalling (Bouché et al. 2003, Zhu et al. 2019, Deng et al. 2020, Li et al. 2020), but many gaps remain

including answering the question of whether GABA is just a stress induced metabolite or a signalling molecule and, if so, how is GABA signalling transduced in plants?

When expression of genes encoding Glutamate Decarboxylase (GAD1, 2) were ablated via T-DNA insertional mutagenesis, the resulting low endogenous GABA corresponded to elevated rates of stomatal conductance (Mekonnen et al. 2016). Members of Aluminium-activated Malate Transporter (ALMT) family have critical roles in both stomatal opening and closing (Meyer et al. 2010, De Angeli et al. 2013b). The family from across plant species is subject to regulation by GABA, and subsequently it was found that they can transport GABA (Ramesh et al. 2015, Ramesh et al. 2018), which suggests that they are promising components of plant GABA signalling ripe for future research (Gilliham and Tyerman 2016, Ramesh et al. 2017). The following chapter will provide an update on research related to plant GABA and the potential for it to be a guard cell signal; further, it will identify knowledge gaps, and research questions that will be addressed in this thesis.

GABA in plants

GABA metabolism

In plants, the main pathway for GABA synthesis is via the GABA shunt (Fig. 1). It starts with glutamate (Glu) synthesis from 2-ketoglutamate (AKG) catalysed by glutamate dehydrogenase (GDH) in the cytosol. Then Glu is converted to GABA by Glu Decarboxylase (GAD), which consumes H^+ and produces CO_2. Then, GABA is transported by a GABA permease into mitochondria (GABAP), where it is catabolized to succinic semi-aldehyde (SSA) by GABA-Transaminase (GABA-T), and further into succinate by SSA dehydrogenase (SSADH) (Fait et al. 2008, Bown and Shelp 2020). This cascade of

reactions bypass two steps of the TCA cycle from AKG to succinyl-CoA by α-ketoglutarate dehydrogenase (OGDC) and succinyl-CoA to succinate catalysed by succinyl-CoA synthetase (SCS) (Fig. 1). Many studies have shown that the GABA shunt and TCA cycle work cooperatively to maintain the level of succinate for the TCA cycle (Hijaz and Killiny 2019). For instance, when OGDC in *Solanum tuberosum* (potato) was selectively inhibited by analogues of AKG, the level of succinate was still elevated after around 2 hours of treatment, most likely due to the upregulation of the GABA shunt (Araújo et al. 2008). Likewise, in *Solanum lycopersicum* (tomato), when succinyl-CoA synthetase gene expression was silenced by RNAi, the expression of *GAD* was transcriptionally upregulated, which consequently supplied succinate to the TCA cycle and maintained the respiration rates at normal levels (Studart-Guimarães et al. 2007). The relationship between the TCA and the GABA shunt has been shown by both GABA accumulation contributing to organic acid synthesis in the TCA cycle (Hijaz and Killiny 2019, Lee et al. 2020) and via the disruption of GABA transport into mitochondria, i.e. the T-DNA insertion mutant of *GABAP*, where carbon oxidation associated with the TCA cycle is increased (Michaeli et al. 2011). As such, the GABA shunt has been proven to be an efficient bypass of the TCA cycle.

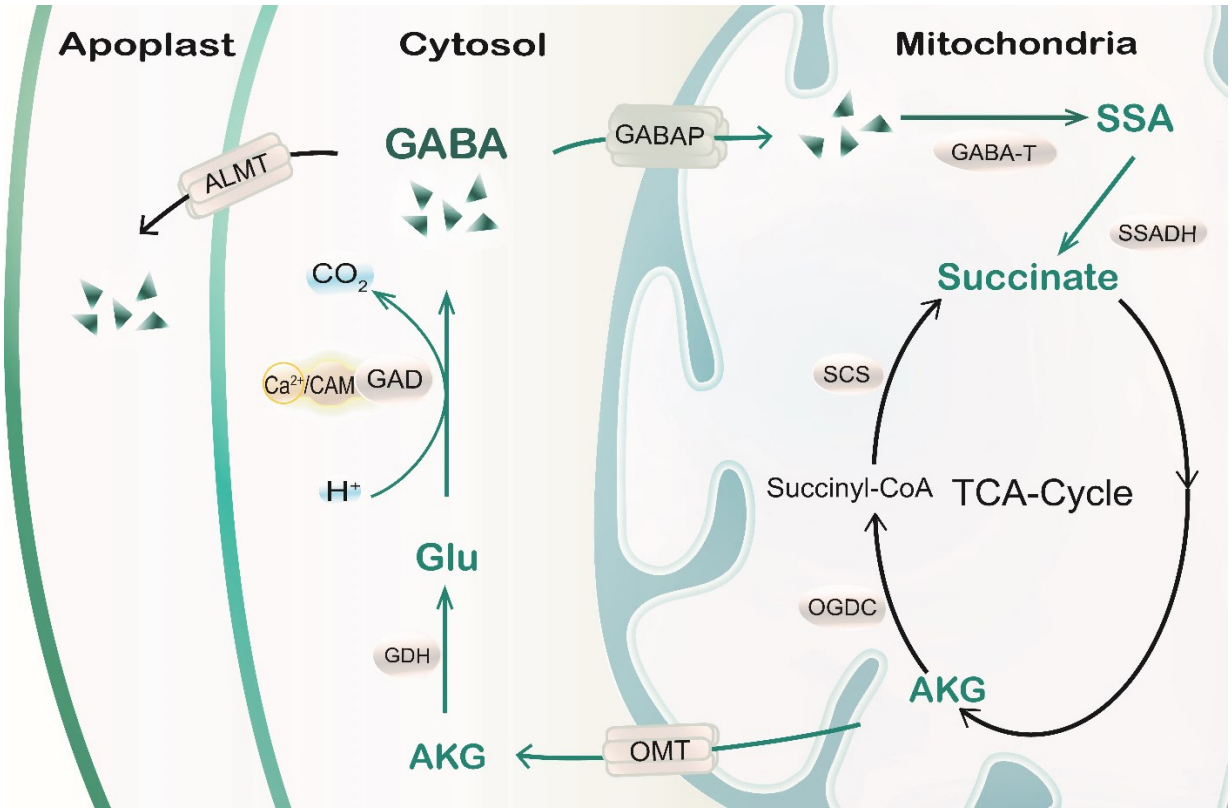

Figure 1. GABA synthesis in plants.

The model illustrates GABA synthesis via GABA shunt. GABA, γ-Aminobutyric Acid (indicated by green triangles); GABAP, GABA permease; GABA-T, GABA-Transaminase; SSA, Succinic Semi-Aldehyde; SSADH, SSA Dehydrogenase; AKG, 2-Ketoglutamate; OMT, AKG transporter; OGDC, A-Ketoglutarate Dehydrogenase; SCS, Succinyl-Coa Synthetase; GDH, Glutamate Dehydrogenase; Glu, Glutamate; GAD, Glutamate Decarboxylase; Ca^{2+}/CaM, Calcium /Calmodulin Complex; ALMT, Aluminium-Activated Malate Transporters.

GABA can also be synthesised from polyamine catabolism from putrescine, catalysed directly by NAD^+-dependent aminoaldehyde dehydrogenases (AMADH) or indirectly by PDH (pyrroline dehydrogenase) (Signorelli et al. 2015). Previous research indicated that these enzymes are NAD^+-dependent enzymes and not induced under abiotic and biotic stress due to an increased $NADH/NAD^+$ ratio, thereby these are unlikely to contribute to

the stress-induced accumulation of GABA (Flores and Filner 1985, Allan et al. 2011, Shelp et al. 2012). Homologues of AMADH in *Arabidopsis*, the aldehyde dehydrogenase 10 family (ALDH10A8 and ALDH10A9), can contribute partially to GABA synthesis in response to saline stress where the mutant lines still had significant lower GABA accumulation comparing to WT (Missihoun et al. 2015, Zarei et al. 2016, Shelp and Zarei 2017). Further, *in vivo* analysis characterized those enzymes as glycine betaine synthetase with an optimal pH over 8.5, suggesting the possible contribution of the enzyme to GABA synthesis would be limited in organelles, such as those with higher pH and likely to be only evoked during rare cases of stress induced alkalisation, such as peroxisome (pH= 8.4) and apoplast (although 6.5-6.7 under normal conditions in *Arabidopsis*, have been proposed to increase by ~2 pH units after encountering pathogen attack in barley from 5 to 7) (Shen et al. 2013, Geilfus 2017, Martinière et al. 2018). Thus, GAD catalysed GABA synthesis should be the main source of GABA production in plants.

Plant GAD commonly contains a C-terminal Ca^{2+}-dependent calmodulin (CaM)-binding domain that acts as an autoinhibitory domain relieved by the binding of Ca^{2+}/CaM (Du et al. 2011), with several exceptions, such as rice OsGAD2, apple MdGAD3, and possibly GAD3 and GAD5 of *Arabidopsis* (Akama and Takaiwa 2007, Trobacher et al. 2013, Shelp and Zarei 2017). Studies have shown that GAD activity is Ca^{2+}/CaM dependent, and optimal at an acidic pH. For instance, both *Arabidopsis* GAD1 and GAD2 has maximum activity at pH 5.8 (cytoplastic pH generally in *Arabidopsis* is 7.3), where Ca^{2+}/CaM can increase the enzyme activity by several fold (Zik et al. 1998, Shen et al. 2013, Trobacher et al. 2013, Demes et al. 2020). *In viv*o analysis suggests an equilibrium of *Arabidopsis* GAD1 between a less active dimer to the fully activate hexamer mediated by a reduction in cytoplasmic pH, and induction of Ca^{2+}/CaM and accumulation of GAD1 (Astegno et al.

2015). This is in accordance with GABA accumulation under varied stress conditions (Locy et al. 2000, Scholz et al. 2017, Fàbregas and Fernie 2019). Cytoplasmic acidification can occur in plants encountering anoxic stress (Felle 2005). Ca^{2+}, as a secondary messenger, mediates signal transduction in response to environmental stimuli, and plant hormones, with high sensitivity (Iqbal et al. 2020). *GAD* expression and protein concentration, also accumulates under stress conditions (Carillo 2018). Increases in cytoplasmic Ca^{2+}, and GAD protein content, and decreases in cytoplasmic pH are all suggested to be the major ways in which GABA synthesis is stimulated (Astegno et al. 2015).

There are 5 homologues of *GAD* in *Arabidopsis*, *GAD1* to *GAD5*. All five members have distinct expression patterns and transcriptional profiles in seedlings (Figure 2). *GAD1* is mainly expressed in roots and has much lower expression in shoots (Bouché et al. 2004), while *GAD2* is the most abundant isoform expressed in shoots (Scholz et al. 2015). Transcript expression of *GAD3* and *GAD5* is mainly detectable in siliques and flowers respectively (Miyashita and Good 2008). While *GAD4* expression is distributed in the whole plants at a relatively low level under normal conditions but is induced under: salt stress and hypoxia in *Arabidopsis* (Zarei et al. 2017, Safavi-Rizi et al. 2020); in the ABA deficit mutant when the key gene (9-cis-epoxycarotenoid dioxygenase) coding ABA synthesis enzyme was mutated; and, in the *gad1/2* mutant (Urano et al. 2009, Scholz et al. 2015). The loss-of-function of single or multiple *GAD* (s) disrupts GABA synthesis in different tissues with distinct plant phenotypes (Bouché et al. 2004, Scala 2015, Mekonnen et al. 2016, Deng et al. 2020). T-DNA insertion of *GAD1* reduced GABA accumulation in roots, which did not contribute to a visible root morphological change under control or hypoxic stress conditions (Bouché et al. 2004, Miyashita and Good 2008). However, additional mutation of *GAD2* in the *gad1* background (*gad1/2*), reduced GABA accumulation in both shoots and roots, had

increased sensitivity to drought stress compared to that of wild type due to elevated stomatal conductance (Mekonnen et al. 2016). *gad1/2* also showed increased susceptivity to salt stress due to an enhanced Reactive oxygen species (ROS) production (Su et al. 2019). The triple mutant *gad1/2/4* and quadruple mutant *gad1/2/4/5*, which had further reduced endogenous GABA concentrations, showed enhanced susceptibility to *Pseudomonas syringae* inoculation (Deng et al. 2020). *GAD1*, *GAD2* and *GAD4* responded differently during immunity against pathogenic microorganisms in *Arabidopsis*, and GABA accumulation during this process appears to be downstream of mitogen-activated protein kinase signalling (MPK3/MPK6) (Deng et al. 2020). Thereby, disrupted GABA synthesis, especially in shoots, seems to contribute to susceptibility of plants to biotic and abiotic stress.

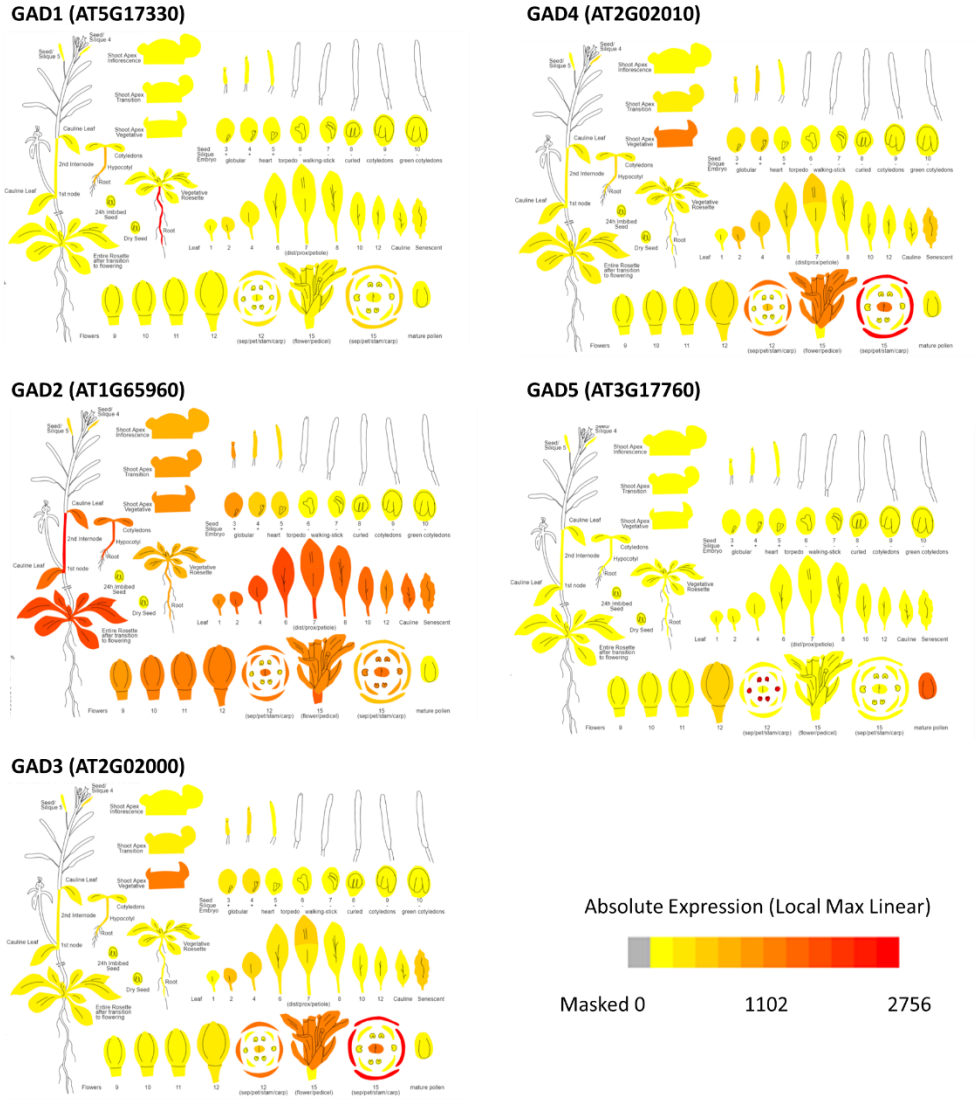

Figure 2. Expression level of *GAD* homologues in *Arabidopsis.*

Colour scale from yellow to red indicates absolute expression level of *GADs*. Data were adapted from The Bio-Analytic Resource for Plant Biology (Schmid et al. 2005, Waese and Provart 2017).

GABA transport in plants

GABA metabolism (from synthesis in the cytosol to catabolism in mitochondria) (Shelp and Zarei 2017), and its potential signalling functions (e.g. immunity response) (Shelp et al. 2006), depends upon the transport of GABA across membranes. So far, several families of transporter proteins have been identified in plants that appear to catalyse the movement of GABA, i.e. ProTs (proline transporters), AAP3 (amino acid/auxin transporter), GAT1 (GABA transporter), GABP (GABA permease) and CAT9 (cationic amino acid transporter), and ALMTs (Fischer et al. 2002, Meyer et al. 2006, Henry et al. 2007, Michaeli et al. 2011, Ramesh et al. 2018). The plasma membrane localised GABA transporters identified so far had either low affinity to GABA (AAP3, ProTs) or no significant impairment on cytosolic GABA level (GAT1) (Grallath et al. 2005, Batushansky et al. 2015). This could be due to presumably existence of other GABA transporters on the plasma membrane, such as ALMTs (Batushansky et al. 2015, Ramesh et al. 2018). Besides, GABA synthesis mainly takes place in cytosol, which is tightly controlled by GAD activity (Bown and Shelp 2020), and thus could hinder the detection of the contribution by plasma membrane GABA importers to cellular GABA concentration . Mitochondria GABAP is the only transporter so far identified mediating GABA uptake into mitochondria, which is required for further GABA catabolism (Michaeli et al. 2011). Perturbed GABA catabolism by mutation of gene encoding *GABAP* led to impaired root and leaf growth in a light dependent manner, possibly due to light dependent activity of TCA cycle in plants (Zhang and Fernie 2018). As for the tonoplast CAT9, mutation in tomato *slcat9* altered GABA/Glu balance in leaves (increase in GABA and reduced in Glu concentration in tomato leaves) (Li et al. 2018). However, less is known about the role of vacuole storage of GABA, Glu and Asp, further data are required to elucidate the role of the tonoplast GABA transporter. GABA transport via ALMTs is more

dynamic. The direction is pH-dependent relying on GABA concentration and the presence of external anions (Ramesh et al. 2018). The influence of GABA on ALMTs has been associated to a putative GABA-binding motif on ALMTs (Ramesh et al. 2015, Long et al. 2020).

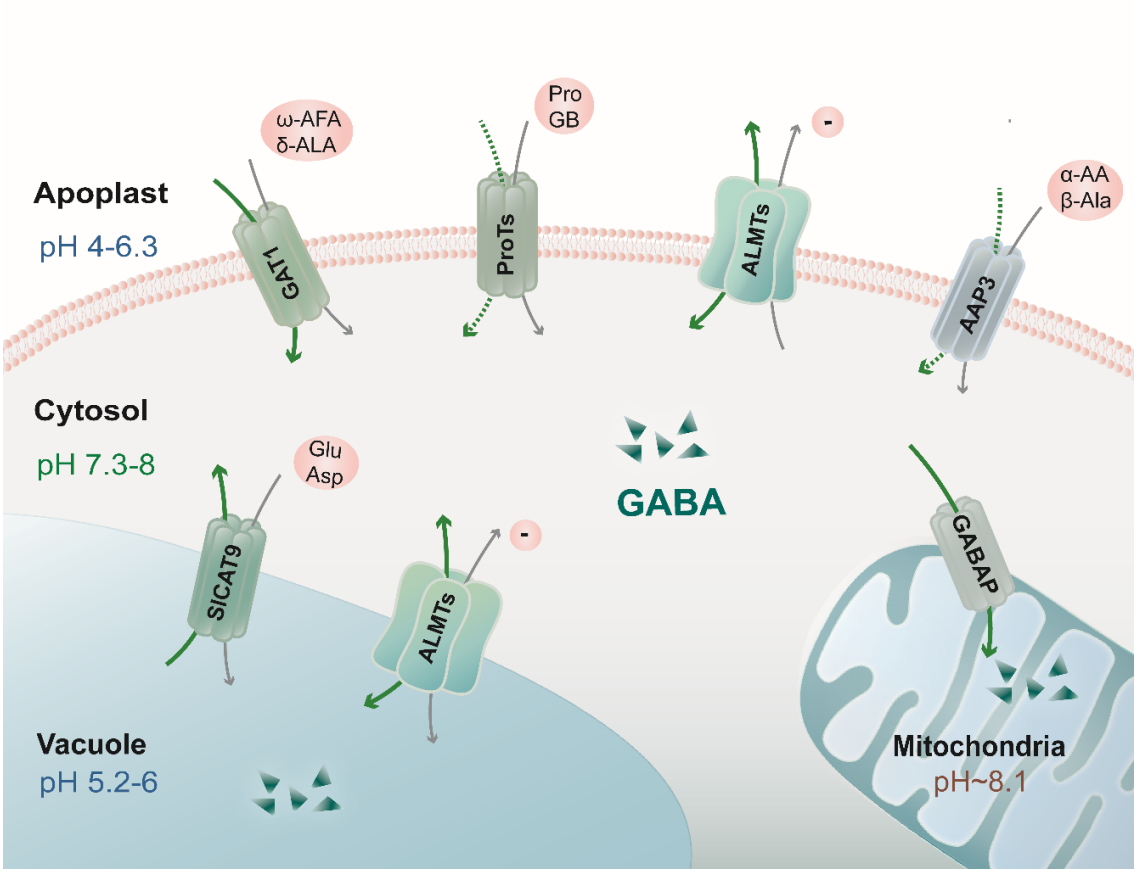

Figure 3. GABA transporters in plants.

The figure illustrates transport activity and subcellular location of currently identified GABA transporters. The green arrows indicate GABA transport direction and affinity (solid arrow: high affinity transport; dotted arrow: low affinity transport). Grey arrows indicate transport activity of the protein to other substrates. Negative charge signs represent varied anions, which can be transport by ALMTs, such as Cl^- and Mal^{2-} (Sharma et al. 2016). Since transport activity of Prots, GAT1 and ALMT was suggested to be pH-dependent (Breitkreuz et al. 1999, Meyer et al. 2006, Ramesh et

al. 2018), pH of varied subcellular compartments is also indicated (Kader and Lindberg 2010, Shen et al. 2013, Bhatti et al. 2017). ω-AFA: ω - aminiofatty acid; δ-ALA: δ- aminolevulinic acid; Pro: proline; GB: Gly Betaine; α-AA: α-Amino Acid; β-Ala: β-Alanine; Glu: Glutamate; Asp: Aspartate; GAT1: GABA Transporter 1; ProTs: Proline transporters; AAP3: amino acid/auxin transporter; GABP: GABA permease; SlCAT9: cationic amino acid transporter; ALMTs: Aluminium-activated malate Transporters.

Stomatal movement

In the majority of dicotyledonous plants, the opening and closing of stomata is controlled by expansion and shrinkage of guard cells respectively (Mano and Hasebe 2021). The driving force for stomatal movement is the change in turgidity of guard cells, which is mediated by varied transporters and channels located on both the plasma membrane and tonoplast membrane of guard cells (Jezek and Blatt 2017, Sato et al. 2018, Xiang et al. 2020). In brief, stomatal opening is initiated by efflux of H^+ from the cytosol via the H^+-ATPase located on both the plasma membrane and tonoplast. This provides a hyperpolarised membrane potential and proton gradient, which are required to activate K_{in}^+ channels (potassium influx channels) and anion importers on the plasma membranes and subsequently sequestration of ions into vacuoles by tonoplast transporters, such as Na^+/H^+ antiporter (NHX) and ALMTs. The increased osmolarity in guard cells leads to a reduced water potential, and subsequent water uptake into guard cells. The built-up turgor pressure expands guard cells to open stomata. On the contrary, stomatal closing is induced by anion efflux initiated by activation of two types of anion channel on the plasma membrane, slow anion channels and its homologues (SLAC/SLAHs) and rapid-type anion channels (QUACs/ALMTs). These depolarise the membrane potential of guard cells and activate

efflux of K^+ via the guard cell outward rectifying K^+ channel (GORK). In the vacuole, K^+ efflux by TPK (two-pore K^+ channel) supports the anion efflux mediated by CLC (chloride channel) and ALMTs. The water potential is then increased in guard cells, which closes stomata due to the loss of water from guard cells (Kollist et al. 2014, Sharma et al. 2016).

Among all the anion transporters involved in stomatal movement, ALMT family members can catalyse malate transport across both plasma membrane and tonoplast membrane. Not only that, malate, the shared target of ALMTs, can be degraded from or converted to starch, which has been suggested to be implicated in stomatal movement (Daloso et al. 2017, Santelia and Lunn 2017). Thus, identification of the ALMT transport activity and regulation could contribute to untangling some of the complexity in the elaborate stomata signalling network.

Varied transport traits of ALMTs and their role in guard cells

Plant ALMTs are named after the first member of the family discovered, wheat ALMT1 (TaALMT1), which mediates tolerance to the Aluminium trivalent cation (Al^{3+}) in acidic soils (Sasaki et al. 2004). However, only a few ALMT family members are Al^{3+} activated (Liu and Zhou 2018). Phylogenetic analysis on anion channels and transporters in plants revealed that ALMTs are evolutionally grouped into different clades, with homologues in *Arabidopsis* divided into four clades (Clade I: ALMT1, 2, 7, 8; Clade II: ALMT3, 4, 5, 6, 9; Clade III: ALMT11-14; Clade IV: ALMT10) (Maia et al. 2011, Sharma et al. 2016) (Fig. 4). *Arabidopsis* ALMT1, in Clade I, is the only member in *Arabidopsis* identified so far with Al^{3+} activation. It is mainly expressed in root tips, from where it catalyses malate efflux to chelate Al^{3+} in acidic soils, Fe^{3+} at low phosphate conditions and facilitates alkaline tolerance (Hoekenga

et al. 2006, Lager et al. 2010, Balzergue et al. 2017, Kamran et al. 2020). Other clade I members, such as barley HvALMT1 (is plasma membrane localised) mediates efflux of malate and other organic acid out of guard cells and the root apex (Gruber et al. 2011). Less is known about the transport activity of ALMT10 in clade IV, except for that it was found to be induced in the *almt12* mutant together with other *ALMTs* (*ALMT3, 4, 5, 11, 13* and *14*) in pollen tubes (Gutermuth et al. 2018, Herbell et al. 2018, Domingos et al. 2019). Evidence are that rice OsALMT7 from clade IV mediates plasma membrane anion export, which is required for panicle growth (Miura et al. 2010). Clade II contains 5 members from *Arabidopsis*. ALMT4, 5, 6 and 9 are targeted on the tonoplast membrane (Fig. 5) (Gruber et al. 2011, Meyer et al. 2011, De Angeli et al. 2013b, Eisenach et al. 2017). ALMT6, which is distributed mainly in guard cells and flowers, is a pH-modulated bidirectional malate and fumarate channel activated by cytosolic Ca^{2+} (Meyer et al. 2011). Mutation of *ALMT6* had reduced malate current of guard cell vacuoles, though the mutant did not show a significant impaired stomatal movement compared to that of wildtype (Meyer et al. 2011). *ALMT9* encodes a malate-activated chloride transporter in leaves and roots, catalysing malate, Cl^- and fumarate uptake into the vacuoles of guard cells (De Angeli et al. 2013b). Mutation of *ALMT9* led to impaired stomatal opening with increased drought performance (De Angeli et al. 2013b) and accumulated NaCl in shoots under saline stress (Baetz et al. 2016). Different from ALMT6 and 9, ALMT4 mediates malate efflux from guard-cell vacuoles, activated by cytosolic malate and MPK4/6. The loss-of-function of *almt4* impairs ABA-induced stomatal closure (Eisenach et al. 2017). Both overexpression of *ALMT4* in *Arabidopsis* and *HvALMT1* in barley result in more closed stomata of plants (Gruber et al. 2011, Eisenach et al. 2017). Another clade member, grape VvALMT9, located on tonoplast of grape fruits, mediates tartaric acid accumulation, which contributes to berry flavour (De Angeli et al. 2013a). The tomato SlALMT5, localised in endoplasmic reticulum (ER),

expressed in tomato fruits and seeds, is an inward rectifying malate transport (Sasaki et al. 2016). The last clade of ALMTs comprise the QUACs in *Arabidopsis* (Dreyer et al. 2012). ALMT12, i.e. QUAC1, is well known for fast activation characteristic during membrane depolarisation (Sussmilch et al. 2019). It is permeable to both organic and inorganic anions, which can be activated by cytosolic SO_4^{2-} , malate and altered membrane potential (Meyer et al. 2010, Sasaki et al. 2010, Malcheska et al. 2017). *ALMT12* disruption caused reduced stomatal closure to CO_2 and darkness (Meyer et al. 2011). Recently, it has been found that QUACs (ALMT12, 13 and 14) act down stream of Ca^{2+} signalling in pollen tubes of plants, in a way by Ca^{2+}-dependent protein kinases (CPKs) activating their anion efflux at the apical area of pollen tubes. These channels worked cooperatively with a Ca^{2+} importer, contributing to a high $[anion]_{cyt}$ /$[Ca^{2+}]_{cyt}$ to maintain pollen tube growth (Gutermuth et al. 2018). A clade III ALMT in grass *Brachypodium distachyon* (BdALMT12), which is also a voltage dependent malate transporter, mediates stomatal closing via activation cooperatively by malate and Ca^{2+} /CaM instead of kinases (Luu et al. 2019). In summary, the ALMTs have varied transport activity in response to diverse regulatory factors within the same species, and homologues exist with high identity between different species. The family have been proven to be involved in multiple physiological processes in plants, in response to divergent signalling pathways (Sharma et al. 2016, Liu and Zhou 2018).

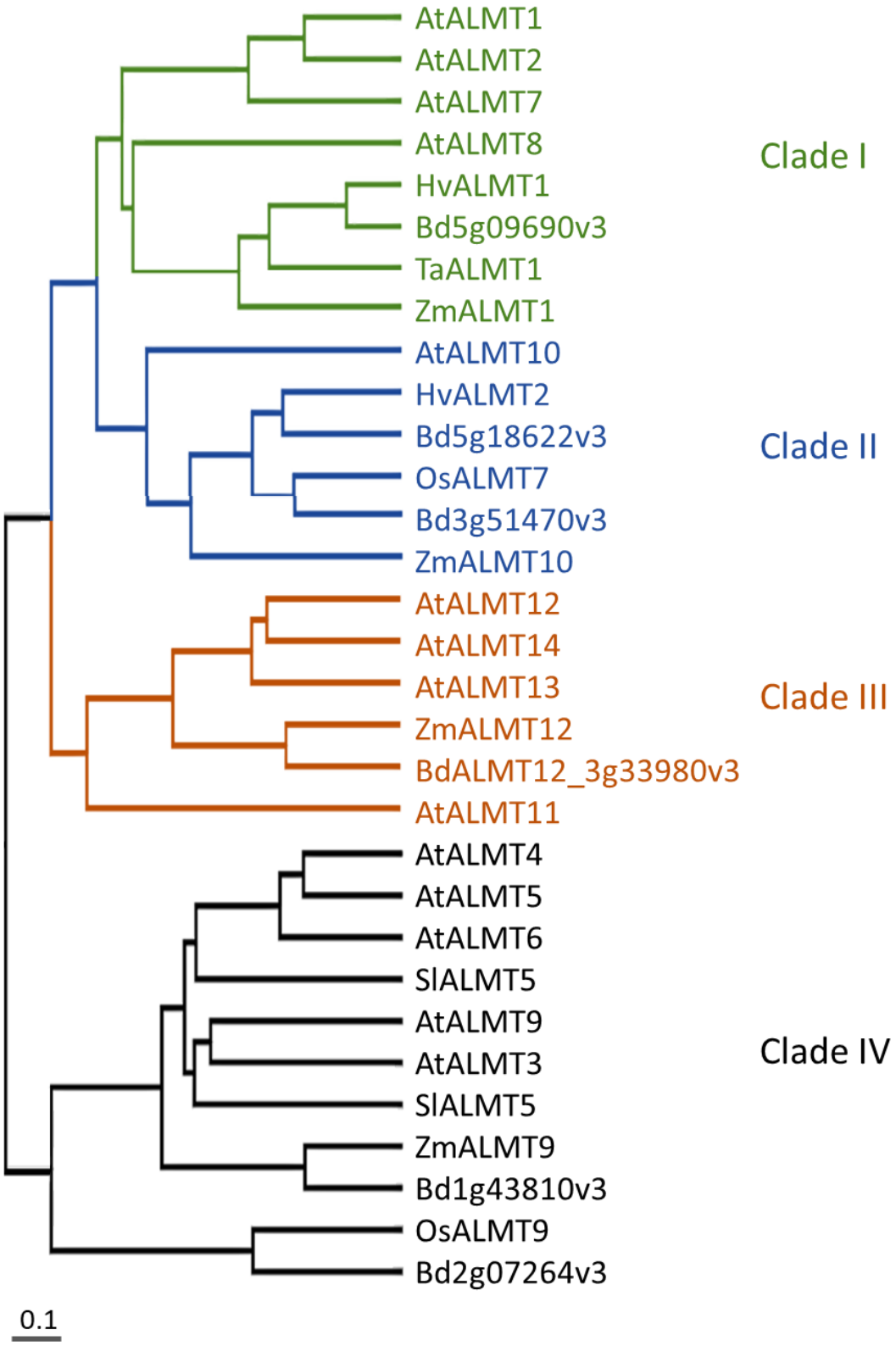
AtALMT1
AtALMT2
AtALMT7
AtALMT8
HvALMT1
Bd5g09690v3
TaALMT1
ZmALMT1
Clade I
AtALMT10
HvALMT2
Bd5g18622v3
OsALMT7
Bd3g51470v3
ZmALMT10
Clade II
AtALMT12
AtALMT14
AtALMT13
ZmALMT12
BdALMT12_3g33980v3
AtALMT11
Clade III
AtALMT4
AtALMT5
AtALMT6
SlALMT5
AtALMT9
AtALMT3
SlALMT5
ZmALMT9
Bd1g43810v3
OsALMT9
Bd2g07264v3
Clade IV
0.1

Figure 4. Phylogenetic analysis of ALMTs.

The phylogenetic tree was established via multiple sequence alignment by MAFFT (EMBL-EBI) using protein sequence of ALMTs from varied plant species (Katoh and Standley 2013, McWilliam et al. 2013, Li et al. 2015). The family members are divided into 4 clades marked in different colours. Branch length indicates genetic change of the branch (substitution per site). At, *Arabidopsis thaliana*; Hv, *Hordeum vulgare*; Ta, *Triticum aestivum*; Zm, *Zea mays*; Os, *Oryza sativa*; Sl, *Solanum lycopersicum*; Bd, Brachypodium distachyon.

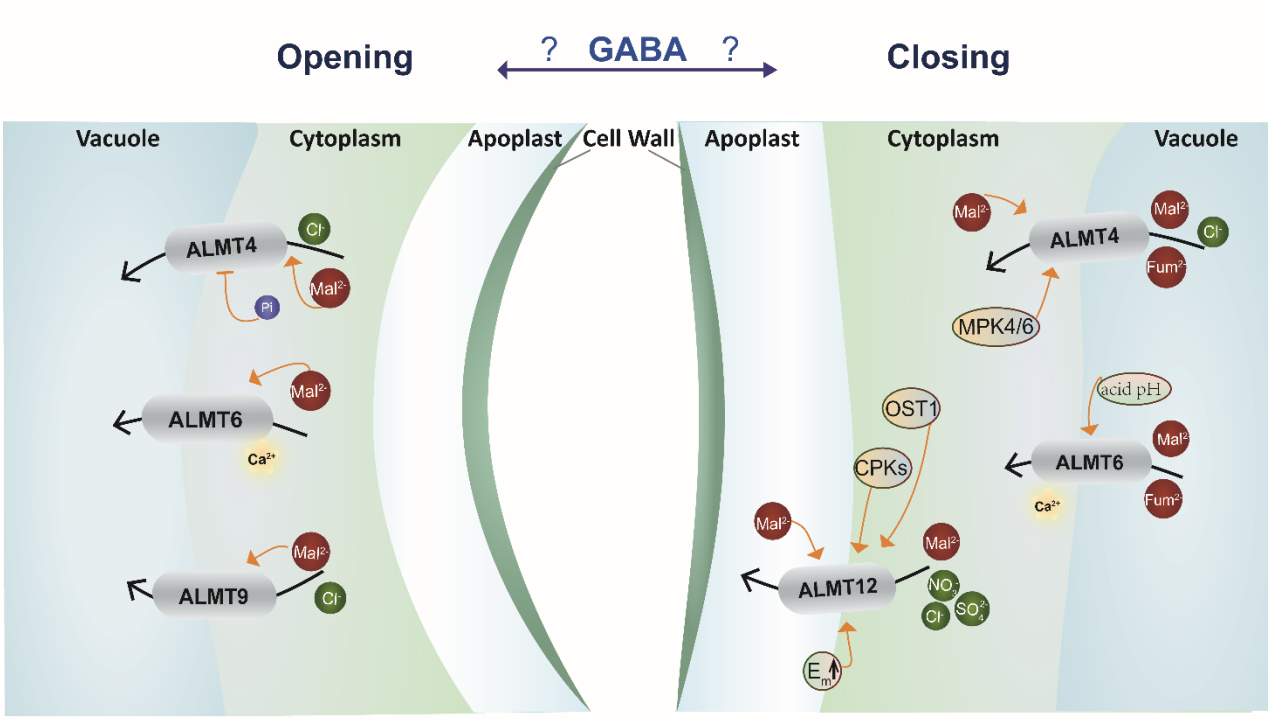

Figure 5. Does GABA play a role in regulating opening and closing of stomatal through regulation of guard cell ALMTs?

The model summarises key transport features of *Arabidopsis* ALMTs in Guard cells. Mal^{2-}, malate; SO_4^{2-}, sulphate; NO_3^-, nitrate; Ca^{2+}, calcium; Em, membrane potential; OST1, Open Stomata 1 (SnrK2.6); CPK, Calcium-dependent protein kinases; MPK, mitogen-activated protein kinase; Pi,

protein phosphorylation. Black arrows indicate transport directions, while orange arrow indicates activation elements of the transporter.

ABA signals in stomatal movement

ABA is a phytohormone involved in many aspects of plant physiological process and stress responses. It is synthesised in the vasculature, as well as in the mesophyll cells and guard cells, and is a key part of signalling networks for stomatal regulation (Askari-Khorsgani et al. 2018, Chen et al. 2020). Sub-cellularly, ABA is synthesized from its chloroplast derived precursor xanthoxin and catabolised to either ABA glucosyl ester (ABA-GE) or dihydrophaseic acid (DPA) in the cytosol (Xiong and Zhu 2003, Zhou et al. 2004). ABA production is regulated by developmental and environmental cues (Xiong and Zhu 2003, Ma et al. 2018), and thereby governs ABA signalling in plants (Sehgal et al. 2018, Kumar et al. 2019). The well-defined ABA signalling pathway, the core signalling pathway, is constituted by Pyrabactin Resistance/Pyrabactin Resistance-Like/Regulatory Components of The ABA Receptor (PYR/PYL/RCAR), type 2C protein phosphatases (PP2Cs) and class III SNF-1-related protein kinase (SnRKs) (Soon et al. 2012, Duarte et al. 2019). When ABA concentration is low, PP2C inhibits target protein activity directly or indirectly through inhibiting kinase activity of SnRKs (Fernando and Schroeder 2016). When a stimulus occurs, such as drought and dark, cytosolic ABA concentration increases and is recognised by PYR/PYL/RCAR, which enhances the interaction of PYLs and PP2C to relieve inhibition of SnRKs (Soon et al. 2012). The kinases then trigger downstream signal transduction of ABA depend signalling (Zhang et al. 2019). For instance, OST1 (SnrK2.6) activates transport activity of SLAC1 and QUAC1 to induce stomatal closing (Eisenach et al. 2017, Hsu et al. 2021).

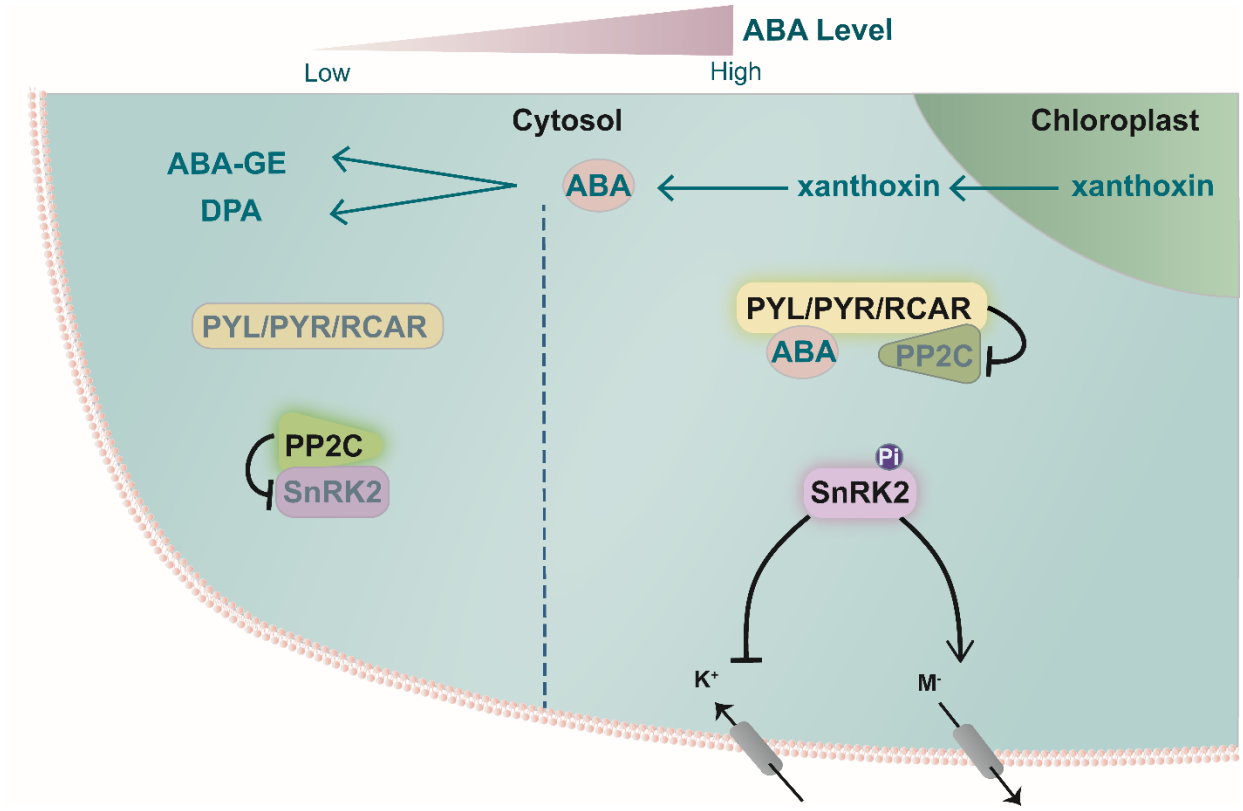

Figure 6. ABA core signalling in plant cells.

ABA metabolism pathway was connected by blue arrows indicated at the top the graph. ABA, abscisic acid; ABA-GE, ABA glucosyl ester; DPA, dihydrophaseic acid; PYR/PYL/RCAR, Pyrabactin Resistance/ Pyrabactin Resistance - Like/Regulatory Components of The ABA Receptor; PP2C, type 2C protein phosphatases; SnRK2, class III SNF-1-related protein kinase. K^+, potassium imports by potassium channel protein (KAT1); M^-, anions exports executed by transports, such as SLAC (slow anion channel) and QUAC (quick anion channel).

Thesis outline/hypotheses generation

As reviewed above, previous research has shown that ALMTs modulate a wide range of developmental and physiological processes (Sharma et al. 2016, Liu and Zhou 2018).

ALMTs can facilitate GABA transport and are also regulated by GABA. The anion transporters are proposed to act as a transducer of GABA signalling (Gilliham and Tyerman 2016, Ramesh et al. 2017, Domingos et al. 2019). In this case, the loss-of-function mutants of *ALMT*(s) may phenocopy knockout mutants associated with impairment in GABA signalling (for instance, *gad(s)* mutant(s)). Further study of gain- and/or loss-of-function mutants of *ALMTs* is a prospective way to uncover roles of GABA signalling in plants. As GABA metabolism may affect stomatal regulation (Mekonnen et al. 2016), and ALMTs are a key transport family involved in regulating stomatal movement, the role of GABA regulation of ALMT in stomata appears to be a perfect test case for studying whether GABA is truly a signal in plants.

The most predominant *GAD* paralogues of *Arabidopsis* are *GAD1* and *GAD2*. Single mutants of *GAD1*, with reduced GABA concentrations in roots, had no visible phenotype (Bouché et al. 2004). Whereas mutation of both *GAD1* and *GAD2* result in enlarged stomatal apertures (Bouché et al. 2004, Mekonnen et al. 2016). In ABA deficient mutants and salinity-stressed wildtype *Arabidopsis* plants, only *GAD4* expression was induced (Urano et al. 2009, Zarei et al. 2017). Thus, further questions should be addressed:

1) Is GABA accumulation linked to stomatal regulation? *Explored in chapter II*

2) Does the disruption of guard-cell ALMT(s) perturb stomatal sensitivity to GABA? *Explored in chapter II and III.*

3) Do GADs other than the major GAD1 and 2 contribute to GABA signalling, and how? *Explored in chapters IV and V.*

Chapter II GABA signalling modulates stomatal opening to enhance plant water use efficiency and drought resilience

Brief introduction

A signalling role for GABA in plants has long been speculated, but evidence was lacking *in planta*. Recently, members of ALMT family specific were found to have their anion transport negatively regulated by GABA and be a facilitator of GABA transport (Ramesh et al. 2015, Ramesh et al. 2018). Two ALMT family members, ALMT9 and ALMT12, have been shown to modulate stomatal opening and closing, respectively in *Arabidopsis* (Meyer et al. 2010, De Angeli et al. 2013b). Furthermore, deficiency in GABA synthesis in leaves was linked to more open stomatal pores of *Arabidopsis* (Mekonnen et al. 2016). Here, we investigate the hypothesis that GABA is a signal in plants by the use of guard cells as an assay system. This allows the examination of the effects of GABA (both exogenous and endogenous) on stomatal guard cell movement, and the manipulation of ALMT9 and ALMT12. The results of this work were accepted by *Nature Communications* in March 2021.

Statement of Authorship

Title of Paper	GABA signalling modulates stomatal opening to enhance plant water use efficiency and drought resilience
Publication Status	☑ Published ☐ Accepted for Publication ☐ Submitted for Publication ☐ Unpublished and Unsubmitted work written in manuscript style
Publication Details	Xu, Bo, Yu Long, Xueying Feng, Xujun Zhu, Na Sai, Larissa Chirkova, Annette Betts, Johannes Herrmann, Everard Edwards, Mamoru Okamoto, Rainer Hedrich, and Matthew Gilliham. "GABA signalling modulates stomatal opening to enhance plant water use efficiency and drought resilience." *Nature Communications* (2021).

Candidate

Name of Candidate:	Xueying Feng

Contribution to the Paper	My primary contribution was the construction and screening of homozygous lines of *almt9-1/35S::ALMT9* and *almt9-1/35S::ALMT9F243C.* I measured stomatal conductance of the transgenic lines under steady state and conducted epidermal strip assay on the transgenic lines in GABA inhibited light induced stomatal opening (Fig 8a, Fig 9; Supp Fig 16a,b). I also ensured that the primary data and hypothesis presented (Fig 10) were accurate by performing independent repeat experiments of the WT and *gad2, almt9* drought assays and stomatal response assays (replicate data for figure 1, 3; Supp Fig 6, 7).		
Overall percentage (%)	20%		
Certification:	This paper reports on original research I conducted during the period of my Higher Degree by Research candidature and is not subject to any obligations or contractual agreements with a third party that would constrain its inclusion in this thesis.		
Signature		Date	06/05/2021

Co-Author Contributions

By signing the Statement of Authorship, each author certifies that:

i. the candidate's stated contribution to the publication is accurate (as detailed above);

ii. permission is granted for the candidate in include the publication in the thesis; and

iii. the sum of all co-author contributions is equal to 100% less the candidate's stated contribution.

Name of Co-Author	Bo Xu		
Contribution to the Paper	Conceived research and designed experiments. Conducted all experiments not listed above or below. Co-wrote paper.		
Signature		Date	6/05/2021

Name of Co-Author	Yu Long		
Contribution to the Paper	Constructed almt9/almt12 knockouts, conducted assays on almt12 and almt9/almt12 plants. Repeated experiments with gad2 and WT.		
Signature		Date	5/5/2021
Name of Co-Author	Xujun Xu		
Contribution to the Paper	Conducted Supp Fig 5a,f.		
Signature		Date	5.5.2021

Name of Co-Author	Na Sai		
Contribution to the Paper	Conducted Supp Fig 5g,h – barley experiments.		
Signature		Date	5/5/2021

Name of Co-Author	Larissa Chirkova		
Contribution to the Paper	Performed UPLC interpreted data. Edited manuscript.		
Signature		Date	5/05/2021

Name of Co-Author	Annette Betts		
Contribution to the Paper	Performed LC interpreted data. Edited manuscript.		
Signature		Date	7/5/21

Name of Co-Author	Johannes Hermann		
Contribution to the Paper	Performed Fig 1. Commented on manuscript.		
Signature		Date	06.05.2021

Name of Co-Author	Everard Edwards
Contribution to the Paper	Supervised LC, interpreted data. Edited manuscript.

Signature		Date	6/5/21

Name of Co-Author	Mamouru Okamoto		
Contribution to the Paper	Supervised UPLC, interpreted data. Edited manuscript.		
Signature		Date	5/05/2021

Name of Co-Author	Rainer Hedrich		
Contribution to the Paper	Designed experiments, interpreted data and edited manuscript.		
Signature		Date	05.05.2021

Name of Co-Author	Matthew Gilliham		
Contribution to the Paper	Conceived research, designed experiments, interpreted data and co-wrote manuscript.		
Signature		Date	10/5/2021

nature COMMUNICATIONS

ARTICLE

https://doi.org/10.1038/s41467-021-21694-3 OPEN

GABA signalling modulates stomatal opening to enhance plant water use efficiency and drought resilience

Bo Xu[1,2], Yu Long[1,2], Xueying Feng[1,2], Xujun Zhu[1,3], Na Sai[1,2], Larissa Chirkova[2,4], Annette Betts[5], Johannes Herrmann[6], Everard J. Edwards[5], Mamoru Okamoto[2,4], Rainer Hedrich[6] & Matthew Gilliham[1,2]✉

The non-protein amino acid γ-aminobutyric acid (GABA) has been proposed to be an ancient messenger for cellular communication conserved across biological kingdoms. GABA has well-defined signalling roles in animals; however, whilst GABA accumulates in plants under stress it has not been determined if, how, where and when GABA acts as an endogenous plant signalling molecule. Here, we establish endogenous GABA as a bona fide plant signal, acting via a mechanism not found in animals. Using *Arabidopsis thaliana*, we show guard cell GABA production is necessary and sufficient to reduce stomatal opening and transpirational water loss, which improves water use efficiency and drought tolerance, via negative regulation of a stomatal guard cell tonoplast-localised anion transporter. We find GABA modulation of stomata occurs in multiple plants, including dicot and monocot crops. This study highlights a role for GABA metabolism in fine tuning physiology and opens alternative avenues for improving plant stress resilience.

[1] Plant Transport and Signalling Lab, ARC Centre of Excellence in Plant Energy Biology, Waite Research Institute, Glen Osmond, SA, Australia. [2] School of Agriculture, Food and Wine, Waite Research Precinct, University of Adelaide, Glen Osmond, SA, Australia. [3] College of Horticulture, Nanjing Agricultural University, Nanjing, China. [4] ARC Industrial Transformation Research Hub for Wheat in a Hot and Dry Climate, Waite Research Institute, University of Adelaide, Glen Osmond, SA, Australia. [5] CSIRO Agriculture & Food, Glen Osmond, SA, Australia. [6] Institute for Molecular Plant Physiology and Biophysics, University of Würzburg, Würzburg, Germany. ✉email: matthew.gilliham@adelaide.edu.au

The regulation of stomatal pore aperture is a key determinant of plant productivity and drought resilience, and profoundly impacts climate due to its influence on global carbon and water cycling[1–3]. The stomatal pore is delineated by a guard cell pair. Fine control of ion and water movement across guard cell membranes, via transport proteins, determines cell volume and pore aperture following opening and closing signals such as light and dark[2,4,5] (Fig. 1). Due to their critical roles and their ability to respond to and integrate multiple stimuli, stomatal guard cells have become a preeminent model system for investigating plant cell signalling[6] resulting in the elucidation of many critical pathways involved in plant biotic and abiotic stress tolerance[7–9].

GABA signalling in mammals relies upon receptor-mediated polarization of neuronal cell membranes[10,11]. Speculation that GABA could be a signal in plants is decades old[12], but a definitive demonstration of its mode of action remains elusive. GABA production in plants is upregulated by stress[13,14]. It is synthesised in the cytosol via the GABA shunt pathway, bypassing two stress-inhibited reactions of the mitochondrial-based tricarboxylic acid (TCA) cycle[15,16]. GABA is therefore well known as a stress-induced plant metabolite that is fed back into the mitochondrial TCA cycle to sustain cellular energy production[12,17]. The discovery that the activity of aluminium-activated malate transporters (ALMTs) can be regulated by GABA[18] represents a plausible mechanism by which GABA signals could be transduced in plants, providing a putative—but unproven—novel signalling link between primary metabolism and physiology[19]. Stomatal guard cells contain a number of ALMTs that impact stomatal movement and transpirational water loss[20–22]. Therefore, stomatal guard cells represent an ideal system to test whether GABA signalling occurs in plants.

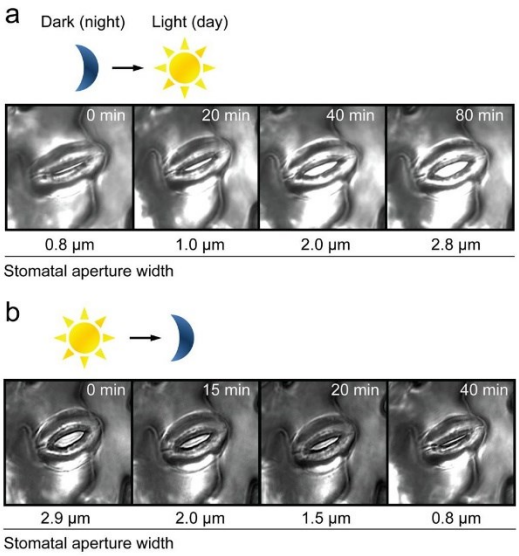

Fig. 1 Guard cells respond to light signals. a, b Time course of light-induced stomatal opening (**a**) and dark-induced stomatal closure (**b**) with actual stomatal aperture width indicated below; dark-to-light transition mimics night-to-day transition which opens stomatal pores (**a**) and light-to-dark transition mimics day-to-night transition which closes stomatal pores (**b**), light intensity 150 µmol m^{-2} s^{-1}.

Significantly, here, we show that GABA does not initiate changes in stomatal pore aperture, rather it antagonises changes in pore size, which differentiates it from many of the signals known to regulate stomatal aperture[3–8]. Specifically, we find that GABA concentration increases under a water deficit and this reduces stomatal opening in an ALMT9-dependant manner. The anion channel ALMT9 is a major pathway for mediating anion uptake into the vacuole during stomatal opening[21]; GABA signal transduction via ALMT9 leads to reduced transpirational water loss, increased water use efficiency (WUE) and improved drought resilience. As such, even though guard cell signalling is relatively well defined[6,23], this study has been able to uncover another pathway regulating plant water loss. Furthermore, by revealing a mechanism by which GABA acts in stomatal guard cells, we demonstrate that GABA is a legitimate plant signalling molecule[16].

Results

GABA antagonises both stomatal pore opening and closure in epidermal peels, but only opening in leaf feeding experiments. To validate whether GABA is a physiological signal that modulates stomatal pore aperture, our initial experiments used excised *Arabidopsis thaliana* epidermal peels where stomatal guard cells are directly accessible to a chemical stimuli[8,24–26]. When exogenous GABA or its analogue muscimol[14] were applied under constant light or dark conditions, neither elicited a change in stomatal aperture (Fig. 2a, b; Supplementary Fig. 1a, b). Interestingly though, we found that both compounds suppressed light-induced stomatal opening and dark-induced stomatal closure (Fig. 2a, b; Supplementary Fig. 1a, b). We then fed intact leaves with an artificial sap solution through the detached petiole with or without the addition of GABA or muscimol and examined whether this affected gas exchange rates. We found, in the GABA and muscimol fed leaves, that the increase in water loss (transpiration) stimulated by a dark-to-light transition was dampened compared to leaves fed just the artificial sap solution due to reduced stomatal conductance (Fig. 2c; Supplementary Figs. 1c, d and 2a). This is consistent with the reduced extent of stomatal opening that we observed in epidermal peels in the presence of GABA or muscimol upon a dark-to-light transition (Fig. 2b; Supplementary Fig. 1a). The gas exchange values of fed leaves were used to calculate instantaneous intrinsic WUE (iWUE) and WUE (ratios of carbon gained through photosynthesis per unit of water lost), which are key traits underpinning drought tolerance in plants[27], and both values were greater (i.e. improved) in GABA fed leaves (Fig. 2d; Supplementary Fig. 2a–c).

GABA is a universal stomatal behaviour modifier. To examine whether GABA or muscimol can modulate stomatal aperture beyond the response to light and dark, we examined their impact on a range of opening and closing signals using epidermal peels of *Arabidopsis*. We found both GABA and muscimol inhibited abscisic acid- (ABA, 2.5 µM) or H_2O_2-stimulated stomatal closure and coronatine-induced opening (Supplementary Fig. 3a, c, e, f)[8,28]. However, stomatal pores were fully closed in response to high concentrations of ABA (25 µM) (Supplementary Fig. 3b, d) or exogenous calcium in the presence of GABA or muscimol (Supplementary Fig. 3g), which indicated stomatal closure could occur in epidermal peels in the presence of GABA when the closing signal was of sufficient magnitude.

We tested whether our results could be explained by GABA or muscimol treatment permanently locking guard cells in a closed (or open) state and preventing further change in stomatal pore aperture, which would argue against GABA being a physiological signal. We did this by incubating epidermal peels in GABA or

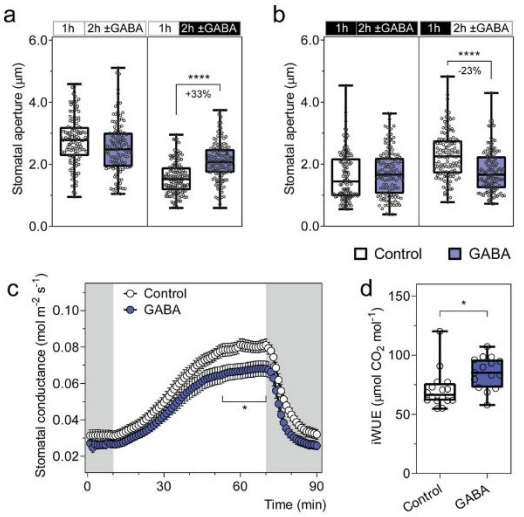

Fig. 2 Exogenous GABA antagonises changes in stomatal pore aperture and increases intrinsic water use efficiency. a, **b** Stomatal aperture of wild-type *A. thaliana* leaves in response to light or dark. Epidermal strips were pre-incubated in stomatal pore measurement buffer for 1 h under light (**a**) or dark (**b**), followed by a 2 h incubation under constant light (**a**), dark (**b**), light-to-dark transition (**a**) or dark-to-light transition (**b**) as indicated in the above graphs by the black (dark) or white (light) bars, together with the application of 2 mM GABA; $n = 129$ for control (constant light), $n = 121$ for GABA (constant light), $n = 137$ for control (light-to-dark transition) and $n = 135$ for GABA (light-to-dark transition) (**a**); $n = 122$ for control (constant dark), $n = 124$ for GABA (constant dark), $n = 123$ for control (dark-to-light transition) and $n = 130$ for GABA (dark-to-light transition) (**b**); all experiments were repeated twice in steady-state conditions (for both light or dark) or four times for dark-to-light or light-to-dark transitions in different batches of plants using blind treatments with similar results (**a**, **b**). GABA feeding of excised leaves reduces stomatal conductance (**c**) and increases intrinsic water use efficiency (iWUE) (**d**). **c** Stomatal conductance of detached leaves from 5- to 6-week-old *A. thaliana* wild-type plants was recorded using a LI-COR LI-6400XT in response to dark (shaded region) and 200 μmol m^{-2} s^{-1} light (white region), fed with artificial xylem sap solutions ± 4 mM GABA. **d** iWUE efficiency of detached leaves was calculated as the ratio of photosynthetic rate (Supplementary Fig. 2b) versus stomatal conductance (**c**); $n = 16$ independent leaves for control and $n = 15$ independent leaves for GABA, data collected from three different batches of plants (**c**, **d**). All data are plotted with box and whiskers plots: whiskers plot represents minimum and maximum values, and box plot represents second quartile, median and third quartile (**a**, **b**, **d**), or data are represented as mean ± s.e.m (**c**); statistical difference was determined by two-way ANOVA (**a**, **b**), or two-sided Student's *t* test (**c**, **d**), $^*P < 0.05$ and $^{****}P < 0.0001$.

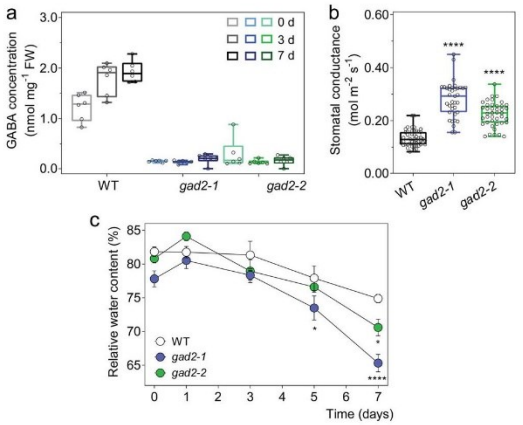

Fig. 3 Leaf GABA concentration regulates transpiration. a Leaf GABA concentration of 5–6-week-old *A. thaliana* wild-type (WT), *gad2-1* and *gad2-2* plants following drought treatment for 0, 3 and 7 days, $n = 6$. **b** Stomatal conductance of *Arabidopsis* WT, *gad2-1* and *gad2-2* plants determined using an AP4 porometer; $n = 48$ for WT, $n = 37$ for *gad2-1* and $n = 41$ for *gad2-2*, data collected from three independent batches of plants. **c** Relative leaf water content of WT, *gad2-1* and *gad2-2* plants following drought treatment for 0, 1, 3, 5 and 7 days, $n = 6$. All data are plotted with box and whiskers plots: whiskers plot represents minimum and maximum values, and box plot represents second quartile, median and third quartile (**a**, **b**), or data are represented as mean ± s.e.m (**c**); statistical difference was determined using two-way ANOVA (**a**, **c**) or one-way ANOVA (**b**); $^*P < 0.05$ and $^{****}P < 0.0001$.

muscimol, then removing this treatment and performing a light or dark transition. As would be expected from viable cells, after removal of the GABA or muscimol treatment, we found that stomatal guard cells responded to a light treatment by opening the pores (Supplementary Fig. 4a, b) or to a dark treatment by closing pores (Supplementary Fig. 4c, d). Collectively, these data again indicate that GABA signals would likely act to modulate stomatal aperture in the face of a stimulus rather than stimulating a transition itself.

To test whether GABA is a universal modulator of stomatal control, we explored whether GABA or muscimol treatment of epidermal strips attenuated stomatal responses of other plant species to light or dark transitions, including the dicot crops *Vicia faba* (broad bean), *Glycine max* (soybean) and *Nicotiana benthamiana* (tobacco-relative) and the monocot *Hordeum vulgare* (barley) (Supplementary Fig. 5). The widespread inhibition of stomatal pore aperture changes suggests that GABA has the potential to be a universal 'brake' on stomatal movement in plants, including valuable crops.

GABA accumulation in guard cells contributes to the regulation of transpiration and drought performance. Stomatal control is explicitly linked with the regulation of plant water loss, which impacts the survival of plants under drought[7]; the wider the stomatal aperture, the greater the water loss of plants, the poorer the survival of plants under a limited water supply, as excessive water use by the plant diminishes the availability of stored soil water. The observation that the stress-induced metabolite GABA[13] reduces plant water loss and improves WUE (Fig. 2d; Supplementary Fig. 2c)—key factors underpinning drought tolerance[27]—implicates GABA as novel signal regulating plant drought resilience. Therefore, to examine the hypothesis that endogenous GABA concentration increases under a water deficit and acts as a signal, we first determined whether we could replicate the previously reported increases in GABA accumulation under drought[13,14,29] (Fig. 3; Supplementary Fig. 6). In wild-type plants, a drought treatment was applied by withholding watering, which resulted in the gradual depletion of soil gravimetric water and a reduction in leaf relative water content (RWC) (Supplementary Fig. 6a, b). We found that GABA accumulation in drought stressed leaves increased by 35% compared to that of well-watered leaves (water versus drought at

7 days: 1.07 ± 0.08 versus 1.44 ± 0.11 nmol mg^{-1} FW) (Supplementary Fig. 6c).

To investigate whether GABA has a role during drought, we obtained *Arabidopsis* T-DNA insertional mutants for the major leaf GABA synthesis gene, *Glutamate Decarboxylase 2* (*GAD2*)[29]. Both *gad2-1* and *gad2-2* had >75% less GABA accumulation in leaves than in wild-type plants, whilst GABA concentrations in roots were unchanged (Fig. 3a; Supplementary Fig. 6d–f). Furthermore, leaves of *gad2* plants did not accumulate additional GABA under drought conditions unlike wild-type controls where GABA increased by 45% after 3 days, and was maintained at this elevated level after 7 days of drought (Fig. 3a). Under standard conditions, both *gad2* mutant lines exhibited greater stomatal conductance and wider stomatal pores than wild-type plants (Fig. 3b; Supplementary Fig. 6g), whereas stomatal density was identical to wild type (Supplementary Fig. 6h). The application of exogenous GABA to *gad2* leaves inhibited stomatal pore aperture changes in response to light treatments (Supplementary Fig. 6i, j), indicating that *gad2* stomata would be competent in a GABA response if sufficient GABA was present. Furthermore, the aperture of GABA pre-treated *gad2* stomata after a dark-to-light transition were statistically insignificant from non-GABA treated wild-type stomata (Supplementary Fig. 6j), which is consistent with GABA playing a role in modulating opening of wild-type stomata under non-stressed conditions. It has been shown previously that both *GAD2* transcription and GABA accumulation exhibit diurnal regulation; GABA usually peaks at the end of the dark cycle prior to stomatal opening and reaches a minimum when stomatal conductance is at its maximum near subjective mid-day[30]. However, during stress, both *GAD2* transcript abundance and GABA accumulation remain high[30]. This suggests GABA may further minimise stomatal opening under stress and contribute to drought tolerance.

Under drought, the leaf RWC of *gad2* plants lowered more quickly than in wild type (Fig. 3c). Transcriptional profiles of key ABA-marker gene (*RD22*) and GABA-related genes (other than *GAD2*) were similar in wild type and *gad2* lines, although *RD29A* was significantly higher in *gad2-1* than wild type and *gad2-2* on day 0 and day 7 of the drought treatment (Supplementary Fig. 7), which is consistent with the lower RWC of *gad2-1* after 7 days (Fig. 3c). These results confirm that *GAD2* is critical for leaf GABA production under stress, and suggests that GABA itself may regulate plant water loss and drought tolerance[29].

Histochemical staining corroborated that *GAD2* is highly expressed in leaves, particularly in guard cells[29] (Supplementary Fig. 8a, b). GAD2 is a cytosolic enzyme[31]; to examine if cytosolic GABA biosynthesis within the guard cell was sufficient to modulate transpiration we expressed—specifically in the guard cell[32]—a constitutively active form of *GAD2* (*GAD2Δ*) that has a C-terminal autoinhibitory domain removed[31,33] (Fig. 4a). This led to a large increase in leaf GABA accumulation (Fig. 4b) and to complementation of the steady-state stomatal conductance and aperture phenotypes of *gad2* plants to wild-type levels (Fig. 4c; Supplementary Fig. 8c, d). At the same time, no change in stomatal density or leaf ABA accumulation was detected under standard conditions (Supplementary Fig. 8e, f), suggesting the complementation of the *gad2* phenotype was due to the restoration of GABA synthesis in the guard cell. Other phenotypes restored to wild-type levels by guard cell-specific expression of *GAD2Δ* included the exaggerated stomatal opening and closure kinetics and decreased instantaneous iWUE/WUE of *gad2-1* (Fig. 4d–f; Supplementary Fig. 8g–i). The drought sensitivity of *gad2*, compared to wild type, was also abolished by guard cell-specific expression of *GAD2Δ* (Fig. 4g, h). This demonstrates GABA synthesis in guard cells was sufficient to modulate stomatal movement, regulate water loss and improve drought resilience.

To examine whether GABA metabolism can be modulated to improve drought resilience beyond wild-type levels, *GAD2Δ* was expressed specifically in the guard cells of wild-type *Arabidopsis* plants (Fig. 5a), this resulted in leaf GABA concentrations being increased to beyond wild-type levels (Fig. 5b). The steady-state stomatal conductance of the GABA overproducing transgenic plants in standard and drought conditions was lowered compared to wild-type plants (Fig. 5c). Consistent with this, the plants overexpressing *GAD2Δ* in the wild-type background maintained higher leaf RWC than wild-type plants after 10 days of drought treatment (Fig. 5d, e). Furthermore, a greater percentage of plants overexpressing *GAD2Δ* in the wild-type background survived following re-watering after a 12-day drought treatment (Supplementary Fig. 9). As such, we show here that GABA overproduction can reduce water loss and improve drought resilience.

Guard cell cytosolic GABA modulates stomatal movement and drought resilience. Our data show that although guard cell synthesised GABA can rescue the *gad2* phenotype, it is clear that exogenously applied GABA can also modulate stomatal movement (e.g. Fig. 2 for wild type or Supplementary Fig. 6i, j for *gad2*). It is known that GABA can pass the membrane through a variety of transporters[34–36], so it is unclear whether the site of guard cell GABA action is from the apoplast or cytoplasm. We expressed *GAD2Δ* specifically in the spongy mesophyll[37], adjacent to the abaxial stomatal layer, to test whether it could complement *gad2* (Supplementary Fig. 10a, b). This resulted in a significant increase in leaf GABA, but no change in stomatal conductance (Supplementary Fig. 10c, d). As such, unlike guard cell-specific expression, *GAD2Δ* in the spongy mesophyll was insufficient to complement the *gad2-1* phenotype.

To further probe the role of guard cell synthesised GABA, we expressed full-length *GAD2* under the guard cell-specific promoter (*gad2-1/GC1::GAD2*) (Supplementary Fig. 11a). This form of GAD2 requires activation by Ca^{2+}/calmodulin or low pH to synthesise GABA[14]. Interestingly, guard cell-specific expression of full-length *GAD2* failed to complement the high stomatal conductance of the *gad2-1* line to wild-type levels under standard conditions, whereas its constitutive expression (driven by pro35S-CAMV) did (Supplementary Fig. 11b, f, g). Under drought, the *gad2-1/GC1::GAD2* lines increased GABA production, reduced their stomatal conductance significantly more than that of *gad2-1* plants and had a comparable leaf RWC to wild-type plants following 5 days of drought (Supplementary Fig. 11c–e). This suggests that activation of full-length GAD2 via its regulatory domain[31] is important in stimulating GABA production under drought in guard cells.

We extended our investigation of GABA's site of action through an epidermal peel experiment. We compared the effects of exogenously applied muscimol or muscimol-BODIPY, a muscimol molecule conjugated with a BODIPY fluorophore, which is active against GABA targets in plants and animals, but lacks cell-membrane permeability[38,39]. We found that unlike muscimol, membrane impermeable muscimol-BODIPY was unable to inhibit stomatal opening or closure (Supplementary Fig. 12). This result—alongside the differential effects of *gad2* complementation by full-length *GAD2* when expressed constitutively or solely in the guard cell (Supplementary Fig. 11a–e)—provides further evidence that GABA is likely to pass the plasma membrane and that it acts from the cytosol, consistent with our feeding assays (e.g. Fig. 2c). Collectively, the data in this section demonstrate that guard cell-specific cytosolic GABA accumulation is sufficient and necessary for controlling stomatal aperture and transpiration under drought, but suggests a role for other cell types in fine-tuning GABA signals under standard conditions.

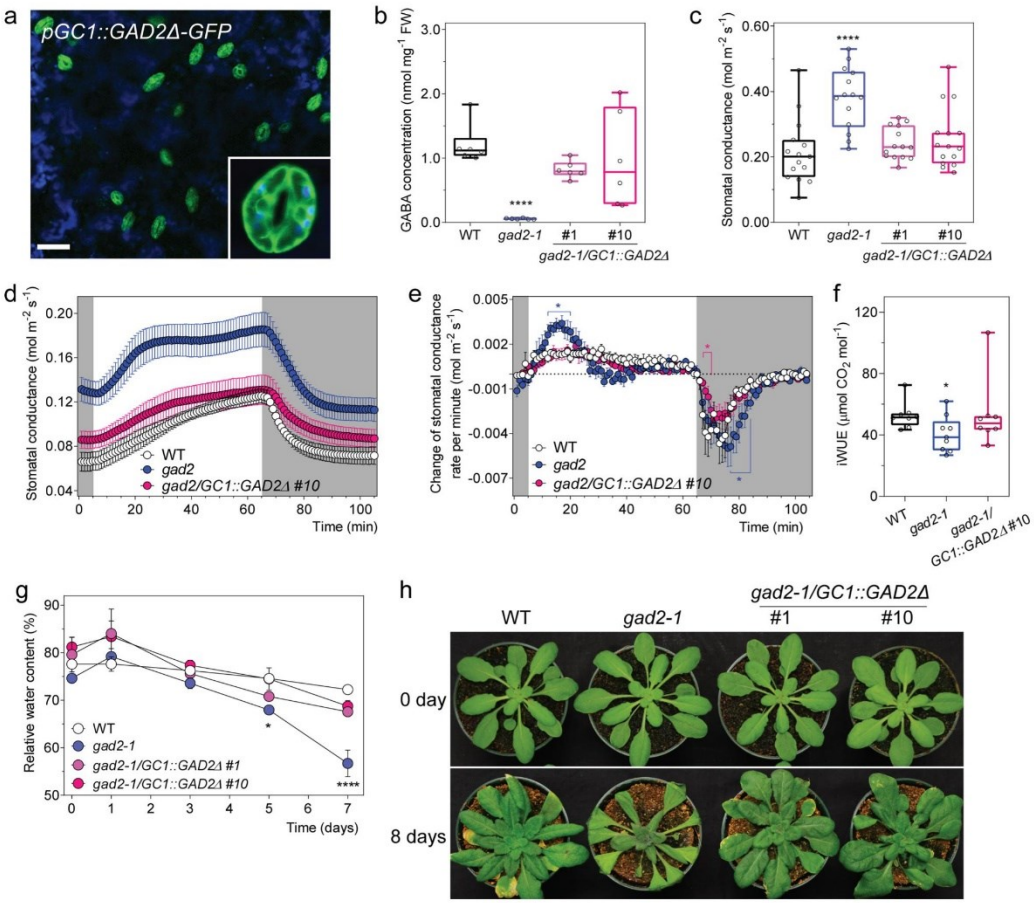

Fig. 4 Guard cell GABA regulates water loss and drought tolerance. a Representative confocal images of *gad2*-1 plants expressing *GC1::GAD2Δ-GFP* (*gad2-1/GC1::GAD2Δ-GFP*); GFP fluorescence and chlorophyll autofluorescence (blue) of the leaf abaxial side of 3–4-week-old *gad2-1/GC1::GAD2Δ-GFP* plant indicates that the *GC1* promoter drives *GAD2Δ* expression specifically in guard cells, similar pattern images are obtained from multiple *gad2-1/GC1::GAD2Δ-GFP* plants, scale bars = 50 μm. **b** Leaf GABA accumulation of 5–6-week-old *A. thaliana* WT, *gad2-1*, *gad2-1/GC1::GAD2Δ* #1 and #10 plants grown under control conditions, $n = 6$. **c** Stomatal conductance of WT ($n = 15$), *gad2-1* ($n = 14$), *gad2-1/GC1::GAD2Δ* #1 ($n = 14$) and #10 ($n = 15$) plants under control conditions determined using an AP4 porometer, data collected from two independent batches of plants. **d** Stomatal conductance of WT, *gad2-1* and *gad2-1/GC1::GAD2Δ* #10 plants in response to dark (shaded region) and 150 μmol m^{-2} s^{-1} light (white region), measured using a LI-COR LI-6400XT. **e** Change in stomatal conductance each minute calculated using dConductance/dt (min) of the data represented in **d**. **f** iWUE of WT, *gad2-1* and *gad2-1/GC1::GAD2Δ* plants was calculated based on the ratio of photosynthetic rate (Supplementary Fig. 8h) versus stomatal conductance represented in **d**; $n = 8$ individual plants for WT, $n = 9$ for *gad2-1* and $n = 8$ for *gad2-1/GC1::GAD2Δ* #10, data collected from two independent batches of plants (**d**–**f**). **g** Relative leaf water content of WT, *gad2-1*, *gad2-1/GC1::GAD2Δ* #1 and #10 plants following drought treatment for 0, 1, 3, 5 and 7 days; $n = 4$ for 0, 1, 3 and 5 days samples and $n = 5$ for 7 days samples, except that $n = 3$ for 0-day *gad2-1* and 1-day *gad2-1/GC1::GAD2Δ* #1. **h** Representative images of WT, *gad2-1*, *gad2-1/GC1::GAD2Δ* #1 and #10 plants (shown in **i**) before (0 day) and after (8 days) drought treatment as indicated. All data are plotted with box and whiskers plots: whiskers plot represents minimum and maximum values, and box plot represents second quartile, median and third quartile (**b**, **c**, **f**), or data are represented as mean ± s.e.m (**d**, **e**, **g**); statistical difference was determined using by two-sided Student's *t* test (**f**), one-way ANOVA (**b**, **c**) or two-way ANOVA (**e**, **g**); $^{*}P < 0.05$ and $^{****}P < 0.0001$.

GABA signalling regulating WUE and drought resilience is ALMT9 dependent. ALMTs are plant-specific anion channels that share no homology to Cys-loop receptors except a region of 12 amino acid residues predicted to bind GABA in $GABA_A$ receptors[14,18]. In animals, ionotropic GABA receptors are stimulated by GABA; in contrast, anion currents through ALMTs are inhibited by GABA[10,11]. There are a number of *ALMT*s expressed in guard cells that contain the putative GABA binding motif and have the potential to transduce the GABA signal, with most having been shown to have a role in regulating stomatal movement[20–22,40]. For instance, ALMT12 (also called QUAC1, quickly-activation anion conductance 1) is a plasma membrane localised anion channel, which moves anions out of the guard cell during guard cell closure[20].

Under the conditions tested here, the impact of GABA on stomatal closure appears to be limited to epidermal peels, it is not

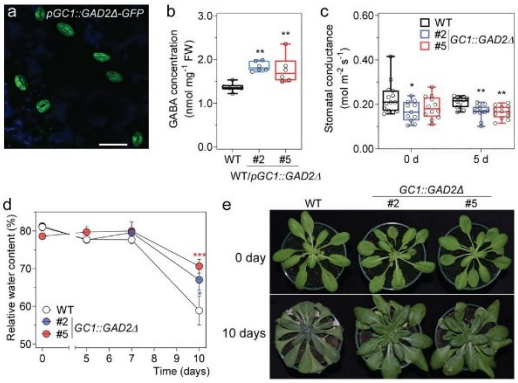

Fig. 5 Guard cell overexpression of *GAD2Δ* decreases plant water loss and increases drought survival. a Representative confocal images of *A. thaliana* wild-type plants expressing *GC1::GAD2Δ-GFP*; GFP fluorescence and chlorophyll autofluorescence (blue) of the leaf abaxial side of 3–4-week-old plants, similar pattern images are obtained from multiple wild-type plants expressing *GC1::GAD2Δ-GFP* plants, scale bars = 50 µm. **b** GABA accumulation in the leaves of 5–6-week-old *Arabidopsis* wild type, *GC1::GAD2Δ* #2 and #5 plants; $n = 6$. **c** Stomatal conductance of WT, wild-type *Arabidopsis* expressing *GAD2Δ* in the guard cells using the *GC1* promoter—*GC1::GAD2Δ* #2 and #5 plants before (0 day) and after (5 days) drought treatment determined using an AP4 porometer; $n = 14$ for WT, $n = 11$ for *GC1::GAD2Δ* #2 and $n = 15$ for *GC1::GAD2Δ* #2 at 0 day and $n = 12$ for WT, *GC1::GAD2Δ* #2 and #5 at 5 days. **d** Relative leaf water content of WT, *GC1::GAD2Δ* #2 and #5 plants following drought treatment for 0, 5, 7 and 10 days; $n = 6$ for 0 and 5 days all samples, except $n = 18$ for WT at 10 days, $n = 12$ for *GC1::GAD2Δ* #2 at 10 days and $n = 13$ for *GC1::GAD2Δ* #5 at 10 days. **e** Representative images of WT, *GC1::GAD2Δ* #2 and #5 plants before (0 day) and after (10 days) drought treatment as indicated. Pot size 2.5 inch diameter × 2.25 inch height (LI-COR). All data are plotted with box and whiskers plots: whiskers plot represents minimum and maximum values, and box plot represents second quartile, median and third quartile (**b**, **c**), or data are represented as mean ± s.e.m (**d**); statistical difference was determined using one-way ANOVA (**b**, **c**) or two-way ANOVA (**d**); $^*P < 0.05$, $^{**}P < 0.01$ and $^{***}P < 0.001$.

seen in intact leaves. However, epidermal peels still represent an assay system that can be used to test whether ALMT might transduce the inhibitory effect of GABA on closure. We observed that, unlike wild-type plants, stomatal closure in *almt12* knockouts was insensitive to GABA or muscimol when transitioning from light-to-dark (Supplementary Fig. 13a). In contrast, stomatal opening of *almt12* lines showed wild-type-like sensitivity to GABA or muscimol when transitioning from dark to light (Supplementary Fig. 13b). These data indicate that ALMT12 is a plasma membrane GABA target that affects stomatal closure in response to dark—in epidermal peels at least.

However, if GABA inhibition of ALMT12/QUAC1 played a significant role during drought, then the resulting inhibition of closure would translate into an increase in water loss compared to wild-type plants during closure. As we found no evidence that GABA had an effect on closure in intact leaves, under a light-to-dark transition as measured by stomatal conductance or transpiration (Fig. 2c; Supplementary Fig. 2a), and the fact that GABA accumulation led to a net decrease in water loss and improvement in drought resilience, ALMT12 is unlikely to be a major target contributing to this outcome. We therefore focused on tonoplast-localised ALMTs that are involved in stomatal pore opening[21], as this is the process where GABA has its predominant affect in intact leaves.

ALMT9 is the major tonoplast-localised channel involved in anion uptake into guard cell vacuoles during stomatal opening, but has no documented role in closure[21]. We hypothesised that GABA might target and inhibit ALMT9 activity to reduce the rate or extent of stomatal opening. We initially attempted in vitro electophysiological studies to examine the impact of GABA on ALMT9-induced currents, but were unable to consistently detect stable currents following heterologous expression in either *Xenopus laevis* oocytes or tobacco mesophyll cells[21,41]. Therefore, we examined the potential regulation of ALMT9 by GABA by focusing solely on in planta studies as it is difficult to faithfully replicate regulatory pathways from guard cells in heterologous systems, e.g.[42–47]. In the first instance, we independently crossed two *almt9* alleles (*almt9-1* and *almt9-2*) with *gad2-1*. We found that, similar to *gad2*, both double mutants (*gad2-1/almt9-1* and *gad2-1/almt9-2*) maintained low GABA accumulation in their leaves (Fig. 6a, b; Supplementary Fig. 14a, e). However, both *gad2-1/almt9-1* and *gad2-1/almt9-2* had wild-type-like stomatal conductance and aperture unlike *gad2-1* where both these parameters are high (Fig. 6c, d; Supplementary Fig. 14d, f). Furthermore, guard cell-specific complementation of *gad2-1/almt9-1* by *GAD2Δ* did not alter stomatal conductance (Supplementary Fig. 14a–d). Collectively, these data are consistent with ALMT9 being required for GABA to regulate gas exchange via stomatal control. An interesting additional observation was that the loss of *ALMT9* in *gad2-1* also resulted in ABA inducing stomatal pore closure to wild-type levels (Supplementary Fig. 14g–j), indicating that, although ALMT9 is a channel that regulates stomatal opening, it can influence the extent to which stomatal pores close under certain conditions (in epidermal peels at least). The incomplete stomatal closure of *gad2* coupled to its greater stomatal opening may further contribute to its drought sensitivity. These findings are consistent with the regulation of stomatal aperture being a dynamic equilibrium between the pathways that regulate stomatal opening and closure, with stomatal aperture being weighted towards a particular state dependent upon the dominant stimuli[48,49].

To further test whether ALMT9 transduces GABA signalling, we examined the effect of GABA on regulating stomatal opening in *almt9* mutant plants. In wild-type plants, we previously showed that light-induced stomatal opening was inhibited by exogenous GABA (Fig. 2a) or muscimol (Supplementary Fig. 1a). In *almt9* lines, exogenous GABA or muscimol did not antagonise stomatal opening (Fig. 7a, b; Supplementary Fig. 15a, b), whereas dark-induced stomatal closure in *almt9* retained its GABA sensitivity (Fig. 7c, d; Supplementary Fig. 15c, d). These results are consistent with GABA reducing stomatal opening via negative regulation ALMT9-mediated Cl^- uptake into guard cell vacuoles. Furthermore, it strongly indicates the corollary of this finding, that the higher stomatal conductance phenotype of *gad2* is the result of greater ALMT9 activity due to its lack of inhibition by GABA.

We tested this hypothesis by attempting to complement *almt9* plants with either the native channel or a site-directed ALMT9 mutant ($ALMT9^{F243C/Y245C}$). The mutations within $ALMT9^{F243C/Y245C}$ are in the 12 amino acid residue motif that shares homology with a GABA binding region in mammalian $GABA_A$ receptors[14,18]. Mutations in the aromatic amino acid residues in this motif have been shown for other ALMTs to result in active channels that are not inhibited by GABA when tested in heterologous systems[36,39] (Fig. 8; Fig. 9). However, no in planta tests have been conducted to date—for any ALMT—to determine whether mutations in this region result in a transport competent protein that lacks GABA sensitivity. Here, we observed that *ALMT9* and $ALMT9^{F243C/Y245C}$ had similar

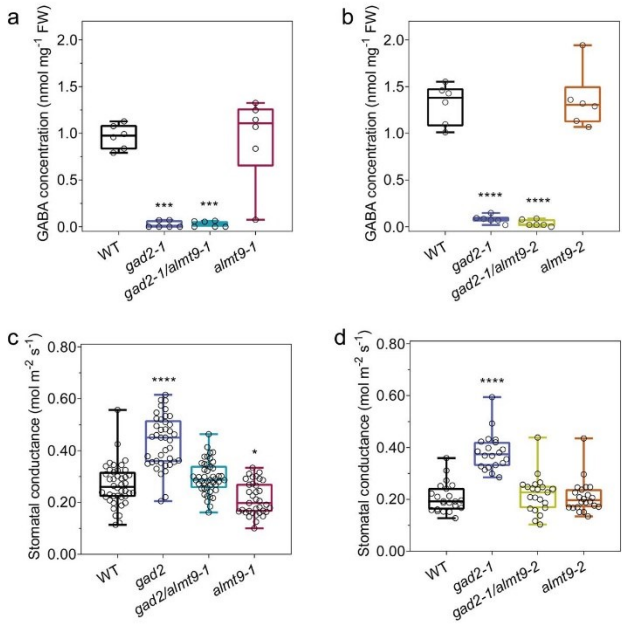

Fig. 6 The loss of ALMT9 suppresses the *gad2* mutant stomatal phenotype. a–d Leaf GABA concentration (**a**, **b**) and stomatal conductance (**c**, **d**) of 5–6-week-old *A. thaliana* WT, *gad2-1*, *gad2-1/almt9-1*, *almt9-1*, *gad2-1/almt9-2* and *almt9-2* plants; $n = 6$ plants (**a**, **b**); $n = 42$ for WT, $n = 40$ for *gad2-1*, $n = 45$ for *gad2-1/almt9-1* and $n = 35$ for *almt9-1*, data collected from four independent batches of plants (**c**); $n = 22$ for WT, $n = 20$ for *gad2-1*, $n = 21$ for *gad2-1/almt9-2* and $n = 22$ for *almt9-2*, data collected from two independent batches of plants (**d**); data (**a**, **c**) were extracted respectively from Supplementary Fig. 13b, c. All data are plotted with box and whiskers plots: whiskers plot represents minimum and maximum values, and box plot represents second quartile, median and third quartile; statistical difference was determined by one-way ANOVA, $^{*}P < 0.05$, $^{***}P < 0.001$ and $^{****}P < 0.0001$.

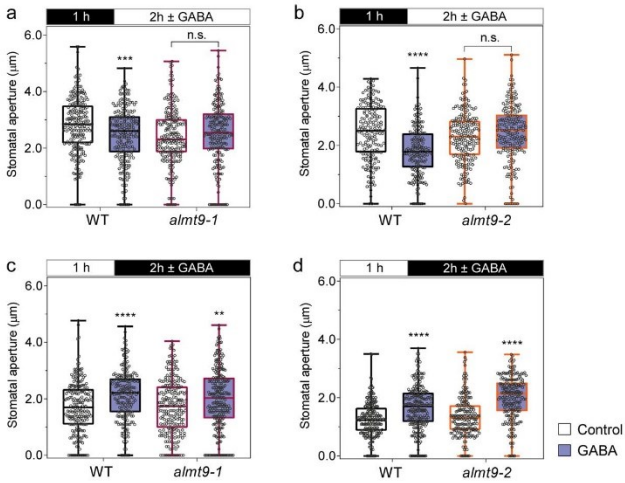

Fig. 7 The loss of *ALMT9* abolishes GABA inhibition of stomatal opening but does not affect closure. a–d *Arabidopsis* WT and *almt9* knockout plant stomatal aperture in response to light or dark. Epidermal strips were pre-incubated in stomatal measurement buffer for 1 h under dark (**a**, **b**) or light (**c**, **d**), followed by 2 h in light (**a**, **b**) or dark (**c**, **d**) as indicated by black (dark) or white (light) bars above graphs with ±2 mM GABA; $n = 236$ for WT and $n = 221$ for *almt9-1* with control treatment, $n = 229$ for WT and $n = 215$ for *almt9-1* with GABA treatment (**a**); $n = 223$ for WT and $n = 242$ for *almt9-1* with control treatment, $n = 215$ for WT and $n = 256$ for *almt9-1* with GABA treatment (**b**); $n = 183$ for WT and $n = 189$ for *almt9-2* with control treatment, $n = 210$ for WT and $n = 197$ for *almt9-2* with GABA treatment (**c**); $n = 236$ for WT and $n = 243$ for *almt9-2* with control treatment, $n = 202$ for WT and $n = 220$ for *almt9-2* with GABA treatment (**d**). All data are plotted with box and whiskers plots: whiskers plot represents minimum and maximum values, and box plot represents second quartile, median and third quartile; statistical difference was determined by two-way ANOVA, $^{**}P < 0.01$, $^{***}P < 0.001$ and $^{****}P < 0.0001$.

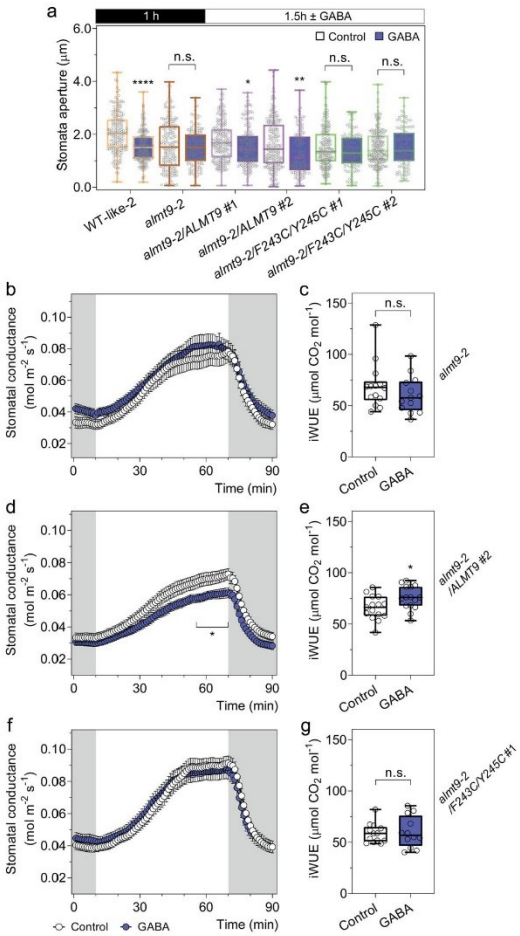

Fig. 8 *ALMT9* but not *ALMT9*$^{F243C/Y245C}$ restores the GABA sensitivity of *almt9-2*. a Stomatal aperture measurement of *A. thaliana* WT, *almt9-2* and complementation lines. Epidermal strips were pre-incubated in stomatal measurement buffer for 1 h under dark, followed by a 1.5 h dark-to-light transition, as indicated above graphs by black (dark) or white (light) bars, ±2 mM GABA; $n = 189$ (control) and $n = 195$ (GABA) for WT-like 2 (segregated from *almt9-2*)[21], $n = 197$ (control) and $n = 153$ (GABA) for *almt9-2*, $n = 213$ (control) and $n = 178$ (GABA) for *almt9-2* complement with *35S::ALMT9* #1 (*almt9-2/ALMT9* #1), $n = 219$ (control) and $n = 127$ (GABA) for *almt9-2/ALMT9* #2, $n = 195$ (control) and $n = 115$ (GABA) for *almt9-2* complemented with *35S::ALMT9* with double mutation F243C/Y245C (*ALMT9*$^{F243C/Y245C}$) targeting the putative GABA interaction residues[18,36,39] (*almt9-2*/F243C/Y245C #1), $n = 221$ (control) and $n = 109$ (GABA) for *almt9-2*/F243C/Y245C #2 with control treatment. **b–g** Leaf feeding assay of *almt9-2* and complementation lines. Stomatal conductance of detached leaves from 5–6-week-old *Arabidopsis almt9-2*, *almt9-2/ALMT9* #2 and *almt9-2*/F243C/Y245C #1 plants was recorded using a LI-COR LI-6400XT in response to dark (shaded region) and 200 μmol m^{-2} s^{-1} light (white region), fed with artificial xylem sap solutions ± 4 mM GABA (**b**, **d**, **f**). The iWUE of *almt9-2* (**c**), *almt9-2/ALMT9* #2 (**e**) and *almt9-2*/F243C/Y245C #1 (**g**) detached leaves was calculated based on the ratio of photosynthetic rate (Supplementary Fig. 17b, e, h) versus stomatal conductance (**b**, **d**, **f**); $n = 14$ (control) and $n = 13$ (GABA) for *almt9-2* (**b**, **c**); $n = 15$ (control and GABA) for *almt9-2/ALMT9* #2 (**d**, **e**); $n = 13$ (control) and $n = 12$ (GABA) for *almt9-2*/F243C/Y245C #1 (**f**, **g**). All data are plotted with box and whiskers plots: whiskers plot represents minimum and maximum values, and box plot represents second quartile, median and third quartile (**a**, **c**, **e**, **g**), or data are represented as mean ± s.e.m (**b**, **d**, **f**); statistical difference was determined by two-sided Student's *t* test; $^*P < 0.05$, $^{**}P < 0.01$, $^{****}P < 0.0001$ (**a**–**g**).

expression in *almt9-2* complementation lines and the mutations (in ALMT9$^{F243C/Y245C}$) did not alter the membrane localisation with both versions of the ALMT9 protein being clearly present on the tonoplast (Supplementary Fig. 16). Further, we found that similar to *almt9* lines, *almt9-2* expressing *ALMT9*$^{F243C/Y245C}$ was insensitive to GABA during a dark-to-light transition assayed on epidermal peels and detached leaves, for stomatal opening and stomatal conductance, respectively; this contrasts the GABA sensitivity of wild-type plants and plants expressing native *ALMT9* in the *almt9-2* background (Figs. 2c and 8a, b, d, f; Supplementary Fig. 17a, b, d, e, g, h). Furthermore, instantaneous iWUE/WUE of *almt9-2* was improved by native *ALMT9* complementation, but not *ALMT9*$^{F243C/Y245C}$ (Fig. 8c, e, g; Supplementary Fig. 17c, f, i). Steady-state stomatal conductance and aperture of *ALMT9*$^{F243C/Y245C}$ lines were also significantly greater than that of wild-type and *almt9* lines and were insignificant from *gad2-1* under standard conditions (Fig. 9; Supplementary Fig. 17j). This result indicates that we successfully complemented *almt9* with an active, but GABA-insensitive form of ALMT9, and that this increased transpirational water loss over wild-

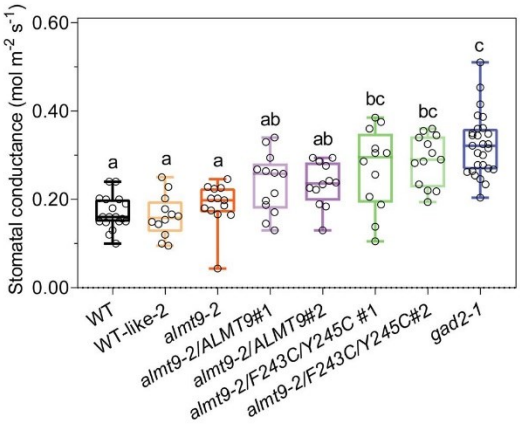

Fig. 9 *ALMT9*$^{F243C/Y245C}$ increases steady-state stomatal conductance. Stomatal conductance of 5–6-week-old *Arabidopsis* WT, *gad2-1*, *almt9-2* and complementation lines determined using an AP4 Porometer; $n = 18$ for WT, $n = 12$ for WT-like 2, *almt9-2/ALMT9* #2 and *almt9-2*/F243C/Y245C #1, $n = 13$ for *almt9-2*, *almt9-2/ALMT9* #1 and *almt9-2*/F243C/Y245C #2, $n = 27$ for *gad2-1*. All data are plotted with box and whiskers plots: whiskers plot represents minimum and maximum values, and box plot represents second quartile, median and third quartile; statistical difference was determined by one-way ANOVA, the letters a, b and c represent data groups that are not statistically different, $P < 0.05$.

type levels. These data are completely consistent with ALMT9 being a GABA target that regulates plant water loss, even under non-stressed conditions, through modulation of ALMT9 activity. The GABA effect is then amplified under a water deficit when GABA concentration increases. We propose that GABA accumulation has a role in promoting drought resilience by reducing the amplitude of stomatal re-opening each morning, which minimises whole plant water loss. As such, the GABA–ALMT pathway is a strong candidate for constituting the ABA-independent stress memory of a decreased soil water status that has been previously proposed without mechanistic attribution[50,51].

Discussion

The data in this manuscript have unveiled a GABA signalling pathway in plants, which can be summarised by the simplified models presented in Fig. 10. We propose that cytosolic GABA signals, generated by GAD2, modulate stomatal opening, WUE and drought resilience transduced through negative regulation of ALMT9 activity (Fig. 10).

Collectively our use of leaf feeding, knockouts, complementation and point mutagenesis strongly suggests ALMT9 is an essential and major component transducing GABA signalling in guard cells during well-watered and drought conditions. As has become evident for other guard cell based signalling pathways through their examination over time[42–47], we are cognizant of the potential that other GABA response elements, including other ALMT, may be involved in transducing and fine-tuning this signalling pathway. Our finding that GABA does not impact stomatal closure in epidermal peels of *almt12* knockouts infers a potential role for this plasma membrane localised ALMT12 in transducing guard cell GABA signals. The fact that light-induced stomatal opening and dark-induced stomatal closure was completely GABA insensitive in *almt9xalmt12* knockouts (Supplementary Fig. 18) suggests that both channels have the potential to transduce the major effects of GABA in guard cells.

However, it is interesting that GABA inhibition of stomatal opening was consistently seen between epidermal peel assays and leaf feeding, whilst GABA only inhibited stomatal closure during isolated epidermal peel experiments, but not when it was fed to leaves. This suggests that GABA acts through ALMT12 on processes associated with stomatal closure, but in the context of an intact leaf this phenotype is lost, which is likely due to the loss of functional epidermal and/or mesophyll cells. This is consistent with the growing body of evidence that indicates stomatal aperture experiments on isolated epidermal peels require validation via studies on intact leaves to avoid overinterpreting potential artifacts from this reductionist system. However, it also means we cannot fully rule out whether GABA inhibition of stomatal closure does have a role under certain physiological scenarios that are yet to be identified. Therefore, in future studies, it would be pertinent to examine whether ALMT12-dependent GABA inhibition of stomatal closure has a physiological role in transducing GABA signals in conditions not examined here, and, more broadly, whether other ALMTs or additional elements are involved in GABA signal transduction.

ALMT activity appears to be regulated by a suite of factors including anions, (Al^{3+} for ALMT1), pH, ATP, voltage and GABA[52]. As such, it is becoming clear that ALMTs have the potential to act as a key signalling hub in a variety of physiological processes. Following on from this study, leading on from the observed GABA modulation of ABA, H_2O_2 and coronatine effects on stomata, the investigation into cross-talk between GABA and other signals for ALMT9, in particular, and ALMTs, in general, provides the basis for future research areas. Such studies will be able to resolve questions such as 'whether GABA can act directly on guard cell ALMTs?', as appears to occur for wheat ALMT1[18,39], or 'whether other signalling intermediates are also involved?'. GABA inhibition of the wheat ALMT1 anion conductance was recently found to occur from the cytosol only, by reducing the open probability of the channel to anions[39]. However, that study was unable to determine whether this occurred through permeation of uncharged GABA through the ALMT

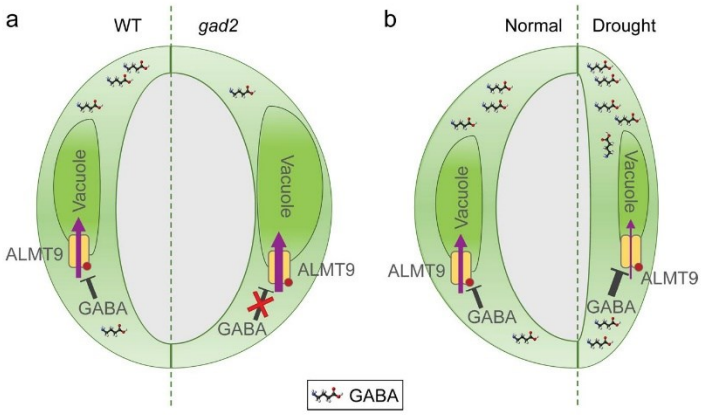

Fig. 10 Proposed model of GABA-mediated signalling for the regulation of water use efficiency. a Cytosolic guard cell GABA negatively regulates ALMT9-mediated anion uptake into guard cell vacuoles, which fine tunes stomatal opening (left guard cell of pair). Depletion of GABA accumulation in the leaves of *GAD2* loss-of-function mutant (*gad2*) de-regulates ALMT9, maximizing anion uptake and accumulation in guard cell vacuoles. This leads to a more open stomatal pore, greater water loss and lower WUE of plants (right guard cell of pair). This stomatal phenotype can be replicated by replacing F243/Y245 (red dot) with two cysteines, which abolishes GABA sensitivity of ALMT9. **b** Leaf GABA synthesized and accumulated during water deficit reduces ALMT9-mediated vacuolar anion uptake into guard cells, which requires amino acid residues F243/Y245 (red dot) (right guard cell of pair). This reduces stomatal opening, reducing the pore aperture and enhances plant WUE under drought stress compared to guard cells under standard conditions in the light (left guard cell of pair). Note: We have excluded ALMT12 from this model as we did not find a role for this protein in GABA modulation of water use efficiency in planta, despite its role in GABA modulation of stomatal aperture found within epidermal peels.

pore or through GABA binding modifying channel structure[39]. Cytosolic GABA inhibition was dependent upon the putative GABA binding residue F213 (equivalent to F243 in ALMT9, which is also predicted to face the cytosol)[39,53]. Our study therefore highlights the real need to definitively determine whether GABA binds to ALMTs or whether the identified amino acid residues affect GABA sensitivity independent of anion permeability through other means. For instance, future studies should address whether GABA permeability of ALMTs has a role in signal transduction in guard cells and the regulation of other physiological processes[36]. These later questions would be aided by the determination of GABA concentrations in different cell types and compartments to further understand the co-ordination of GABA signalling across membranes, leaves and other organs, and this could be achieved through the deployment of novel GABA sensors, as recently used in animal tissues[54,55].

GABA concentration oscillates over diel cycles and increases in response to multiple abiotic and biotic stresses including drought, heat, cold, anoxia, wounding pathogen infection and salinity[13]. ALMTs have been implicated in modulating multiple developmental and physiological processes in plants[20–22,56–58] including those underpinning nutrient uptake and fertilization that are affected by GABA[18,59,60]. Therefore, the discovery that GABA regulates ALMT to form a physiologically relevant signalling mechanism in guard cells is likely to have broad significance beyond stomata, particularly during plant responses to environmental transitions and stress.

GABA's effect on stomata appears to be conserved across a large range of crops from diverse clades including important monocot and dicot crops (Supplementary Fig. 5), indicating that GABA may well be a stomatal signal of economic significance. As we find that the genetic manipulation of cell-type specific GABA metabolism can reduce water loss leading to improved drought performance, our work opens up alternative ways for manipulating crop stress resilience. This statement is tempered in the knowledge that GABA modulated stomatal signalling in the face of another signal and did not stimulate changes in stomatal aperture itself. GABA's role appears to be that of fine-tuning stomatal aperture. Our data suggest that GABA modulated stomatal movement occurs in response to light and dark and low concentrations of signal intermediates, but in the face of a strong stress stimulus its affects may be overridden. As such, GABA may well provide a direct link between the metabolic status of the cell —GABA being produced in the cytosol in times of stress as a bypass of several reactions of the TCA cycle—to regulate and sustain a certain physiological process prior to it being shut down via a more severe stress response pathway. More broadly, this study also provides proof that GABA is a plant signalling molecule and not just a plant metabolite[12,16], and in so doing, we conclude that GABA is an endogenous signalling molecule beyond the animal and bacterial kingdoms, enacted through distinct and organism specific mechanisms.

Methods

Plant materials and growth conditions. All experiments were performed on *A. thaliana* were in the Columbia-0 (Col-0) ecotype background, unless stated. *Arabidopsis* wild type, T-DNA insertion mutant and other transgenic plants were germinated and grown on ½ Murashige and Skoog (MS) medium with 0.8% phytagel for 10 days before being transferred to soil for growth in short-day conditions (100–120 μmol m^{-2} s^{-1}, 10 h light/14 h dark) at 22 °C. The T-DNA insertion mutant *gad2-1* (GABI_474_E05) and *gad2-2* (SALK_028819) were obtained from the Arabidopsis Biological Resource Centre (ABRC). *gad2-1* was selected using primer sets:

gad2_LP1 (5′-TATCACGCTAACACCTAACGC-3′), gad2_RP1 (5′-TTCAAGGTTTGTCGGTATTGG-3′) and GABI_LB (5′-GGGCTACAC TGAATTGGTAGCTC-3′) for removing the second T-DNA insert; gad2_LP2 (5′-ACGTGATGGATCCAGACAAAG-3′), gad2_RP2 (5′-TCTTCATTTCCAC ACAAAGGC-3′) and GABI_LB for isolation of the *GAD2* (At1g65960) T-DNA insertion. *gad2-2* was selected using primer sets: gad2-2_LP (5′-AGTTGTATGAA AGTTCATGTGGC-3′), gad2-2_RP (5′-TCGACCACGAGATTTTAATGG -3′) and SALK_LB (5′-ATTTTGCCGATTTCGGAAC-3′). *almt9-1* (SALK_055490), *almt9-2* (WiscDsLox499H09)), *almt12-1* (SM_3_38592) and *almt12-2* (SM_3_1713) were selected as described previously[20,21]. The double mutant lines *gad2-1/almt9-1*, *gad2-1/almt9-2*, *almt9-2/12-1* and *almt9-2/12-2* were obtained, respectively, from crossing the respective mutants. The mesophyll enhancer-trap line JR11-2 in the Col-0 background was kindly provided by K. Baerenfaller (ETH Zurich)[61]. JR11-2 (Col-0) and *gad2-1*/JR11-2 were segregated from crossing *gad2-1* with JR11-2. JR11-2 was selected using primer sets: JR11-2_LP (5′-TTATTTAGGG AAATTACAAGTTGC-3′), JR11-2_RP (5′-AGACACATTTAATAACATTACAAC AAA-3′) and JR11-2_LB (5′-GTTGTCTAAGCGTCAATTTGTTT-3′)[62]. All experiments were performed on stable T_3 transgenic plants or confirmed homozygous mutant lines. The other plants *V. faba*, *N. benthamiana* and *G. max* were grown in soil in long-day conditions (400 μmol m^{-2} s^{-1}, 16 h light/8 h dark, 28 °C/25 °C). *H. vulgare* (barley) cv. Barke was grown in a hydroponic system with half-strength Hoagland's solution in long-day conditions (150 μmol m^{-2} s^{-1}, 16 h light/8 h dark, 23 °C)[63].

Gene cloning and plasmid construction. For guard cell-specific complementation, the constitutively active form of *GAD2* with a truncation of the calmodulin binding domain (*GAD2Δ*)[31,33] and the full-length *GAD2* coding sequence (*GAD2*) was driven by a guard cell-specific promoter *GC1* (−1140/+23)[32], as designated *GC1::GAD2Δ* and *GC1::GAD2*, respectively. PCR reactions first amplified the truncated *GAD2Δ* with a stop codon and *GC1* promoter (*GC1*) separately using Phusion® High-Fidelity DNA Polymerase (New England Biolabs) with the primer sets: GAD2_forward (5′-CACTACTCAAGAAATATGGTTTTGACAAAAACC GC-3′) and GAD2_truncated_reverse (5′-TTATACATTTTCCGCGATCCC-3′); GC1_forward (5′-CACCATGGTTGCAACAGAGAGGATG-3′) and GC1_reverse (5′-ATTTCTTGAGTAGTGATTTTGAAG-3′). This was followed by an overlap PCR to fuse the *GC1* promoter to *GAD2Δ* (*GC1::GAD2Δ*) with the GC1_forward and GAD2_truncated_reverse primer set. The same strategy was used to amplify *GC1::GAD2Δ* without a stop codon (*GC1::GAD2Δ-stop*), *GC1::GAD2* and *GC1::GAD2* without a stop codon (*GC1::GAD2-stop*) with different primer sets: (1) *GC1::GAD2Δ-stop* amplified with GAD2_forward and GAD2_truncated-stop_reverse (5′-TACATTTTCCGCGATCCCT-3′); (2) *GC1::GAD2* amplified with GAD2_forward and GAD2_reverse (5′-TTAGCACACACCATTCATCTTCTT-3′) and (3) *GC1::GAD2-stop* amplified with GAD2_forward and GAD2-stop_reverse (5′-CACACCATTCATCTTCTTCC-3′). The fused PCR products were cloned into the pENTR/D-TOPO vector via directional cloning (Invitrogen). pENTR/D-TOPO vectors containing *GC1::GAD2Δ* or *GC1::GAD2* were recombined into a binary vector pMDC99[64] by an LR reaction using LR Clonase II Enzyme mix (Invitrogen) for guard cell-specific complementation, after an insertion of a NOS Terminator into this vector. A pMDC99 vector was cut by *Pac*I (New England Biolabs) and ligated with NOS terminator flanked with *Pac*I site using T4 DNA ligase (New England Biolabs). This NOS terminator flanked with *Pac*I site was amplified with primer set: nos_PacI_forward (5′-TACGTTAATTAAGAATTTCCCCGAT-3′) and nos_PacI_reverse (5′-GCATTTAATTAAAGTAACATAGATGACACC-3′) and cut by restriction enzyme *Pac*I before T4 DNA ligation. *GC1::GAD2Δ-stop* and *GC1::GAD2-stop* were recombined from the pENTR/D-TOPO vector into a pMDC107 vector that contained a GFP tag on the C-terminus (*GC1::GAD2Δ-GFP* and *GC1::GAD2-GFP*)[64].

To create *GAD2* complementation driven by a constitutive 35S promoter, the full-length *GAD2* was also amplified using primer set GAD2_forward2 (5′-CACC ATGGTTTTGACAAAAACCGC-3′) and GAD2_reverse and cloned into pENTR/D-TOPO vector via directional cloning (Invitrogen), followed by an LR reaction recombinant into pMDC32[64]. For mesophyll specific complementation, *GAD2Δ* with a stop codon was amplified with the GAD2_forward2 and GAD2_truncated_reverse primer set, and cloned into the pENTR/D-TOPO vector, followed by an LR reaction recombined into the pTOOL5 vector (*UAS::GAD2Δ*)[65].

For *almt9-2* complementation, the pART27 binary vector containing the *ALMT9* coding sequence[21] was used for native *ALMT9* complementation driven by the 35S promoter, and also used as a template for a site-direct mutagenesis PCR to replace F243 and Y245 of *ALMT9* with two cysteines (*ALMT9*$^{F243C/Y245C}$) using the primer sets: ALMT9_DoubleF (5′-GTTTAGGTGTTAATATGTGTATCTGT CCTATATGGGCTGGAGAGG-3′) and ALMT9_DoubleR (5′-CCATATAGGACA GATACACATATTAACACCTAAACTAACACCAGCACC-3′).

For *GAD2* expression analysis, a 1 kb sequence upstream of the *GAD2* start codon was designated as the *GAD2* promoter (*pGAD2*) and amplified using primer set proGAD2_F (5′-ATTTTGAATTTGCGGAGAATCT-3′) and proGAD2_R (5′-CTTTGTTTCTGTTTAGTGAAAGAGAA-3′). The *pGAD2* PCR product was cloned into pCR8/GW/TOPO via TA cloning and recombined via an LR reaction into the pMDC162 vector containing the *GUS* reporter gene for histochemical assays[64]. The binary vectors, pMDC32, pMDC99, pMDC107, pMDC162, pTOOL5 and pART27 carrying sequence-verified constructs, were transformed into *Agrobacterium* strain *AGL1* for stable transformation in *Arabidopsis* plants.

Stomatal aperture and density measurement. Soil-grown *Arabidopsis* (5–6-week-old) were used for stomatal aperture and density measurements. Two-to-three-week-old soybean, broad beans and barley and 5–6-week-old tobacco were used for

stomatal aperture assays. Epidermal strips from *Arabidopsis*, soybean, faba bean and tobacco were peeled from abaxial sides of leaves, pre-incubated in stomatal pore measurement buffer containing 10 mM KCl, 5 mM L-malic acid, 10 mM 2-ethanesulfonic acid (MES) with pH 6.0 by 2-amino-2-(hydroxymethyl)-1,3-propanediol (Tris) under light (200 μmol m^{-2} s^{-1}) or darkness and transferred into stomatal pore measurement buffer with blind treatments as stated in the figure legend. For barley epidermal stomatal assays, a modified method was used[66]: the second fully expanded leaf from 2-week-old seedlings was used as experimental material, leaf samples were first detached and bathed in a modified measurement buffer (50 mM KCl, 10 mM MES with pH 6.1 by KOH) under light (150 μmol m^{-2} s^{-1}) for 1.5 h or darkness for 1 h, then pre-treated in the same buffer with or without 1 mM GABA for 0.5 h; after this pre-treatment, samples were incubated in continuous dark, light, light-to-dark or dark-to-light transition for an additional 1 h as indicated in the figure legend before leaf epidermal strips were peeled for imaging. For *Arabidopsis* stomatal density measurement, epidermal strips were peeled from abaxial sides of young and mature leaves, three leaves per plants, three plants per genotype. Epidermal strips for both aperture and density measurement were imaged using an Axiophot Pol Photomicroscope (Carl Zeiss) apart from the barley epidermal strips imaged using an Nikon Diaphot 200 Inverted Phase Contrast Microscope (Nikon). Stomatal aperture and density were analyzed using particle analysis (http://rsbweb.nih.gov/ij/).

Stomatal conductance measurement. All stomatal conductance measurements were performed on 5–6-week-old *Arabidopsis* plants. The stomatal conductance determined by the AP4 Porometer (Delta-T Devices) was calculated based on the mean value from 2–3 leaf recordings per plant (Figs. 3b, 4c, 5c, 6c, d and 9; Supplementary Fig. 10d, 11d, g and 14c). The time-dependent stomatal conductance, transpiration and photosynthetic rate was recorded using LI-6400XT Portable Photosynthesis System (LI-COR Biosciences) equipped with an *Arabidopsis* leaf chamber fluorometer (under 150 μmol m^{-2} s^{-1} light with 10% blue light, 150 mmol s^{-1} flow rate, 400 ppm CO_2 mixer, ~50 % relative humidity at 22 °C) as indicated (Fig. 4d; Supplementary Fig. 8g, h).

ABA measurement. The analysis of *Arabidopsis* leaf ABA concentration followed a method as described previously[67]. Briefly, >50 mg of ground fresh leaf samples were used to determine ABA concentration using an Agilent 6410 Series Triple Quad liquid chromatography (LC)-mass spectrometer (MS)/MS, equipped with Agilent 1200 series HPLC (Agilent Technologies) using a Phenomenex C18 column (75 mm × 4.5 mm × 5 μm) with a column temperature set at 40 °C. Solvents were nanopure water and acetonitrile, both with 0.05% acetic acid. Samples were eluted with a linear 15-min gradient from 10 to 90% acetonitrile. Compounds were identified by retention times and mass/charge ratio.

Water-deficit drought assay. Plants were germinated on ½ MS medium with 0.8% phytagel for 10 days in short-day conditions (100–120 μmol m^{-2} s^{-1}, 10 h light/14 h dark) at 22 °C before being transferred to pots (size 2.5 inch diameter × 2.25 inch height, LI-COR Bioscience) with soil, containing coco peat/Irish peat (1:1 ratio). Prior to 10-day-old seedling transfer, all pots were weighed on an Ohaus ARA520 Adventurer Balance and soil was aliquoted into the pots within ±0.1 g between all replicates within an experimental run, randomly placed in growth cabinet and moved every other day in the same environmental conditions stated above. The starting weight varied amongst experimental runs dependent upon soil moisture (from 75 to 78 g). The drought assay was performed on 5–6-week-old *Arabidopsis* plants (Figs. 3, 4g, h and 5; Supplementary Figs. 6a–c, 9 and 11c–e). All plants were well-watered (saturated) the night before the drought assay, but not watered again during the assay. During the drought assay, all plants were randomly moved around once a day to avoid any bias of uneven light distribution or air flow within the cabinet that may differentially affect water loss.

At each sampling point, fresh weight of 2–3 leaves per plant was determined on an Ohaus Explorer E02140 balance (in Fig. 3a, Supplementary Figs. 6c and 11c, this occurred immediately after the rest of the leaf rosette was snap frozen in liquid nitrogen for later GABA measurement). Sampled leaves were then rehydrated to full turgid weight in ultrapure water overnight and measured after surface water was dried with paper towel. Dry weight was determined at 65 °C for 1 day. Leaf RWC was calculated as (Figs. 3c, 4g and 5d; Supplementary Figs. 6a and 11e)

$$\mathrm{RWC} = \frac{\text{Fresh weight} - \text{Dry weight}}{\text{Turgid weight} - \text{Dry weight}} \times 100\% \quad (1)$$

At each sampling point, fresh soil weight of the whole pot (Mwet) and dry soil weight after drying the soil (Mdry) at 105 °C for 3 days was measured using an Ohaus ARA520 Adventurer Balance (Supplementary Fig. 6b). Gravimetric soil water content (θg) of the whole soil in the pots was calculated as

$$\theta g = \frac{\mathrm{Mwet} - \mathrm{Mdry}}{\mathrm{Mdry}} \quad (2)$$

Leaf feeding assay. The stomatal conductance, transpiration and photosynthetic rate of the detached leaf feeding assay was recorded using either a LCpro-SD Portable Photosynthesis System (ADC Bioscientific) with 350 μmol m^{-2} s^{-1} light, 200 μmols s^{-1} flow rate and 400 ppm CO_2 at 22 °C (Supplementary Fig. 1c, d) or LI-COR LI-6400XT (LI-COR Biosciences) with 200 μmol m^{-2} s^{-1} light, 150 μmols s^{-1} flow rate and 400 ppm CO_2 at 22 °C (Figs. 2c and 8b, d, f; Supplementary Figs. 2a, b and 17a, b, d, e, g, h). The detached leaf was fed with artificial xylem sap solution modified as described[68], containing 1 mM KH_2PO_4, 1 mM K_2HPO_4, 1 mM $CaCl_2$, 0.1 mM $MgSO_4$, 1 mM KNO_3, 0.1 mM $MnSO_4$, 1 mM K-H-malate, pH 6.0 (KOH) with or without GABA or muscimol supplement as indicated, detached leaves were pre-fed under 150 μmol m^{-2} s^{-1} light to allow the uptake of treatments for 45–60 min before recording. iWUE and WUE were calculated based on the equation as described in ref. [27].

GABA measurement. GABA concentration was determined using ultra performance LC (UPLC) as described previously[36]. Briefly, GABA was extracted from samples using 10 mM sodium acetate and derivatized with the AccQ Tag Ultra Derivatization Kit (Waters). Chromatographic analysis of GABA was performed on an Acquity UPLC System (Waters) with a Cortecs or Phenomenex UPLC C18 column (1.6 μm, 2.1 × 100 mm). The gradient protocol for amino acids analysis was used to measure GABA with mobile solvents AccQ Tag Ultra Eluents A and B (Waters). Standard GABA solution was used for calibration ranging from 0 to 150 μM. The results were analyzed by Empower chromatography software version 3 (Waters).

GUS histochemical staining assays. A GUS histochemical assay was performed using the methods described previously[69]. Three-to-four-week-old transgenic *pGAD2::GUS* plants were stained in buffer containing 50 mM Na phosphate pH = 7.0, 10 mM EDTA, 2 mM potassium ferrocyanide, 2 mM potassium ferricyanide, 0.1% (v/v) Triton X-100 and 0.1% (w/v) X-Gluc (5-bromo-4-chloro-3-indolyl β-D-glucuronide) during a 1.5 h incubation at 37 °C in the dark. The stained plants were destained in 70% ethanol. GUS-stained plants were imaged using an Axiophot Pol Photomicroscope (Carl Zeiss).

Fluorescence microscopy. The fluorescence of fluorescent proteins in transgenic *gad2-1/GC1::GAD2Δ-GFP*, *gad2-1/GC1::GAD2-GFP* and WT/*GC1::GAD2Δ-GFP* plants was imaged by confocal laser scanning microscopy using a Zeiss Axioskop 2 mot plus LSM5 PASCAL and argon laser (Carl Zeiss). Sequential scanning and laser excitation was used to capture fluorescence via the LSM5 PASCAL from GFP (excitation = 488 nm, emission band-pass = 505–530 nm), chlorophyll autofluorescence (excitation = 543 nm, emission long-pass = 560 nm). The fluorescence of fluorescent proteins in the mesophyll protoplasts of transgenic *almt9-2* complementation lines and *N. benthamiana* (Supplementary Fig 16c, d) was imaged using Nikon A1R Laser Scanning Confocal with DS-Ri1 CCD camera. Sequential scanning and laser excitation was used to capture fluorescence via the Nikon A1R Laser Scanning Confocal from GFP (excitation = 488 nm, emission = 525–575 nm), chlorophyll autofluorescence (excitation = 561 nm, emission = 595–645 nm).

Reverse transcriptional PCR. Reverse transcriptional PCR was determined by PCR amplification on cDNA synthesized from RNA extracted from plants as indicated. PCR amplified *GAD2, Actin2, GFP, GAD2 mRNA, UAS::GAD2Δ* and *ALMT9* using Phire Hot Start II DNA Polymerase (Invitrogen) with primer sets:
GAD2_rt_F (5′-ACGTGATGGATCCAGACAAAG-3′) and
GAD2_rt-R (5′-TACATTTTCCGCGATCCCT-3′);
Actin2_rt_F (5′-CAAAGGCCAACAGAGAGAAGA-3′) and
Actin2_rt_R (5′-CTGTACTTCCTTTCAGGTGGTG-3′);
GFP_rt_F (5′-GGAGTTGTCCCAATTCTTGTT-3′) and
GFP_rt_R (5′-CGCCAATTGGAGTATTTTGT-3′);
GAD2mRNA_rt_F (5′-ACGTGATGGATCCAGACAAAG-3′) and
GAD2mRNA_rt_R (5′-TCTTCATTTCCACACAAAGGC-3′);
UAS_GAD2_rt_F (5′-TCACTCTCAATTTCTCCAAGG-3′) and
UAS_GAD2_rt_R (5′-CGGCAACAGGATTCAATCTTAAG-3′);
ALMT9_rt_F (5′-AATACTCGAGAAACGGGAGAG-3′) and
ALMT9_rt_R (5′-CATCCCAAAACACCTACGAAT-3′).

Quantitative real-time PCR analysis. Quantitative reverse transcription PCR was performed using KAPA SYBR FAST ABI PRISM kit (Kapa Biosystems) using a QuantStudio™ 12K Flex Real-Time PCR System (Thermo Fisher Scientific) to determine the expression levels of *GAD1*, *GAD2*, *GAD3*, *GAD4*, *GAD5*, *GABA-T*, *ALMT9*, *ALMT12*, *RD29A* and *RD22* genes with primer sets:
GAD1_qF (5′-TCTCAAAGGACGAGGGAGTG-3′) and
GAD1_qR (5′-AACCACACGAAGAACAGTGATG-3′);
GAD2_qF (5′-GTCTCAAAGGACCAAGGAGTG-3′) and
GAD2_qR (5′-CATCGGCAGGCATAGTGTAA-3′);
GAD3_qF (5′-CCGTTAGTGGCGTTTTCTCT-3′) and
GAD3_qR (5′-TCTCTTTGCGTCTCCTCTGG-3′);
GAD4_qF (5′-GTGTTCCGTTAGTGGCGTT-3′) and
GAD4_qR (5′GTCTCCTCTGGCGTCTTCTT-3′);
GAD5_qF (5′-TCAACCCACTTTCACTCTCA-3′) and
GAD5_qR (5′-TTCCTTCTCTTAGCCTCCTT-3′);
GABA-T_qF (5′-AGGCAGCACCTGAGAAGAAA-3′) and
GABA-T_qR (5′-GGAGTGATAAAACGGCAAGG-3′);

ALMT9_qF (5′-CAGAGAGTGGGCGTAGAAGG-3′) and
ALMT9_qR (5′-GGATTTGAAGGCGTAGATTGG-3′);
ALMT12_qF (5′-TTGACGGAACTCGCAGATAG-3′) and
ALMT12_qR (5′-CGATGGAGGTTAGAGCCAAG-3′);
RD29A_qF (5′-AAACGACGACAAAGGAAGTG-3′) and
RD29A_qR (5′-ACCAAACCAGCCAGATGATT-3′);
RD22_qF (5′-AGGGCTGTTTCCACTGAGG-3′) and
RD22_qR (5′- CACCACAGATTTATCGTCAGACA-3′).
Expression levels of each gene was normalised to three control genes—*Actin2*, *EF1α* and *GAPDH-A*—that were amplified with primer sets:
Actin2_qF (5′-TGAGCAAAGAAATCACAGCACT-3′) and
Actin2_qR (5′-CCTGGACCTGCCTCATCATAC-3′);
EF1α_qF (5′-GACAGGCGTTCTGGTAAGGAG-3′) and
EF1α_qR (5′-GCGGAAAGAGTTTTGATGTTCA-3′);
GAPDH-A_qF (5′-TGGTTGATCTCGTTGTGCAGGTCTC-3′) and
GAPDH-A_qR (5′-GTCAGCCAAGTCAACAACTCTCTG-3′).

Reporting summary. Further information on research design is available in the Nature Research Reporting Summary linked to this article.

Data availability

Sequence data used in this paper can be found in The Arabidopsis Information Resource database (https://www.arabidopsis.org/) under the following accessions: *GAD1* (At5g17330), *GAD2* (At1g65960), *GAD3* (At2g02000), *GAD4* (At2g02010), *GAD5* (At3g17760), *GABA-T* (At3g22200), *ALMT9* (At3g18440), *ALMT12* (At4g17970), *RD29A* (At5g52310) and *RD22* (At5g25610). Other data that support the findings of this study are available from the corresponding author upon request. Source Data are provided with this paper.

Received: 19 December 2019; Accepted: 4 February 2021;
Published online: 29 March 2021

References

1. Keenan, T. F. et al. Increase in forest water-use efficiency as atmospheric carbon dioxide concentrations rise. *Nature* **499**, 324 (2013).
2. Papanatsiou, M. et al. Optogenetic manipulation of stomatal kinetics improves carbon assimilation, water use, and growth. *Science* **363**, 1456–1459 (2019).
3. Hetherington, A. M. & Woodward, F. I. The role of stomata in sensing and driving environmental change. *Nature* **424**, 901 (2003).
4. Shimazaki, K.-i, Doi, M., Assmann, S. M. & Kinoshita, T. Light regulation of stomatal movement. *Annu. Rev. Plant Biol.* **58**, 219–247 (2007).
5. Sussmilch, F. C., Schultz, J., Hedrich, R. & Roelfsema, M. R. G. Acquiring control: the evolution of stomatal signalling pathways. *Trends Plant Sci.* **24**, 342–351 (2019).
6. Kim, T.-H., Böhmer, M., Hu, H., Nishimura, N. & Schroeder, J. I. Guard cell signal transduction network: advances in understanding abscisic acid, CO_2, and Ca^{2+} signaling. *Annu. Rev. Plant Biol.* **61**, 561–591 (2010).
7. Murata, Y., Mori, I. C. & Munemasa, S. Diverse stomatal signaling and the signal integration mechanism. *Annu. Rev. Plant Biol.* **66**, 369–392 (2015).
8. Melotto, M., Underwood, W., Koczan, J., Nomura, K. & He, S. Y. Plant stomata function in innate immunity against bacterial invasion. *Cell* **126**, 969–980 (2006).
9. Liu, Y. et al. Anion channel SLAH3 is a regulatory target of chitin receptor-associated kinase PBL27 in microbial stomatal closure. *eLife* **8**, e44474 (2019).
10. Žárský, V. Signal transduction: GABA receptor found in plants. *Nat. Plants* **1**, 15115 (2015).
11. Owens, D. F. & Kriegstein, A. R. Is there more to GABA than synaptic inhibition? *Nat. Rev. Neurosci.* **3**, 715 (2002).
12. Bouche, N. & Fromm, H. GABA in plants: just a metabolite? *Trends Plant Sci.* **9**, 110–115 (2004).
13. Kinnersley, A. M. & Turano, F. J. Gamma aminobutyric acid (GABA) and plant responses to stress. *Crit. Rev. Plant Sci.* **19**, 479–509 (2000).
14. Ramesh, S. A., Tyerman, S. D., Gilliham, M. & Xu, B. γ-Aminobutyric acid (GABA) signalling in plants. *Cell Mol. Life Sci.* **74**, 1577–1603 (2017).
15. Bouché, N., Lacombe, B. & Fromm, H. GABA signaling: a conserved and ubiquitous mechanism. *Trends Cell Biol.* **13**, 607–610 (2003).
16. Bown, A. W. & Shelp, B. J. Plant GABA: not just a metabolite. *Trends Plant Sci.* **21**, 811–813 (2016).
17. Michaeli, S. & Fromm, H. Closing the loop on the GABA shunt in plants: are GABA metabolism and signaling entwined? *Front. Plant Sci.* **6**, 419 (2015).
18. Ramesh, S. A. et al. GABA signalling modulates plant growth by directly regulating the activity of plant-specific anion transporters. *Nat. Commun.* **6**, 7879 (2015).
19. Gilliham, M. & Tyerman, S. D. Linking metabolism to membrane signaling: the GABA-malate connection. *Trends Plant Sci.* **21**, 295–301 (2016).
20. Meyer, S. et al. AtALMT12 represents an R-type anion channel required for stomatal movement in *Arabidopsis* guard cells. *Plant J.* **63**, 1054–1062 (2010).
21. De Angeli, A., Zhang, J., Meyer, S. & Martinoia, E. AtALMT9 is a malate-activated vacuolar chloride channel required for stomatal opening in *Arabidopsis*. *Nat. Commun.* **4**, 1804 (2013).
22. Eisenach, C. et al. ABA-Induced stomatal closure involves ALMT4, a phosphorylation-dependent vacuolar anion channel of *Arabidopsis*. *Plant Cell* **29**, 2552–2569 (2017).
23. Hauser, F., Li, Z., Waadt, R. & Schroeder, J. I. SnapShot: abscisic acid signaling. *Cell* **171**, 1708–1708 (2017).
24. Peiter, E. et al. The vacuolar Ca^{2+}-activated channel TPC1 regulates germination and stomatal movement. *Nature* **434**, 404 (2005).
25. Meidner, H. Measurements of stomatal aperture and responses to stimuli. in *Stomatal Physiology* (ed. Jarvis, P. D. & Mansfield, T. A.) 25–28 (Cambridge University Press, 1981).
26. Mori, I. C. et al. CDPKs CPK6 and CPK3 function in ABA regulation of guard cell S-type anion-and Ca^{2+}-permeable channels and stomatal closure. *PLoS Biol.* **4**, 1749–1762 (2006).
27. Leakey, A. D. et al. Water use efficiency as a constraint and target for improving the resilience and productivity of C_3 and C_4 crops. *Annu. Rev. Plant Biol.* **70**, 781–808 (2019).
28. Desikan, R. et al. Hydrogen peroxide and nitric oxide signalling in stomatal guard cells. *J. Exp. Bot.* **55**, 205–212 (2004).
29. Mekonnen, D. W., Flügge, U.-I. & Ludewig, F. Gamma-aminobutyric acid depletion affects stomata closure and drought tolerance of *Arabidopsis thaliana*. *Plant Sci.* **245**, 25–34 (2016).
30. Espinoza, C. et al. Interaction with diurnal and circadian regulation results in dynamic metabolic and transcriptional changes during cold acclimation in *Arabidopsis*. *PLoS ONE* **5**, e14101 (2010).
31. Zik, M., Arazi, T., Snedden, W. A. & Fromm, H. Two isoforms of glutamate decarboxylase in *Arabidopsis* are regulated by calcium/calmodulin and differ in organ distribution. *Plant Mol. Biol.* **37**, 967–975 (1998).
32. Yang, Y., Costa, A., Leonhardt, N., Siegel, R. S. & Schroeder, J. I. Isolation of a strong *Arabidopsis* guard cell promoter and its potential as a research tool. *Plant Methods* **4**, 6 (2008).
33. Akama, K. & Takaiwa, F. C-terminal extension of rice glutamate decarboxylase (OsGAD2) functions as an autoinhibitory domain and overexpression of a truncated mutant results in the accumulation of extremely high levels of GABA in plant cells. *J. Exp. Bot.* **58**, 2699–2707 (2007).
34. Lehmann, S. et al. In planta function of compatible solute transporters of the AtProT family. *J. Exp. Bot.* **62**, 787–796 (2011).
35. Meyer, A., Eskandari, S. & Grallath, S. Rentsch D. AtGAT1, a high affinity transporter for γ-aminobutyric acid in *Arabidopsis thaliana*. *J. Biol. Chem.* **281**, 7197–7204 (2006).
36. Ramesh, S. A. et al. Aluminium-activated malate transporters can facilitate GABA transport. *Plant Cell* **30**, 1147–1164 (2018).
37. Martí, M. C., Stancombe, M. A. & Webb, A. Cell-and stimulus-type-specific intracellular-free Ca^{2+} signals in *Arabidopsis thaliana*. *Plant Physiol.* **163**, 625–634 (2013).
38. Kowada, T., Maeda, H. & Kikuchi, K. BODIPY-based probes for the fluorescence imaging of biomolecules in living cells. *Chem. Soc. Rev.* **44**, 4953–4972 (2015).
39. Long, Y., Tyerman, S. D. & Gilliham, M. Cytosolic GABA inhibits anion transport by wheat ALMT1. *New Phytol.* **225**, 671–678 (2019).
40. Meyer, S. et al. Malate transport by the vacuolar AtALMT6 channel in guard cells is subject to multiple regulation. *Plant J.* **67**, 247–257 (2011).
41. Kovermann, P. et al. The *Arabidopsis* vacuolar malate channel is a member of the ALMT family. *Plant J.* **52**, 1169–1180 (2007).
42. Negi, J. et al. CO_2 regulator SLAC1 and its homologues are essential for anion homeostasis in plant cells. *Nature* **452**, 483–486 (2008).
43. Vahisalu, T. et al. SLAC1 is required for plant guard cell S-type anion channel function in stomatal signalling. *Nature* **452**, 487–491 (2008).
44. Geiger, D. et al. Activity of guard cell anion channel SLAC1 is controlled by drought-stress signaling kinase-phosphatase pair. *Proc. Natl Acad. Sci. USA* **106**, 21425–21430 (2009).
45. Geiger, D. et al. Guard cell anion channel SLAC1 is regulated by CDPK protein kinases with distinct Ca^{2+} affinities. *Proc. Natl Acad. Sci. USA* **107**, 8023–8028 (2010).
46. Hedrich, R. & Geiger, D. Biology of SLAC1-type anion channels-from nutrient uptake to stomatal closure. *New Phytol.* **216**, 46–61 (2017).
47. Takahashi, Y. et al. MAP3Kinase-dependent SnRK2-kinase activation is required for abscisic acid signal transduction and rapid osmotic stress response. *Nat. Commun.* **11**, 1–12 (2020).
48. Chen, Z.-H. et al. Systems dynamic modeling of the stomatal guard cell predicts emergent behaviors in transport, signaling, and volume control. *Plant Physiol.* **159**, 1235–1251 (2012).

49. Hills, A., Chen, Z.-H., Amtmann, A., Blatt, M. R. & Lew, V. L. OnGuard, a computational platform for quantitative kinetic modeling of guard cell physiology. *Plant Physiol.* **159**, 1026–1042 (2012).
50. Takahashi, F. et al. A small peptide modulates stomatal control via abscisic acid in long-distance signalling. *Nature* **556**, 235 (2018).
51. Kuromori, T., Seo, M. & Shinozaki, K. ABA transport and plant water stress responses. *Trends Plant Sci.* **23**, 513–522 (2018).
52. Sharma, T., Dreyer, I., Kochian, L. & Piñeros, M. A. The ALMT family of organic acid transporters in plants and their involvement in detoxification and nutrient security. *Front. Plant Sci.* **7**, 1488 (2016).
53. Zhang, J. et al. Identification of a probable pore-forming domain in the multimeric vacuolar anion channel AtALMT9. *Plant Physiol.* **163**, 830–843 (2013).
54. Marvin, J. S. et al. A genetically encoded fluorescent sensor for in vivo imaging of GABA. *Nat. Methods* **16**, 763–770 (2019).
55. Fromm, H. GABA signaling in plants: targeting the missing pieces of the puzzle. *J. Exp. Bot.* **71**, 6238–6245 (2020).
56. Liu, J., Zhou, M., Delhaize, E. & Ryan, P. R. Altered expression of a malate-permeable anion channel, OsALMT4, disrupts mineral nutrition. *Plant Physiol.* **175**, 1745–1759 (2017).
57. Balzergue, C. et al. Low phosphate activates STOP1-ALMT1 to rapidly inhibit root cell elongation. *Nat. Commun.* **8**, 15300 (2017).
58. Jie, Y. et al. An InDel in the promoter of Al-activated malate transporter 9 selected during tomato domestication determines fruit malate contents and aluminum tolerance. *Plant Cell* **29**, 2249–2268 (2017).
59. Palanivelu, R., Brass, L., Edlund, A. F. & Preuss, D. Pollen tube growth and guidance is regulated by POP2, an *Arabidopsis* gene that controls GABA levels. *Cell* **114**, 47–59 (2003).
60. Domingos, P. et al. Molecular and electrophysiological characterization of anion transport in *Arabidopsis thaliana* pollen reveals regulatory roles for pH, Ca^{2+} and GABA. *New Phytol.* **223**, 1353–1371 (2019).
61. Svozil, J., Gruissem, W. & Baerenfaller, K. Proteasome targeting of proteins in *Arabidopsis* leaf mesophyll, epidermal and vascular tissues. *Front. Plant Sci.* **6**, 376 (2015).
62. Prusko, K. *Identifizierung Cis-Regulatorischer Elemente der Transkriptionskontrolle in Photosynthetisch Aktiven Blattzellen von Arabidopsis thaliana*, PhD thesis (Heinrich-Heine-Universität Düsseldorf, 2010).
63. Conn, S. J. et al. Protocol: optimising hydroponic growth systems for nutritional and physiological analysis of *Arabidopsis thaliana* and other plants. *Plant Methods* **9**, 4 (2013).
64. Curtis, M. D. & Grossniklaus, U. A gateway cloning vector set for high-throughput functional analysis of genes *in planta*. *Plant Physiol.* **133**, 462–469 (2003).
65. Møller, I. S. et al. Shoot Na^+ exclusion and increased salinity tolerance engineered by cell type–specific alteration of Na^+ transport in *Arabidopsis*. *Plant Cell* **21**, 2163–2178 (2009).
66. Shen, L. et al. Measuring stress signaling responses of stomata in isolated epidermis of graminaceous species. *Front. Plant Sci.* **6**, 533 (2015).
67. Speirs, J., Binney, A., Collins, M., Edwards, E. & Loveys, B. Expression of ABA synthesis and metabolism genes under different irrigation strategies and atmospheric VPDs is associated with stomatal conductance in grapevine (*Vitis vinifera* L. cv Cabernet Sauvignon). *J. Exp. Bot.* **64**, 1907–1916 (2013).
68. Wilkinson, S. & Davies, W. J. Xylem sap pH increase: a drought signal received at the apoplastic face of the guard cell that involves the suppression of saturable abscisic acid uptake by the epidermal symplast. *Plant Physiol.* **113**, 559–573 (1997).
69. Xu, B. et al. A calmodulin-like protein regulates plasmodesmal closure during bacterial immune responses. *New Phytol.* **215**, 77–84 (2017).

Acknowledgements

The authors would like to thank Dr Katja Bärenfaller from the University of Zurich for providing JR11-2 (Col-0) seeds; Prof. Zhonghua Chen from Western Sydney University for assisting with barley epidermal assays; Dr Cornelia Eisenach from the University of Zurich for providing *ALMT9* constructs, *almt12* and *almt9* seeds and Prof. Stephen D Tyerman, Prof. Enrico Martinoia and Dr Alexis De Angeli for valuable discussions. This work was funded by Waite Research Institute, funding to M.G. and B.X., ARC Discovery grants DP170104384 and DP21012828 to M.G. and R.H. and ARC Centre of Excellence (CE14010008) and Grains Research and Development Corporation funding (UWA00173) to M.G. Author X.F. was supported by supported by a Chinese Scholarship Council. X.Z. was supported by a Chinese Scholarship Council Travelling Fellowship.

Author contributions

B.X. constructed all materials and performed all experiments except the following: Y.L. generated *almt9/almt12* mutants and performed experiments on stomatal aperture assays treated with hydrogen peroxide and calcium and of *almt12* and *almt9/12* mutants. X.F. generated *almt9* complementation lines, performance aperture and conductance measurement of complementation plants. X.Z. performed all non-*Arabidopsis* aperture measurements, except for barley performed by N.S. Author L.C. performed GABA measurements supervised by M.O. Author A.B. performed ABA quantification supervised by E.J.E. Author J.H. acquired images used in Fig. 1. M.G., B.X. and R.H. conceived the research. B.X. drafted all figures. M.G. and B.X. drafted the manuscript. All authors provided edits.

Competing interests

The authors declare no competing interests.

Additional information

Supplementary information The online version contains supplementary material available at https://doi.org/10.1038/s41467-021-21694-3.

Correspondence and requests for materials should be addressed to M.G.

Peer review information *Nature Communications* thanks the anonymous reviewers for their contribution to the peer review of this work. Peer review reports are available.

Reprints and permission information is available at http://www.nature.com/reprints

Publisher's note Springer Nature remains neutral with regard to jurisdictional claims in published maps and institutional affiliations.

GABA signalling modulates stomatal opening to enhance plant water use efficiency and drought resilience

Bo Xu[1,2], Yu Long[1,2], Xueying Feng[1,2], Xujun Zhu[1,3], Na Sai[1,2], Larissa Chirkova[2,4], Annette Betts[5], Johannes Herrmann[6], Everard J Edwards[5], Mamoru Okamoto[2,4], Rainer Hedrich[6] & Matthew Gilliham[1,2]*

[1] Plant Transport and Signalling Lab, ARC Centre of Excellence in Plant Energy Biology, Waite Research Institute, Glen Osmond, SA 5064, Australia

[2] School of Agriculture, Food and Wine, Waite Research Precinct, University of Adelaide, Glen Osmond, SA 5064, Australia

[3] College of Horticulture, Nanjing Agricultural University, Nanjing 210095, China

[4] ARC Industrial Transformation Research Hub for Wheat in a Hot and Dry Climate, Waite Research Institute, University of Adelaide, Glen Osmond, SA 5064, Australia

[5] CSIRO Agriculture & Food, Locked Bag 2, Glen Osmond, SA, 5064, Australia

[6] Institute for Molecular Plant Physiology and Biophysics, University of Würzburg, Würzburg 97070, Germany

SUPPLEMENTARY INFORMATION

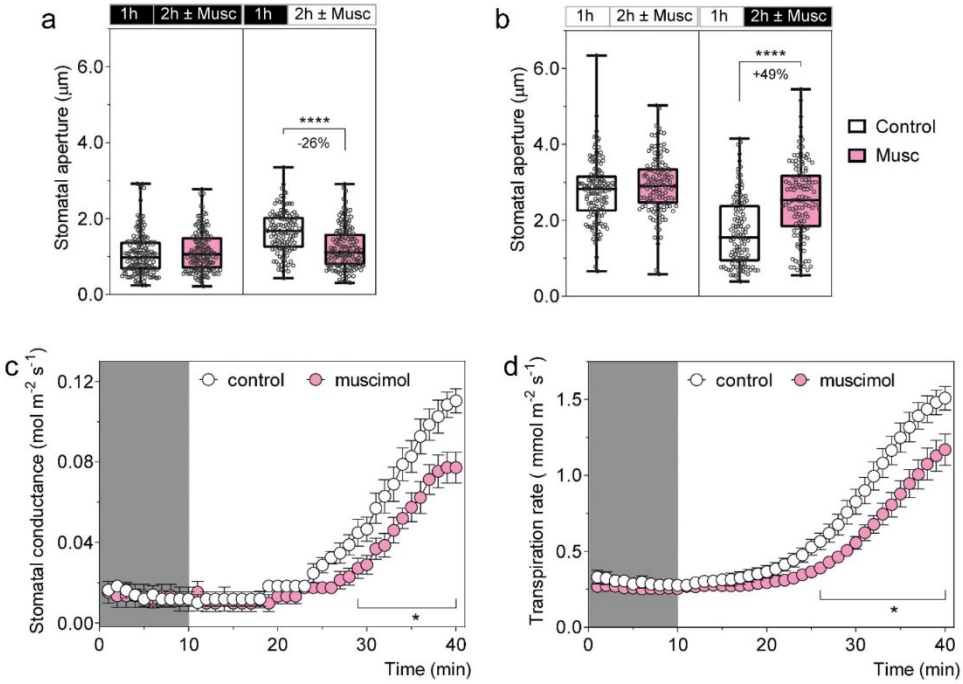

Supplementary Figure 1. Muscimol antagonises stomatal aperture changes initiated by light and dark treatments a-b, Exogenous muscimol application reduces stomatal pore movement in response to light or dark. Epidermal strips were pre-incubated in stomatal pore measurement buffer for 1 h under dark (**a**) or light (**b**), followed by 2 h incubation under constant dark (**a**), light (**b**), dark-to-light transition (**a**) or light-to-dark transition (**b**) as indicated above graphs by black (dark) or white (light) bars, together with the application of 10 µM muscimol (Musc); n = 156 for control (constant dark), n = 151 for muscimol (constant dark), n = 127 for control (dark-to-light transition) and n = 151 for muscimol (dark to light transition) (**a**); n = 134 for control (constant light), n = 132 for muscimol (constant light), n = 118 for control (light-to-dark transition) and n = 120 for muscimol (light-to-dark transition) (**b**). **c-d**, Muscimol feeding reduces stomatal conductance, transpiration rate of detached leaves. Stomatal conductance (**c**), transpiration rate (**d**) of detached leaves of wildtype Arabidopsis plants determined by LCpro-SD Portable Photosynthesis System was fed by artificial

xylem sap solution with or without 10 μM muscimol supplement; n = 7 for control and n = 8 for muscimol (**c, d**). All data are plotted with box and whiskers plots: whiskers plot represents minimum and maximum values, and box plot represents second quartile, median and third quartile (**a, b**) or data are represented mean ± s.e.m (**c, d**); statistical difference was determined by Two-way ANOVA (**a, b**), or two-sided Student's *t-test* (**c, d**), *P<0.05 and ****P<0.0001.

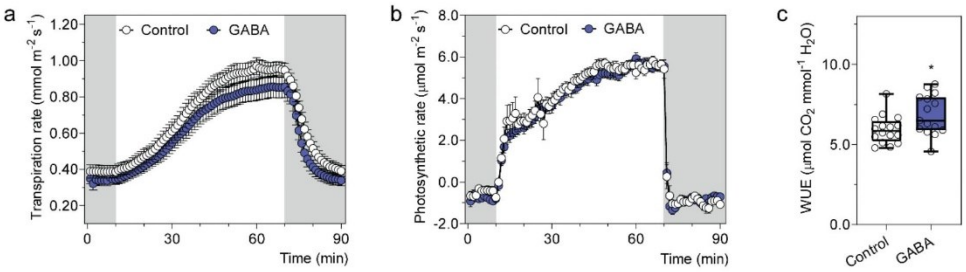

Supplementary Figure 2. GABA feeding increases WUE of detached leaves. GABA feeding reduces transpiration rate and increases water use efficiency (WUE) of detached leaves. Transpiration (**a**) and photosynthetic rate (**b**) of 5-6 week-old leaves of 5-6 week-old *A. thaliana* wildtype plants was recorded using a LiCor LI-6400XT in response to dark (shaded region) and 200 µmol m^{-2} s^{-1} light (white region), fed with artificial xylem sap solutions ± 4 mM GABA. **c**, WUE of detached leaves was calculated based on the ratio of photosynthetic rate (**b**) versus transpiration rate (**a**), n = 16 independent leaves for control and n = 15 for GABA (**a-c**). All data are plotted with box and whiskers plots: whiskers plot represents minimum and maximum values, and box plot represents second quartile, median and third quartile (**c**) or data are represented mean ± s.e.m (**a, b**), statistical difference was determined by two-sided Student's *t-test*, *P<0.05

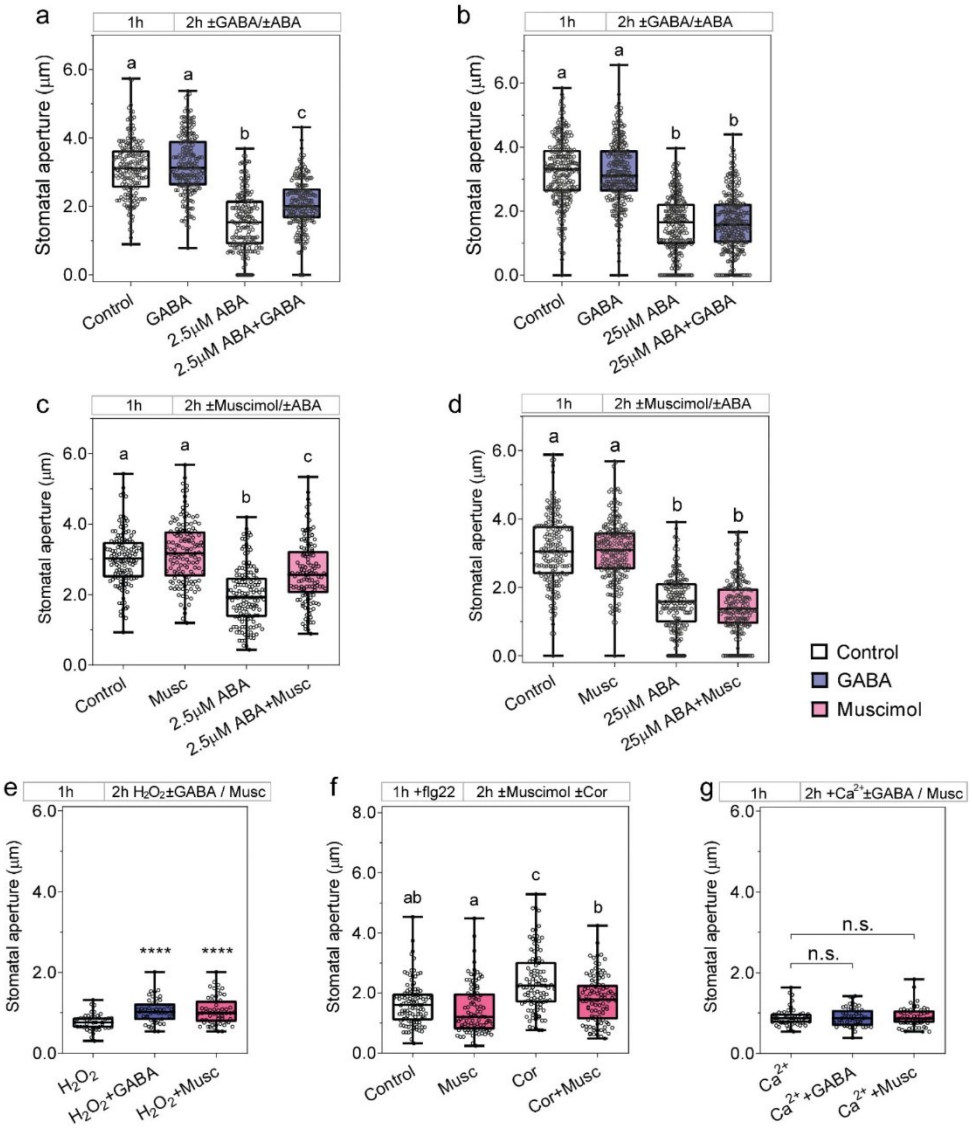

Supplementary Figure 3. GABA and muscimol inhibit stomatal aperture changes triggered by signaling molecules. a-g, Exogenous GABA or muscimol application reduces stomatal closure in response to 2.5 µM ABA (**a, c**), 50 µM H_2O_2[1] (**e**) and stomatal opening to 0.5 µg ml^{-1} coronatine[2] (**f**), but not to 25 µM ABA (**b, d**) and 2 mM $CaCl_2$[1] (**g**). Epidermal strips were pre-incubated in stomatal pore measurement buffer for 1 h under light, followed by 2 h treatment under light with or

without combination of ABA ± 2 mM GABA (**a, b**) / 10 µM muscimol (**c, d**), H_2O_2 ± 2 mM GABA/10 µM muscimol (Musc) (**e**), coronatine (Cor) ± 10 µM muscimol (**f**), and $CaCl_2$ (Ca^{2+}) ± 2 mM GABA/10 µM muscimol (**g**) as indicated; n = 183 for control, n = 191 for GABA, n = 171 for ABA and n = 201 for ABA+GABA (**a**); n = 249 for control, n = 249 for GABA, n = 243 for ABA and n = 261 for ABA+GABA (**b**); n = 133 for control, n = 137 for muscimol, n = 142 for ABA and n = 131 for ABA+muscimol (**c**); n = 180 for control, n = 222 for muscimol, n = 176 for ABA and n = 179 for ABA+muscimol (**d**); n = 44 for H_2O_2, n = 47 for H_2O_2+GABA and n = 54 for H_2O_2+Musc (**e**); n = 103 for control, n = 103 for Cor, n = 101 for Cor+muscimol and n = 91 for muscimol (**f**);); n = 52 for Ca^{2+}, n = 52 for Ca^{2+}+GABA and n = 54 for Ca^{2+}+Musc (**g**). All data are plotted with box and whiskers plots: whiskers plot represents minimum and maximum values, and box plot represents second quartile, median and third quartile; statistical difference as determined by One-Way ANOVA (**a-g**), **** $P<0.0001$, a, b and c represent groups without significant difference, $P<0.05$ (**a-d, f**).

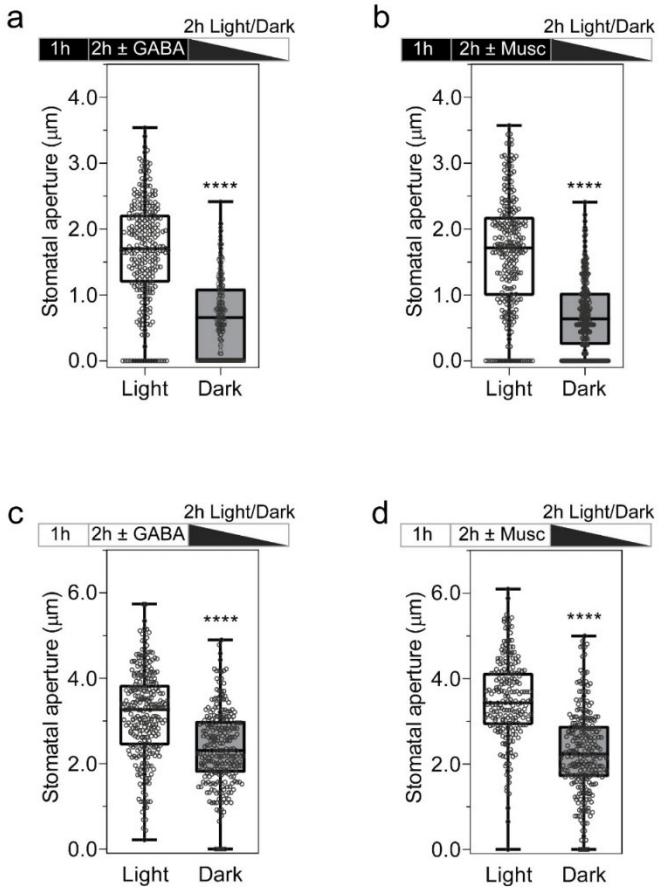

Supplementary Figure 4. Guard cells are viable after treatment with GABA and muscimol. a-d, Guard cells were competent in movement after removal of GABA or muscimol treatments, as closed pores opened when exposed to light (**a-b**) or open pores closed when exposed to dark (**c-d**) following removal of GABA or muscimol. Epidermal strips were incubated under dark (**a-b**) or light (**c-d**) for 1 h, followed by 2 h treatment of 2 mM GABA (**a, c**) or 10 µM muscimol (**b, d**), then epidermal strips were transferred into fresh stomatal measurement buffer with 2 h light or dark treatment before measurement; n = 272 for light and n = 247 for dark (**a**); n = 251 for light and n = 251 for dark (**b**); n = 275 for light and n = 248 for dark (**c**); n = 217 for light and n = 261 for dark (**d**). All data are plotted with box and whiskers plots:

whiskers plot represents minimum and maximum values, and box plot represents second quartile, median and third quartile; statistical difference as determined by two-sided Student's *t*-test (**a-d**), **** $P<0.0001$.

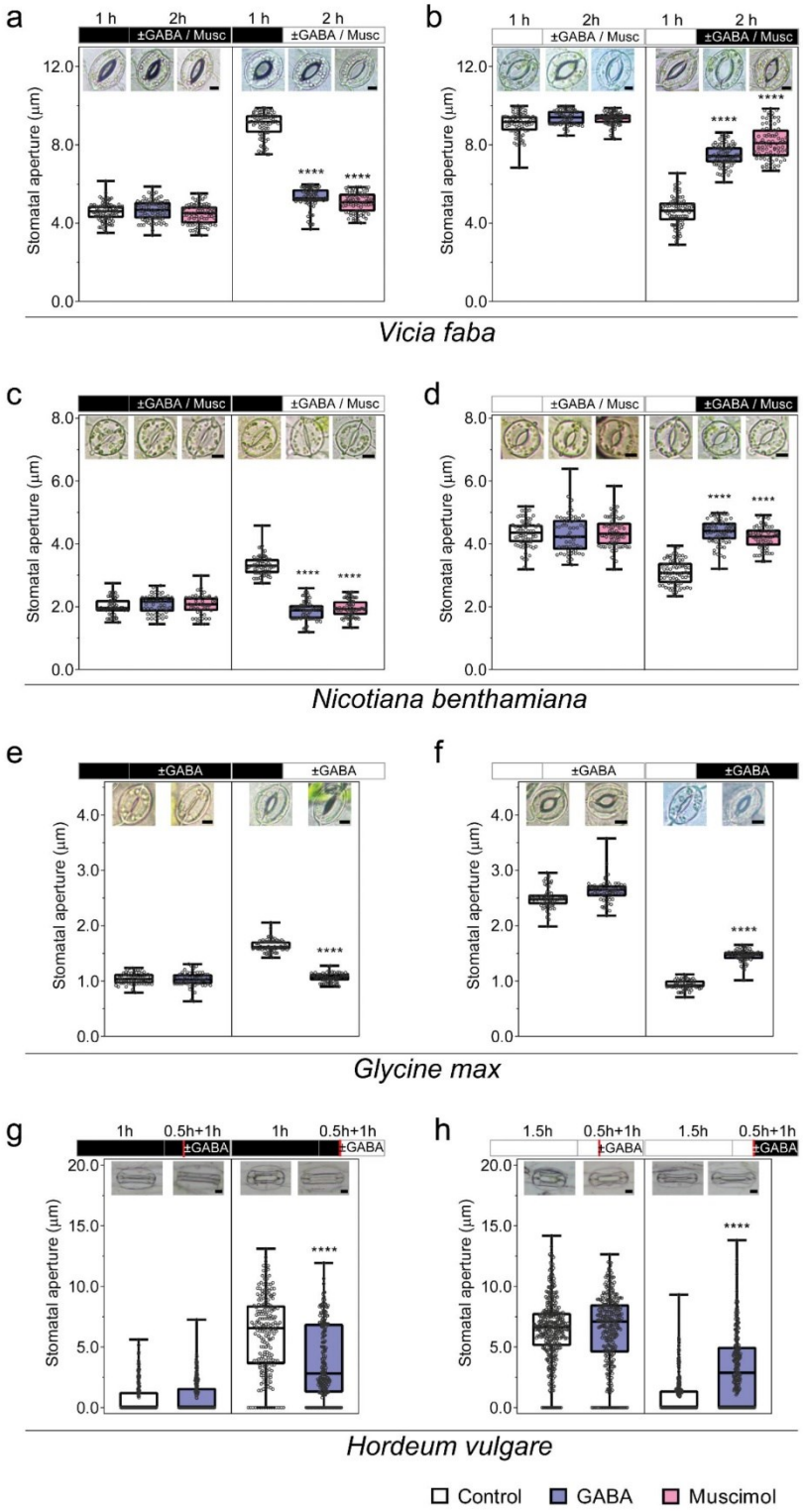
a
b
1 h
2h
1 h
2 h
±GABA / Musc
Stomatal aperture (µm)
****
Vicia faba
c
d
Nicotiana benthamiana
e
f
±GABA
Glycine max
g
h
1h
0.5h+1h
1.5h
Hordeum vulgare
Control
GABA
Muscimol

Supplementary Figure 5. **GABA and muscimol inhibit stomatal aperture changes in response to light and dark in *Vicia faba* (broad bean), *Nicotiana benthamiana* (tobacco), *Glycine max* (soybean) and *Hordeum vulgare* (barley).** Epidermal strips were pre-incubated in stomatal measurement buffer for 1 h under dark (**a, c, e**) or light (**b, d, f**), followed by 2 h incubation under constant dark (**a, c, e**), light (**b, d, f**) as illustrated by black (dark) or white (light) bars, ± 2 mM GABA or 10 μM muscimol (Musc) as indicated; barley leaf samples were first detached and bathed in a modified measurement buffer under 2h dark (**g**) or light (100 μmol m^{-2} s^{-1}) (**h**), then pre-treated in the fresh buffer ±1 mM GABA for 0.5 h as indicated by black or white bars; after this pre-treatment (break by red line), leaf samples were incubated in continuous dark (**g**), light (**h**), dark-to-light (**g**) or light-to-dark (**h**) transition for additional 1 h before the epidermal strips were peeled for imaging. n = 88 for control (constant dark), n = 85 for GABA (constant dark), n = 82 for muscimol (constant dark), n = 78 for control (dark-to-light transition), n = 106 for GABA (dark-to-light transition) and n = 76 for muscimol (dark-to-light transition) (**a**); n = 73 for control (constant light), n = 65 for GABA (constant light), n = 76 for muscimol (constant light), n = 89 for control (light-to-dark transition), n = 85 for GABA (light-to-dark transition) and n = 84 for muscimol (light-to-dark transition) (**b**); n = 50 for control (constant dark), n = 52 for GABA (constant dark), n = 50 for muscimol (constant dark), n = 63 for control (dark-to-light transition), n = 65 for GABA (dark-to-light transition) and n = 64 for muscimol (dark to light transition) (**c**); n = 73 for control (constant light), n = 60 for GABA (constant light), n = 78 for muscimol (constant light), n = 78 for control (light-to-dark transition), n = 67 for GABA (light-to-dark transition) and n = 65 for muscimol (light-to-dark transition) (**d**); n = 61 for control (constant dark), n = 60 for GABA (constant dark), n = 63 for control (dark-to-light transition) and n = 62 for GABA (dark-to-light transition) (**e**); n = 59 for control (constant light), n = 59 for GABA (constant light), n = 60 for control (light-to- dark transition) and

n = 60 (dark-to-light transition) (**f**); n = 177 for control (constant dark), n = 220 for GABA (constant dark), n = 201 for control (dark-to-light transition) and n = 203 for GABA (dark-to-light transition) (**g**); n = 350 for control (constant light), n = 301 for GABA (constant light), n = 289 for control (light-to-dark transition) and n = 228 for GABA (light-to dark-transition) (**h**). All data are plotted with box and whiskers plots: whiskers plot represents minimum and maximum values, and box plot represents second quartile, median and third quartile; statistical difference was determined by Two-way ANOVA, ****$P< 0.0001$; scale bars = 5 μm (**a-h**).

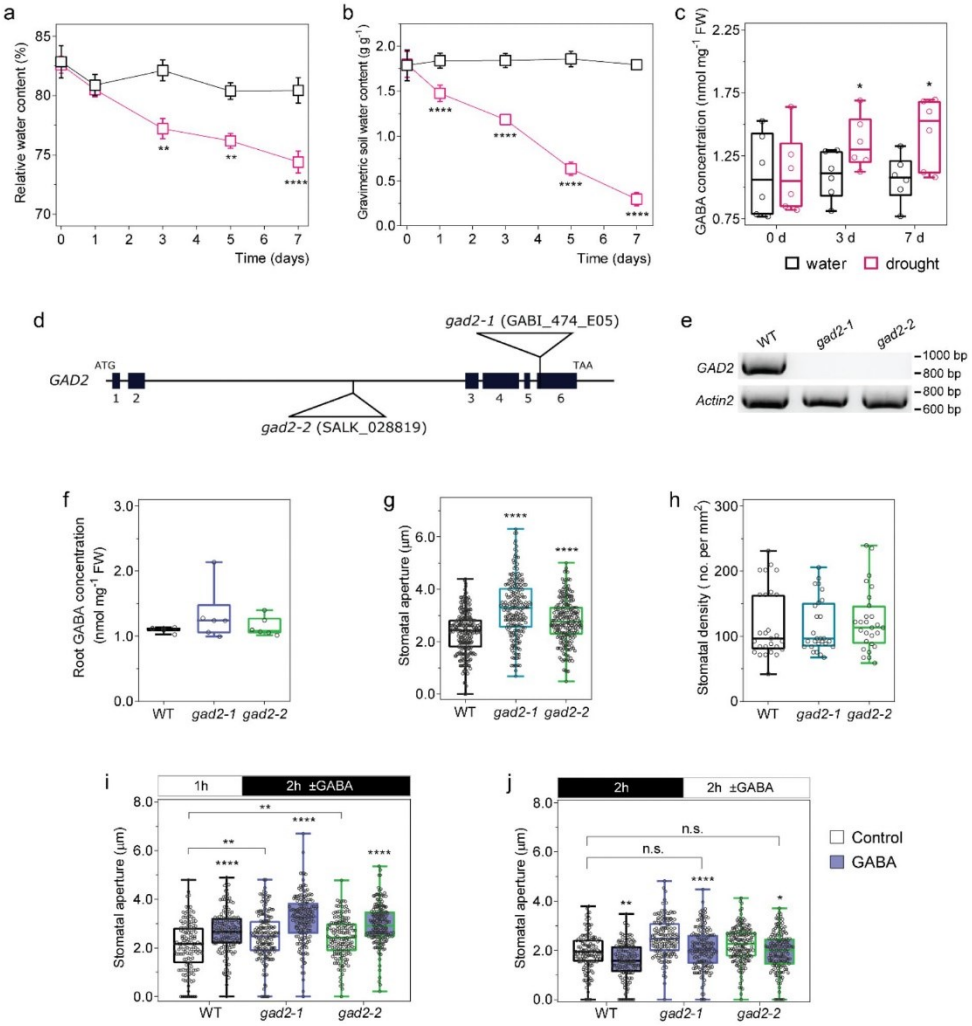

Supplementary Figure 6. **GABA accumulates in leaves of Arabidopsis upon drought, and *gad2* knockout plants have greater stomatal apertures but show wildtype (WT)-like responses to exogenous GABA and root GABA accumulation.** **a,** Relative water content in wildtype Arabidopsis leaves under well-water (black) or drought (red) treatments as indicated. **b,** Water content in the potted soil corresponding to the plants sampled in (**a**). **c,** Leaf GABA concentration of wildtype Arabidopsis following well-watered control treatment (black) or drought (red). 2-3 leaves per plant were sampled for relative water content measurement, as shown in

(**a**); the whole rosette from the sampled plant in (**a**) was harvested and snap frozen in liquid nitrogen for later GABA measurement, as shown in (**c**); and the pot soil of corresponding plants harvested in (**a, b**) was sampled to determine gravimetric soil water content, as shown in (**b**); n = 6 (**a-c**). **d,** A diagram of *GAD2* T-DNA insertional mutant alleles in the Arabidopsis genome. **e,** Reverse transcriptional PCR semi-quantification of *GAD2* transcripts in Arabidopsis WT and *gad2* knockout plants, *Actin2* used as an internal control, similar results were obtained from three independent biological replicates. **f,** Root GABA concentration of WT, *gad2-1* and *gad2-2* plants. Roots were harvested from 5-6 week-old plants grown hydroponically in basal nutrient solution (2 mM NH_4NO_3, 3 mM KNO_3, 0.1 mM $CaCl_2$, 2 mM KCl, 2 mM $Ca(NO_3)_2$, 2 mM $MgSO_4$, 0.6 mM KH_2PO_4, 1.5 mM NaCl, 50 μM NaFe(III)EDTA, 50 μM H_3BO_3, 5 μM $MnCl_2$, 10 μM $ZnSO_4$, 0.5 μM $CuSO_4$, 0.1 μM Na_2MoO_3, pH = 5.6 by KOH)[3], n = 6 plants. **g-j,** Stomatal aperture and density on the leaf abaxial side of Arabidopsis WT and *gad2* knockouts; epidermal strips were peeled and incubated in stomatal measurement buffer for 1 h under light before measurement n = 254 for WT, n = 215 for *gad2-1* and n = 226 for *gad2-2* (**g**); n = 27 sampling areas (0.57 x 0.42 mm) consisting of three areas per leaf, three leaves per plant and three plants per line sampled (**h**). **i-j,** Epidermal strips were pre-incubated in stomatal measurement buffer for 1 h under light (**i**) or 2 h dark (**j**), followed by 2 h incubation dark (**i**) or light (**j**) as indicated by black (dark) or white (light) bars ± blind treatment of 2 mM GABA or control; n = 135, 166 and 157 for WT, *gad2-1* and *gad2-2* with control treatment, n = 146, 162 and 174 for WT, *gad2-1* and *gad2-2* with GABA treatment (**i**); n = 139, 155 and 160 for WT, *gad2-1* and *gad2-2* with control treatment, n = 136, 155 and 153 for WT, *gad2-1* and *gad2-2* with GABA treatment (**j**). All data are plotted with box and whiskers plots: whiskers plot represents minimum and maximum values, and box plot represents second quartile, median and third quartile (**c, f-j**); or data are represented

by mean ± s.e.m. (**a, b**); statistical difference was determined by two-sided Student's *t*-test (**c**), One-way ANOVA (**f-h**) or Two-way ANOVA (**a, b, i, j**), *P< 0.05, **P< 0.01 and ****P< 0.0001.

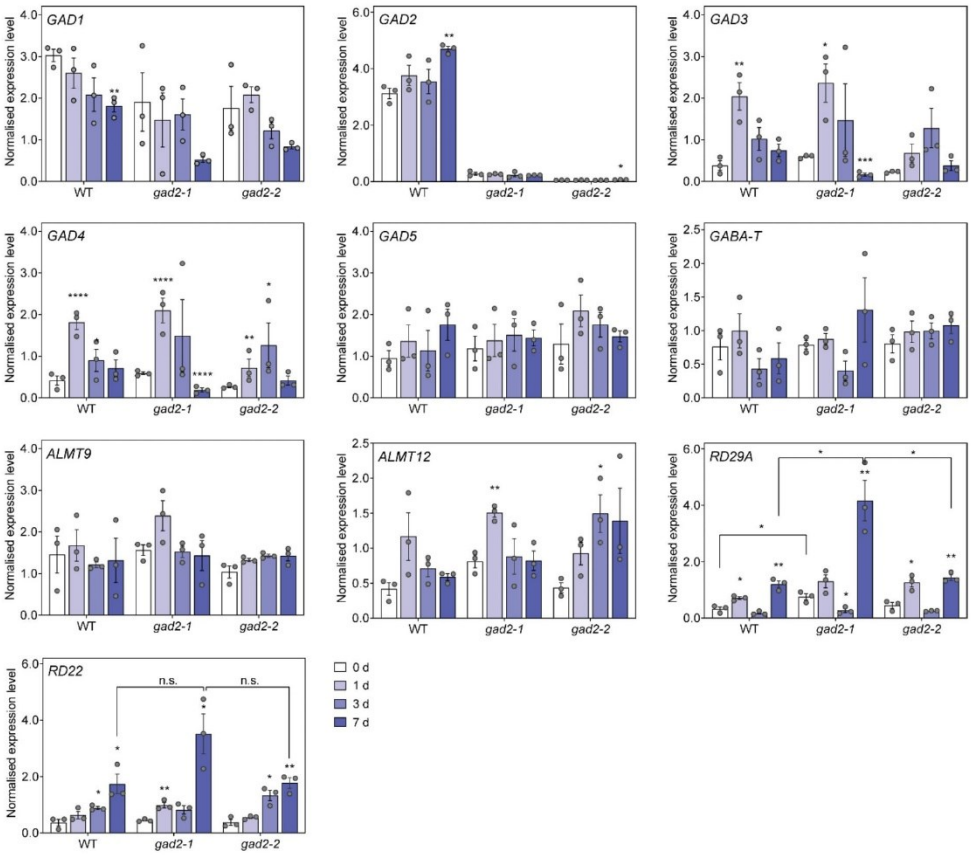

Supplementary Figure 7. ***gad2* knockouts have similar transcriptional profiles to wildtype plants of other *GADs*, *GABA-T*, *ALMT9*, *ALMT12* or ABA responsive genes under drought stress.** Quantitative real time PCR of *GAD1*, *GAD2*, *GAD3*, *GAD4*, *GAD5, GABA-T*, *ALMT9*, *ALMT12* and ABA marker genes –*RD29A* and *RD22*[4] in the leaves of Arabidopsis wildtype (WT), *gad2-1* and *gad2-2* plants following drought treatment for 0, 1, 3 and 7 days as indicated, expression levels were normalized against three control genes –*Actin2*, *EF1α* and *GAPDH-A*; data are represented by means ± s.e.m; n = 3, statistical difference as determined via the comparison of genes from drought-treated plants (1, 3 and 7 days) with non-droughted (0 day) plants within the same genotype by two-sided Student's *t-test*, *$P< 0.05$ **$P< 0.01$, ***$P< 0.001$ and ****$P< 0.0001$.

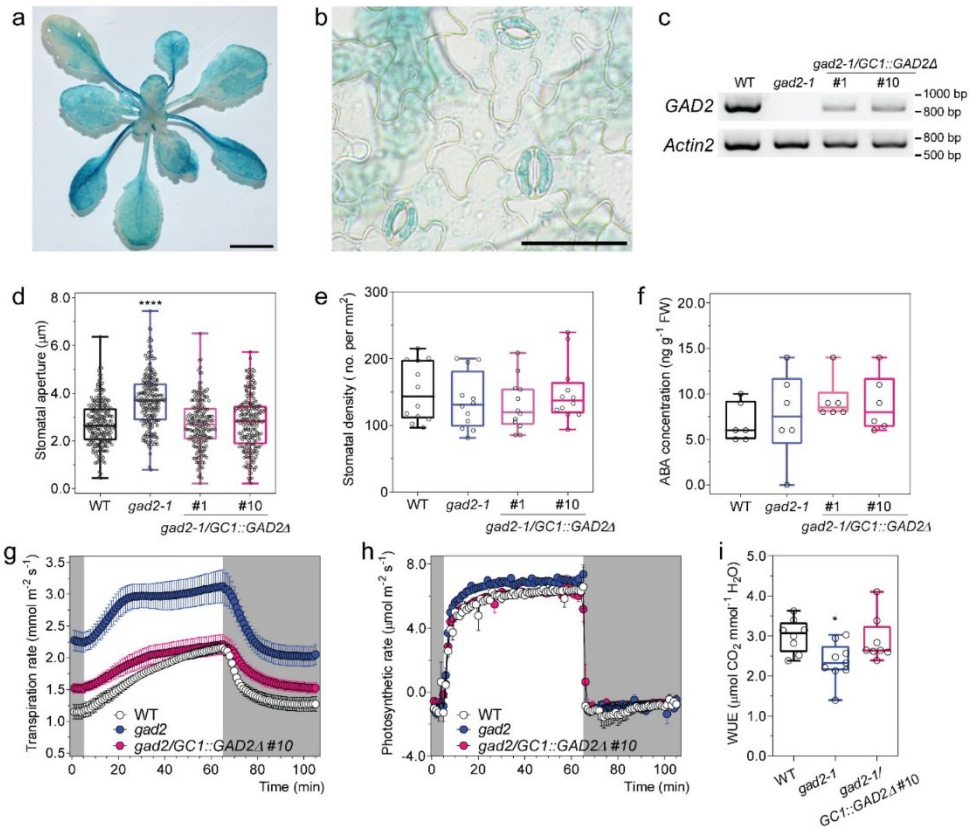

Supplementary Figure 8. *GAD2* is highly expressed in leaves and guard cells, and guard-cell cell complementation of *GAD2Δ* restores stomatal aperture and WUE without modifying stomatal density. a-b, Representative GUS histochemical staining of *pGAD2::GUS* whole rosette**;** image of 3-4 week-old *pGAD2::GUS* plants after staining in histochemical staining buffer, GUS staining of the guard cells was observed in all plants examined that were expressing *pGAD2::GUS*, scale bar = 5 mm (**a**) and epidermal peels from 3-4 week-old *pGAD2::GUS* leaves (**a**), scale bar = 50 µm (**b**). **c,** Reverse-transcriptional PCR quantification of *GAD2* transcripts in Arabidopsis wildtype (WT), *gad2-1*, *gad2-1/GC1::GAD2Δ* #1 and #10 plants, similar results were obtained from three independent biological replicates. **d-e,** Stomatal aperture (**d**) and density (**e**) on the leaf abaxial side of Arabidopsis WT, *gad2-1*, *gad2-*

1/GC1::GAD2Δ #1 and #10 plants; epidermal strips were peeled and incubated in stomatal measurement buffer for 1 h under light before measurement, n = 223 for WT, n = 212 for *gad2-1*, n = 197 for *gad2-1/GC1::GAD2Δ* #1 and n = 224 for *gad2-1/GC1::GAD2Δ* #10 (**d**); n = 12 leaf areas (0.57 x 0.42 mm); two areas per leaf, two leaves per plant and three plants per line were sampled (**e**). **f**, ABA accumulation in rosette leaves of 5-6 week-old Arabidopsis WT, *gad2-1*, *gad2-1/GC1::GAD2Δ* #1 and #10 plants, n = 6. **g-h**, Transpiration (**g**), photosynthetic rate (**h**) of 5-6 week-old Arabidopsis WT, *gad2-1* and *gad2-1/GC1::GAD2Δ* #10 plants in response to dark (shaded region) and 150 µmol m^{-2} s^{-1} light (white region), measured using a LiCor LI-6400XT, n = 8 for WT, n = 9 for gad2-1 and n = 8 for *gad2-1/GC1::GAD2Δ* #10 (**g-h**). **i,** WUE of of 5-6 week-old Arabidopsis WT, *gad2-1* and *gad2-1/GC1::GAD2Δ* #10 plants was calculated based on the photosynthetic rate (**h**) against transpiration rate (**g**). All data are plotted with box and whiskers plots: whiskers plot represents minimum and maximum values, and box plot represents second quartile, median and third quartile (**d-f, i**) or data are represented mean ± s.e.m (**g, h**); statistical difference was determined by One-way ANOVA (**d-f, i**), *P <0.05 and ****P <0.0001.

a

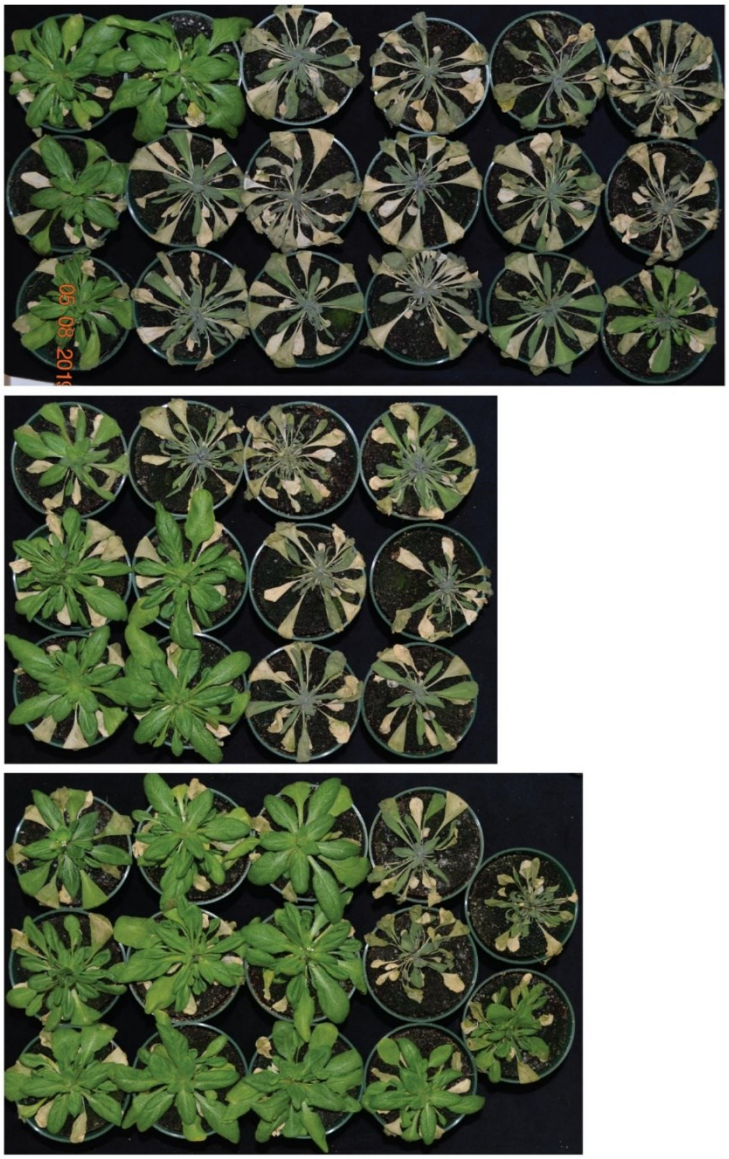

b

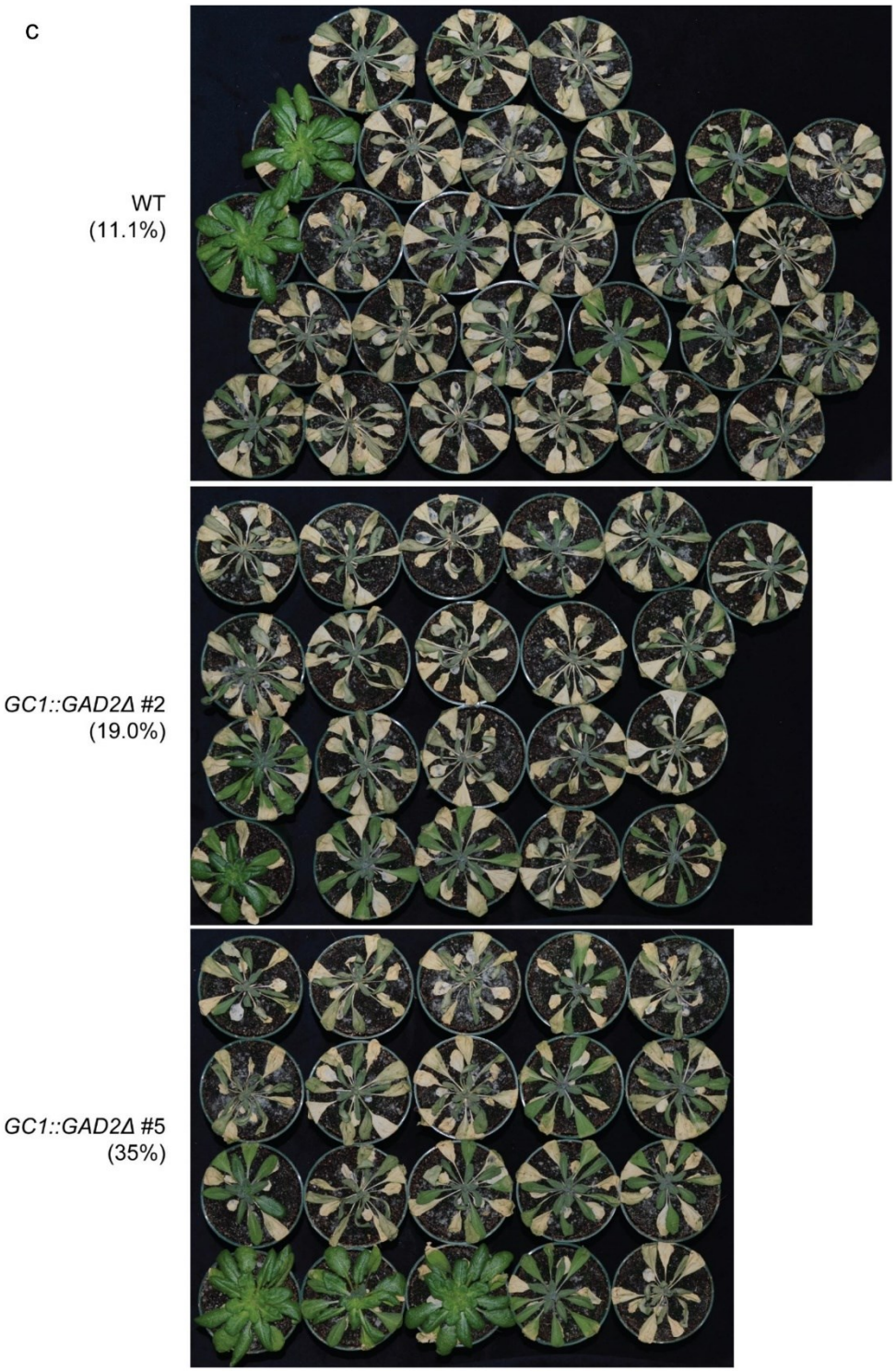
c
WT
(11.1%)
GC1::GAD2Δ #2
(19.0%)
GC1::GAD2Δ #5
(35%)

Supplementary Figure 9. Recovery of re-watered Arabidopsis WT, *GC1::GAD2Δ* #2 and #5 from drought treatment. a-c, Re-water recovery of wildtype, *GC1::GAD2Δ* #2 and #5 plants from drought in three different batches of experiments, plants were re-watered at 2 days after all plant wilting by drought. A higher recovery rate of *GC1::GAD2Δ* #2 and #5 plants than WT was observed from re-watering in all three experiments (**a-c**); 4 out of 18 (22%) wildtype, 5 out of 12 (41.7%) *GC1::GAD2Δ* #2 and 11 out of 14 (78.6%) *GC1::GAD2Δ* #5 plants were recovered from re-water in the first trail (**a**); 21 out of 27 (77.8%) wildtype, 24 out of 27 (88.9%) *GC1::GAD2Δ* #2 and 16 out of 18 (88.9%) *GC1::GAD2Δ* #5 plants were recovered from re-water in the second trail (**b**); 3 out of 27 (11.1%) wildtype, 4 out of 21 (19.0%) *GC1::GAD2Δ* #2 and 7 out of 20 (35%) *GC1::GAD2Δ* #5 plants were recovered from re-water in the third trail (**c**).

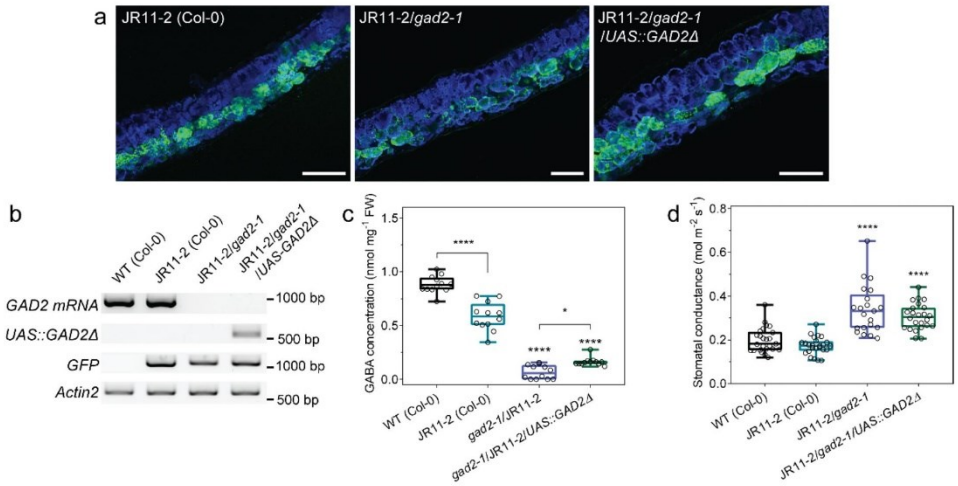

Supplementary Figure 10. **Spongy mesophyll-cell specific expression of *GAD2Δ* in *gad2-1* fails to restore stomatal conductance back to wildtype (WT) levels. a,** Representative images of leaf transverse cross-sections (30 µm thickness) of 3-4 week-old segregated mesophyll-specific enhancer-trap line JR11-2[5] backcrossed into Arabidopsis Col-0 background[6], JR11-2 in *gad2-1* background (JR11-2*/gad2-1*) and JR11-2*/gad2-1* expressing *UAS::GAD2Δ* (JR11-2*/gad2-1*/*UAS::GAD2Δ*), similar images were obtained from all examined lines, scale bars = 100 µm. GFP fluorescence shown in green indicates cells in which *GAD2* expression will be activated by the yeast transcription factor GAL4, blue indicates chlorophyll autofluorescence. **b,** Reverse-transcriptional PCR quantification of native *GAD2* mRNA (*GAD2mRNA*), *GAD2Δ* driven by *UAS* element (*UAS::GAD2Δ*), *GFP* and *Actin2* transcripts in Arabidopsis WT (Col-0), JR11-2 (Col-0), JR11-2*/gad2-1* and JR11-2*/gad2-1*/*UAS::GAD2Δ* plants, *Actin2* used as an internal control; similar results were obtained from three independent biological replicates. **c-d,** Leaf GABA concentration (**c**) and stomatal conductance (**d**) of 5-6 week-old Arabidopsis WT (Col-0), JR11-2 (Col-0), JR11-2*/gad2-1* and JR11-2*/gad2-1*/*UAS::GAD2Δ* plants, stomatal conductance was measured by AP4 Leaf Porometer (**d**); n = 12 (**c**); n = 25 for WT and JR11-2, n = 21

for JR11-2*/gad2-1* and n = 24 for JR11-2*/gad2-1*/*UAS::GAD2Δ*, data collected from two different batches of plants (**d**). All data are plotted with box and whiskers plots: whiskers plot represents minimum and maximum values, and box plot represents second quartile, median and third quartile (**c, d**); statistically differences were determined by One-way ANOVA by comparing with JR11-2 (**c, d**), *P< 0.05 and ****P< 0.0001.

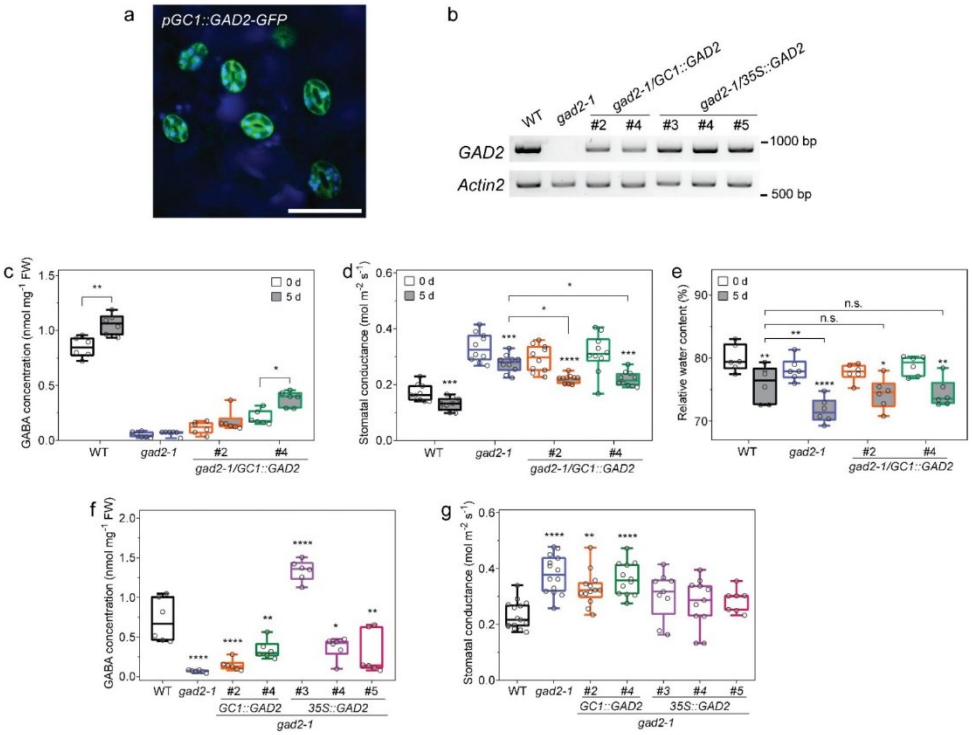

Supplementary Figure 11. Guard-cell specific expression of full-length *GAD2* only reduces the stomatal conductance of *gad2* knockout plants under drought. **a,** Representative confocal image of *gad2*-1 leaves expressing full-length *GAD2* tagged with *GFP* driven by *GC1* promoter (*GC1::GAD2-GFP*), similar images were obtained from all *gad2-1*/ *GC1::GAD2-GFP* plants examined, scale bar = 50 µm. **b,** Reverse-transcriptional PCR quantification of *GAD2* transcripts in wildtype (WT), *gad2-1* and *gad2-1* complementation with full-length *GAD2* driven by guard-cell promoter *GC1* (*gad2-1/GC1::GAD2* #2 and #4) or by a pro35S-CAMV constitutive promoter (*gad2-1/35S::GAD2* #3, #4 and #5), *Actin2* used as an internal control; similar results were obtained from three independent biological replicates. **c-e,** Leaf GABA concentration, stomatal conductance and relative water content of Arabidopsis WT, *gad2-1*, *gad2-1/GC1::GAD2* #2 and #4 plants; n = 6 plants for GABA measurement before (0 d) and after drought treatment for 5 days (5 d) as indicated

(**c**); the stomatal conductance of 5-6 week-old plants was determined by AP4 Leaf Porometer at 0 d and 5 d after drought treatment, n = 9 for WT and n = 10 for *gad2-1*, *gad2-1/GC1::GAD2* #2 and #4 (**d**); relative leaf water content of corresponding leaf samples at 0 d and 5 d after drought treatment, as shown in (**e**). **f-g,** Leaf GABA concentration and stomatal conductance of WT, *gad2-1*, *gad2-1/GC1::GAD2* #2, #4, *gad2-1/35S::GAD2* #3, #4 and #5 plants; n = 6 plants (**f**); the stomatal conductance of WT, *gad2-1*, and *gad2-1* complementation lines; stomatal conductance of 5-6 week-old plants was determined by AP4 Leaf Porometer in normal conditions, n = 15 plants for WT, n = 14 for *gad2-1*, n = 13 for *gad2-1/GC1::GAD2* #2, n = 12 for *gad2-1/GC1::GAD2* #4, n = 9 for *gad2-1/35S::GAD2* #3, n = 11 for *gad2-1/35S::GAD2* #4 and n = 7 for *gad2-1/35S::GAD2* #5 (**g**). All data are plotted with box and whiskers plots: whiskers plot represents minimum and maximum values, and box plot represents second quartile, median and third quartile (**c-g**); statistically differences were determined by One-way ANOVA by comparing with WT (**f, g**), or within genotypes or treatment by Two-way ANOVA (**c-e**), $^{*}P < 0.05$, $^{**}P < 0.01$, $^{***}P < 0.001$ and $^{****}P < 0.0001$.

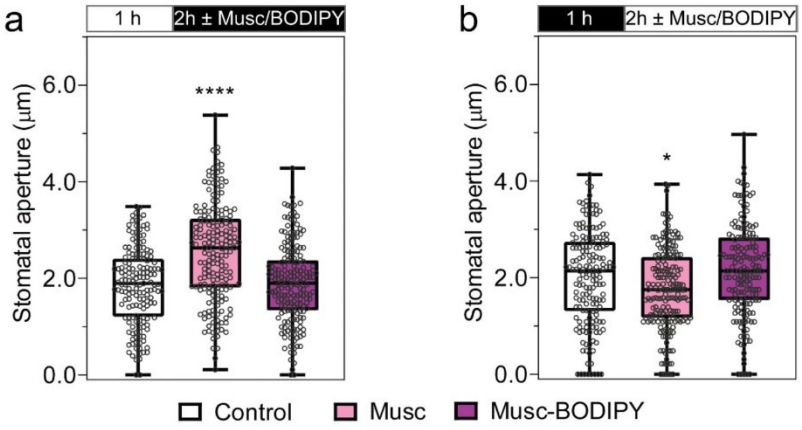

Supplementary Figure 12. Membrane impermeable muscimol does not antagonises stomatal movement initiated by light and dark treatments a-b, Exogenous muscimol-BODIPY application does not affect stomatal movement. Epidermal strips were pre-incubated in stomatal measurement buffer for 1 h under light (**a**) or dark (**b**), followed by 2 h incubation under light-to-dark transition (**a**) or dark-to-light transition (**b**) as indicated above graphs by black (dark) or white (light) bars, together with the application of 10 µM muscimol (Musc) or muscimol-BODIPY (Musc-BODIPY); n = 161 for control, n = 185 for muscimol and n = 188 for muscimol-BODIPY (**c**); n = 168 for control, n = 190 for muscimol and n = 175 for muscimol-BODIPY. All data are plotted with box and whiskers plots: whiskers plot represents minimum and maximum values, and box plot represents second quartile, median and third quartile (**a-b**); statistical difference was determined by One-way ANOVA, *P<0.05 and ****P<0.0001.

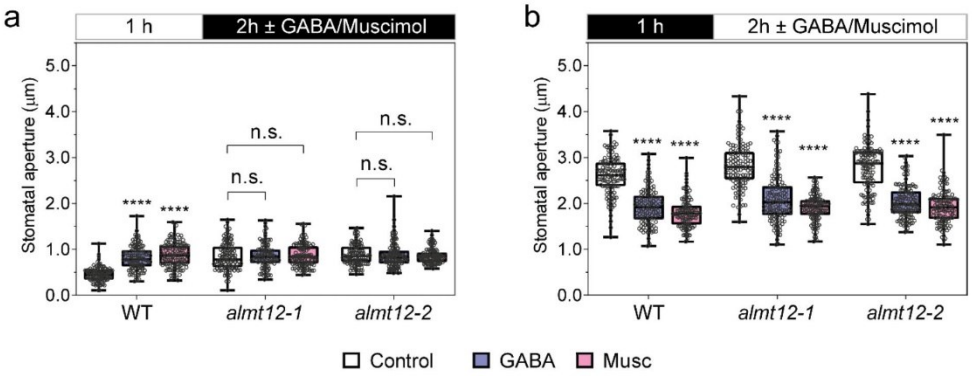

Supplementary Figure 13. Stomatal aperture measurement of WT, *almt12-1* and *almt12-2* knockout plants in response to dark or light. Epidermal strips were pre-incubated in stomatal measurement buffer for 1 h in the light (**a**) or dark (**b**), followed by 2 h incubation in the dark (**a**) or light (**b**) as indicated by black (dark) or white (light) bars above the plots ± 2 mM GABA or 10 µM muscimol (Musc); n = 105 for WT (control), n = 115 for *almt12-1* (control), n = 122 for *almt12-2* (control), n = 122 for WT (GABA), n = 100 for *almt12-1* (GABA), n = 131 for *almt12-2* (GABA), n = 122 for WT (Musc), n = 107 for *almt12-1* (Musc) and n = 118 for *almt12-2* (Musc) (**a**); n = 116 for WT (control), n = 119 for *almt12-1* (control), n = 120 for *almt12-2* (control), n = 113 for WT (GABA), n = 123 for *almt12-1* (GABA), n = 124 for *almt12-2* (GABA), n = 117 for WT (Musc), n = 122 for *almt12-1* (Musc) and n = 116 for *almt12-2* (Musc) (**b**). All data are plotted with box and whiskers plots: whiskers plot represents minimum and maximum values, and box plot represents second quartile, median and third quartile; statistical difference was determined using Two-way ANOVA, ****$P < 0.0001$; all experiments were repeated at least twice from different batches of plants with blind treatments.

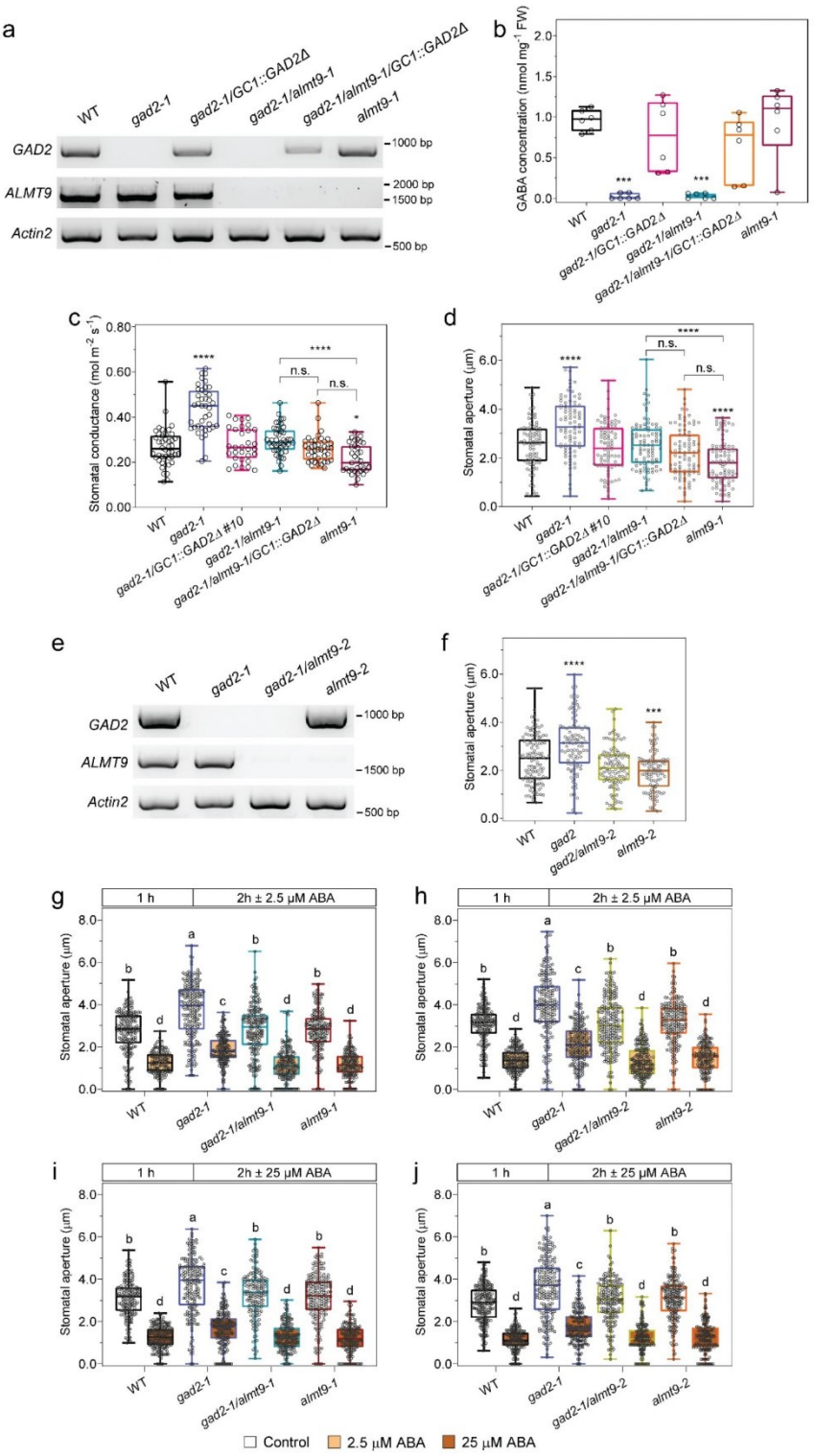
a
WT
gad2-1
gad2-1/GC1::GAD2Δ
gad2-1/almt9-1
gad2-1/almt9-1/GC1::GAD2Δ
almt9-1
GAD2
ALMT9
Actin2
1000 bp
2000 bp
1500 bp
500 bp
b
GABA concentration (nmol mg-1 FW)
c
Stomatal conductance (mol m-2 s-1)
d
Stomatal aperture (µm)
gad2-1/GC1::GAD2Δ#10
n.s.
e
gad2-1/almt9-2
almt9-2
f
gad2
gad2/almt9-2
g
h
i
j
1 h
2h ± 2.5 µM ABA
2h ± 25 µM ABA
Control
2.5 µM ABA
25 µM ABA

Supplementary Figure 14. The loss of *ALMT9* rescues the larger stomatal aperture and ABA response of *gad2* knockout plants. a, Reverse-transcriptional PCR quantification of *GAD2*, *ALMT9* and *Actin2* transcripts in Arabidopsis wildtype (WT), *gad2-1*, *gad2-1/GC1::GAD2Δ* #10, *gad2-1/almt9-1*, *gad2-1/almt9-1/GC1::GAD2Δ* and *almt9-1* plants, *Actin2* used as an internal control; similar results were obtained from three independent biological replicates. **b-d,** Leaf GABA accumulation, stomatal conductance and aperture of WT, *gad2-1*, *gad2-1/GC1::GAD2Δ* #10, *gad2-1/almt9-1*, *gad2-1/almt9-1/GC1::GAD2Δ* and *almt9-1* plants. The whole rosette leaves of 5-6 week-old plants were harvested for GABA measurement (**b**) and used for stomatal conductance measurement, as determined by AP4 porometer; n = 6 plants (**b**); n = 42 for WT, n = 40 for *gad2-1*, n = 31 for *gad2-1/GC1::GAD2Δ* #10, n = 45 for *gad2-1/almt9-1*, n = 40 for *gad2-1/almt9-1/GC1::GAD2Δ* and n = 35 for *almt9-1*, data collected from four independent batches of plants (**c**). Epidermal strips were peeled and incubated in stomatal measurement buffer for 2 h under light before measurement; n = 86 for WT, *gad2-1*, *gad2-1/GC1::GAD2Δ* #10 and *almt9-1*, n = 95 for *gad2-1/almt9-1* and n = 87 for *gad2-1/almt9-1/GC1::GAD2Δ* (**d**). **e,** Reverse-transcriptional PCR quantification of *GAD2*, *ALMT9* and *Actin2* transcripts in WT, *gad2-1*, *gad2-1/almt9-2* and *almt9-2* plants, *Actin2* used as an internal control; similar results were obtained from three independent biological replicates. **f,** Stomatal aperture of WT (n = 115), *gad2-1* (n = 100), *gad2-1/almt9-2* (n = 106) and *almt9-2* (n = 104) plants; epidermal strips were incubated under light for 2 h before measurement. **g-j**, Stomatal response to ABA of Arabidopsis wildtype (WT), *gad2-1*, *gad2-1/almt9-1*, *almt9-1*, *gad2-1/almt9-2* and *almt9-2* plants. Epidermal strips were pre-incubated in stomatal measurement buffer for 1 h under light, followed by 2 h treatment under light with or without 2.5 μM or 25 μM ABA as indicated; n = 189 (control) and n = 145 (ABA) for WT, n = 208 (control)

and n = 192 (ABA) for *gad2-1*, n = 200 (control) and n = 183 (ABA) for *gad2-1/almt9-1*, n = 182 (control) and n = 181 (ABA) for *almt9-1* (**g**); n = 184 (control) and n = 186 (GABA) for WT, n = 188 (control) and n = 207 (ABA) for *gad2-1*, n = 222 (control) and n = 224 (ABA) for *gad2-1/almt9-2*, n = 197 (control) and n = 182 (ABA) for *almt9-2* (**h**); n = 172 (control) and n = 196 (ABA) for WT, n = 190 (control) and n = 182 (ABA) for *gad2-1*, n = 162 (control) and n = 183 (ABA) for *gad2-1/almt9-1*, n = 192 (control) and n = 181 (ABA) for *almt9-1* (**i**); n = 215 (control) and n =178 (ABA) for WT, n = 197 (control) and n = 174 (ABA) for *gad2-1*, n = 189 (control) and n = 174 (ABA) for *gad2-1/almt9-2*, n = 195 (control) and n =180 (ABA) for *almt9-2* (**j**). All data are plotted with box and whiskers plots: whiskers plot represents minimum and maximum values, and box plot represents second quartile, median and third quartile (**b-d, f, g-i**); statistically differences were determined by One-way ANOVA, *$P < 0.05$, ***$P < 0.001$ and ****$P < 0.0001$ (**b-d, f**), or by Two-way ANOVA, a, b, c and d represent data groups that are not statistically different, $P < 0.05$ (**g-i**).

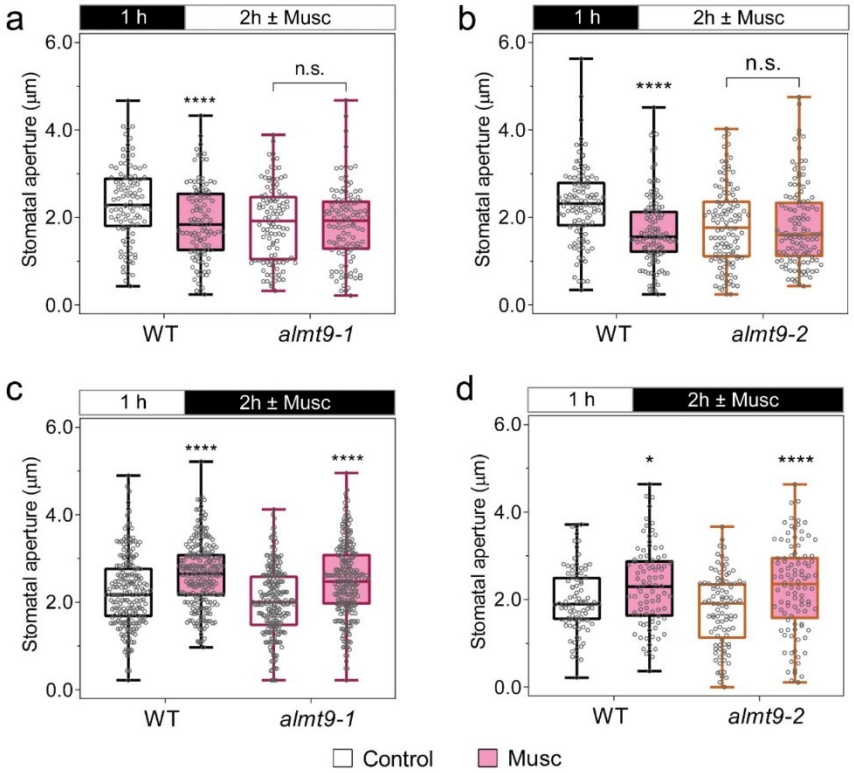

Supplementary Figure 15. *almt9* knockouts abolish muscimol-inhibition of stomatal opening but not affect closure. a-d, Stomatal aperture of wildtype (WT) and *almt9* knockout plants in response to dark or light. Epidermal strips were pre-incubated in stomatal measurement buffer for 1 h under dark (**a-b**) or light (**c-d**), followed by light (**a-b**) or dark (**c-d**) for 2 h as indicated by black (dark) or white (light) bars above graphs, ± 10 µM muscimol (Musc); n = 105 for WT and n = 106 for *almt9-1* with control treatment, n = 106 for WT and n = 111 for *almt9-1* with muscimol treatment (**a**); n = 88 for wildtype (WT) (control); n = 108 for WT (control), n = 116 for *almt9-2* (control), n = 119 for WT (muscimol) and n = 121 for *almt9-2* (muscimol) (**b**); n = 210 for WT and n = 233 for *almt9-1* with control treatment, n = 240 for WT and n = 245 for *almt9-1* with muscimol treatment (**c**); n = 88 for WT (control), n = 96 for *almt9-2* (control), n = 90 for WT (muscimol) and n = 100 for *almt9-2* (muscimol) (**d**); all

experiments were repeated at least twice from different batches of plants with blind treatments (**a-d**). All data are plotted with box and whiskers plots: whiskers plot represents minimum and maximum values, and box plot represents second quartile, median and third quartile (**a-d**); statistically differences were determined by Two-way ANOVA (**a-d**), $*P < 0.05$ and $****P < 0.0001$.

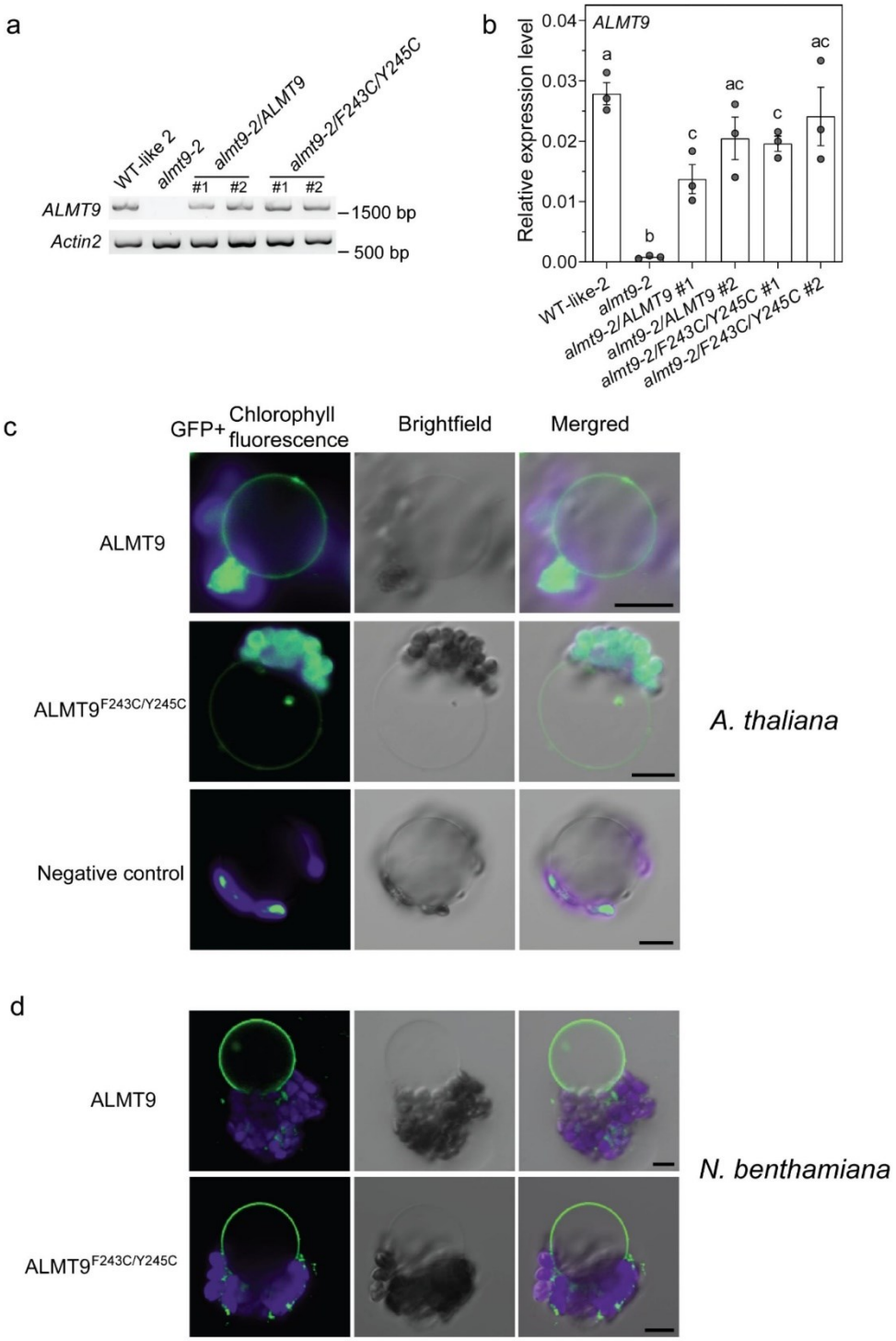
a
WT-like 2
almt9-2
almt9-2/ALMT9
almt9-2/F243C/Y245C
#1 #2 #1 #2
ALMT9
Actin2
–1500 bp
– 500 bp
b
ALMT9
Relative expression level
0.04
0.03
0.02
0.01
0.00
a
b
c
ac
c
ac
WT-like-2
almt9-2
almt9-2/ALMT9 #1
almt9-2/ALMT9 #2
almt9-2/F243C/Y245C #1
almt9-2/F243C/Y245C #2
c
GFP+ Chlorophyll fluorescence
Brightfield
Mergred
ALMT9
ALMT9F243C/Y245C
Negative control
A. thaliana
d
ALMT9
ALMT9F243C/Y245C
N. benthamiana

Supplementary Figure 16. *ALMT9* and *ALMT9*$^{F243C/Y245C}$ show similar expression in *almt9-2* complementation lines and both are present on the tonoplast membrane. a-b, Reverse-transcriptional PCR (**a**) and quantitative real-time PCR (**b**) of *ALMT9* and *Actin2* transcripts in WT-like 2, *almt9-2*, *almt9-2/ALMT9* and *almt9-2/*F243C/Y245C plants. Similar results were obtained from three independent biological replicates (**a**); n = 3 plants and data represented by mean ± s.e.m, statistical difference was determined by two-sided Student's *t*-test, a, b and c represent data groups that are not statistically different, $P < 0.05$ (**b**). **c-d,** Subcellular localisation of ALMT9 and ALMT9$^{F243C/Y245C}$ in Arabidopsis (**c**) and *N. benthamiana* (**d**). Representative confocal image of ALMT9 and ALMT9$^{F243C/Y245C}$ tagged with GFP in the mesophyll protoplasts of *almt9-2/ALMT9* and *almt9-2/*F243C/Y245 complementation lines, repeated on 3 occasions with consistent results (**c**), or transiently expressed in *N. benthamiana* by Agrobacterium infiltration, repeated on 3 occasions with consistent results (**d**); the mesophyll protoplasts of wildtype (WT) Arabidopsis leaves were imaged as control (**c**), using the exact same setting to capture the fluorescence of GFP-tagged ALMT9 and ALMT9$^{F243C/Y245C}$. The mesophyll protoplasts were prepared and lysis as described[7, 8], GFP fluorescence (green) and chlorophyll autofluorescence (purple) captured by Nikon A1R Laser Scanning Confocal (**c, d**).

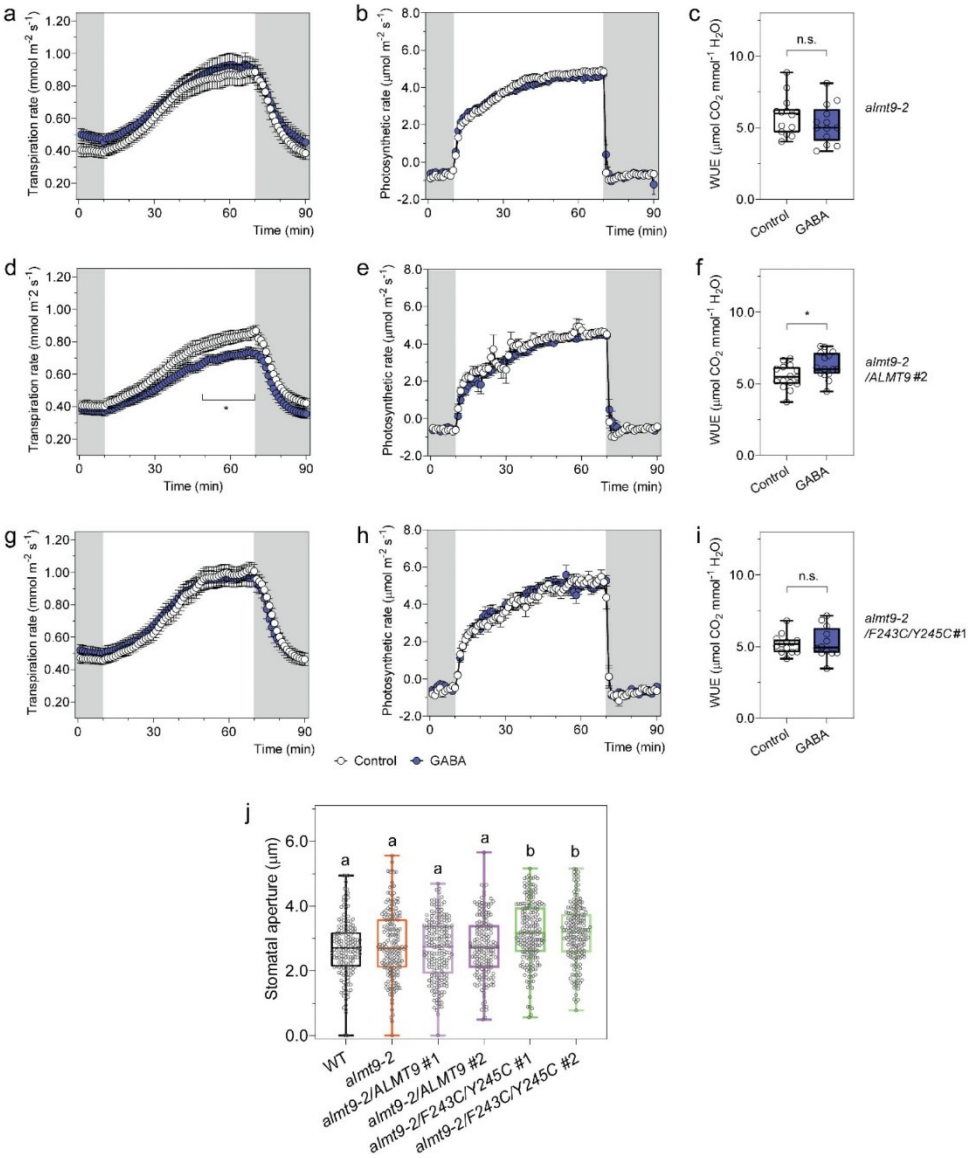

Supplementary Figure 17. *ALMT9* complementation but not by *ALMT9*$^{F234C/245C}$. **a-i**, Transpiration, photosynthetic rate and WUE of detached leaves from Arabidopsis *almt9-2* (**a-c**), *almt9-2/ALMT9* #2 (**d-f**) and *almt9-2/*F243C/Y245C #1 (**g-i**) fed with artificial xylem sap solution ± 4 mM GABA using a LiCor LI-6400XT. The WUE of *almt9-2* (**c**), *almt9-2/ALMT9* #2 (**f**) and *almt9-2/*F243C/Y245C #1 (**i**) was calculated the ratio of photosynthetic rate (**b, e, h**) versus transpiration rate (**a, d, g**); n = 14 (control)

and n = 13 (GABA) for *almt9-2* (**a-c**); n = 15 (control and GABA) for *almt9-2/ALMT9* #2 (**d-f**); n = 13 (control) and n = 12 (GABA) for *almt9-2*/F243C/Y245C #1 (**g-i**). **j**, Stomatal aperture of WT, *almt9-2* and complementation lines. Epidermal strips were peeled and incubated in stomatal measurement buffer for 2 h under light before measurement; n = 164 for WT, n = 185 for *almt9-2*, n = 190 for *almt9-2/ALMT9* #1, n = 169 for *almt9-2/ALMT9* #2, n = 198 for *almt9-2*/F243C/Y245C #1 and n = 186 for *almt9-2*/F243C/Y245C #2 (**j**). All data are plotted with box and whiskers plots: whiskers plot represents minimum and maximum values, and box plot represents second quartile, median and third quartile (**c, f, i, j**); or data are represented by means ± s.e.m (**a, b, d, e, g, h**); statistically differences were determined by two-sided Student's *t*-test (**a-i**), $^*P < 0.05$; or by One-way ANOVA, a and b represent data groups that are not statistically different, $P < 0.05$ (**j**).

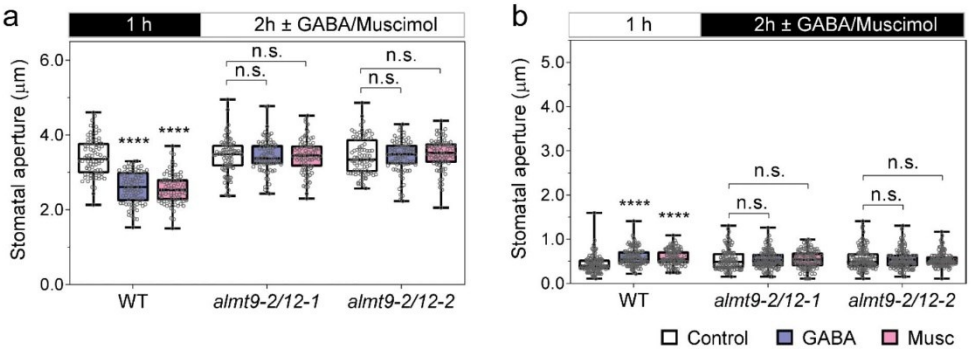

Supplementary Figure 18. The loss of *ALMT9* and *ALMT12* impairs both stomatal opening and closure sensitivity to GABA. Epidermal strips were pre-incubated in stomatal measurement buffer for 1 h in the dark (**a**) or light (**b**), followed by 2 h incubation in the light (**a**) or dark (**b**) as indicated by black (dark) or white (light) bars above the plots ± 2 mM GABA or 10 µM muscimol (Musc); n = 78 for WT (control), n = 82 for *almt9-2/12-1* (control), n = 83 for *almt9-2/12-2* (control), n = 77 for WT (GABA), n = 77 for *almt9-2/12-1* (GABA), n = 81 for *almt9-2/12-2* (GABA), n = 75 for WT (Musc), n = 81 for *almt9-2/12-1* (Musc) and n = 81 for *almt9-2/12-2* (Musc) (**a**); n = 114 for WT (control), n = 104 for *almt9-2/12-1* (control), n = 120 for *almt9-2/12-2* (control), n = 113 for WT (GABA), n = 114 for *almt9-2/12-1* (GABA), n = 123 for *almt9-2/12-2* (GABA), n = 107 for WT (Musc), n = 106 for *almt9-2/12-1* (Musc) and n = 127 for *almt9-2/12-2* (Musc) (**b**). All data are plotted with box and whiskers plots: whiskers plot represents minimum and maximum values, and box plot represents second quartile, median and third quartile; statistical difference was determined using Two-way ANOVA, ****$P < 0.0001$; all experiments were repeated at least twice from different batches of plants with blind treatments.

References

1. Desikan R, Cheung MK, Bright J, Henson D, Hancock JT, Neill SJ. ABA, hydrogen peroxide and nitric oxide signalling in stomatal guard cells. *J Exp Bot* **55**, 205-212 (2004).

2. Melotto M, Underwood W, Koczan J, Nomura K, He SY. Plant stomata function in innate immunity against bacterial invasion. *Cell* **126**, 969-980 (2006).

3. Conn SJ*, et al.* Protocol: optimising hydroponic growth systems for nutritional and physiological analysis of *Arabidopsis thaliana* and other plants. *Plant Methods* **9**, 4 (2013).

4. Sánchez JP, Duque P, Chua NH. ABA activates ADPR cyclase and cADPR induces a subset of ABA-responsive genes in Arabidopsis. *Plant J* **38**, 381-395 (2004).

5. Martí MC, Stancombe MA, Webb A. Cell-and stimulus-type-specific intracellular-free Ca^{2+} signals in *Arabidopsis thaliana*. *Plant Physiol*, **163,** 625-634 (2013).

6. Svozil J, Gruissem W, Baerenfaller K. Proteasome targeting of proteins in Arabidopsis leaf mesophyll, epidermal and vascular tissues. *Front Plant Sci* **6**, 376 (2015).

7. De Angeli A, Zhang J, Meyer S, Martinoia E. AtALMT9 is a malate-activated vacuolar chloride channel required for stomatal opening in Arabidopsis. *Nat Commun* **4**, 1804 (2013).

8. Yoo S-D, Cho Y-H, Sheen J. Arabidopsis mesophyll protoplasts: a versatile cell system for transient gene expression analysis. *Nat Protoc* **2**, 1565 (2007).

Brief discussion

The data presented in this publication demonstrate that GABA is a signalling molecule in plants through revealing a role in modulating stomatal pore movement in response to stimuli, including ABA, light, and drought. Furthermore, it was unveiled that the important role of GABA in improving plant acclimation to drought stress was enacted through a genetic interaction with ALMT9, and that guard cell derived GABA synthesis is required in such process. As such it corroborated the role of ALMT in transducing GABA signals in plants.

This work raises several questions:

1. It was shown that GABA negatively regulates ALMT9 to reduce stomatal opening, but how does the release of the GABA-ALMT9 interaction through mutation of the putative GABA-binding site in ALMT9 lead to a similar stomatal phenotype as *gad2*?
2. What is the scenario for the GABA-ALMT12 interaction, does this alter stomatal closure?
3. GABA deficiency appears positively correlated with more open stomata; however, this has been examined so far in only single (*gad2*) and double (*gad1/gad2*) mutants (Mekonnen et al. 2016, Xu et al. 2021). There are 5 homologues of *GAD* identified in *Arabidopsis*, do they also contribute to the modulation of stomatal movement?
4. Exogenous GABA impaired ABA induced stomatal closure on epidermal strips. Does GABA deficiency lead to altered ABA sensitivity in intact leaves? How does GABA interact with ABA to modulate stomatal regulation?

In the following chapter I will conduct experiments to further examine the role of the ALMT9-GABA interaction in stomatal opening and build resources to address the question for

ALMT12, to answer question 1 and 2. And then concentrate on question 3 and 4 in Chapter IV and V, respectively.

Chapter III ALMT9-mediated GABA inhibition of light induced stomatal opening: a focused study

Introduction

Stomatal guard cell movement, which results in the opening and closing of the stomatal pore, is driven by change in guard cell osmolarity (Sussmilch et al. 2019). Guard cell ALMTs are involved in both stomatal opening and closing processes (Meyer et al. 2010, Meyer et al. 2011, De Angeli et al. 2013b, Zhang 2014, Eisenach et al. 2017). Ablation of *ALMT9* function impairs light induced stomatal opening; whilst ablation of *ALMT12* reduced dark induced stomatal closure (Meyer et al. 2010, De Angeli et al. 2013b). Light dependent changes in stomatal pore aperture is antagonized by exogenous application of GABA (Xu et al. 2021). Xu et al (2021) showed that both ALMT12 and ALMT9 are potentially targeted by GABA during stomatal regulation, as outlined in Chapter II.

A 12 amino-acid residue motif within plant ALMTs, that shares homology with the GABA binding motif from mammalian ionotropic $GABA_A$ receptors, contributes to GABA sensitivity (Ramesh et al. 2015, Ramesh et al. 2018, Long et al. 2020). Expression of site-directed mutants of ALMTs within this motif, mutations of the first and/or second aromatic amino acid residues to a cysteine, resulted in the lack of negative regulation of anion transport by and of GABA by ALMTs when assayed in *Xenopus laevis* oocytes (Ramesh et al. 2015, Ramesh et al. 2018, Long et al. 2020). Here, we attempt to corroborate whether mutation of this motif results in a functional ion transport protein that lacks GABA sensitivity. This was achieved by comparing the GABA sensitivity of plants expressing the putative GABA-insensitive ALMTs with those expressing the standard unmutated ALMT. We perform these studies *in planta* to provide data on GABA regulation of ALMT within the native environment

to give it a physiological context, specifically in the regulation of stomata pore aperture and stomatal conductance. In this chapter, such an attempt was made for *ALMT9*. Physiological experiments focused on *almt9-2*/*35S::ALMT9* and *almt9-2*/*35S::A*LMT9^{F243CY245C}. Note, the data contained within this chapter on ALMT9 are foundational to, and extend upon, those shown in Chapter II.

Results

Complementation assays of *almt9* mutant lines by *35S::ALMT9* and *35S::ALMT9*^{F243CY245C}

To construct complementation lines via floral dip mediated transformation, the *almt9* mutant lines were firstly genotyped and found to be a homozygous knockout lines (Fig. 1). The pART27 vector carries the *neomycin phosphotransferase II* (*nptII*) gene, which confers transformed plants resistance to kanamycin (Gleave 1992). *almt9-1* (SALK_055490) is from the SALK seed collection, which harbour T-DNA insertional mutations using the pBIN-pROK2 vector with kanamycin resistance (Fig. 1A) (Alonso et al. 2003). Another allele, *almt9-2* (WiscDsLox499H09) was generated using the T-DNA vector pDs-Lox, conferring plants with BASTA and hygromycin resistance (Fig. 1A) (Woody et al. 2007). Despite the common resistance to kanamycin of *almt9-1* and pART27-nptII, this was used in addition to *almt9-2*, given that the transgenic lines harbouring a GFP tag could conceivably be selected via fluorescence. The use of fluorescence as a screening tool for the transgenic lines was confirmed, but for an unknown reason the fluorescence in *almt9-1* lines selected was weak comparing to the autofluorescence background and more diffuse observed

under confocal microscope (Suppl. Fig. 3A and Suppl. Fig. 4A), which led to higher false detection rate when confirmed by genotyping using PCR (Suppl. Fig. 3B). Therefore, homozygous transgenic lines of only *almt9-2* were progressed further for phenotyping experiments (Suppl. Fig. 4).

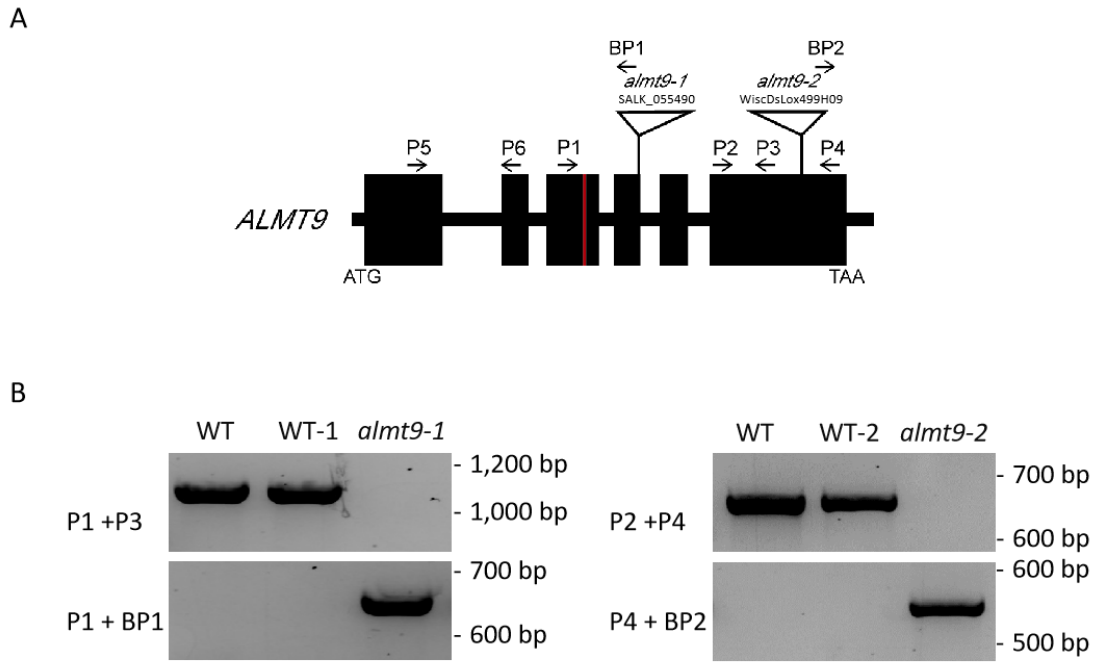

Figure 1. Confirmation of *ALMT9* T-DNA insertion in *almt9* mutants.

A. Schematic of *ALMT9* gene and insertion sites of the *almt9-1* and *almt9-2.* The putative GABA-binding motif is marked in red. Primers were designed to flank both the insertion site and the putative GABA-binding motif to genotype complementation lines. **B.** Genotyping result on agarose gel. *almt9* mutant lines are genotyped using primers (*ALMT9* gene specific primers P 1-4, and insertion sequence border primers, BP 1-2). Both WT and corresponding wild types of mutant lines were used as control.

Stomatal conductance of *almt9-2/35S::ALMT9* and *almt9-2/35S::ALMT9*^{F243CY245C}

For physiological experiments, WT-like-2 were used, which is an out-crossed wild type like line whilst screening for homozygous *almt9-2* plants (i.e. does not contain the T-DNA insertion) (De Angeli et al. 2013b). This makes a more suitable control than the WT genotype as the ancestral line went through the transformation process. Expression of *ALMT9* in homozygous transgenic lines were checked by both reverse-transcriptional PCR (RT-PCR) (Fig. 2A) and quantitative real-time PCR (qPCR) (Fig. 2B). Expression of *ALMT9* and *ALMT9*^{F243CY245C} were detected from cDNA of corresponding complemented lines (Fig. 2A). This was also confirmed in qPCR, where expression level of *ALMT9* and *ALMT9*^{F243CY245C} in complemented lines were significantly higher than that of *almt9-2* (Fig. 2B). The result of both analyses indicated *ALMT9* and *ALMT9*^{F243CY245C} had been successfully restored into transgenic lines.

For physiological experiments, initially, stomatal conductance of *almt9-2/35S::ALMT9* and *almt9-2/35S::ALMT9*^{F243CY245C} were measured comparing to that of WT-like-2 and *almt9-2* (Fig. 3). The data were collected at two separate times, either 2.5 hr after the start of the light period (Fig. 3A), or after 5 hr (Fig. 3B). This was selected as being either ¼ or ½ into the light period, given the role of ALMT9 in light induced stomatal opening and the potential influence of circadian rhythms on stomatal movement (Dodd et al. 2004, De Angeli et al. 2013b). The result showed that at the earlier stage of light period, stomatal conductance was similar across all plant lines except for *almt9-2*, which had significantly lower stomatal conductance than the control WT-like-2 (Fig. 3A). At the middle of the light period, where

stomatal conductance is likely to be at its peak and have reached steady state, *almt9-2* had a similar level of stomatal conductance to that of WT-like-2 and *almt9-2*/*35S:ALMT9* lines (Fig. 3B). Meanwhile, both lines of *almt9-2/35S::ALMT9*^{F243CY245C} showed significantly higher stomatal conductance than that of the rest of genotypes (Fig. 3B).

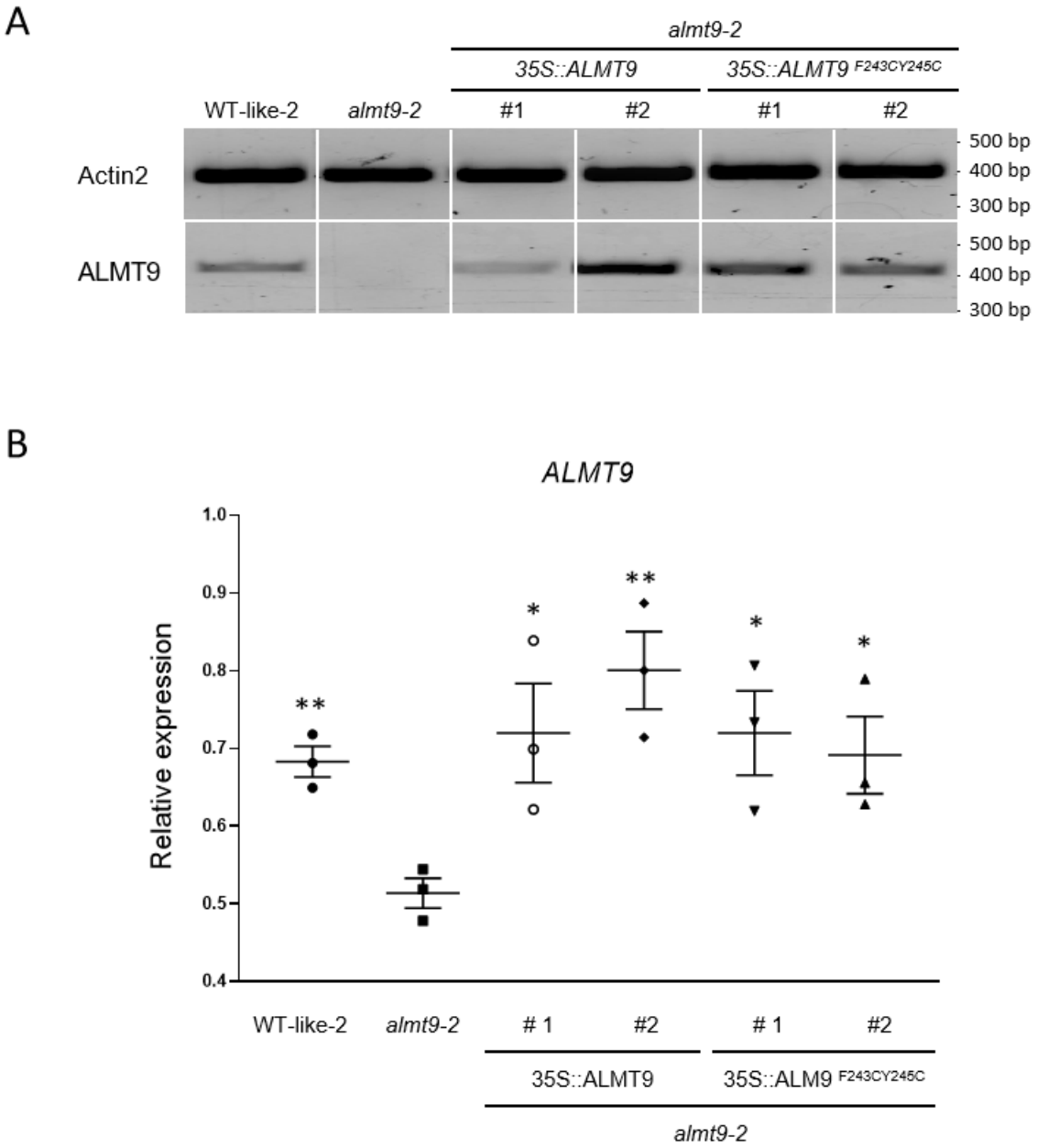

Figure 2. Expression of *ALMT9* / *ALMT9*^{F243CY245C} in the *almt9-2* background.

A. Semi-qPCR of *ALMT9* expression in WT, *almt9-2/35S::ALMT9* and *almt9-2/35S::ALMT9*^{F243CY245C}. 25-cycles were used for each cDNA sample. *Actin2* (AT3G18780) was used as an internal control. **B.** qPCR analysis of *ALMT9* expression in WT, *almt9-2/35S::ALMT9* and *almt9-2/35S::ALMT9*^{F243CY245C} using primers (P5-P6) in Fig. 1A. Expression level was normalised to that of *Actin2* (AT3G18780). Hashtag numbers indicates T4 plants originated from varied T1 plants. Asterisks represent statistical significance comparing expression of *ALMT9* in all genotypes comparing to that of *almt9-2* after one-way ANOVA analysis. F (5, 12) = 4.245, p=0.0187, η^2= 0.2119 (p<0.05 *, p<0.01 **, n=3).

A

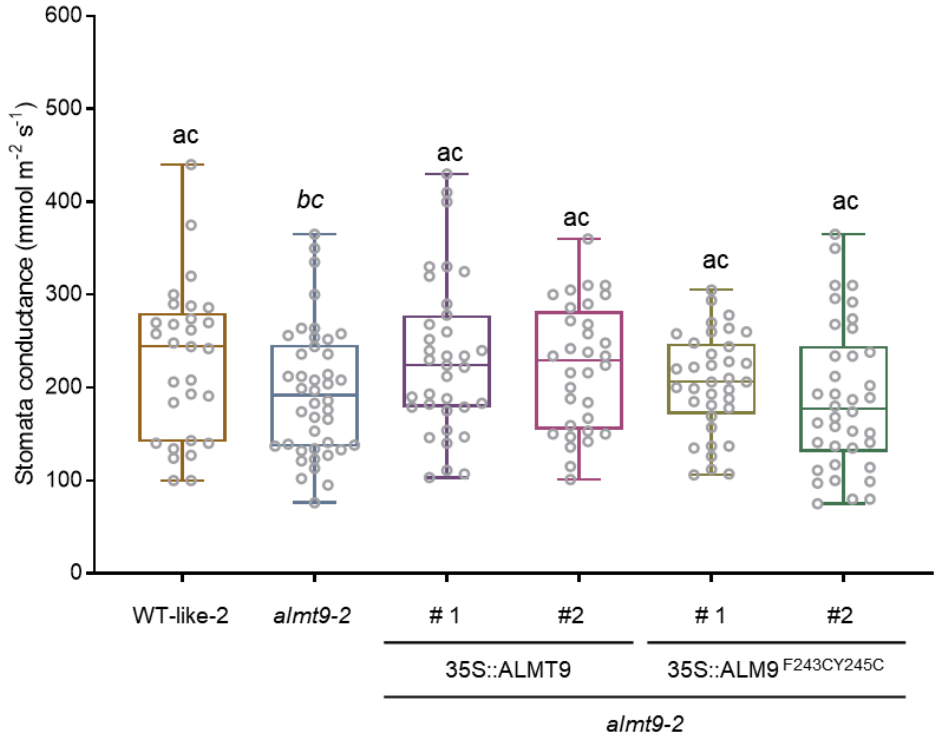
Stomata conductance (mmol m-2 s-1)
600
500
400
300
200
100
0
ac
bc
ac
ac
ac
ac
WT-like-2
almt9-2
1
#2
1
#2
35S::ALMT9
35S::ALM9 F243CY245C
almt9-2

B

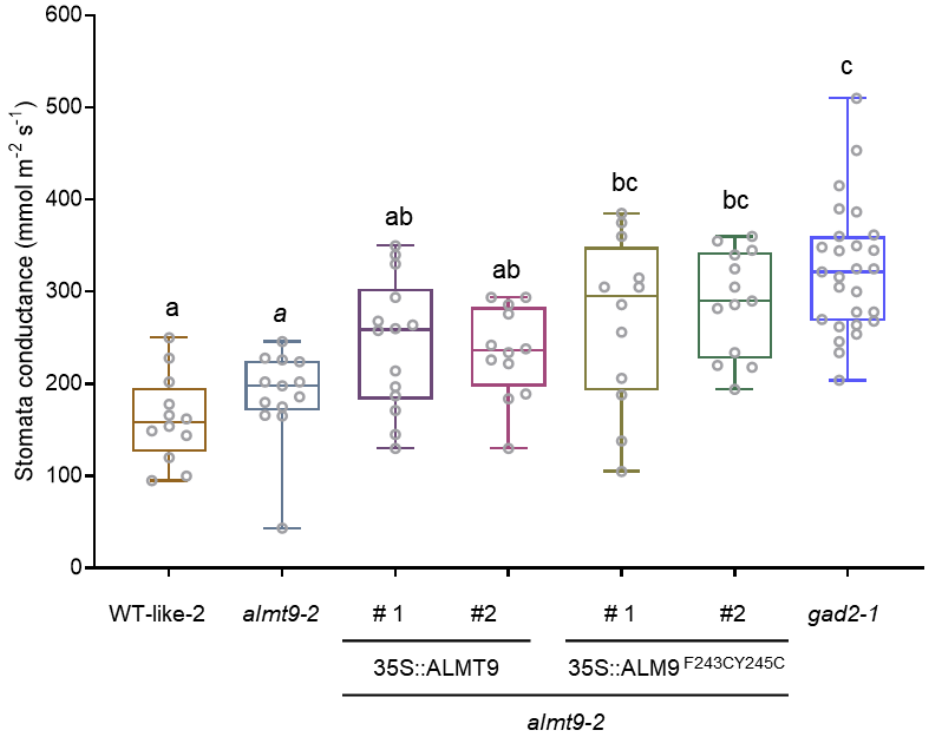
Stomata conductance (mmol m-2 s-1)
600
500
400
300
200
100
0
a
a
ab
ab
bc
bc
c
WT-like-2
almt9-2
1
#2
1
#2
gad2-1
35S::ALMT9
35S::ALM9 F243CY245C
almt9-2

Figure 3. Stomatal conductance of *almt9-2* and complementation lines expressing *ALMT9* and *ALMT9^{F243CY245C}*.

A. Stomatal conductance of *almt9-2/35S::ALMT9* and *almt9-2/35S::ALMT9^{F243CY245C}* measured 2.5 hr after the light is on, n=12 for WT-2, n=12 for *almt9-2*, n=14 for *almt9-2/35S::ALMT9* #1, n=12 for *almt9-2/35S::ALMT9* #2, n=12 for *almt9-2/35S::ALMT9^{F243CY245C}* #1, n=13 for *almt9-2/35S::ALMT9^{F243CY245C}* #2. The top panel indicated the time where stomatal conductance was measured (A- 2.5 hr) **B.** Stomatal conductance of *almt9-2/35S::ALMT9* and *almt9-2/35S::ALMT9 ^{F243CY245C}* measured 5 hr after the light is on, *n* = 12 for WT-like 2, *almt9-2/ALMT9* #2 and *almt9-2/*F243C/Y245C #1, *n* = 13 for *almt9-2*, *almt9-2/ALMT9* #1 and *almt9-2/*F243C/Y245C #2, *n* = 27 for *gad2-1*. For each genotype, 4-5 biological replicate plants were measured. Asterisks represent statistical significance comparing between genotypes after one-way ANOVA. Light induced stomatal movement in epidermal peels of the complementation plants. *Note: Figure 6B is presented as Fig 9 in Chapter II (Xu et al. 2021).*

Stomatal aperture of *almt9-2/35S::ALMT9* and *almt9-2/35S::ALMT9*^{F243CY245C} in response to light induced stomatal opening

The result above suggests that mutation of the putative GABA binding site within ALMT9 led to an eventual increased stomatal conductance, phenocopying *gad2* (Fig 3B; also presented by Xu et al. 2021). Further experiments were conducted with epidermal strip assays on Wildtype-like-2, *almt9-2, almt9-2/35S::ALMT9* and *almt9-2/35S::ALMT9^{F243CY245C}* with half an hour of pre-treatment with 2 mM GABA and 1.5 hr light exposure (also presented as Figure 8a in Xu et al., 2021). Different batches of experiments were conducted, and the data were combined to analyse consistent differences between genotypes (Suppl. Fig. 7B, C). Both the combined data by absolute stomatal aperture (Fig.

4) and by normalised stomatal aperture to that of WT under control condition (Suppl. Fig. 7A) indicate consistent results. Only WT-like-2 and *35S::ALMT9* showed GABA inhibition of light-induced stomatal opening, whereas *almt9-2* and the *35S::ALMT9*^{F243CY245C} showed insensitivity to such effect of GABA (Fig. 4A). Following the dark-to-light transition both the WT-like-2 (25.3% reduction) and the native *ALMT9* complemented lines (11% reduction in #1, 19.8% reduction in #2) had significantly reduced stomatal aperture following a 2 mM GABA treatment, unlike *almt9-2* and the *35S::ALMT9*^{F243CY245C} (Fig. 4A, B).

A

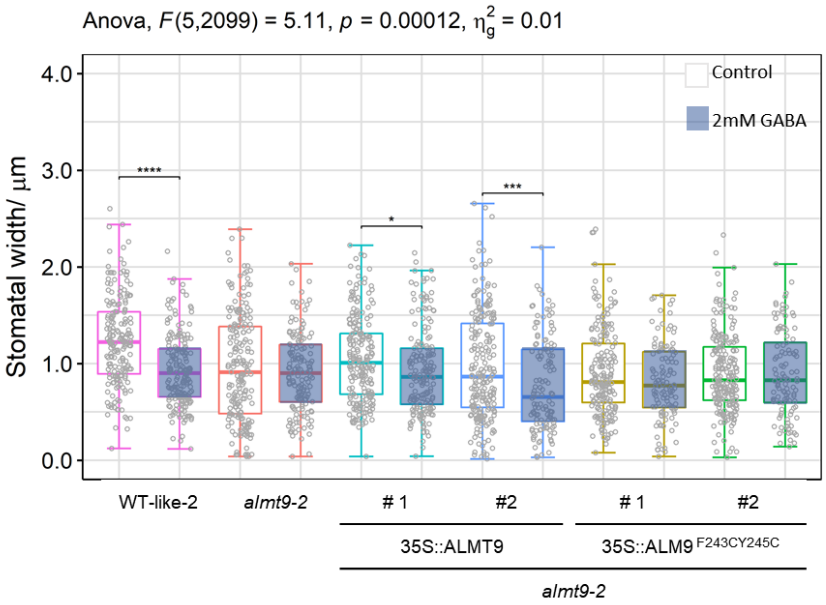
Anova, $F(5,2099) = 5.11$, $p = 0.00012$, $\eta_g^2 = 0.01$
Control
2mM GABA
Stomatal width/ µm
4.0
3.0
2.0
1.0
0.0
****
*
***
WT-like-2
almt9-2
1
#2
1
#2
35S::ALMT9
35S::ALM9 F243CY245C
almt9-2

B

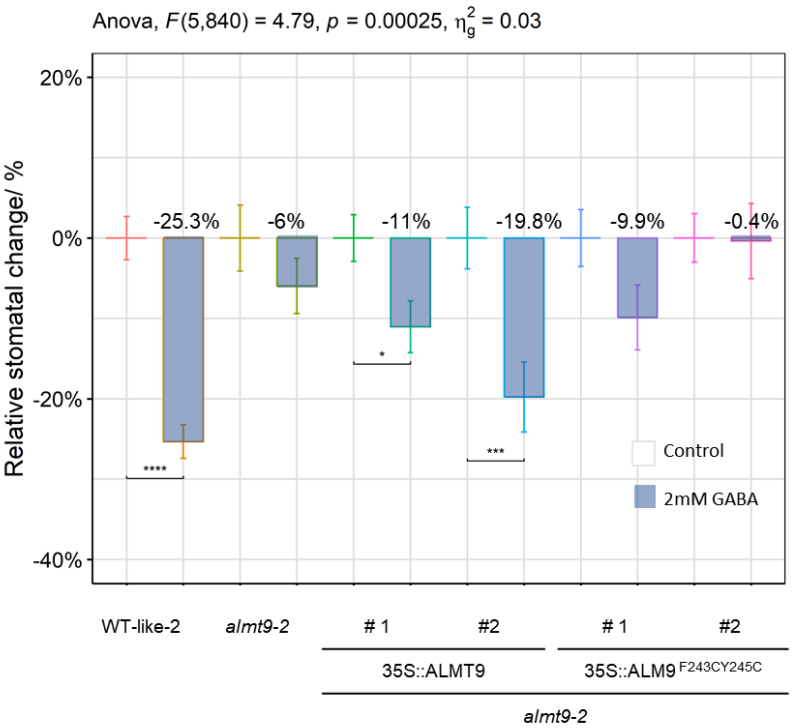
Anova, $F(5,840) = 4.79$, $p = 0.00025$, $\eta_g^2 = 0.03$
Relative stomatal change/ %
20%
0%
-20%
-40%
-25.3%
-6%
-11%
-19.8%
-9.9%
-0.4%
****
*
***
Control
2mM GABA
WT-like-2
almt9-2
1
#2
1
#2
35S::ALMT9
35S::ALM9 F243CY245C
almt9-2

Figure 4. Stomatal response of *almt9-2* and complementation lines expressing *ALMT9* and *ALMT9^{F243CY245C}*.

A. Stomatal aperture of plants in response to GABA inhibited stomatal opening. **B.** Relative change of stomata of plants in response to GABA inhibited stomatal opening. In control group, n = 189 for WT-like2, n = 197 for *almt9-2*, n = 213 for *almt9-2*/*35S::ALMT9* #1, n = 219 for *almt9-2*/*35sS::ALMT9* #1, n = 195 for *almt9-2*/*35S::*ALMT9^{F243CY245C} #1, n = 221 for *almt9-2*/*35S::*ALMT9^{F243CY245C} #2; In GABA treated group, n = 195 for WT-like2, n = 153 for *almt9-2*, n = 178 for *almt9-2*/*35S::ALMT9* #1, n = 127 for *almt9-2*/*35S::ALMT9* #1, n = 115 for *almt9-2*/*35S::*ALMT9^{F243CY245C} #1, n = 109 for *almt9-2*/*35S::*ALMT9^{F243CY245C} #2. Asterisks represent statistical significance comparing influence of GABA on single genotypes after one-way ANOVA (indicated on top of plots). p = 0.005. *, $p < 0.05$; **, $p < 0.01$; ***, $p < 0.001$; ****, $p < 0.0001$.

Exploring the role of GABA in light induced stomatal opening in WT and *almt9-2*

It was noticed that with a 1.5 hr light exposure, which is half an hour less than what was used as standard in Chapter II (Xu et al. 2021), GABA occasionally exert inhibit effect on *almt9-2* in light induced stomatal opening (Suppl. Fig. 7B-C). Given that the time which the epidermis is exposed to light can influence the extent of stomatal opening (Shimono et al. 2016), it was explored whether there was time dependency in the GABA effect on WT and *almt9-2* stomatal pore opening induced by light in epidermal strip assays (Fig. 5). The result showed that under sustained light exposure, both WT and *almt9-2* had increased stomatal aperture regardless of whether GABA was applied (Fig. 5A, Suppl. Tab. 2). This suggests a positive correlation between time and stomatal aperture. At 5 of the 7 timepoints GABA significantly inhibited stomatal opening in WT plants, whereas GABA inhibition of stomatal

opening was completely absent in *almt9-2* plants (Fig. 5B). Furthermore, during the extended light exposure, the extent of opening of *almt9-2* with or without GABA is equivalent to WT with GABA (Fig. 5B). This therefore did not back up the occasional observation made in Suppl. Fig 7B-C about GABA inhibiting stomatal opening of *almt9-2*. This is possibly due to the limit of resolution of epidermal strip assay in such condition or the skewed data distribution caused by sampling during microscopy of the epidermis.

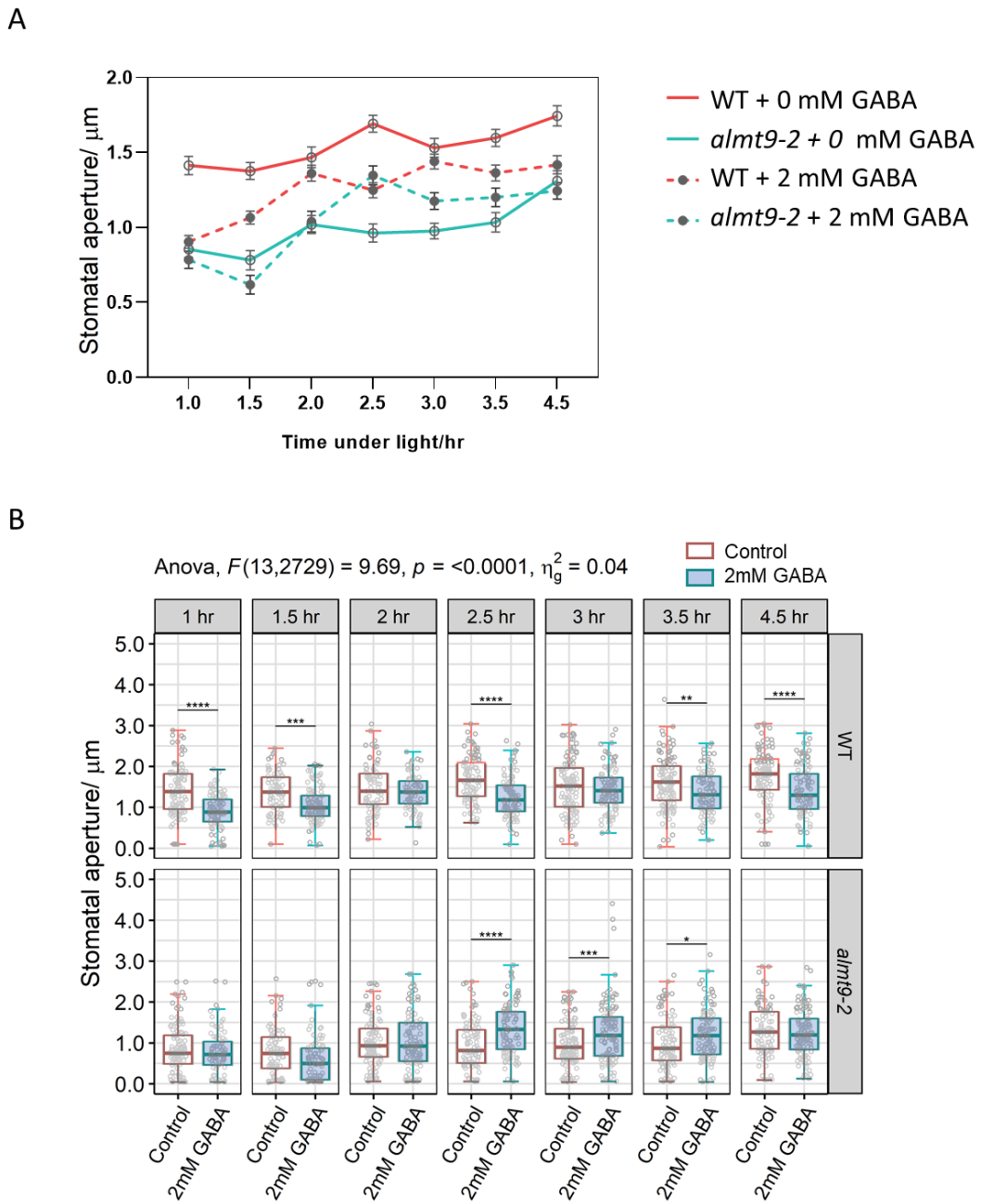

Figure 5. Time-course of stomatal opening of WT and *almt9-2*.

A. Timecourse record of stomatal opening with or without 2 mM GABA treatment. Symbols indicate mean ± SE. **B.** Details of stomata aperture width measured with or without GABA under each time point as indicated. The figure shows a 4.5-hr timecourse record of stomatal aperture in response

to light with or without 2 mM GABA. For 1 hr light exposure, n = 101 for WT_Control, n = 97 for WT_2 mM GABA, n = 112 for *almt9-2*_Control, n = 86 for *almt9-2*_2 mM GABA; For 1.5 hr light exposure, n = 79 for WT_Control, n = 101 for WT_2 mM GABA, n = 82 for *almt9-2*_Control, n = 90 for *almt9-2*_2 mM GABA; For 2 hr light exposure, n = 78 for WT_Control, n = 73 for WT_2 mM GABA, n = 100 for *almt9-2*_Control, n = 100 for *almt9-2*_2 mM GABA; For 2.5 hr light exposure, n = 98 for WT_Control, n = 98 for WT_2 mM GABA, n = 95 for *almt9-2*_Control, n = 97 for *almt9-2*_2 mM GABA; For 3 hr light exposure, n = 111 for WT_Control, n = 109 for WT_2 mM GABA, n = 118 for *almt9-2*_Control, n = 118 for *almt9-2*_2 mM GABA; For 3.5 hr light exposure, n = 117 for WT_Control, n = 99 for WT_2 mM GABA, n = 98 for *almt9-2*_Control, n = 102 for *almt9-2*_2 mM GABA; For 4.5 hr light exposure, n = 101 for WT_Control, n = 97 for WT_2 mM GABA, n = 87 for *almt9-2*_Control, n = 113 for *almt9-2*_2 mM GABA. Asterisks represent statistical significance comparing influence of GABA on either WT or *almt9-2* at single time point after one-way ANOVA, $F(2, 15) = 22.02$, $p < 0.0001$ for GABA concentration analysis; $F(2, 15) = 10.07$, $p = 0.0017$ for Glu concentration analysis. *, $p < 0.05$; **, $p < 0.01$; ***, $p < 0.001$; ****, $p < 0.0001$.

Discussion

Mutagenesis of putative GABA interaction site of ALMT9 abolished GABA inhibition of stomatal opening

As a major agent of anion sequestration across the tonoplast membrane of guard cells, the loss of *ALMT9* results in impaired stomatal opening (De Angeli et al. 2013b). As presented here and in Chapter II, 2 mM GABA inhibited light induced stomatal opening, which was abolished if *ALMT9* was ablated (Fig. 4, 5, Suppl. Fig. 7). Furthermore, GABA treatment of WT plants resulted in equivalent stomatal apertures to those in *almt9-2* plants after 4.5 hr

(Fig. 4), which is consistent with the GABA inhibitory effect targeting ALMT9 as a major anion sequestration pathway in the vacuole controlling stomatal opening. Since the mutation of the putative GABA binding site impaired the GABA sensitivity of anion transport (and GABA transport capacity) of TaALMT1 rather than anion transport *per se* we hypothesised that this would be the case for ALMT9 (Ramesh et al. 2015, Long et al. 2020). This appears to be the case as mutation of the putative GABA binding domain (35S::ALMT9^{F243CY25C}) resulted in stomatal conductance that was higher than that of *35S::ALMT9* and WT at steady state, and equivalent to that of *gad2* (Fig. 3B). Perturbed GABA sensitivity of ALMT9 activity, or absence of GABA leading to similar stomatal conductance suggests that ALMT9 is the major target of GABA modulating stomatal opening.

Epidermal peel assays on the complemented lines broadly backup this model, where a mutation in the putative GABA-binding motif disrupts GABA mediated ALMT9 transport activity, since *35S::ALMT9*, but not *35S::ALMT9*^{F243CY25C}, recovered *almt9-2* stomatal opening sensitivity to GABA (Fig. 4, Suppl. Fig. 7). However, with 1.5 hr of light exposure, enlarged stomata of *almt9-2/*35S::ALMT9^{F243CY25C} was not observed in the epidermal strip assay (Fig. 4A; Suppl. Fig. 7B-C). This is similar to the situation where stomatal conductance of the *almt9-2/*35S::ALMT9^{F243CY25C} was similar to that of other genotypes before it reached the steady state (Fig. 3A). Stomatal aperture is positively corelated to duration of light exposure (Fig. 5A) (Shimono et al. 2016), and as confirmed later with extended time in exposure to light, the *almt9-2/*35S::ALMT9^{F243CY25C} did show enlarged stomatal aperture (Chapter II, Supplementary Figure 17j). The role of GABA in regulating stomatal opening via a GABA-ALMT9 interaction thereby is corroborated in this chapter. Drought experiment on WT, *almt9-2*, *35S::ALMT9* and *35S::ALMT9*^{F243CY25C} was also

attempted to see whether higher steady state conductance in *35S::ALMT9*^{F243CY25C} could lead to increased drought sensitivity, as occurs in *gad2*. However, our results failed to replicate the drought insensitive phenotype of *almt9-2* (De Angeli et al. 2013b), and all genotypes had similar relative water content during the process (Suppl. Fig. 8). Thus, repeat experiments should be conducted in future to optimise conditions so we can obtain the baseline for the experiment i.e. *almt9* improved resistance to drought, and therefore be able to study the influence of the GABA-ALMT9 interaction on drought adaptation of plants. Due to time limitations, further experiments on guard cells specific complemented plants of *ALMT12* are pending, with plants only generated at the T_0 generation of complemented lines, but not phenotyped. The filial materials are now available for screening for homozygousity to explore the role of the GABA-ALMT12 interaction in stomatal closing at a later date.

Materials and Methods

Gene cloning

ALMT12 native CDS was first constructed into the pCR8 vector (pCR8/GW/TOPO TA Cloning Kit - Thermo Fisher Scientific). Site directed mutation was conducted on *pCR8-ALMT12* with Phusion High-Fidelity DNA Polymerase (NEB) for *pCR8-ALMT12*^{L205CY207C}. The entry clone constructions were then recombined into binary vectors driven by guard cells specific promoter *pGC1*. Subsequently, the coding sequences were cloned into binary vector pMDC32-pGC1 with Gateway LR Clonase II Enzyme mix (Invitrogen). For each construction, the PCR products using vector specific and target gene specific primers were

checked by electrophoresis on a 1% (w/v) agarose gel, and then purified using the illustra GFX PCR DNA and Gel Band Purification Kit (GE Healthcare). The plasmid carries bacterial kanamycin resistance gene. Positive construction was selected on LB medium containing 25 µg/mL kanamycin, and was stored and enriched in *E. coli* competent cells (Chung et al. 1989). The *pAR27-35S::ALMT9-GFP*, *pAR27-35S::ALMT9*^{F243CY245C}*-GFP* constructs were available at the beginning of my projects (B. Xu, University of Adelaide). The plasmids were selected and enriched with LB medium containing 50 µg/mL spectinomycin. Positive constructions of pAR27-35S::ALMT9-GFP, pAR27-35S::ALMT9^{F243CY245C}-GFP, pMDC32-proGC1::ALMT12 and pMDC32-proGC1::ALMT12^{L205CY207C} were checked by Sanger sequencing after transformation into *Agrobacterium* strain *AGL1* (Höfgen and Willmitzer 1988).

Plant materials and growth condition

The *Arabidopsis* wildtype used in this study was ecotype Columbia-0 (Col-0) unless otherwise specified. The single mutant *almt9-1* (SALK_055490), *almt9-2* (WiscDsLox499H09) are previously described (De Angeli et al. 2013b, Baetz et al. 2016). Mutant lines of *ALMT12* were JIC mutation lines, which carries a single defective Spm (dSpm) transposon element as a stable insertion in the genome (Meyer et al. 2010). All mutants used in this study were homozygous, confirmed by PCR using a pair of gene specific primers and the T-DNA insertion border primer. Details of primers are listed in Supplementary Table 1.

For the *almt9-2*/*35S::ALMT9-GFP* and *almt9-2/35S::ALMT9*^{F243CY245C}*-GFP,* these were constructed by *Agrobacterium tumefaciens* mediated floral dipping assay (Harrison et al.

2006, Zhang et al. 2006). Seeds of transgenic plants (T_0) and subsequent filial generations were then selected by resistance to kanamycin (Kanamycin Monosulphate, Melford Laboratories Ltd.) (Harrison et al. 2006). In brief, seeds were harvested in 2 mL tubes and mixed with silica gel beads (Silica gel orange, Sigma) in a ratio of 1:1. The tube was then sealed with a cotton ball and placed on the bench at room temperature for 10-14 days. Subsequently, the seeds were sterilised with 0.5% (m/v) sodium hypochlorite and 0.01% (v/v)triton-x solution for 10-15 min and washed with sterilised pure water (by Milli Q Plus 185 Water Purification System) 5-6 times, before being placed on half-MS medium containing 50 µg/mL kanamycin in a petri dish (Murashige and Skoog medium, Duchefa-Biochemie; 1% Sucrose, Chem-supply; 0.8% Phytagel, Sigma Aldrich). The seeds were then stratified at 4°C under dark for 2 days, and then placed horizontally under the light for 6 hr, covered under dark for 2 days and exposed to light again for 1 day. The seedlings that had a greener appearance were transferred to soil and covered with cling wrap to maintain high humidity for 5-7 days. After that, the cling wrap was removed and the plants (T1 generation) were kept under long-day conditions (16-hr light/ 8-hr dark, 22 °C, 60-70 % relative air humidity) for seed harvesting (Rivero et al. 2014). The kanamycin selected plants were double confirmed by genotyping using PCR with primers indicated in Fig. 1A and Suppl. Table 1 (Lu 2011). For each genotype, around 20 plants were kept for seeds harvesting. The filial T_2 generation was then selected with the same method on ½ MS medium containing 50 µg/mL kanamycin. Around 100 seeds of each genotype were selected on the medium and those with kanamycin resistance were kept for seeds harvesting. Finally, the T_3 generation was screened by the same method and only that the ones showed 100% resistance were kept. And the T_4 generation, the homozygous lines, were used for phenotyping experiments. The transgenic plants (4-day-old) were observed

under Olympus Fluorescence Microscope and screened to check the fluorescence emitted from the GFP tag.

For phenotyping experiments, all materials for were sown on half-MS medium and stratified at 4°C for 4 days, and then grew in short-day condition unless otherwise specified (100-150 μmol $\cdot m^{-2} \cdot s^{-}$,10-hr light/ 14-hr dark, 22 °C, 60-70 % relative air humidity).

Quantitative PCR

For qPCR, total RNA samples were extracted from rosette leaves of 5-week-old plants using TRIzol Reagent (TRIzol RNA Isolation Reagents, Invitrogen) and purified with DNase (TURB DNase, Invitrogen). cDNA was synthesized with SuperScript III Reverse Transcriptase (Invitrogen) from 1μg mRNA. Real time qPCR was performed with KAPA SYBR® FAST qPCR Kit (Roche) in QuantStudio 12 Flex Real-Time PCR System (Thermo Fisher Scientific) with cDNA synthesized from 1ug mRNA. Each experiment was repeated containing 3 biological replicate plants with 3 technical replicates.

Semi-quantitative PCR

Semi-qPCR was conducted with PCR reaction on cDNA from plants as indicated. The PCR system used in this study is KAPA2G Fast HotStart ReadyMix. 50 × dilution of cDNA was made from 1 μg RNA then used in the PCR reaction. The products were then checked with electrophoresis after 25 cycles of PCR.

Stomatal pore assay

For stomatal aperture measurement, epidermal strips were peeled from the abaxial side of mature leaves of 4-6 week-old plants. The peels were then submerged in KCl-MES buffer (10 mM MES, 10 mM KCl, 5 mM Malate, pH 6.0 by Tris base) (Xu et al. 2021), with or without 2 mM GABA, under light (200 μmol photons m^{-2} s^{-1}) or in the dark. Stomatal status was captured under Zeiss Axiophot Fluorescence Phase Microscope, and then measured by ImageJ. 3 biological replicate plants, 2 leaves of each, were used in each experiment. Stomatal conductance was measured with AP4 Leaf Porometer (Delta-T) on 4 leaves of each plant from 5 biological replicate plants.

Drought treatment

Drought assays was performed as in Chapter 2. 4-5 weeks old plants were grown in short-day conditions (100- 150 μmol photons m^{-2} s^{-1},10-hr light/ 14-hr dark, 22 °C, 40-60 % RH), in equally weighed out soils containing 1:1 ratio Irish Peat and coco peat. The soil water content was saturated at Day-0 before withdrawing water. Leaves ware harvested and weighed for fresh weight, turgid weight and dry weight during the drought process. Water content and relative water content (RWC) was then calculated by the equation below.

$$\mathrm{RWC} = \frac{\text{Fresh Weight} - \text{Dry Weight}}{\text{Turgid Weight} - \text{Dry Weighta}}$$

Construction of *almt12/proGC1:: ALMT12*, *almt12/GC1:: ALMT 12*^{L203CY205C}, *almt9-2/ 35S::ALMT9* and *almt9-2/ 35S:: ALMT9*^{F243CY245C}

Protein sequences of *Arabidopsis* ALMTs family members were aligned to that of wheat TaALMT1 to identify the putative GABA binding motif in ALMT9 and ALMT12 and for the location of the first two aromatic amino acids in this motif (Ramesh et al. 2015). Putative GABA binding motif was located at residues 243-254 in ALMT9 and residues 205-216 in ALMT12 (Suppl. Fig. 1, 2A). For *ALMT9*, *pART27-35S::ALMT9* (native *ALMT9* coding sequence) was used as template for site-directed mutagenesis to construct *pART27-35S::ALMT9*^{F243CY245C} (De Angeli et al. 2013a) (Chapter II) (Suppl. Fig. 2B). The plasmid construction was checked by Sanger sequencing (Suppl. Fig. 2C). With the same method, primers were designed for the cloning of *ALMT12*^{L205CY207C}, using the GATEWAY entry vector pCR8 carrying *ALMT12* as a template (Suppl. Tab. 1, Suppl. Fig. 6A). Since *ALMT12* is mainly expressed in guard cells, both the native and mutated fragments were cloned into binary vectors driven by the guard cell specific promoter *GC1* (At1g22690, −1140/+23 relative to the transcriptional start site, size of 1163 bp) (Yang et al. 2008, Meyer et al. 2010) (Suppl. Fig. 5A). The binary vector construction was then transformed into *E. coli* competent cells and checked by colony PCR (Suppl. Fig. 6B). Final plasmid constructions were checked by Sanger sequencing (Suppl. Fig. 6C).

Statistical analysis

Statistical analysis was conducted in GraphPad Prizm. One-way ANOVA was applied when comparing the influence of one factor. For datasets with multiple groups, homogeneity and

normal distribution of data in each group were checked. Afterwards, the dataset was tested by ANOVA to test if there was significant difference between groups. Then multiple comparisons were conducted after Tukey post-hoc tests. Asterisks represent statistical significance. *, $p < 0.05$; **, $p < 0.01$; ***, $p < 0.001$; ****, $p < 0.0001$. Different letters indicate significant difference if $p < 0.05$.

Supplementary materials

Supplementary Table 1. Primers used in this Chapter.

Primer names	Primer sequence: 5'- 3'	Purpose of using
alnt9-1-LP	TGGTGGATCTGAATCTTCGAG	almt9-1 genotyping
alnt9-1-RP	GTTCCGGGTTTTCTTGCTTAC	almt9-1 genotyping
BP	ATTTTGCCGATTTCGGAAC	almt9-1 genotyping
alnt9-2-LP	CGTGGATGAACAAAACATGTG	almt9-2 genotyping
alnt9-2-RP	AGAGAGTGGGCGTAGAAGGAG	almt9-2 genotyping
almt9-2-BP	AACGTCCGCAATGTGTTATTAAGTTGTC	almt9-2 genotyping
ALMT9-qPCR_F	ACCTAATCCGGATCTTAGTCGATACT	ALMT9 qPCR
ALMT9-qPCR_R	TCACCGAATAAAGTGGAAAGCTCAG	ALMT9 qPCR
actin2_F	TGGAATCCACGAGACAACCTA	qPCR reference gene
actin2_R	TTCTGTGAACGATTCCTGGAC	qPCR reference gene
ALMT9-F	ATGGCGGCGAAGCAAG	ALMT9 Gateway Cloning
ALMT9-R	CATCCCAAAACACCTACGAATCTTC	ALMT9 Gateway Cloning
ALMT9-nonter-R	CCCAAAACACCTACGAATCTTC	ALMT9 Gateway Cloning
KpnI-ALMT9-F	GGGGTACCATGGCGGCGAAGCAAGGTT	pART27/ 35S:: ALMT9F243C Cloning
KpnI-ALMT9-R	ACGGTACCCATCCCAAAACACCTACGAAT	pART27/ 35S:: ALMT9F243C Cloning
atalmt12-1_F	GTTGTGCAAAGGGCTTAATAGAG	almt12-1 genotyping
atalmt12-1_R	CAAGAAGGCTCATGAAAAGACAG	almt12-1 genotyping
atalmt12-2_F	ACAAGACCACCGTTGGTAAACTC	almt12-1 genotyping
atalmt12-2_R	CTCCGGCTAATCTTACACAAGG	almt12-1 genotyping
Spm32	TACGAATAAGAGCGTCCATTTTAGAGT	almt12 genotyping
ALMT12-L205C_F	CTGTCTTTTCATGAGCCTTTGTGTT	Site-directed mutation of ALMT12
ALMT12-L205C_R	CCAGACCAAATAGGAAAAACACAAAGG	Site-directed mutation of ALMT12
ALMT12-Y207C_F	GAGCCTTCTTGTTTGTCCTATTTGGTC	Site-directed mutation of ALMT12
ALMT12_Y07C_R	CTTCACCAGACCAAATAGGACAAACAA	Site-directed mutation of ALMT12
ALMT12-L205CF207C_F	GGAATCTGTCTTTTCATGAGCCTTTGTGTTTGTCC	Site-directed mutation of ALMT12
ALMT12-L205CF207C_R	GATCTTCACCAGACCAAATAGGACAAACACAAAGG	Site-directed mutation of ALMT12

Supplementary Table 2. Statistical summary of data shown in Fig. 5.

The table summarized the statistical analysis of the time-lapse data comparing stomatal aperture of single genotypes between a light exposure duration of 1hr and 4.5 hr.

Time/ hr	GABA /mM	Genotype	n	Mean/ µm	SD	t-test	P
1	0	WT	101	1.41	0.61	-3.64	3.45E-04
4.5	0	WT	101	1.74	0.68		
1	2	WT	97	0.9	0.42	-6.93	7.86E-11
4.5	2	WT	97	1.42	0.6		
1	0	almt9-2	112	0.85	0.59	-5.18	5.96E-07
4.5	0	almt9-2	87	1.31	0.64		
1	2	almt9-2	86	0.78	0.53	-5.68	2.05E-08
4.5	2	almt9-2	113	1.24	0.58		

A

```
ALMT9            1 MAAKQGSFRHGILEKRERLLSNNGFSDFRFTDIESNDLLENENCGRRTRLCCCCSCGNLS 60
ALMT9F243CY245C  1 ............................................................ 60
ALMT9           61 EKISGVYDDAKDVARKAWEMGVSDPRKIVFSAKIGLALTIVALLIFYQEPNPDLSRYSVW 120
ALMT9F243CY245C 61 ............................................................ 120
ALMT9          121 AILTVVVVFEFTIGATLSKGFNRALGTLSAGGLALGMAELSTLFGDWEEIFCTLSIFCIG 180
ALMT9F243CY245C 121 ........................................................... 180
ALMT9          181 FLATFMKLYPSMKAYEYGFRVFLLTYCYILISGFRTGQFIEVAISRFLLIALGAGVSLGV 240
ALMT9F243CY245C 181 ........................................................... 240
ALMT9          241 NMFIYPIWAGEDLHNLVVKNFMNVATSLEGCVNGYLRCLEYERIPSKILTYQASEDPVYK 300
ALMT9F243CY245C 241 ..C.C...................................................... 300
ALMT9          301 GYRSAVESTSQEESLMSFAIWEPPHGPYKSFNYPWKNYVKLSGALKHCAFTVMALHGCIL 360
ALMT9F243CY245C 301 ........................................................... 360
ALMT9          361 SEIQAPEERRQVFRQELQRVGVEGAKLLRELGEKVKKMEKLGPVDLLFEVHLAAEELQHK 420
ALMT9F243CY245C 361 ........................................................... 420
ALMT9          421 IDKKSYLLVNSECWEIGNRATKESEPQELLSLEDSDPPENHAPPIYAFKSLSEAVLEIPP 480
ALMT9F243CY245C 421 ........................................................... 480
ALMT9          481 SWGEKNHREALNHRPTFSKQVSWPARLVLPPHLETTNGASPLVETTKTYESASALSLATF 540
ALMT9F243CY245C 481 ........................................................... 540
ALMT9          541 ASLLIEFVARLQNVVDAFKELSQKANFKEPEIVTTGTDVEFSGERVGLGQKIRRCFGM 598
ALMT9F243CY245C 541 ........................................................... 598
```

B

```
ALMT12            1 MSNKVHVGSLEMEEGLSKTKWMVLEPSEKIKKIPKRLWNVGKEDPRRVIHALKVGLSLTL  60
ALMT12L205CF207C  1 ............................................................  60
ALMT12           61 VSLLYLMEPLFKGIGSNAIWAVMTVVVVLEFSAGATLCKGLNRGLGTLIAGSLAFFIEFV  120
ALMT12L205CF207C 61 ............................................................  120
ALMT12          121 ANDSGKVLRAIFIGTAVFIIGAAATYIRFIPYIKKNYDYGVVIFLLTFNLITVSSYRVDS  180
ALMT12L205CF207C 121 ...........................................................  180
ALMT12          181 VINIAHDRFYTIAVGCGICLFMSLLVFPIWSGEDLHKTTVGKLQGLSRSIEACVDEYFEE  240
ALMT12L205CF207C 181 .......................C.C................................  240
ALMT12          241 KEKEKTDSKDRIYEGYQAVLDSKSTDETLALYANWEPRHTLRCHRFPCQQYVKVGAVLRQ  300
ALMT12L205CF207C 241 ...........................................................  300
ALMT12          301 FGYTVVALHGCLQTEIQTPRSVRALFKDPCVRLAGEVCKALTELADSISNHRHCSPEILS  360
ALMT12L205CF207C 301 ...........................................................  360
ALMT12          361 DHLHVALQDLNSAIKSQPKLFLGSNLHRHNNKHQNGSISNNKHHQRNSSNSGKDLNGDVS  420
ALMT12L205CF207C 361 ...........................................................  420
ALMT12          421 LQNTETGTRKITETGSRQGQNGAVSLSSFRTDTSALMEYRRSFKNSNSEMSAAGERRMLR  480
ALMT12L205CF207C 421 ...........................................................  480
ALMT12          481 PQLSKIAVMTSLEFSEALPFAAFASLLVEMVARLDNVIEEVEELGRIASFKEYDNKRDQT  540
ALMT12L205CF207C 481 ...........................................................  540
ALMT12          541 ADDVRCENPANVTISVGAAE  560
ALMT12L205CF207C 541 ....................  560
```

Supplementary Figure 1. Protein sequence alignment of ALMT9 and ALMT9^{F243CY245C}

Protein sequence alignment of ALMT9 and ALMT9F243CY245C (**A**) and ALMT12 and ALMT12$^{L205C/F207C}$ (**B**). Dots indicate identical amino acid residues. The mutation sites are marked in red.

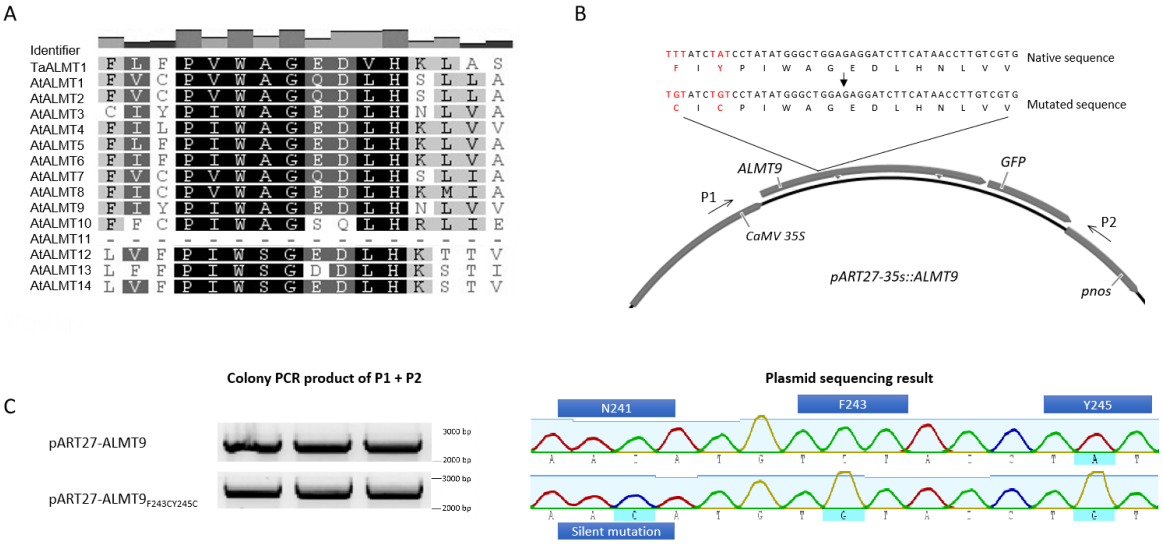

Supplementary Figure 2. Putative GABA binding motif of *Arabidopsis* ALMTs.

A. Sequence alignment of *Arabidopsis* ALMTs to TaALMT1 to identify putative GABA-binding motif. The top panel indicates the identity level of each amino acid locus. Grey scale of the background indicated extent of conservatism of the single amino acid residue. *ALMT11* encodes a protein with 152-aa, where the putative GABA binding motif is absence. Grayscale of shading indicates score of conservation, where black represents the most conserved residues. **B.** Schematic of the T-DNA part of pART27-*35S::ALMT9* illustrating vector construction. Mutation sites on the putative GABA binding motif are indicated on the top panel. Side-directed mutations are indicated in red, where the phenylalanine (F) and/or tyrosine (Y) were mutated into a cysteine (C). **C.** Identification of *Agrobacterium* harbouring the various target pART27-*35S::ALMT9* constructs. *Agrobacterium* used for floral dipping assays were identified through colony PCR; plasmid DNA were extracted for Sanger sequencing.

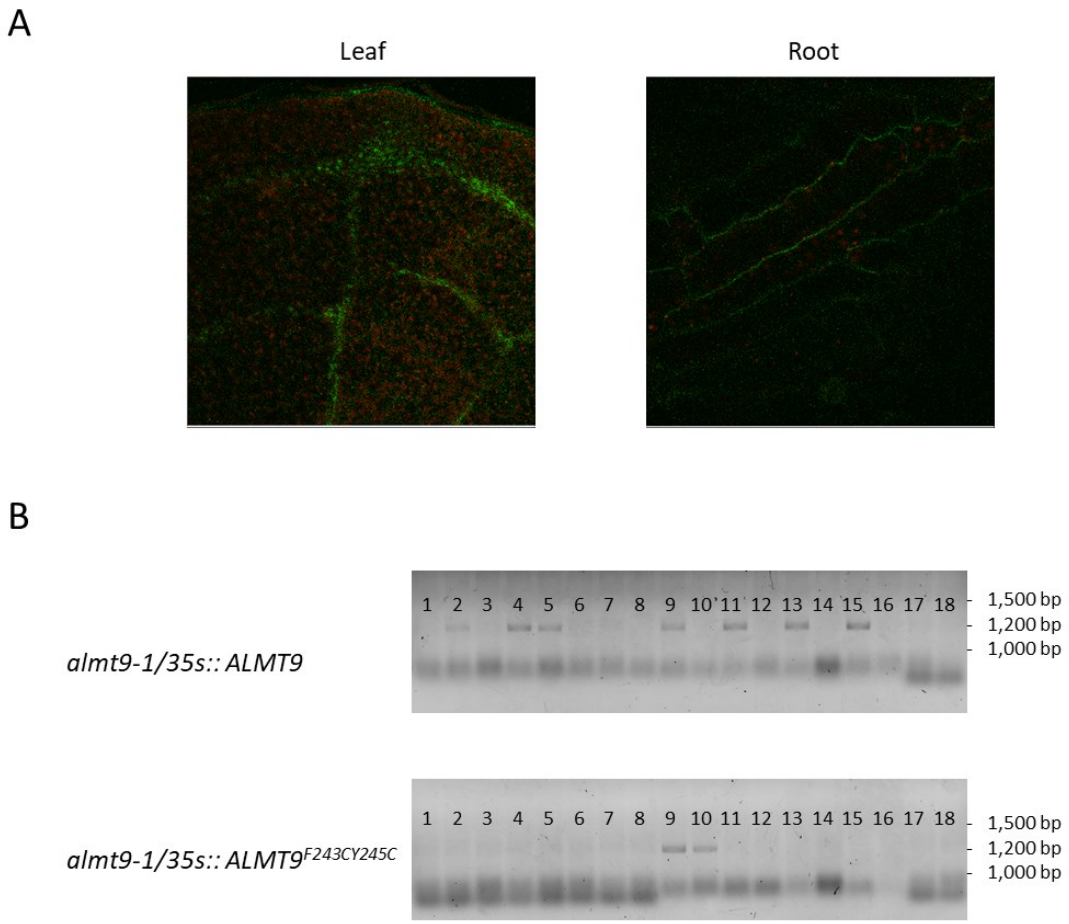

Supplementary Figure 3. Selection of complementation lines in the *almt9-1* background.

A. Confocal images of *almt9-1/35S::ALMT9* and *almt9-1/35S::ALMT9*^{F243CY245C}. GFP fluorescence from GFP tag in transformed lines was detected and identified by green fluorescence. Red fluorescence was from autofluorescence of chloroplast. **B.** Genotyping of filial T2 plants of plants selected by fluorescence under confocal microscope. Genomic DNA was extracted from plants rosette leaves. Primer P1 and P4 in Fig. 1A were used for genotyping. The result indicates that line 2, 4, 5, 9, 11, 13 ,15 of *almt9-1/ 35S::ALMT9* and line 9, 10 of *almt9-1/ 35S::ALMT9*^{F243CY245C} are the positive transgenic lines.

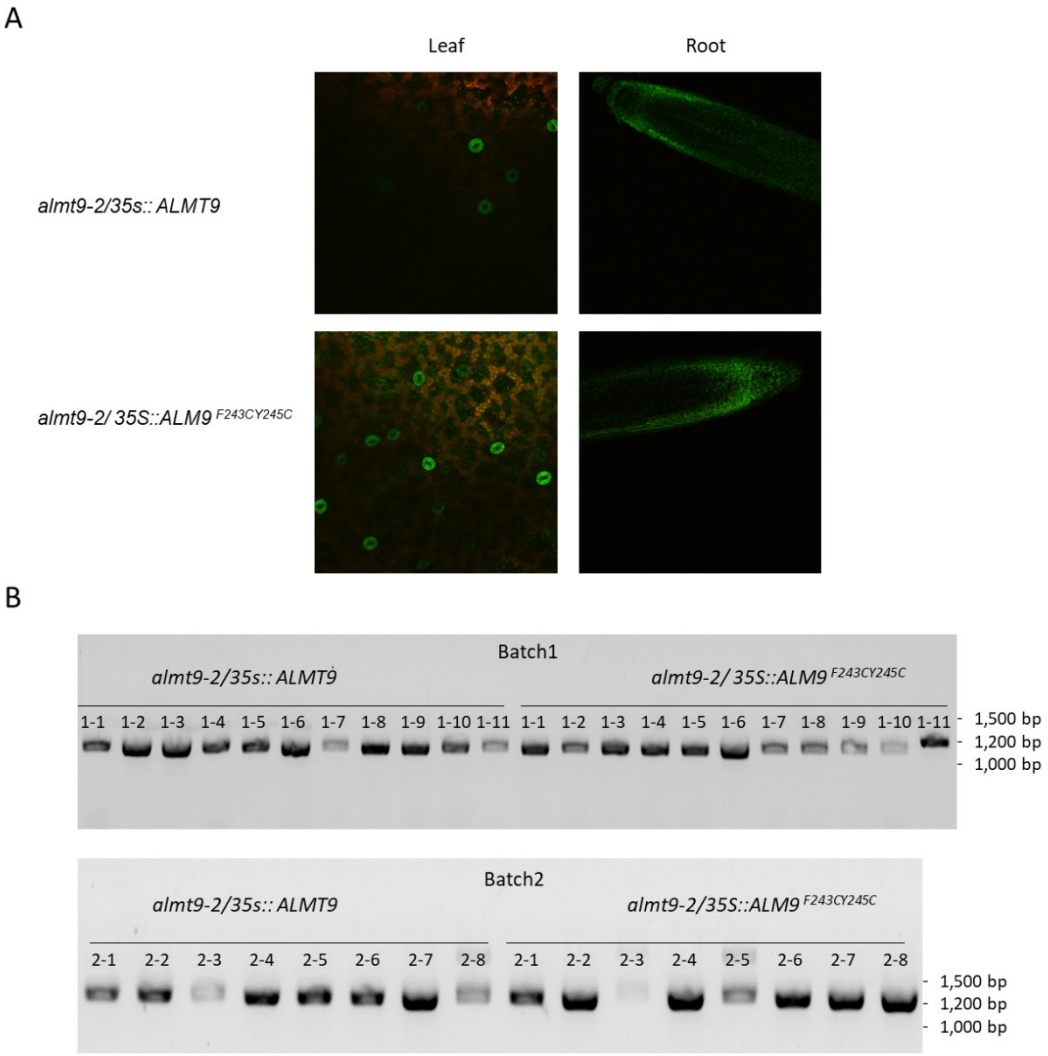

Supplementary Figure 4. Selection of complementation lines in the *almt9-2* background.

A. Confocal images of *almt9-2/35S::ALMT9* and *almt9-2/35S::ALMT9*^{F243CY245C} showing GFP fluorescence in positive transformants. **B.** Genotyping of filial T_2 generation of transgenic plants in A. Primer P2 and P4 in Fig.2A were used for genotyping. The result showed a low proportion of negative transformants (those with no and slightly larger size band, such as line 1-11 of *almt9-2/ 35S::ALMT9* from batch 1 and line 2-3 of *almt9-2/35S::ALMT9*^{F243CY245C} from batch 2).

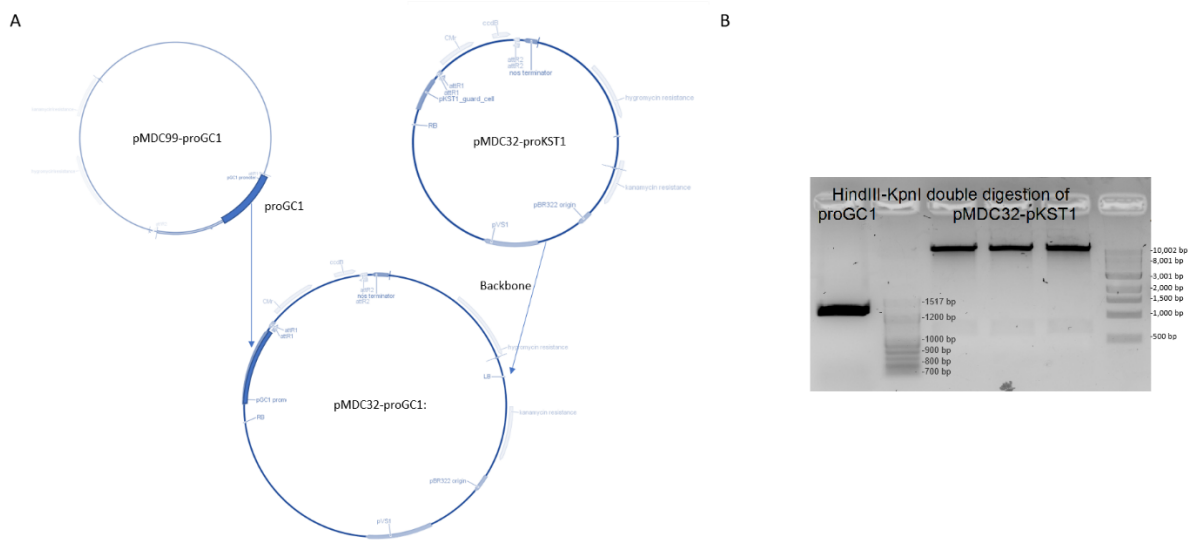

Supplementary Figure 5. Construction of pMDC32 vector carrying *proGC1.*

A. Schematic of entry cloning of pMDC32-*proGC1* construction. The backbone of the new vector was from another binary vector *pMDC32-proKST1*. CDS sequence of *proGC1* was amplified from binary vector *pMDC99-proGC1*. The two parts was ligated together with T4 ligase. **B**. Digestion product of *proGC1* and the backbone with HindIII and KpnI on electrophoresis gel.

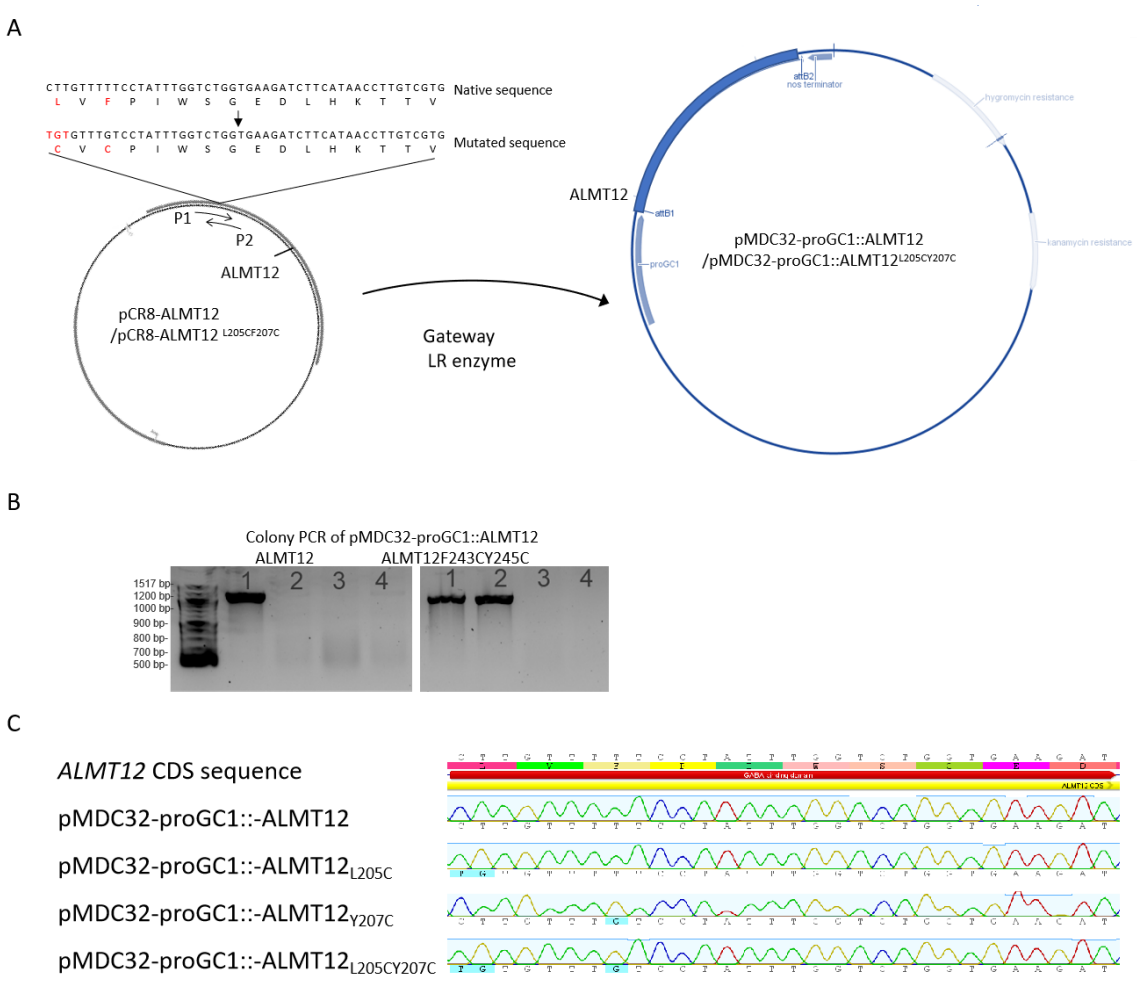

Supplementary Figure 6. *pMDC32-proGC1::ALMT12* construction.

A. Schematic of GATEWAY cloning of *ALMT12* from pCR8 entry vector to the binary vector pMDC32-proGC1. **C.** Colony PCR of pMDC32-*proGC1::ALMT12* transformed *E. coli* and *A. tumefaciens*. Positive and negative signs indicate positive and negative colonies identified by PCR reaction. **C.** Sequencing result focusing on the GABA-binding motif coding region of pMDC32-*proGC1::ALMT12* and pMDC32-*proGC1::ALMT12*^{F243CY245C} plasmid DNA.

A

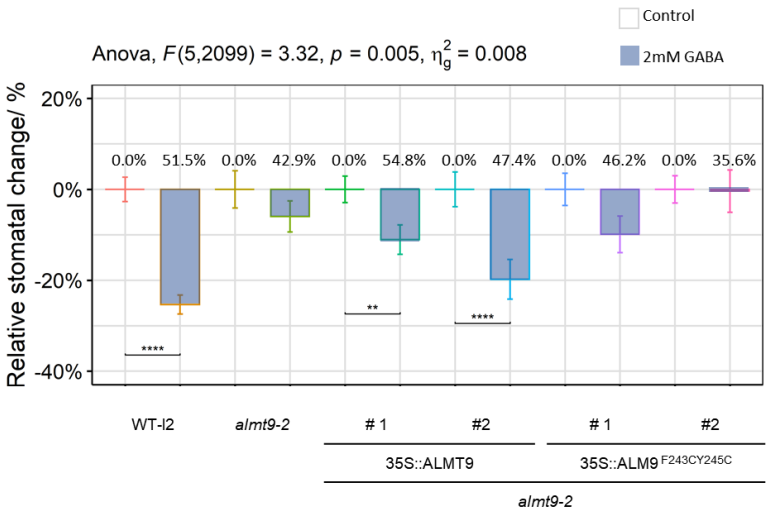
Control
2mM GABA
Anova, F(5,2099) = 3.32, p = 0.005, η_g^2 = 0.008
Relative stomatal change/ %
20%
0%
-20%
-40%
0.0% 51.5% 0.0% 42.9% 0.0% 54.8% 0.0% 47.4% 0.0% 46.2% 0.0% 35.6%
****
**
****
WT-l2
almt9-2
1
#2
1
#2
35S::ALMT9
35S::ALM9 F243CY245C
almt9-2

B

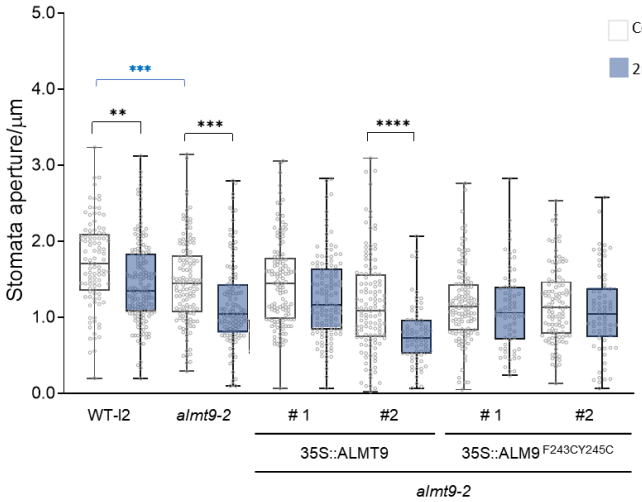
Control
2mM GABA
Stomata aperture/µm
5.0
4.0
3.0
2.0
1.0
0.0
***
**
***
****
WT-l2
almt9-2
1
#2
1
#2
35S::ALMT9
35S::ALM9 F243CY245C
almt9-2

C

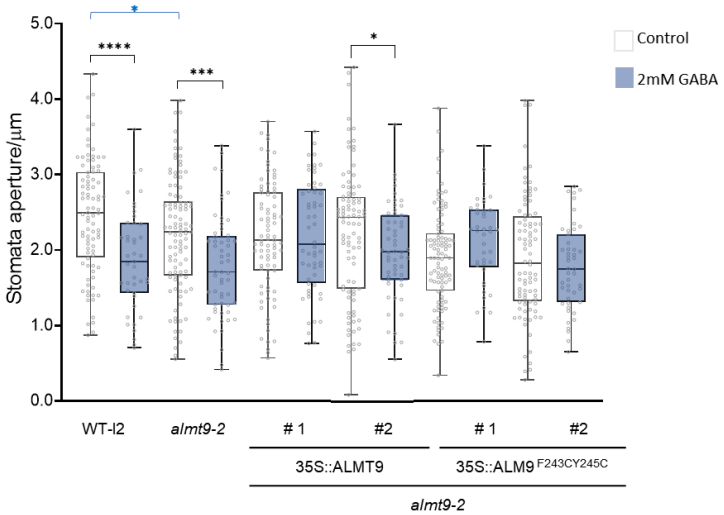
Control
2mM GABA
Stomata aperture/µm
5.0
4.0
3.0
2.0
1.0
0.0
*
****
***
*
WT-l2
almt9-2
1
#2
1
#2
35S::ALMT9
35S::ALM9 F243CY245C
almt9-2

Supplementary Figure 7. Stomatal aperture of the complementation lines.

A. Relative stomatal aperture response of *almt9-2/ 35S::ALMT9* and *almt9-2/ 35S::ALMT9*^{F243CY245C} under dark to light condition with or without 0.5 hr pre-treatment of 2 mM GABA in the dark. **B-C**. Stomata aperture of result measured from different batch of experiments. In control group, n = 189 for WT-like2, n = 197 for *almt9-2*, n = 213 for *almt9-2/35S::ALMT9* #1, n = 219 for *almt9-2/35S::ALMT9* #1, n = 195 for *almt9-2/35S::ALMT9*^{F243CY245C} #1, n = 221 for *almt9-2/35S::ALMT9*^{F243CY245C} #2; In GABA treated group, n = 195 for WT-like-2, n = 153 for *almt9-2*, n = 178 for *almt9-2/35S::ALMT9* #1, n = 127 for *almt9-2/35S::ALMT9* #1, n = 115 for *almt9-2/35S::ALMT9*^{F243CY245C} #1, n = 109 for *almt9-2/35S::ALMT9*^{F243CY245C} #2. Asterisks in black represent statistical significance comparing between genotypes after Two-way ANOVA (indicated on top of plots). Asterisks in black represent statistical significance comparing between genotypes after Two-way t-test. p = 0.005. *, p < 0.05; **, p < 0.01; ***, p < 0.001; ****, p < 0.0001.

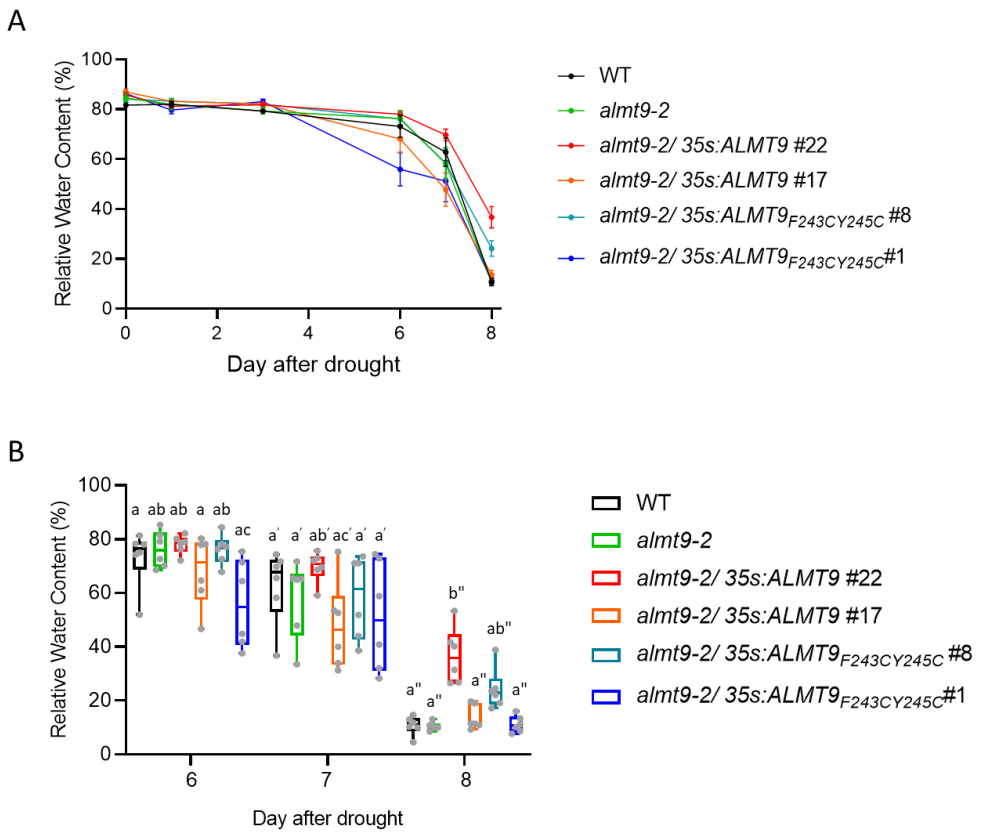

Supplementary Figure 8. Relative water content of the complementation lines during drought process.

A. Time-course recording of plant relative water content over drought process. **B.** Data from day-6 to day-8 in **A** were pulled out to comparing water status between genotypes. Different letters indicate statistical significance comparing between genotypes at the same day of drought process after two-way ANOVA, *p val* <0.05, n=6.

Chapter IV GABA regulation of stomata aperture in Arabidopsis: beyond a simple dose-response relationship

Introduction

Results in previous chapters showed that GABA acts on ALMT9 and ALMT12 to modulate stomatal movement, and that the defect in leaf GABA synthesis (*gad2-1*) led to enlarged stomatal aperture and increased susceptibility to drought stress. On the contrary, cell specific manipulation of GABA synthesis improves drought tolerance of WT and recovers the stomatal phenotype of the single (*gad2*) mutant to that of the wildtype (Xu et al. 2021). There is extensive literature that shows that GABA application improves plants tolerance to stresses, including herbivory, salt, pathogen infection, heat and drought (Park et al. 2010, Scholz et al. 2015, Priya et al. 2019, Su et al. 2019). Furthermore, GABA synthesis deficiency increases sensitivity to biotic stress, such as salinity, drought and pathogenesis (Mekonnen et al. 2016, Su et al. 2019, Deng et al. 2020). As reviewed in chapter I, there are 5 *GAD* homologues in *Arabidopsis* that have distinct expression patterns and contribution to GABA synthesis (Bouché et al. 2004, Miyashita et al. 2007, Scholz et al. 2015, Zarei et al. 2017, Safavi-Rizi et al. 2020). The fact that disruption of a particular GAD function may not always be associated with visible phenotypes, suggests that there are divergent roles for the *GAD* homologues (Bouché et al. 2004, Miyashita and Good 2008). Thus, in this chapter, to further explore the relationship between GABA synthesis and stomatal pore aperture regulation in *Arabidopsis*, higher order mutants of the major *GAD* isoforms expressed in plants were generated and analysed. Here, an unexpected complexity in the relationship between endogenous GABA concentration and stomatal pore

aperture control was revealed, which indicates that normal function of stomata may require more *GAD*s than just *GAD2*.

Results

Genotyping and stomatal phenotype of *gad1/2/4/5*

To follow up on our finding that GABA synthesised via a *GAD2* mediated pathway impacts plant gas exchange (Chapter II and III), it was further investigated whether there is a correlation between GABA metabolism and stomatal movement by characterising the stomatal pore regulation of higher order *GAD* mutants. We obtained seeds from the lab of Prof. Shuqun Zhang, Zheijang University, China (Deng et al. 2020), where *GAD1, 2, 4* and *5* are knocked out simultaneously in the quadruple mutant line *gad1/2/4/5* for near complete disruption of GAD-mediated, Glu-derived, GABA synthesis. *GAD3* is barely expressed through the whole plant (Miyashita and Good 2008) and appears not to impact vegetative GABA concentration (Deng et al., 2020).

As we were unable to obtain the heritage of the lines in addition to the seeds at the beginning of the project, the T-DNA insertion sites present in the proposed *gad1/2/4/5* mutant line were checked (Fig. 1A). With gene specific primers and T-DNA border primers (Suppl. Tab. 1), the T-DNA insertion within *GAD1,2,4* and *5* was located, and thus with this I was able to identify the parental lines used to create the quadruple mutant (Fig. 1A). The quadruple mutant was also verified as homozygous (Fig. 1B). Of importance here, it was confirmed that the *gad1/2/4/5* harbours the *gad2-1* T-DNA insertional mutation in *GAD2* (Suppl. Tab. 2, Suppl. Fig. 1) so it is useful material to compare with the *gad2-1* parental

line. The expression of *GAD* genes was measured in both WT and the quadruple-mutant by quantitative PCR. Real-time quantitative PCR (RT-qPCR) confirmed that *GAD2* was the most dominant *GAD* homologue expressed in the rosette leaves of 5-6-week-old *Arabidopsis*, where *GAD4* was the second most highly expressed *GAD* (Fig. 1C). This is consistent with results obtained using reverse-transcriptional PCR (semi-qPCR), where only expression of *GAD1, 2* and *4* was detected in wildtype (WT) leaves, while no *GAD3 or 5* transcription was detected in *gad1/2/4/5* after 34 cycles of replication (Fig. 1D). *GAD3* and *GAD4*, which are located on chromosome 2 adjacent to each other, share 91% identity in their coding regions (Suppl. Fig. 2). Since T-DNA insertion in salk lines were identified by sanger sequencing (Alonso et al. 2003), a further experiment was required to confirm the T-DNA insertional position within *GAD3* and/or *GAD4* to see whether the sanger sequence result was a mismatch with the T-DNA insertion site in *Arabidopsis* genome. With primers designed flanking the genomic sequence of *GAD4* and *GAD3,* the PCR result indicated that T-DNA is only inserted in *GAD4* of *gad1/2/4/5* (Suppl. Fig. 3).

Subsequently, endogenous GABA concentration of the mutant lines was measured using Ultra-Performance Liquid Chromatography (UPLC). The quadruple mutant had very low GABA content (0.0396 ± 0.005 nmol/ mg FW), slightly lower than that of the *gad2-1* single mutant (0.0527 ± 0.009 nmol/ mg FW), and only maintained approximately 5.8% of GABA accumulation of WT seedlings (0.901 ± 0.182 nmol/ mg FW) (Fig. 1E). As could be reasonably expected, disruption of GABA synthesis accumulated greater Glu in the mutant lines compared to that of WT (3.313 ± 0.151 nmol/ mg FW in *gad2-1*, 3.062 ± 0.089 nmol/ mg FW in *gad1/2/4/5* and 2.418 ± 0.180 nmol/ mg FW in WT) (Fig. 1F).

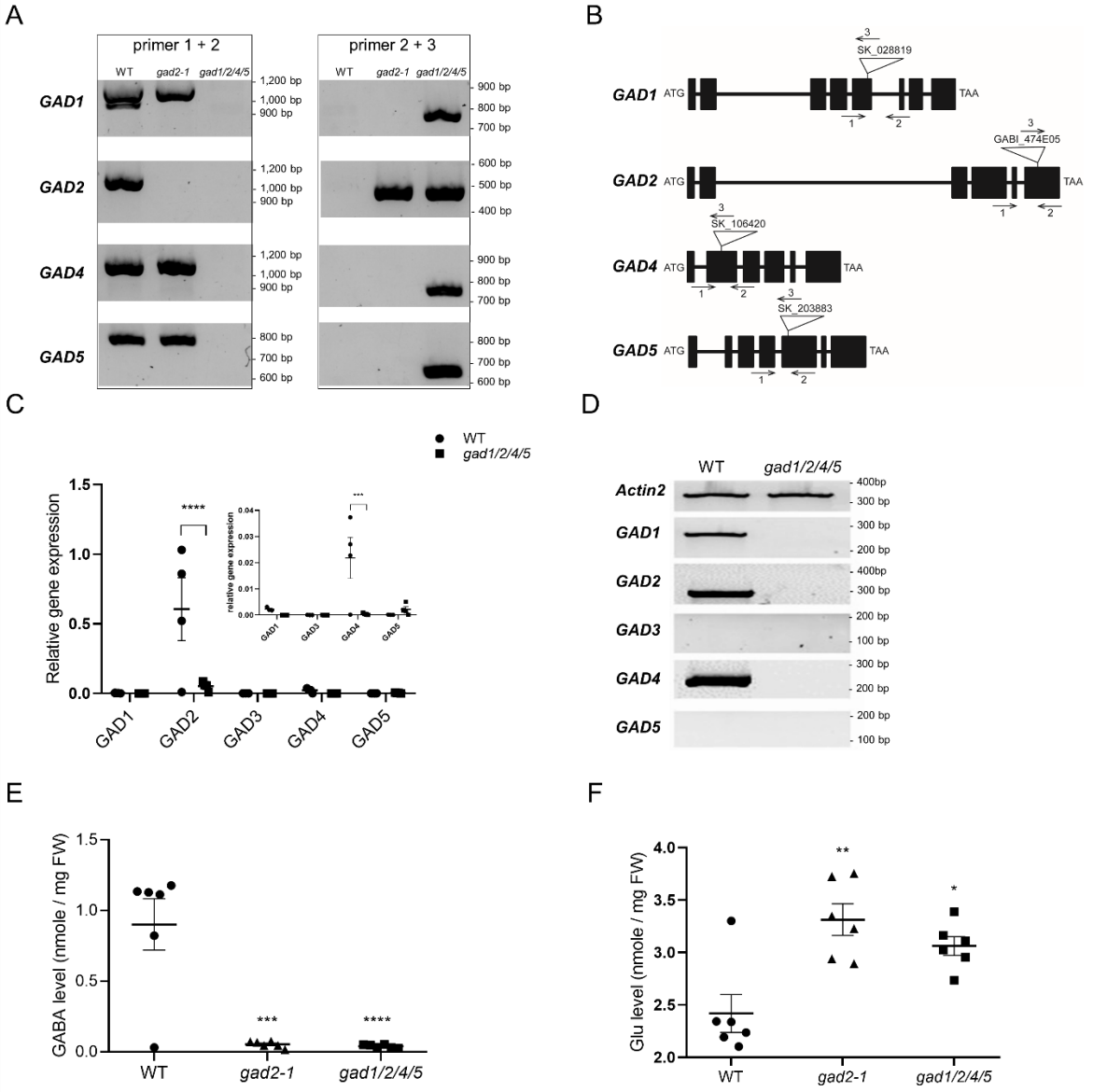

Figure 1. *gad2-1* and *gad1/2/4/5* reduce GABA concentration in leaves.

A. Schematic representation of *GAD* genes; black boxes and solid lines represent exons and introns, respectively. T-DNA insertional map is indicated by triangles and identifying code, while arrows represent primers used for genotyping. **B.** Identification of genotype and T-DNA location of mutants via PCR-based screening of gDNA template of plants with primers indicated in **A**. **C.** qPCR analysis of *GAD* expression relative to that of *Actin2* in WT and *gad1/2/4/5.* **D.** Semi-qPCR analysis of *GAD* expression in rosette leaves of WT and *gad1/2/4/5*. GABA (**E**) and Glu (**F)** level in rosette

leaves of plants was measured by UPLC (n=6). For qPCR, asterisks represent statistical significance after Two-way ANOVA (**C**), $F_{Interaction}$ (4, 30) = 16.96, $p < 0.0001$; F_{Gene} (4, 30) = 0.7503, $p = 0.5657$; $F_{Genotype}$ (1, 30) = 5.830, $p = 0.0221$. For metabolite concentrations, asterisks represent statistical significance comparing mutants to WT after one-way ANOVA, F (2, 15) = 22.02, $p < 0.0001$ for GABA concentration analysis; F (2, 15) = 10.07, $p = 0.0017$ for Glu concentration analysis. *, $p < 0.05$; **, $p < 0.01$; ***, $p < 0.001$; ****, $p < 0.0001$.

The stomatal phenotypes of *gad1/2/4/5* compared to *gad2-1* and WT were then examined. Intriguingly and much to our surprise, unlike *gad2-1 (*and *gad2-2*, Chapter II), the disruption of the four *GADs* simultaneously did not result in a larger stomatal aperture than wildtype, as in the single mutants of *GAD2*; instead *gad1/2/4/5* had a WT-like aperture width (Fig. 2a). Width/length ratios and stomatal conductance of *gad1/2/4/5* were both WT-like (Fig. 2B Suppl. Fig. 4A), suggesting that *gad1/2/4/5* did not alter stomatal pore size and demonstrated a phenotypic reversion of the *gad2-1* single mutant phenotype back to WT.

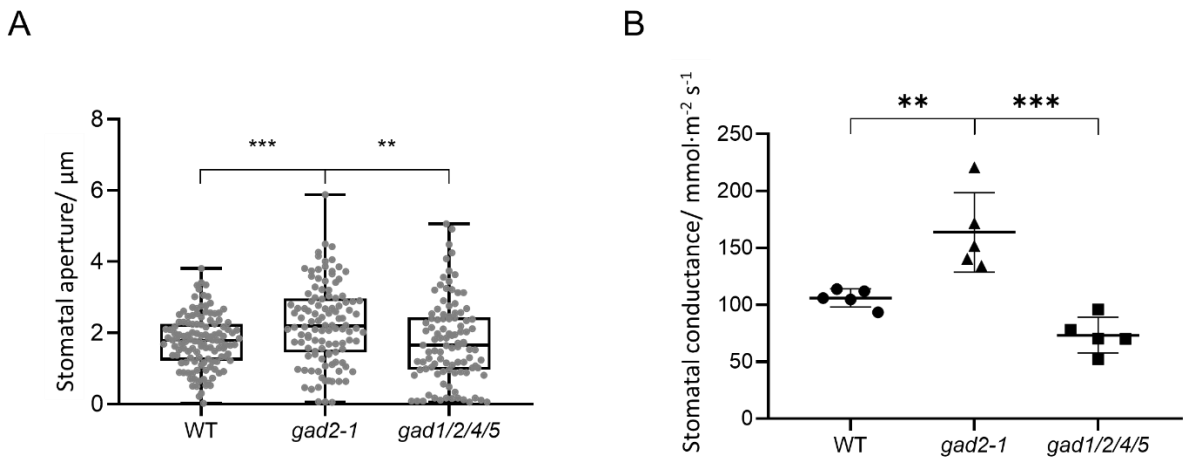

Figure 2. Stomatal aperture and conductance of WT, *gad2-1* and *gad1/2/4/5*.

A. Stomatal aperture of 5-week-old plants were measured under 2 hr of constant light, n= 123 for WT, n= 112 for *gad2-1*, n= 101 for *gad1/2/4/5*. **B**. Stomatal conductance of 5-week-old plants measured at steady state (6 hr after the light is on). 4 leaves per plant, 5 plants per genotype were measured, the mean ± SE of each genotype are indicated. Asterisks represent statistical significance comparing between genotypes after one-way ANOVA in A, $F (2, 333) = 8.465$, $p = 0.0003$; and B, $F (2, 12) = 20.57$, $p = 0.0001$. **, $p < 0.01$; ***, $p < 0.001$.

Drought sensitivity of GABA deficient mutants

Given that the higher water loss rate of *gad2-1* is associated with lower water use efficiency (Chapter II, Fig. 3), here, it was examined whether *gad1/2/4/5* again failed to properly close stomata following water deficiency, despite its WT-like gas exchange of steady state undre light conditions (Fig. 2). This was performed in an attempt to understand whether the near complete interruption of GABA synthesis via the GABA shunt could affect drought performance, i.e. whether there is correlation between GABA concentration and drought sensitivity, by monitoring stomatal conductance following drought treatment. The *gad2-1* mutant again maintained significantly higher water loss rate than that of WT, until it was thoroughly wilted after 5 days of withholding watering (Fig. 3A). Instead, *gad1/2/4/5* consistently behaved like WT and wilted at day 6 (Fig. 3B). In a repeated experiment, leaf tissue was sampled for GABA and Glu concentration during the drought process (Fig. 3C-D). The result indicated that GABA concentrations were consistently lower in both mutants whereas the WT plants had greater GABA concentration upon drought treatment at day 3 (Fig. 3C). Interestingly Glu synthesis was promoted in both mutant lines and peaked at day 3 (Fig. 3D), suggesting that GABA accumulation in response to drought was induced by

fuelling the GABA shunt with Glu, but impaired GABA synthesis led to Glu accumulation in *gad2-1* and *gad1/2/4/5* mutants instead.

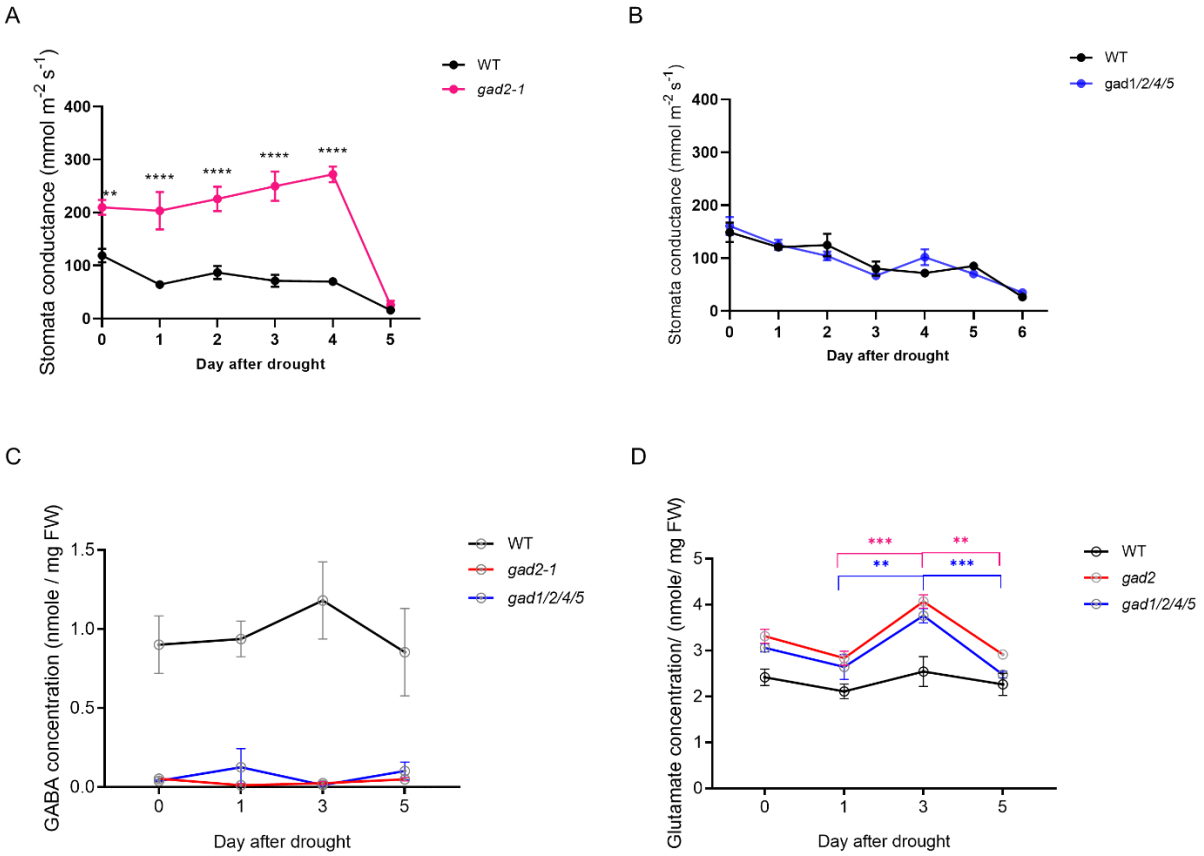

Figure 3. Drought response of WT, *gad2-1* and *gad1/2/4/5*.

A. Stomatal conductance of WT and *gad2-1* were monitored after withholding water for 5 days. 4 leaves of each plant were used to measure stomatal conductance, the mean value of 6 biological replicate plants at each data point is indicated. **B**. Stomatal conductance of WT and *gad1/2/4/5* were monitored after withholding water for 5 days. 4 leaves of each plant were used to measure stomatal conductance, the mean value of 8 biological replicate plants at each data point is indicated. GABA (**C**) and Glu (**D**) concentrations in leaves of WT, *gad2-1* and *gad1/2/4/5* during drought process. Rosette leaves of 6 plants of each genotype were sampled at each data point. Asterisks represent statistical significance comparing between genotypes after Two-way ANOVA

in A, $F_{Interaction}$ (5, 36) = 8.045, $p < 0.0001$; F_{Days} (5, 36) = 22.18, $p < 0.0001$; $F_{Genotypes}$ (1, 36) = 163.5, $p < 0.0001$, and B, $F_{Interaction}$ (6, 56) = 1.272, $p = 0.2851$; F_{Days} (6, 56) = 25.29, $p < 0.0001$; $F_{Genotypes}$ = 0.01755, $p = 0.8951$. Asterisks represent statistical significance comparing metabolite concentrations between days for each genotype (blue: *gad1/2/4/5*; pink: *gad2-1*) after one-way ANOVA in C, F (2, 333) = 8.465, $p = 0.0003$; and D, F (2, 12) = 20.57, $p = 0.0001$). All data points indicate mean ± SE. **, $p < 0.01$; ***, $p < 0.001$; ****, $p < 0.0001$.

Influence of endogenous GABA synthesis on stomatal movements

To further investigate the role of GABA in stomatal regulation and how the disparity between *gad2-1* and *gad1/2/4/5* may occur, ♂ *gad2-1* x ♀ *gad1/2/4/5* (*gad2-1×gad1/2/4/5*) were crossed to generate the first filial generation (F_1). The F_1 generation contained homozygous T-DNA insertions in the *GAD2* alleles, but were heterologous in the other *GAD* alleles – *GAD1*, *GAD4* and *GAD5*. As such, this F_1 was expected to mimic the *gad2-1* single mutant (Fig. 4A). Initially, stomatal conductance of F_1 with WT and parental lines were compared. Since the stomatal conductance level in WT, *gad2-1* and *gad1/2/4/5* has demonstrated both divergence between lines and variability within lines during repeated previous measures, and to have an accurate determination of the F_1 phenotype, a large number of biological replicates were used (n=11 for F_1, n=6 for other genotypes) (Fig. 4B). Our result indicated a similar level of stomatal conductance in the F_1 *gad2-1×gad1/2/4/5* to that of *gad2-1*, which was significantly higher than that of WT and *gad1/2/4/5* (Fig. 4B). This is consistent with the higher stomatal conductance of *gad2-1* mutant being caused by the knockout of the *GAD2* gene as shown with the two independent *gad2-1* and *gad2*-2

mutant lines, respectively from GABI-KAT and SALK mutant seed collections, both of which had higher stomatal conductance than wildtype plants (Chapter II, Fig. 3).

Subsequently, the second (F_2) and third (F_3) filial generation segregated from the F_1 generation were used to segregate homozygote double or triple *GAD* mutants (Suppl. Fig. 4A). For the F_2 generation, plants were genotyped with gene specific primers used in Fig. 1A, thus could be homozygous or heterologous in single locus of either *GAD1*, *GAD4* or *GAD5* alleles, such as *gad1/2* double mutants, *gad1/2/4* and *gad1/2/5* triple mutants (Suppl. Fig. 5A). *gad1/2*, similar to the *gad2-1* mutant, had higher stomatal conductance than that of wildtype plants, consistent with previous research (Mekonnen et al. 2016); however, the loss of either *GAD4* or *GAD5* in addition to the *gad1/2* mutation compromised the higher stomatal conductance of the *gad2* and *gad1/2* mutant and re-produced the *gad1/2/4/5* and WT-like phenotype (Fig. 4C). This was also found in individual lines of the F_2 generation, where the triple mutants, *gad1/2/4* and *gad1/2/5*, had similar levels of stomatal conductance to that of *gad1/2/4/5* and WT (Suppl. Fig. 6). All double and triple mutants harbouring T-DNA insertions in *GAD2*, had low levels of GABA accumulation in rosette leaves, whereas *gad1* single mutant had WT-like GABA level in leaves (Fig. 4D). The result based on the F_2 plants indicated that only *gad2* and *gad1/2* mutants showed a correlation between lower endogenous GABA and higher stomatal conductance, but the additional disruption of *GAD4* or *5* within the *gad2-1* background may alter other aspects to compromise the GABA-deficiency effect on the stomatal phenotype back to wildtype like (Fig. 4C).

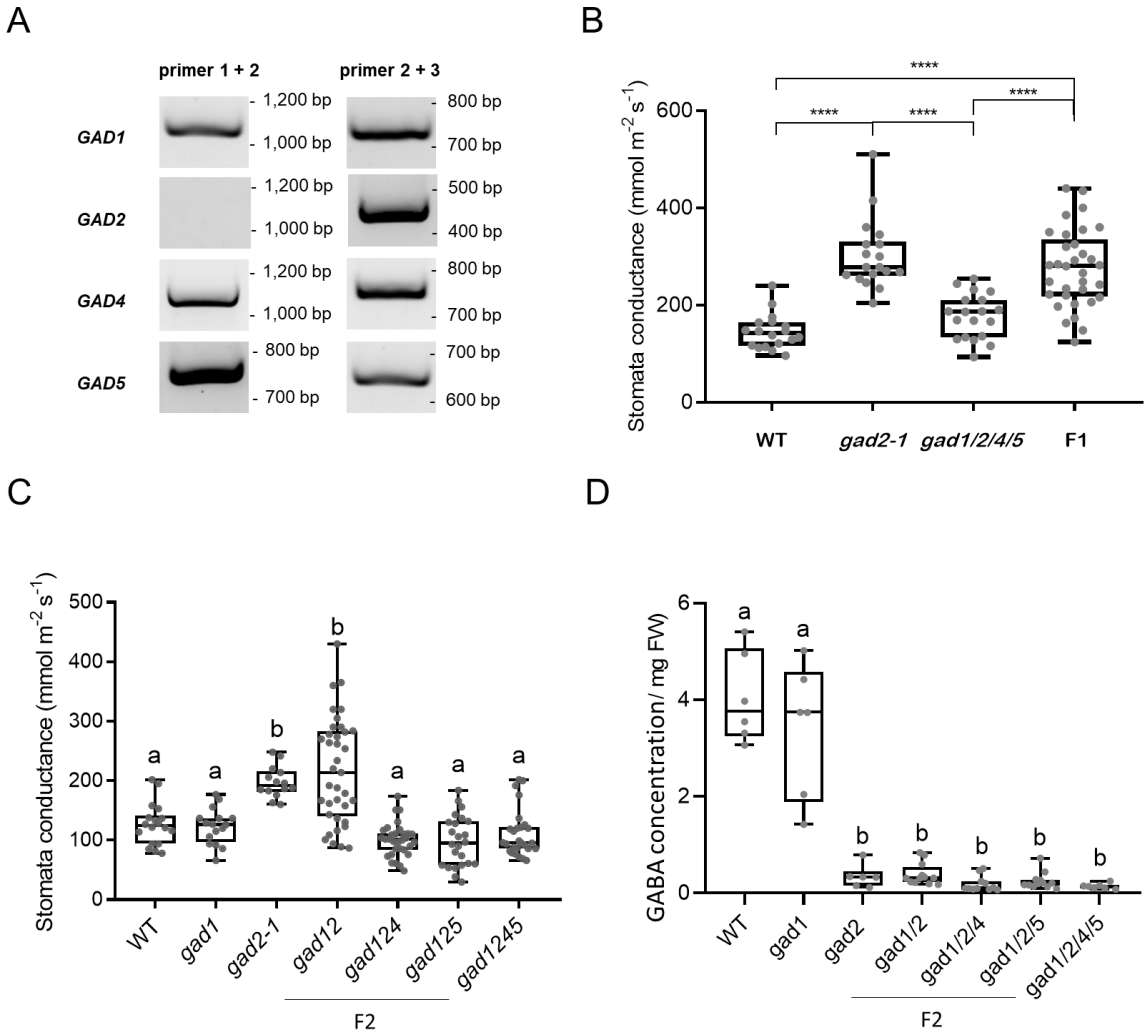

Figure 4. Effect of impaired GABA synthesis on stomatal movement.

A. Genotype of the F_1 generation from a *gad2-1*×*gad1/2/4/5* cross. Primers used are as described in Fig. 1A. **B**. Stomatal conductance of WT, *gad2-1*, *gad1/2/4/5* and F_1. 4 leaves of each plant were used to measure stomatal conductance of plants, the mean value of individual plants of each genotype are indicated. n= 6 for WT, n= 6 for *gad2-1*, n= 6 for *gad1/2/4/5*, n= 11 for F_1. **C**. Stomatal conductance of WT, *gad2-1*, *gad1/2/4/5* and F_2. n= 6 for WT, n= 5 for *gad1*, n= 7 for *gad2-1*, n= 11 for *gad1/2*, n= 10 for *gad1/2/4*, n= 8 for *gad1/2/5*, n= 10 for *gad1/2/4/5*. **D**. GABA level of WT, *gad2-1*, *gad1/2/4/5* and F_2. n=6. Different letters denote significant difference ($p < 0.05$) between

genotypes after one-way ANOVA, B, F (3, 84) = 27.25, P<0.0001; **C**, F (6, 50) = 13.65, P<0.0001; **D**, F (10, 54) = 34.53, P<0.0001.

To determine whether mutation of *GAD4* or *GAD5* eliminated the higher stomatal conductance of *gad1/2* and *gad2-1*, epidermal strip assays were conducted on F_3 of *gad2-1 x gad1/2/4/5* and *gad4*. All mutants were genotyped with both gene specific primers and T-DNA border primers and were deemed homozygous (Suppl. Fig. 5). Epidermal strip assay under constant light showed that gad1, *gad4*, *gad2/4*, *gad1/2/4*, *gad1/2/5* had similar level of stomatal aperture as that in WT and *gad1/2/4/5* (around 1.4 μm) (Fig.5). T-DNA insertion in either *GAD1* or *GAD4* alone did not result in more opened stomatal aperture than WT, unlike the *gad2-1* mutant (2.05 ± 0.08 μm). which had significantly more open stomata than that of other genotypes tested (Fig. 5).

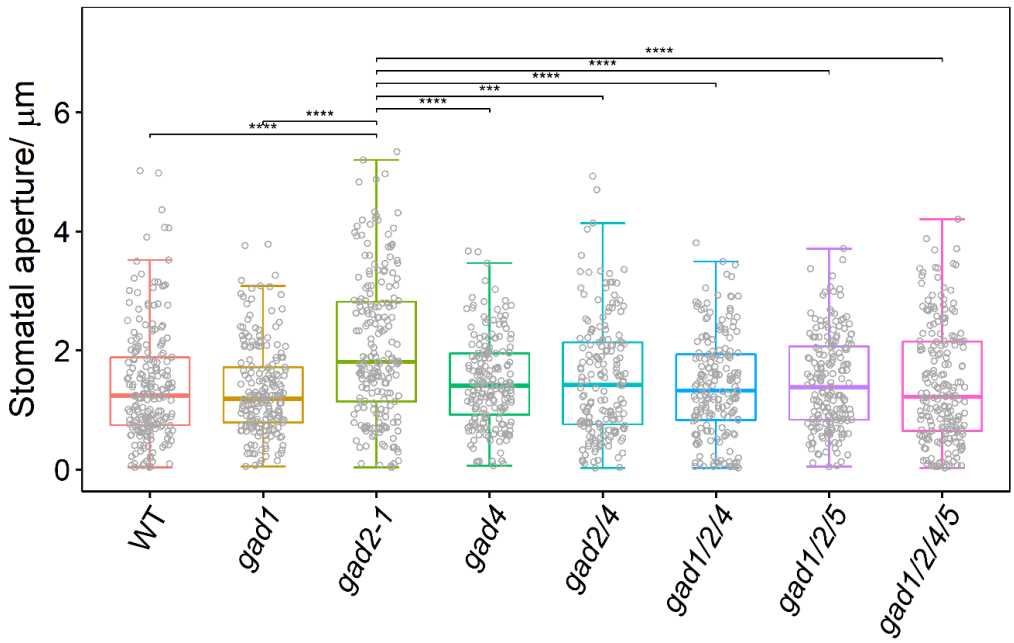

Figure 5. Effect of serial *GAD* knock outs on stomatal opening following a dark to light transition.

The effect of exogenous GABA on stomatal aperture of WT and homozygous mutants of GADs. Black brackets and asterisks indicate significant difference comparing all genotypes, the orange ones indicate significant difference comparing all genotypes excluding *gad2-1*. n= 208 for WT, n= 198 for *gad1*, n= 201 for *gad2-1*, n= 193 for gad4b, n= 173 for *gad2/4*, n= 187 for *gad1/2/4*, n= 187 for *gad1/2/5*, n= 199 for *gad1/2/4/5*. Asterisks indicate significant difference between different pharmacological treatments of each genotype including watered control after one-way ANOVA, $F_{Interaction}$ (7, 2655) = 3.260, p = 0.002; $F_{Genotypes}$ (7, 2655) = 15.488, p <0.0001; $F_{Treatment}$ (1, 2655) = 7.753, p = 0.005. *, p < 0.05; **, p < 0.01; ***, p < 0.001; ****, p < 0.0001.

In another experiment, I measured the stomatal conductance of WT and the mutants (Fig.6A). Interestingly, in contrast to the aperture data, both *gad4* and *gad2/4* had higher stomatal conductance, which was similar to that of *gad2-1* and was significantly higher than other mutants being used (Fig. 6A). It was also checked if expression of other *GAD* homologues was altered in the *gad4* mutant. As indicated in the qPCR result, *GAD4* expression was eliminated in *gad4*, and that the expression of *GAD1*, *GAD2* and *GAD5* was not induced in rosette leaves of the mutant (Fig. 6B).

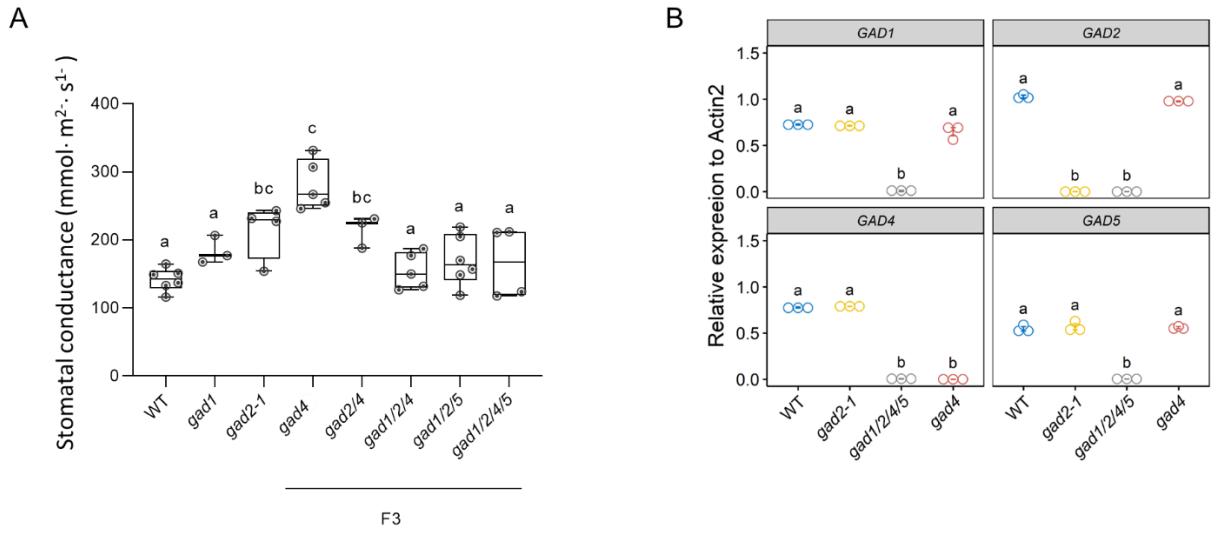

Figure 6. Effect of impaired GABA synthesis on stomatal conductance.

A. Stomatal conductance of WT and homozygous mutants of *GADs* at steady state (6 hr after the light is on). n= 6 for WT, n= 3 for *gad1*, n= 4 for *gad2-1*, n= 5 for *gad4b*, n= 3 for *gad2/4*, n= 5 for *gad1/2/4*, n= 6 for *gad1/2/5*, n= 4 for *gad1/2/4/5*. Different letters in denote significant difference ($p < 0.05$) between genotypes. **B**. qPCR analysis of *GAD*s expression relative to that of *Actin2* in WT and mutant lines. 3 biological replicate plants and 3 technical replicates were used for expression of each gene in each genotype.

Characterisation of *gad1/2/4/5* plants expressing *GAD2Δ* in guard cells

Expression of *GAD2* and *GAD4* can be found in both mesophyll and guard cells of *Arabidopsis* (Leonhardt et al. 2004), to see whether restoring GABA synthesis specifically in guard cells of *gad1/2/4/5* lines altered the stomatal phenotype, the truncated version of *GAD2* lacking the C-terminal auto-inhibitory domain (*GAD2Δ*) with or without a C-terminal GFP tag were expressed in *gad1/2/4/5* driven by guard cell specific promoter of promoter of *GC1* (At1g22690, −1140/+23 relative to the transcriptional start site, size of 1163 bp)

(Yang et al. 2008). Leaf sections of the complemented plants, *gad1/2/4/5/GC1::GAD2Δ-GFP* were observed using confocal microscopy. The GFP fluorescence was exclusively shown in guard cells (Fig. 7A). semi-qPCR analysis on rosette leaves also suggested expression of *GAD2Δ* successfully in both *gad1/2/4/5 /GC1:: GAD2Δ-GFP* and *gad1/2/4/5 /GC1:: GAD2Δ (*Fig. 7B).

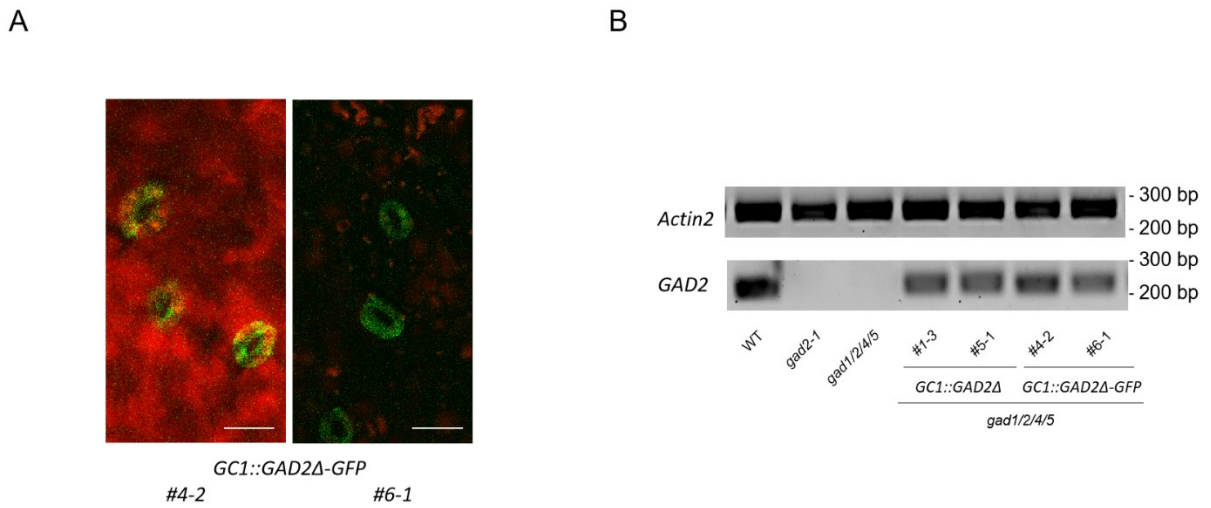

Figure 7. Guard cells specific complementation of *GAD2Δ in gad1/2/4/5*.

A. GFP fluorescence image of guard specific expression of *GAD2Δ-GFP* in the leaves of a *gad1/2/4/5* mutant line observed under confocal microscope, scale bar = 20 μm **B**. semi-qPCR analysis of *GAD2* transcript levels in WT, *gad1/2/4/5* and complementation lines as indicated.

Stomatal conductance of the lines expressing *GAD2Δ* was recorded. Two individual *gad1/2/4/5 /GC1:: GAD2Δ* complemented lines had higher stomatal conductance than that of WT and *gad1/2/4/5 (*Fig. 8A). This was also reflected in stomatal aperture data obtained with *gad1/2/4/5 /GC1:: GAD2Δ-GFP*, where it had significantly more open stomata than

that of both WT and *gad1/2/4/5* (Fig. 8B). Both results indicated a similar stomatal opening of the complemented lines to that of *gad2-1* (Fig. 8).

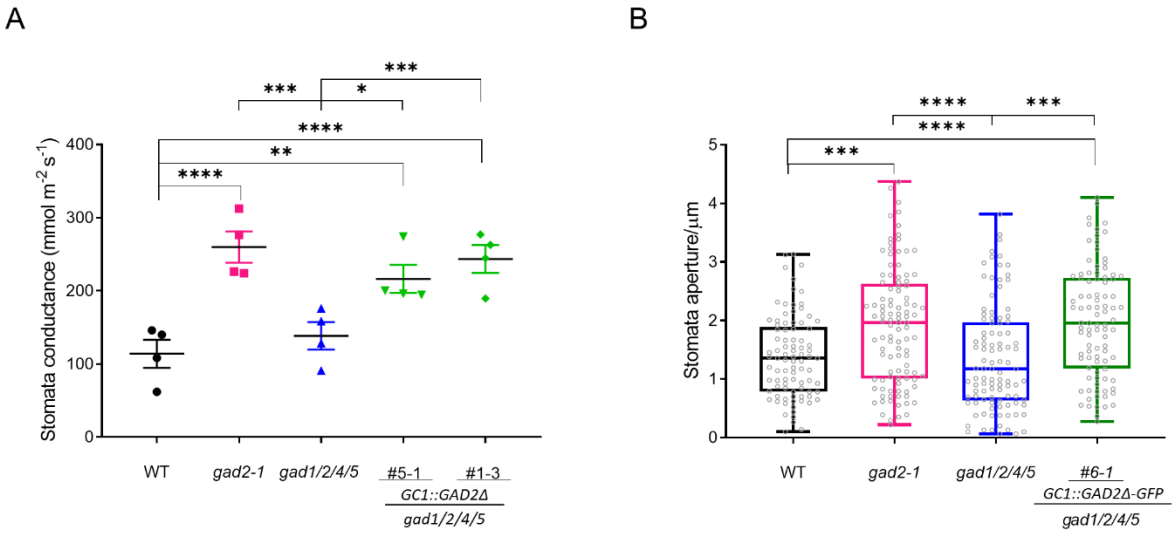

Figure 8. Stomatal movement of WT, *gad2-1*, *gad1/2/4/5* and *GC1: GAD2Δ/gad1/2/4/5*.

A. Stomatal aperture of plants. n= 113 for WT, n= 125 for *gad2-1*, n= 125 for *gad1/2/4/5*, n= 133 for *gad1/2/4/5/GAD2Δ-GFP #6-1*. **B**. stomatal conductance of plants. 4 leaves of each plant and 4 plants of each genotype were used. Asterisks represent statistical significance comparing between genotypes after one-way ANOVA in **A**, F (4, 15) = 10.97, p = 0.0002; and in **B**, F (3, 384) = 13.33, P<0.0001.

Discussion

Stomatal opening and GABA concentrations can be decoupled in *gad* mutants

With similar level of endogenous GABA in both *gad2-1* and *gad1/2/4/5* (Fig. 1E), the discovery that *gad1/2/4/5* failed to resemble *gad2* phenotype was intriguing (Fig. 2). This stomatal phenotype of *gad1/2/4/5* was consistent with its drought performance, as *gad1/2/4/5* had WT-like stomatal behaviour and drought sensitivity (Fig. 3B). A high transpiration rate and drought sensitivity had also been shown in the *gad1/2* double mutant, but not in *gad1* (Mekonnen et al. 2016). In chapter II, it was shown that both *gad2-1 and gad2-2* mutants had enlarged stomatal pores and thus showed increased drought sensitivity (Xu et al. 2021). Similar here with heterologous F_1 of ♂*gad2-1* × ♀*gad1/2/4/5*, which mimics the genotype of *gad2-1*, this ascertained that the loss of *GAD2* is associated with impaired gas exchange and the additional loss of *GAD4* (simultaneously with *GAD1*) or *GAD5* can alter this phenotype back to wildtype (Fig. 4A). The F_1 filial generation had increased stomatal conductance, which is significantly higher than that of WT and *gad1/2//4/5* (Fig. 4B). Thus, the disrupted function of *GAD2*, which leads to more open stomata in *gad2* and the F_1, is corroboration that mutation of *GAD2* leads to enlarged stomata and increased drought sensitivity as suggested previously in Chapter II.

Change in GABA level alone in guard cells can alter stomatal movement in *Arabidopsis*

Apart from the discrepancy in stomatal movement of *gad2* and *gad1/2/4/5*, the guard cell specific complemented lines, *gad1/2/4/5 /GC1:: GAD2Δ*, had increased stomatal aperture and conductance compared to that of *gad1/2/4/5* (Fig. 8A, B). This is also distinct from *gad2-1*, where the *GC1:: GAD2Δ* complementation reduced stomatal opening of *gad2-1* to the level of that in the WT (Xu et al. 2021). Both *gad2* and *gad1/2/4/5* had drastically reduced GABA level in leaves (Fig. 1C, 3C), thus the opposite effect of *GC1:: GAD2Δ* in the two mutants suggests that varying GABA concentration *per se* can create an altered stomatal response, which may vary dependent upon the genetic background and physiological address of the mutants. Expression data sets from the Bio-Analytic Resource for Plant Biology suggest a relatively higher expression level of *GAD2* and *GAD4* in leaves and that expression of *GAD4* is only significant in mesophyll cell (Yang et al. 2008, Pandey et al. 2010, Fucile et al. 2011). Thus the divergence of *gad1/2/4/5 /GC1:: GAD2Δ* vs. *gad2 /GC1:: GAD2Δ* could be due to different compartmentation of GABA within the leaf, which may be further impacted by variation in ALMT activity caused by unbalanced GABA distribution (Meyer et al. 2010, Meyer et al. 2011, De Angeli et al. 2013b, Ramesh et al. 2015, Sharma et al. 2016, Ramesh et al. 2018, Xu et al. 2021). This could lead to varied turgidity status of guard cells and cells surrounding it. For example, turgidity of epidermal cells has been suggested to have a transient effect at early stage of stomatal opening (Buckley 2019).

Both *GAD4* and *GAD5* could contribute to wildtype-like stomatal phenotype in the *gad1/2 background*

It was confirmed in the presented study, that within the scope of the *gad* mutants being tested, only *gad2* and *gad1/2* had more increased stomatal aperture, but not in *gad1* (Fig. 4C, Suppl. Fig. 6). This confirmed that the enlarged stomata in *gad1/2* is due to a mutation in *GAD2*, instead of *GAD1*, probably due to the prominence of *GAD2* in shoot part of plants (Fig. 1E). As aforementioned, further mutation of *GAD4* or *GAD5* may contribute to the difference between *gad2-1* and *gad1/2/4/5*. And the speculation was that *GAD4* could be a potent candidate since its expression is more predominant in rosette leaves and has been shown to be induced in the *gad1/2* mutant and in WT under salt stress and hypoxia (Scholz et al. 2015, Zarei et al. 2017, Safavi-Rizi et al. 2020). Our observation on *gad4* showed that none of the expression of *GAD1*, *GAD2* and *GAD5* was induced in the mutant (Fig. 5B). The single *gad4* mutant had stomatal aperture similar to that of WT and *gad1/2/4/5*, but significantly smaller than that of *gad2-1*. On the other hand, higher stomatal conductance was observed in *gad4* and *gad2/4* (Fig. 6A), although repeat experiments are required to further verify both stomatal aperture and conductance of the two mutants. Stomatal density of the mutants should also be measured to identify whether the divergence is caused by varied stomatal movement or density. This result could again highlight the differences one can obtain between whole leaves and epidermal peel experiments (Chapter II) (Buckley 2019). On the other hand, given our experience that stomata can continuously open with prolonged duration exposure to light with a variance in response speed of different genotypes (chapter III, Fig. 9), it is possible that for the epidermal strip assay, the stomatal aperture of *gad4* was not open enough to match the steady state of stomatal conductance.

Further experiments on stomatal aperture of these mutants under constant light are also required to explore whether there is a perturbed stomatal opening in the mutant.

Experiments on the triple mutants, *gad1/2/4* and *gad1/2/5*, indicated that additional mutation of both *GAD4* and *GAD5* could bring enlarged stomatal of *gad1/2* to the wildtype-like level (Fig. 5, 6A). The discrepancy between *gad2-1* and *gad1/2/4/5* could possibly be due to the mutation of *GAD1* in addition to either *GAD4* or *GAD5*. Recently, research in plant immunity showed that *Pseudomonas syringae* type III effector induced both expression of *GAD1* and *GAD4* in 14-day-old seedlings, while such response was significantly impaired in single mutants of mitogen-activated protein kinases, *mpk6* and *mpk9* (Deng et al. 2020). Furthermore, another study suggested that GABA accumulation by the mutation of *GABA-T/POP2* reduced sensitivity of plant to H_2O_2 possibly by impaired response in Reactive oxygen species (ROS) production gene (Su et al. 2019). ROS synthesis in plants involves Ca^{2+} signalling, MPK (including MPK6/9) and is influenced by circadian rhythms (Lai et al. 2012, Wrzaczek et al. 2013, Grundy et al. 2015, Singh et al. 2017). Whether mutation of *GAD1* and *GAD4* in addition to *GAD2* may perturb stomatal regulation mediated by these signaling pathways and leads to wild type like phenotype of *gad1/2/4* and *gad1/2/4/5* would need to be examined via transcriptional status of the mutants.

The reason why *gad1/2/4*, *gad1/2/5* and *gad1/2/4/5* had wildtype-like levels of gas exchange may also be linked with alteration of other metabolites in these mutants. Previous research showed that impaired GABA metabolism via either GABA depletion (in *gad1/2*) or overaccumulation (in *gaba-t/pop2*) alters the amino acid pool (Renault et al. 2010, Scholz et al. 2015), and a range of amino acids have been demonstrated to act on glutamate

receptor homologs (GLR) to prime Ca^{2+} signalling (Demidchik et al. 2018). For instance, Glu and L-Met can activate GLR-mediated Ca^{2+} signalling and stimulate stomatal closure (Kong et al. 2016). In this case, knock-out multiple *GAD*(s) may block GABA biosynthesis in the whole plants and in response to developmental and growth regulation, changing a range of metabolites that compromise effect by the loss of *GAD2* in plants. Therefore, global metabolic analysis in WT, *gad2-1* and *gad1/2/4/5* is expected to find clues as to the differential performance between single and multiple *GAD* mutants (Yoshida et al. 2016).

Materials and Methods

Plant materials and growth conditions

The *Arabidopsis* WT used in this study was Col-0 unless otherwise specified. The single mutant lines *gad1* (SALK_017810) and *gad2-1*(GABI_474E05) are previously described (Bouché et al. 2004, Mekonnen et al. 2016, Xu et al. 2021). Seeds of *gad1/2/4/5* were obtained from Shuqun Zhang (Deng et al. 2020). Seeds of *gad4a* (SALK_146398), *gad4b* (SALK_106240) mutants were ordered from ABRC. All mutants used in this study were homozygous, checked by a pair of gene specific primers and the T-DNA insertion border primer on genomic DNA. Details of insertion site and primers used are listed in Suppl. Table 1, 2.

Genomic DNA extraction was conducted on leaf tissue of plants. Basically, leaf were excised from plants and immersed in Edward buffer in 1.5 mL centrifuge tubes (Axygen) (Edwards et al. 1991). Then the tissue was thoroughly ground with a pestle and centrifuged at 14,000 x g for 1min. Subsequently, the supernatant was then mixed with 75% (v/v)

isopropanol (Chem Supply) with a ratio of 1:1 (v/v) and centrifuged at the same speed again. The sediment was then washed with 60% ethanol (Chem Supply) and centrifuged at the same speed. Final sediment was dissolved in ultrapure water (Milli Q Plus 185 Water Purification System) after ethanol was fully evaporated.

Mutants constructed from *gad2-1 x gad1/2/4/5* were identified by sequencing extracted DNA and examining the PCR products using the left boarder primer of T-DNA with a gene specific primer (Fig. 1B, right panel). The mutant strains were then confirmed by alignment of the sequencing result to genome sequence of relative genes to find the insertion sites. This was used to compare with the information from T-DNA Express: *Arabidopsis* Gene Mapping Tool by Salk Institute Genomic Analysis Laboratory to find the corresponding ID of mutants, which are indicated in the schematics in Fig. 1A.

The transgenic lines, *proGC1:: GAD2Δ-GFP*/*gad1/2/4/5* and *proGC1:: GAD4-mGFP*/ *gad1/2/4/5* had been constructed by *Agrobacterium tumefaciens* mediated transformation of target genes. Seeds of transgenic plants (T0) were selected by hygromycin-B (hygromycin-B, Monosulphate, Melford Laboratories Ltd.) for filial generations (Harrison et al. 2006). Basically, seeds were harvested in 2 mL tubes and mixed with silica gel beads (Silica gel orange, Sigma) in a ratio of 1:1. The tube was then sealed with cotton ball and placed on bench at room temperature for 10-14 days. Subsequently, the seeds were sterilised with 0.5% sodium hypochlorite and 0.01% triton-x solution for 10-15 min and washed with sterilised pure water (Milli Q Plus 185 Water Purification System) for 5-6 times before placed on half-MS medium containing 50ug / mL hygromycin-B in petri dish (Murashige and Skoog medium, Duchefa-Biochemie; 1% Sucrose, Chem-supply; 0.8% Phytagel, Sigma Aldrich). The seeds were then stratified at 4 °C under dark for 2-days, and

then placed horizontally under light for 6 hr, covered under dark for 2-days and exposed to light again for 1-day. The seedlings that looked greener were transferred to soil and covered with cling wrap to maintain the high humidity for 5-7 days. After that, the cling wrap was removed and the plants (T1 generation) were kept under long-day conditions (16-hr light/ 8-hr dark, 22 °C, 60-70 % relative air humidity) for seed harvesting (Rivero et al. 2014). The hygromycin-B selected plants were confirmed by genotyping (Lu 2011). For each genotype, around 20 plants were kept for seed harvesting. The filial T2 generation was then selected with same method on half-MS medium containing 50 µg/ mL hygromycin-B. Around 100 seeds of each genotype were selected on media and those with higher ratio of resistant plants were kept for seeds harvesting. Finally, the T3 generation was screened by the same method; only that the ones that showed 100% resistance were kept. And the T4 generation, the homozygous lines, were used for phenotyping experiments. The transgenic plants were observed under Olympus Fluorescence Microscope and screened to check the guard cell specific expression. All materials for phenotyping were sown on half-MS medium and stratified at 4°C for 4 days, then grew in short-day conditions unless otherwise specified (100- 150 $\mu mol \cdot m^{2-} \cdot s^{-1}$,10-hr light/ 14-hr dark, 22 °C, 60-70 % relative air humidity). Plants for transgenic construction and seed harvest were grown in long-day conditions (16-hr light/ 8-hr dark, 22 °C, 60-70 % relative air humidity).

Quantitative PCR

For qPCR, total RNA samples were extracted from rosette leaves using TRIzol Reagent (TRIzol RNA Isolation Reagents, Invitrogen) and purified with DNase (TURB DNase,

Invitrogen). cDNA was synthesized with SuperScript III Reverse Transcriptase (Invitrogen). Real time qPCR was performed with KAPA SYBR® FAST qPCR Kit (Roche) in QuantStudio 12 Flex Real-Time PCR System (Thermo Fisher Scientific). Each experiment was performed with 3 biological replicate plants and 3-4 technical replicates.

Semi-qPCR

Semi-qPCR was conducted with PCR reaction on cDNA from plants indicated. The PCR system used in this study is KAPA2G Fast HotStart ReadyMix. 100 × dilution of cDNA made from 1 μg RNA was used in the PCR reaction. The products were then checked with electrophoresis after 34 cycles of PCR reaction.

Stomata assay

For stomata aperture measurement, epidermal strips were peeled from the abaxial side of mature leaves, harvested from 4-6 weeks old plants. The peels were then floated in KCl-MES buffer (10 mM MES, 10 mM KCl, 5 mM Malate, pH 6.0 adjusted with Tris base) (Xu et al. 2021), with or without ABA or GABA, under light (200 μmol photons m^{-2} s^{-1}) or dark conditions. Stomatal status was captured under a Zeiss Axiophot Fluorescence Phase Microscope, and then measured by ImageJ. 3 biological replicate plants, 2 leaves per plant, were used in each experiment. Stomatal conductance was measured with a leaf porometer on 4 leaves of each plant from 5 biological replicate plants.

Drought treatment

Drought assays was performed as in Chapter 2. 4-5 weeks old plants were grown in short-day conditions (100- 150 μmol photons m^{-2} s^{-1},10-hr light/ 14-hr dark, 22 °C, 40-60 % RH), in equally weighed out soils containing 1:1 ratio Irish Peat and coco peat. The soil water content was saturated at Day-0 before withdrawing water. Leaves ware harvested and weighed for fresh weight, turgid weight and dry weight during the drought process. Water content and relative water content (RWC) was then calculated by the equation below.

$$\text{Water Content} = \frac{\text{Fresh Weight} - \text{Dry Weight}}{\text{Fresh Weight}}$$

$$\text{RWC} = \frac{\text{Fresh Weight} - \text{Dry Weight}}{\text{Turgid Weight} - \text{Dry Weight}}$$

Pharmacological treatment

Topical treatment with ABA and GABA were modified from previous research (Söderman et al. 2000). 4-week-old plants were sprayed daily with 0.01% Triton-X solution, with or without GABA (0.5 mM) and/ or ABA (5 μM ±-ABA), under both control and drought condition. Each solution was freshly prepared before the experiment. Stomatal conductance was measured with leaf porometer 3-hr after spray.

GABA concentration measurement

Rosette leaves from indicated materials were excised and snap-frozen in liquid nitrogen. Subsequently, materials were homogenised in liquid nitrogen. For Ultra Performance Liquid Chromatography (UPLC) analysis, around 50 mg fresh tissue were sent out for further analysis by our collaborators (Dr M. Okamoto, University of Adelaide) using Acquity UPLC System (Waters) with a Cortecs or Phenomenex UPLC C18 column (1.6 μm, 2.1x100 mm) as described in previous publication (Xu et al. 2021).

Vector constructions

pMDC32-proGC1:mGFP6 was constructed from pMDC32-35s as a backbone (Curtis and Grossniklaus 2003). The promoter of *GC1* (-1140/ +23 relative to transcriptive starting site, size of 1163 bp) was cloned from the GC1:: GAD2 construct as described in Xu et al., 2021, and the GFP fragment was amplified based on the template of pMDC83 plasmid DNA carrying mGFP6 sequence (Curtis and Grossniklaus 2003). Promoter sequence of proGC1 was amplified with primers containing restriction sites of KpnI and HindIII flanked at the 3' and 5' end, these two restriction sites are located in pMDC32-35s within the region of left border and attR1. Similarly, CDS sequence of mGFP6 was amplified from pMDC83-mGFP6 with primers flanked by restriction site of SpeI, which existed only between attR2 and the nos-terminator of the backbone. PCR amplification products Kpni-proGC1-HindIII, SpeI-Mgfp6-SpeI and pMDC32-35s backbone was respectively digested by HindIII and KpnI or by SpeI. The products digested by same restriction enzyme were then purified with illustra GFX PCR DNA and Gel Band Purification Kit (GE Healthcare), and then ligated with

T4 Ligase (NEB). The ligation product was then transformed into competent cell of *E. coli* DB3.1. Colony PCR was used to select positive colonies, and then the culture of the colony was used to extract plasmid using ISOLATE II Plasmid Mini Kit (Bioline). The plasmid was then checked by sanger sequencing.

Cloning of *GAD4*

CDS sequence of *GAD4 (*A2G02010) was amplified from cDNA of rosette leaves of 5-week-old WT (Col-0) with Phusion High-Fidelity DNA Polymerases (Thermo Scientific). The PCR products (Supplementary Figure 8A) were then checked by electrophoresis and then purified with illustra GFX PCR DNA and Gel Band Purification Kit (GE Healthcare). Subsequently, A-tailing of the purified products was performed with Taq DNA Polymerase (NEB) and purified with the purification kit again. The A-tailed GAD4 was then cloned into entry clone vector pCR™8/GW/TOPO™ (Invitrogen) through TA Cloning (Supplementary Figure 8B). The entry clone constructions were then checked by sequencing. Finally, Gateway LR Clonase II Enzyme mix (Invitrogen) was used to recombinant *GAD4* from pCR8 entry clone to the binary vector *pMDC32-35S:: mGFP6 (*Supplementary Figure 7). Final construction was checked by sanger sequencing (Supplementary Figure 8C).

Statistical analysis

Statistical analysis was conducted in R. For the dataset with only 2 groups, t-test analysis was applied. For dataset with multiple groups, homogeneity and normal distribution of data in each group are checked. Afterwards, for the dataset with one type of variable, ANOVA test was applied first to test if it has significant difference between groups (Fig. 1, 2, 3, 6,

8, and 9). Then multiple comparisons were conducted after Tukey post-hoc tests. For those with two types of variables, an ANOVA test was applied first to test if both have significant effects (Fig. 1, 4, 5, 6 and 7). Then multiple comparisons were conducted after Tukey post-hoc tests. Asterisks represent statistical significance. *, $p < 0.05$; **, $p < 0.01$; ***, $p < 0.001$; ****, $p < 0.0001$. Different letters indicate significant difference if $p < 0.05$.

Supplementary materials

Supplementary Table 1. Primers used in this chapter.

Primer names	Primer sequence: 5'- 3'	Purpose of using
SALK_017931_LP	ATGACTTGACTTGAACCTGCG	gad1 genotyping
SALK_017931_RP	GGAGCCAATGTTCAAGTAACG	gad1 genotyping
GABI_474E05_LP	ACGTGATGGATCCAGACAAAG	gad2 genotyping
GABI_474E05_RP	TCTTCATTTCCACACAAAGGC	gad2 genotyping
SK_106240_LP	CAATAAAAAGATGACGGTCGG	gad4 genotyping
SK_106240_RP	TTGAACCGGAAATTGAGTCAC	gad4 genotyping
GAD5-seq1_F	TGGATGGAACCTGAGTGTGA	gad5 genotyping
GAD5-seq3_R	CCATCCTGTCTCTGCGTTTT	gad5 genotyping
GAD1-qPCR _F	GCTGACCAACCCACCTTTAC	GAD1 qPCR
GAD1-qPCR_R	CGGCACTATCCATCCATACC	GAD1 qPCR
GAD2-qPCR _F	GCGGAGAGACTTGTTGCTGA	GAD2 qPCR
GAD2-qPCR_R	TTTCCACACAAAGGCAACAC	GAD2 qPCR
GAD3-qPCR _F	ACAGCTTCCAAATCCGATGA	GAD3 qPCR
GAD3-qPCR_R	TCCATCCAAGTGGTCACAAA	GAD3 qPCR
GAD4-qPCR _F	TACGTCCGCAACTCTCTTCC	GAD4 qPCR
GAD4-qPCR_R	TGAAGCTCAGTGGTGACAGG	GAD4 qPCR
GAD5-qPCR _F	TGCTTGCTGGTTTGGCTTTC	GAD5 qPCR
GAD5-qPCR_R	CCATCCTGTCTCTGCGTTTT	GAD5 qPCR
GAD4-CDS _F	ATGGTTTTGTCTAAGACAGTTTC	GAD4 cloning

GAD4-CDS_R	CATGCAAATTGTGTTCTTGTTG	GAD4 cloning
HindIII-proGC1_F	GCCAAGCTTTTTATAAGTTTTCAA	Binary vector construction
proGC1-KpnI_R	AAGGTACCGCCACCACATTCATC	Binary vector construction
CCA1-qPCR_F	CCTCAAACTTCAGAGTCCAATGC	CCA1-qPCR
CCA1-qPCR_R	GACCCTCGTCAGACACAGACTTC	CCA1-qPCR
LHY-qPCR_F	GAAGTCTCCGAAGAGGGTCG	LHY-qPCR
LHY-qPCR_R	TATTCACATTCTCTGCCACTTGAG	LHY-qPCR
TOC1-qPCR_F	GCTATGAACAGAAGTAAAGATTCG	TOC1-qPCR
TOC1-qPCR_R	GGATATCCCGTCATTCCATTCGGA	TOC1-qPCR
eIF4a-F	TGACCACACAGTCTCTGCAA	qPCR reference gene
eIF4a-R	ACCAGGGAGACTTGTTG	qPCR reference gene
actin2_F	TGGAATCCACGAGACAACCTA	qPCR reference gene
actin2_R	TTCTGTGAACGATTCCTGGAC	qPCR reference gene

Supplementary Table 2. Details of insertion site in GAD1, GAD2, GAD4 and GAD5 of gad1/2/4/5.

Gene name	Locus	Insertion site	Mutant line
GAD1	AT5G17330	Base 2486 5th exon	SALK_017810
GAD2	AT1G65960	Base 4868 6th exon	GABI_474E05 (gad2-1)
GAD4	AT2G02010	Base 474 2nd exon	Salk_106240 (gad4b)
GAD5	AT3G17760	Base 1391 4th exon	SALK_203883

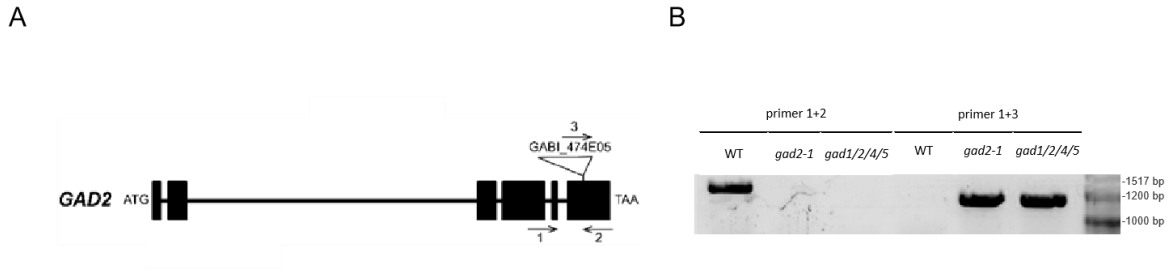

Supplementary Figure 1. Mutation specificity of *GAD2* in *gad2-1* and *gad1/2/4/5*.

A. Schematic of *gad2-1 (*GABI_474_E05) T-DNA insertion. **B**. The primer designed specifically for GABI insertion lines and *GAD2* gene specific primers (primer1-3 in a.) were used for genotyping. Identical in size of PCR products suggests the same mutation of *GAD2* in *gad2-1* and *gad1/2/4/5*.

```
GAD3  68    AAGAAG--ATGGTTTTATCTAAGACAGCTTCCAAATCCGATGATTCAATCCATTCAACTT  125
            ||||||  |||||||| |||||||||| |||| |||| ||||  |||||||||||||||
GAD4  148   AAGAAGACATGGTTTTGTCTAAGACAGTTTCCGAATCTGATGTCTCAATCCATTCAACTT  207

GAD3  126   TTGCTTCCCGTTATGTCCGCAACTCTATCTCACGATTCGAAATACCTAAGAACTCGATCC  185
            ||||||| ||||| ||||||||||||  |  ||||||||||||| ||| ||||||| ||||
GAD4  208   TTGCTTCTCGTTACGTCCGCAACTCTCTTCCACGATTCGAAATGCCTGAGAACTCAATCC  267

GAD3  186   CTAAGGAAGCAGCATACCAAATCATCAACGACGAGCTCAAGTTTGACGGTAACCCGAGGC  245
            | || |||||||| ||||||||||||||||||||||||| | | | || |||||||| ||||
GAD4  268   CAAAAGAAGCAGCTTACCAAATCATCAACGACGAGCTAATGCTCGATGGTAACCCAAGGC  327

GAD3  246   TAAACCTGGCCTCCTTTGTGACCACTTGGATGGAGCCAGAATGTGACAAGCTCATGATGG  305
            | ||||| || ||||| |||||||| ||||||||||||||||||||||||||||||||||||
GAD4  328   TGAACCTAGCTTCCTTCGTGACCACATGGATGGAGCCAGAATGTGACAAGCTCATGATGG  387

GAD3  306   AATCCATCAACAAGAACAACGTTGAGATGGACCAATACCCTGTTACCACCGACCTTCAGA  365
            | ||||||||||||||| ||||| || |||||| | |||||||| ||||| || |||||||
GAD4  388   AGTCCATCAACAAGAACTACGTCGACATGGACGAGTACCCTGTCACCACTGAGCTTCAGA  447

GAD3  366   ATCGATGCGTTAACATGATTGCGCGTCTCTTCAACGCGCCTTTAGGTGACGGTGAAGCCG  425
            | ||||| ||||||||||| || |||||||||||||||||  | ||||||||||||||| |
GAD4  448   ACCGATGTGTTAACATGATAGCACGTCTCTTCAACGCGCCGCTTGGTGACGGTGAAGCTG  507

GAD3  426   CCATTGGTGTTGGCACGGTGGGGTCATCGGAGGCAGTGATGTTGGCCGGACTGGCCTTTA  485
            || ||||||||||||| || || || ||||||||  | ||||||||||||  |||| ||||
GAD4  508   CCGTTGGTGTTGGCACCGTCGGATCGTCGGAGGCGATTATGTTGGCCGGTTTGGCTTTTA  567

GAD3  486   AGAGACAGTGGCAGAACAAGCGTAAGGCCCTAGGGCTGCCTTATGATAGACCTAATATTG  545
            ||||||| |||||||| ||||||||||||| |||||| ||||||||||  || ||||| |
GAD4  568   AGAGACAATGGCAGAATAAGCGTAAGGCCCAAGGGCTTCCTTATGATAAGCCCAATATCG  627

GAD3  546   TAACCGGAGCCAATATTCAGGTTTGCTTGGAGAAATTTGCAAGGTATTTTGAAGTGGAGC  605
            ||||||| || ||| | |||||||||| |||||||| |||||||||| ||||||||||
GAD4  628   TAACCGGTGCTAATGTCCAGGTTTGCTGGGAGAAATTCGCAAGGTATTTCGAAGTGGAGC  687

GAD3  606   TTAAGGAAGTGAAGCTGAGAGAAGGATATTACGTGATGGACCCTGACAAAGCGGTTGAAA  665
            ||||||||||||| || |||||||  ||||||||||||||||||  || ||||| ||||
GAD4  688   TTAAGGAAGTGAACCTAAGAGAAGACTATTACGTGATGGACCCTGTAAAGGCGGTCGAAA  747

GAD3  666   TGGTAGACGAAAACACTATATGCGTCGTGGCCATCCTCGGTTCGACACTAACCGGAGAAT  725
            ||||||||||||||| || || ||||  |||||||||||||| ||  ||||||| ||||
GAD4  748   TGGTAGACGAAAACACAATTTGTGTCGCTGCCATCCTCGGTTCAACGTTAACCGGTGAAT  807

GAD3  726   TCGAAGACGTTAAGCTCCTCAACGACCTTTTAGTCGAGAAAAACAAGAAAAACCGGATGGG  785
            |||||||||||||||||||||||||||||  | ||||||||||||||| ||||||||||||
GAD4  808   TCGAAGACGTTAAGCTCCTCAACGACCTCCTTGTCGAGAAAAACAAGCAAACCGGATGGG  867

GAD3  786   ATACGCCGATTCACGTGGACGCAGCGAGTGGTGGGTTTATTGCTCCCTTCTTGTATCCGG  845
            | ||||| || |||||||||||||||||||||||||||||||||||||| ||||||||||||
GAD4  868   ACACGCCAATACACGTGGACGCAGCGAGTGGTGGGTTTATTGCTCCGTTCTTGTATCCGG  927

GAD3  846   ACTTGGAGTGGGATTTCCGGTTACCGTTGGTTAAGAGCATAAATGTGAGTGGTCACAAAT  905
            |  |||||||||||||||| |||||||||||||||| || ||||||||||||||||||||
GAD4  928   AGCTGGAGTGGGATTTCCGGCTACCGTTGGTTAAGAGTATTAATGTGAGTGGTCACAAAT  987

GAD3  906   ACGGTTTGGTTTACGCCGGTATCGGTTGGGTCGTATGGAGAACCAAAACCGATTTGCCTG  965
            |||||||||||||||||||||| |||||||| ||||||||||||||||||||||||||||
GAD4  988   ACGGTTTGGTTTACGCCGGTATTGGTTGGGTTGTATGGAGAACCAAAACCGATTTGCCTG  1047

GAD3  966   ATGAACTTATCTTCCATATCAATTATCTTGGAGCTGATCAACCCACATTTACCCTCAACT  1025
            |||||||||||||||||||||||||||||||| |||||||||| || ||||| |||||||
GAD4  1048  ATGAACTTATCTTCCATATCAATTATCTTGGCGCTGATCAACCAACCTTTACACTCAACT  1107

GAD3  1026  TCTCTAAAGGGTCAAGTCAAGTGATTGCTCAGTACTACCAGTTGATTCGTCTTGGATTCG  1085
            |||| ||||| |||||||||||||||||||||||||||||||| ||||||||||||||||||
GAD4  1108  TCTCCAAAGGTTCAAGTCAAGTGATTGCTCAGTACTACCAGCTGATTCGTCTTGGATTCG  1167

GAD3  1086  AGGGATATCGCAACGTGATGGATAATTGCCGCGAGAACATGATGGTACTAAGACAAGGAT  1145
            |||| |||||||| ||||||||||||| || || ||||||||||||||||||||||||||
GAD4  1168  AGGGTTATCGCAATGTGATGGATAATTGTCGGGAAAACATGATGGTACTAAGACAAGGAT  1227

GAD3  1146  TAGAGAAAACGGGACGTTTTAACATCGTCTCCAAAGAAAACGGTGTTCCGTTAGTGGCGT  1205
            |||||||||||||||||||||| ||||||||||||||||||||||||||||||||||||||
GAD4  1228  TAGAGAAAACGGGACGTTTTAAAATCGTCTCCAAAGAAAACGGTGTTCCGTTAGTGGCGT  1287

GAD3  1206  TTTCTCTCAAAGATAGTAGCCGCCACAACGAGTTCGAGGTGGCCGAAATGCTTCGTCGCT  1265
            |||||||||||||||||||||||||||||||||||||||||||||| | |  || |||||||
GAD4  1288  TTTCTCTCAAAGATAGTAGCCGCCACAACGAGTTCGAGGTGGCCCATACACTCCGTCGCT  1347

GAD3  1266  TCGGCTGGATCGTTCCGGCCTACACGATGCCTGCGGATGCGCAACATGTCACGGTCCTTC  1325
            |||||||||||||||||||||||||||||||||||||||||||||| |||||||| |||||||
GAD4  1348  TCGGCTGGATCGTTCCGGCCTACACGATGCCTGCGGATGCGCAGCATGTCACTGTCCTTC  1407

GAD3  1326  GAGTTGTTATCCGAGAAGATTTCTCTCGAACCTTAGCTGAGAGATTGGTAGCCGATTTCG  1385
            |||||||||||||||||||||||||||||||||||||| ||||||||||||||| |||||||
GAD4  1408  GAGTTGTTATCCGAGAAGATTTCTCTCGAACCTTAGCCGAGAGATTGGTAGCTGATTTCG  1467

GAD3  1386  AGAAGGTTCTACACGAGCTCGATACGCTTCCCGCGAGGGTTCACGCCAAGATGGCTAGTG  1445
            |||||||||||||||||||||||||||||||| |||||||||||||||||||||||||| ||
GAD4  1468  AGAAGGTTCTACACGAGCTCGATACGCTTCCGGCGAGGGTTCACGCCAAGATGGCTAATG  1527

GAD3  1446  GAAAAGTTAACGGTGTTAAGAAGACGCCAGAGGAGACGCAAAGAGAAGTCACGGCCTACT  1505
            |||||||||||||||||||||||||||||||||||||||||||| |||||||||||||||||
GAD4  1528  GAAAAGTTAACGGTGTTAAGAAGACGCCAGAGGAGACGCAGAGAGAAGTCACGGCCTACT  1587

GAD3  1506  GGAAGAAGTTTGTGGACACTAAGA  1529
            ||||||||||  |||| |||||||
GAD4  1588  GGAAGAAGTTGTTGGAGACTAAGA  1611
```

Supplementary Figure 2. Genome DNA sequence alignment of GAD3 and GAD4.

The alignment was conducted by NCBI BLASTN. The mRNA sequence of the two genes shared 91% identity in a 1478 bp region.

A

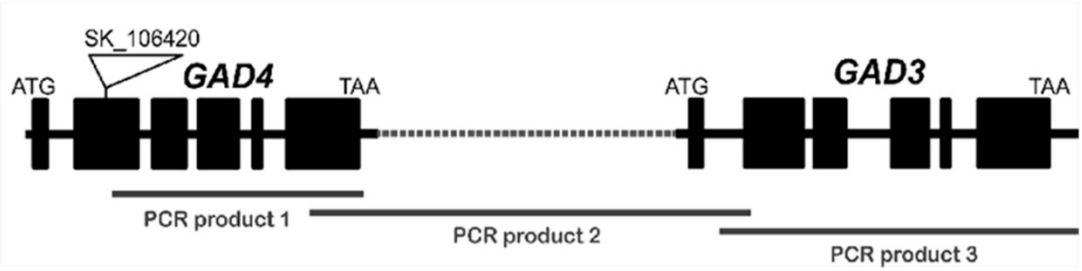

B

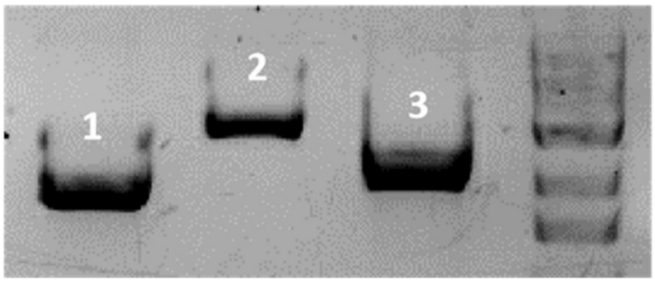

Supplementary Figure 3. Identify T-DNA insertion between *GAD3* and *GAD4*.

Since *GAD3* and *GAD4* locus are adjacent to each other on chromosome 2 (**A**), T-DNA insertion were also checked in *GAD3* by six pairs of primers targeting three segments after the insertion site in *GAD4*. **B.** Electrophoresis result of PCR products corresponding to A.

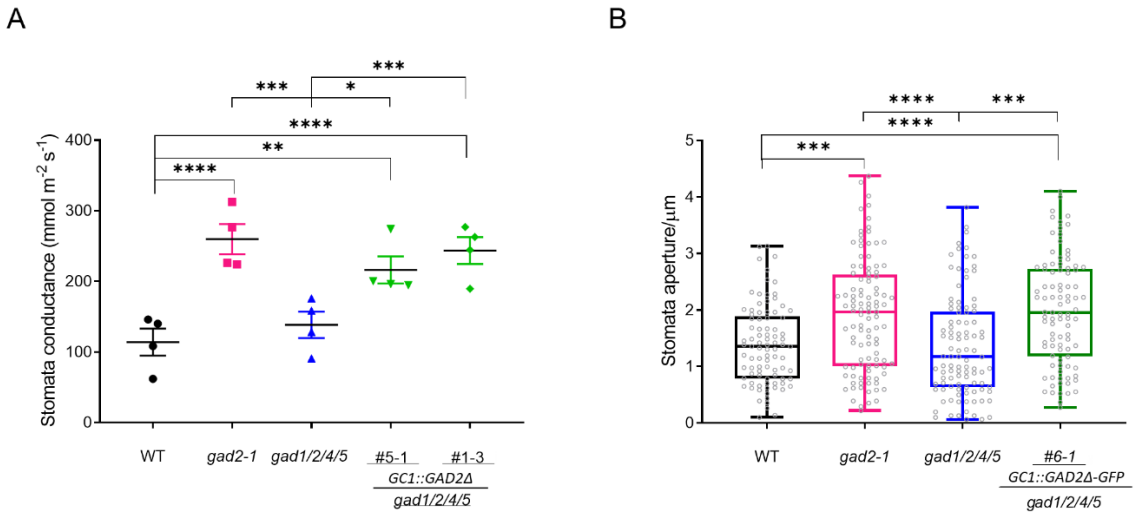

Supplementary Figure 4. Width/ length ratio of stomata in plants.

A. WT, *gad2-* and *gad1/2/4/5.* n= 123 for WT, n= 112 for *gad2-1*, n= 101 for *gad1/2/4/5*. **B**. WT, *gad2-*, *gad1/2/4/5* and *gad1/2/4/5/ΔGAD2-GFP*, n= 113 for WT, n= 125 for *gad2-1*, n= 125 for *gad1/2/4/5*, n= 133 for *gad1/2/4/5/ΔGAD2-GFP #6-1*.

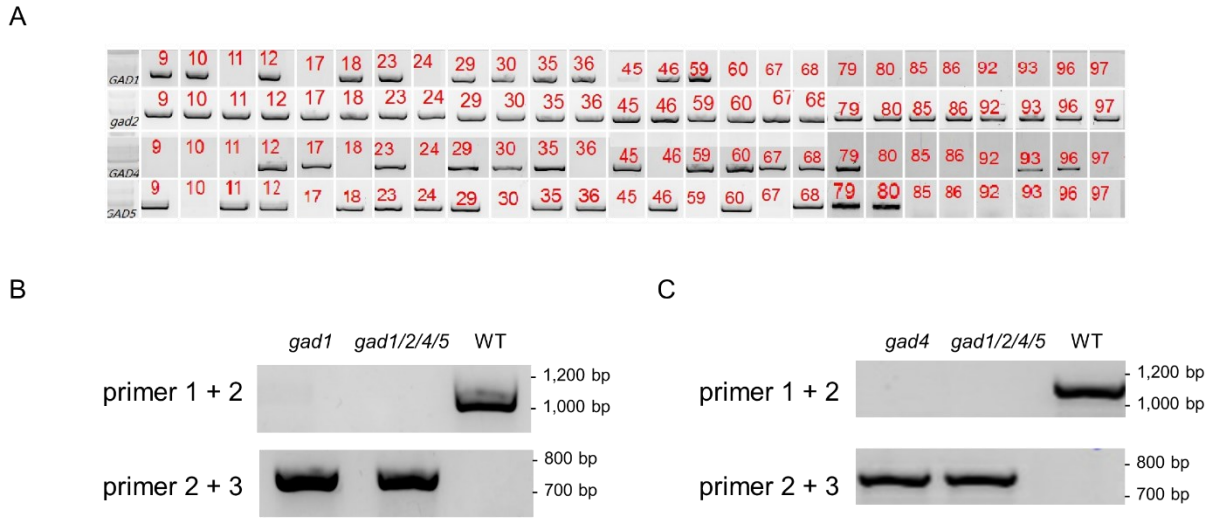

Supplementary Figure 5. Genotyping of *gad2-1* x *gad1/2/4/5* filial generation.

A. Electrophoresis result of genotyping of F_1 from *gad2-1* x *gad1/2/4/5*. **B-C**. Electrophoresis result of genotyping of *gad1* and *gad4*. Primers used are as described in Fig. 1A.

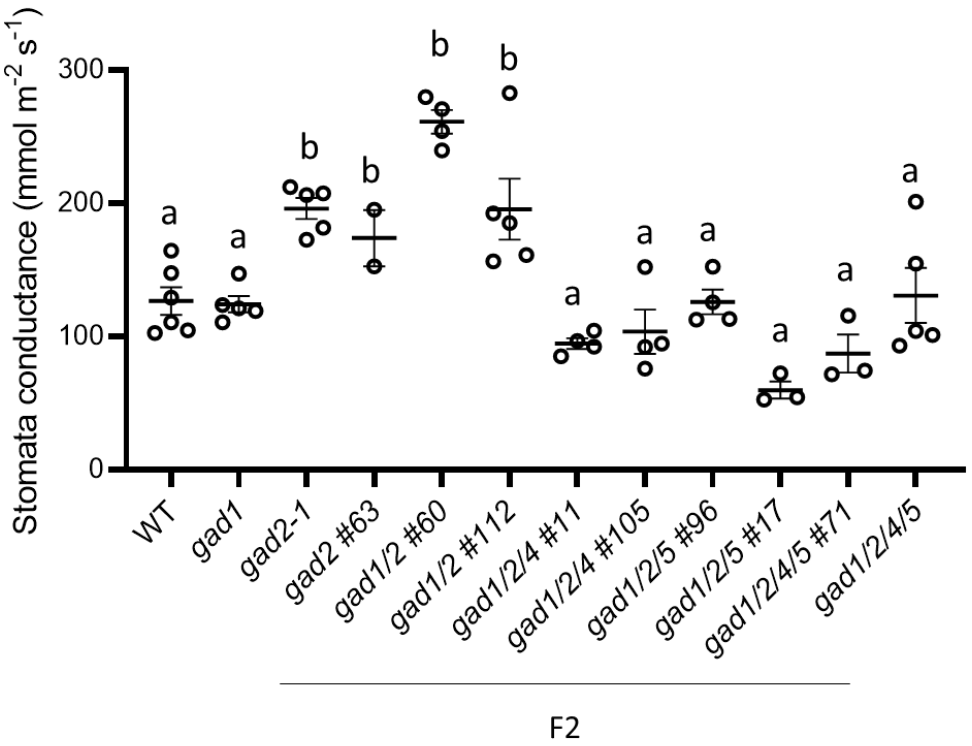

Supplementary Figure 6. Stomatal conductance of individual lines of F_2 mutants.

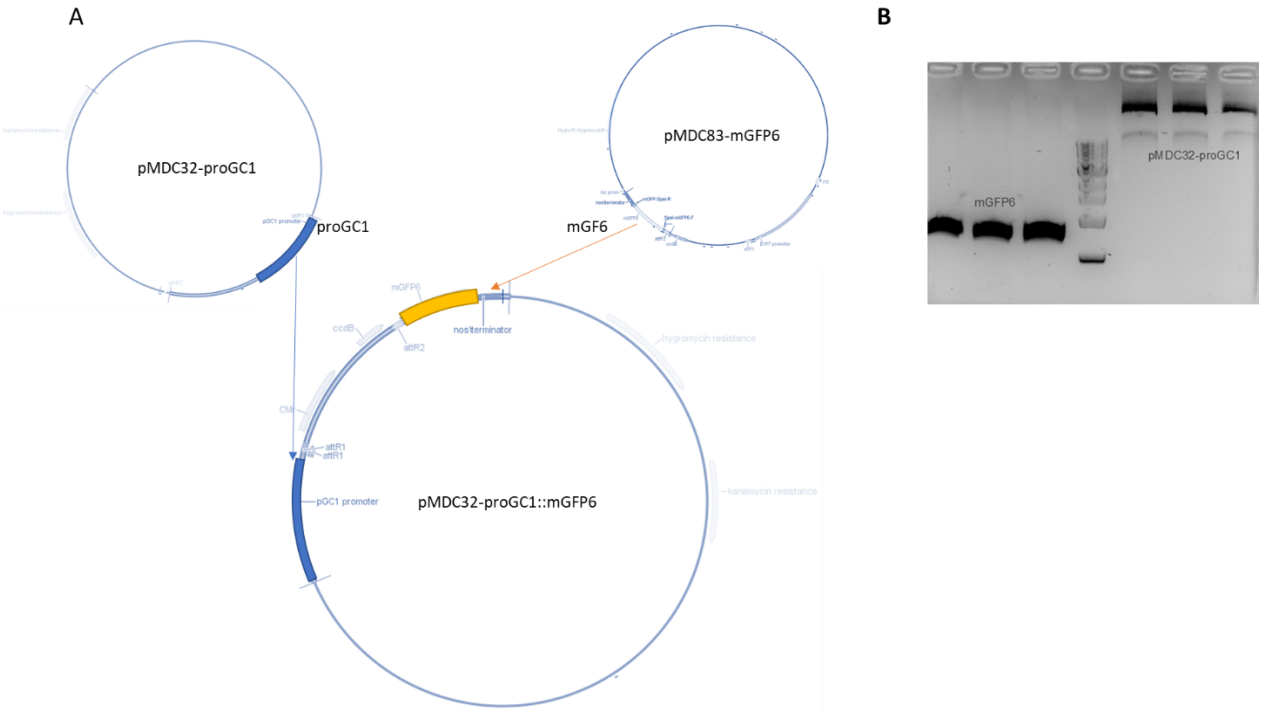

Supplementary Figure 7. Construction of *pMDC32-pGC1:: mGFP6*.

A. Schematic of construction of binary vector *pMDC32-pGC1:: mGFP6*. **B.** Enzyme digestion products of *pMDC32-pGC1* backbone and *mGFP6* coding sequence from donation vectors.

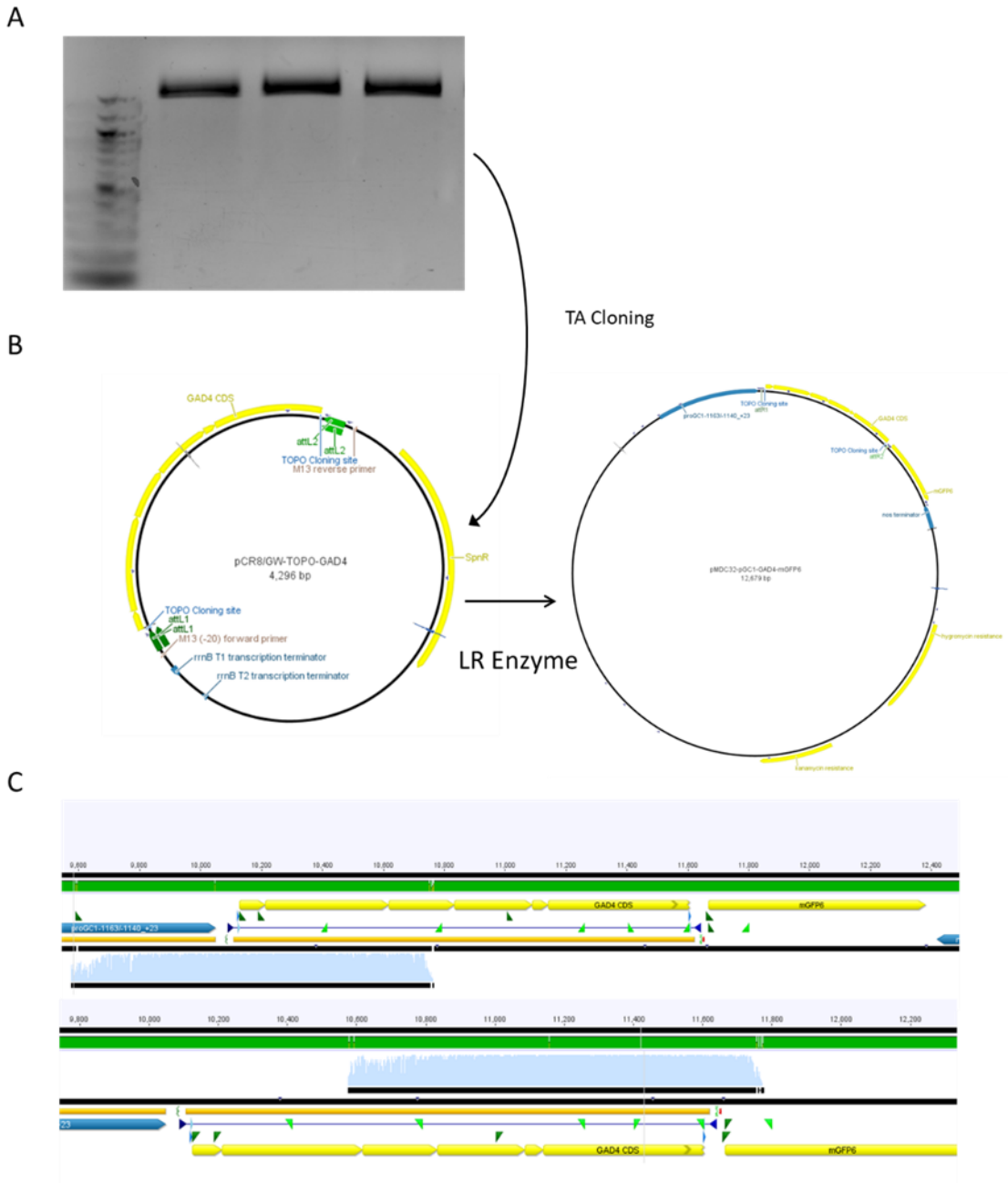

Supplementary Figure 8. Cloning of *GAD4*.

A. Electrophoresis result showing amplified CDS sequence of GAD4 from cDNA of WT. **B.** Schematic of entry cloning of *GAD4* to pCR8 via TA cloning and then to binary vector pMDC32-pGC1:: mGFP6. **C.** Sequence result of pMDC32-pGC1:: *GAD4*-mGFP6 construction.

Chapter V Investigating GABA-ABA crosstalk during stomatal regulation

Introduction

The results in chapter II suggests that that loss function of GAD2 leads to impaired ABA-induced stomatal closing, which is proposed to be due to de-regulation of ALMT9 (Chapter II, Suppl. Fig. 13 g-j). On the other hand, ABA induced stomatal closing was perturbed by application of 2 mM GABA at an ABA concentration of 2.5 μM but not 25 μM (Chapter II, Suppl. Fig. 3). Previous studies also suggests that *gad2-1* and *gad1/2/4/5* mutants appear to have altered responses to ABA (Lancien and Roberts 2006, Scala 2015, Mekonnen 2017). Collectively, these studies suggest that either interrupted or enhanced GABA signalling impaired ABA induced stomatal closing, which suggests crosstalk between the signalling pathways via either sharing elements (Eisenach et al. 2017), or via response to the same cues of stomatal movement (such as stress and circadian rhythm) (Michael et al. 2008b, Espinoza et al. 2010, Yong et al. 2017, Adams et al. 2018, Pelvan et al. 2021). Thus, this chapter aims to answer: 1) whether GABA deficiency led to altered ABA sensitivity of plants; 2) whether exogenous GABA application will alter ABA sensitivity of plants; and 3) whether there was interaction of GABA and ABA for regulation of stomata in *Arabidopsis*. For this purpose, first, ABA efficacy on stomatal closing with single and higher order of mutants of *GADs* were tested. Then drought stress and a dark-light transition were examined to see whether degree of stress, or time of day, may act as the shared cues mediating possible crosstalk between ABA and GABA signalling.

Results

ABA induced stomatal closure in *gad2-1* and *gad1/2/4/5* plants

Given the time interval that is required for preparation of epidermal strips for three bioreplicates of each genotype, and the fact that a time range of 0.5hr – 2hr is often used in such experiments (Prokic et al. 2006, Eisenach et al. 2017, Zhu and Assmann 2017), two different batch of experiments were conducted with a 1 hr (Fig. 1) and 2 hr treatment of ABA (Fig. 2). The epidermal strip assays were used to explore the impact of ABA on the stomatal closing of WT, *gad2-1* and *gad1/2/4/5*, and whether the ABA sensitivity of each line varied with duration of treatment. It is noticed that in those experiments, the quadruple mutant showed more opened stomata aperture after post hoc analysis of Two-way ANOVA (Fig. 1A, 2A). By focusing on the control group alone, the statistical difference between each genotype using post hoc of one-way ANOVA was checked. The result indicated that there was no significant difference between stomatal aperture of *gad1/2/4/5* and WT either for a treatment of 1hr ($F(2, 330) = 28.71$, $P<0.0001$; mean stomatal aperture for WT =1.299 ± 0.08 µm, for *gad1/2/4/5* =1.546 ± 0.07 µm; Adjusted P Value= 0.0823 for Tukey's multiple comparisons test) or 2hr ($F(8, 1182) = 119.8$, $P<0.0001$; mean stomata aperture for WT =1.619 ± 0.06 µm, for *gad1/2/4/5* = 1.901 ± 0.09 µm; Adjusted P Value= 0.0959 for Tukey's multiple comparisons test). The significance after Two-way ANOVA, after checking the algorithm, was due to excluded variation contributed by the ABA effect when looking at the genotype effect alone in Two-way ANOVA. Thus, the quadruple *gad1/2/4/5* mutant had a similar aperture to that of wildtype plants, whereas *gad2-1* constantly had more opened stomata (Fig. 1A, 2A).

Since the influence of both factors on stomatal aperture were of interest, a Two-way ANOVA was interpreted. Under 1hr of ABA treatment, showed that both 2.5 µM and 5 µM ABA closed stomata of each genotype (Fig 1B), suggesting that the depletion of GABA synthesis in *gad2-1* and *gad1/2/4/5* mutants did not prevent the genotypes from being ABA responsive; however, the final apertures achieved by the same ABA treatment was not identical between genotypes (Fig 1A). For each genotype, treatment with either 2.5 or 5 µM ABA closed stomata to a similar level, with no significant difference between the two doses of ABA (Fig. 1B). To clarify the effect of ABA, the stomatal closing extent were calculated as a percentage using Equation 1. Stomatal aperture of *gad2-1* closed to a lesser extent compared to that of other genotypes in response to 5 µM ABA (Suppl. Fig. 4A). To be specific, 2.5 µM ABA caused a closure of between 40-50% of the stomatal width of all genotypes, while 5 µM ABA had a greater effect in WT (54.3 ± 0.03%) and *gad1/2/4/5 (*57.4 ± 0.02%) but not in *gad2-1 (*37.7 ± 0.03%) (Suppl. Fig. 4A).

$$Closing\ extent = \frac{(a_i - \bar{a}_{Ctrl})}{\bar{a}_{Ctrl}} \qquad \text{Equation 1}$$

- a_i: Individual stomatal width;
- $\bar{a}_{Ctrl}$: Mean stomatal width of the genotype under control condition.

A

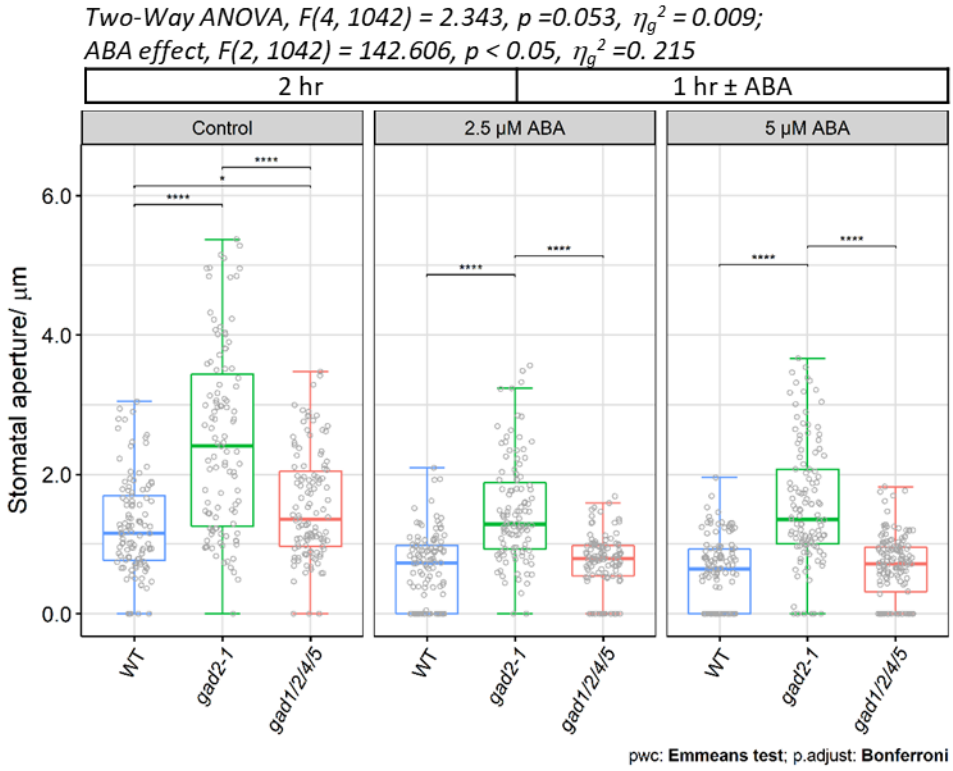
Two-Way ANOVA, F(4, 1042) = 2.343, p =0.053, η_g^2 = 0.009;
ABA effect, F(2, 1042) = 142.606, p < 0.05, η_g^2 =0. 215
2 hr
1 hr ± ABA
Control
2.5 µM ABA
5 µM ABA
Stomatal aperture/ µm
6.0
4.0
2.0
0.0
WT
gad2-1
gad1/2/4/5
pwc: Emmeans test; p.adjust: Bonferroni

B

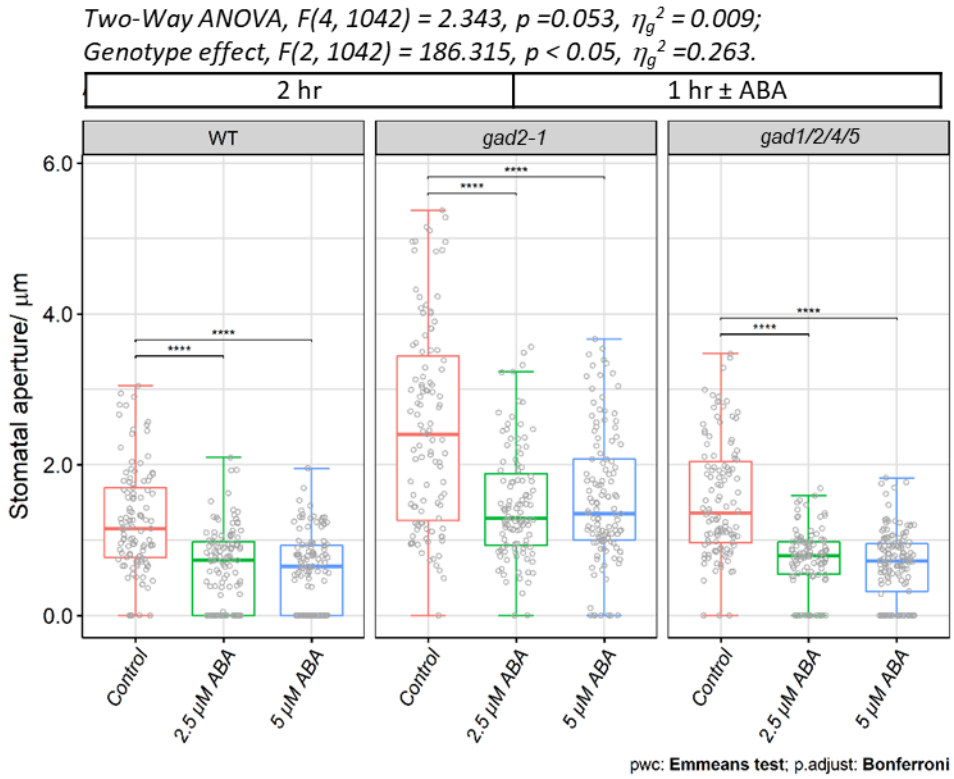
Two-Way ANOVA, F(4, 1042) = 2.343, p =0.053, η_g^2 = 0.009;
Genotype effect, F(2, 1042) = 186.315, p < 0.05, η_g^2 =0.263.
2 hr
1 hr ± ABA
WT
gad2-1
gad1/2/4/5
Stomatal aperture/ µm
6.0
4.0
2.0
0.0
Control
2.5 µM ABA
5 µM ABA
pwc: Emmeans test; p.adjust: Bonferroni

±

Figure 1. Stomatal width of WT, *gad2-1* and *gad1/2/4/5* following ABA induced stomatal closing, with 1 hr of ABA treatment.

A. Comparing dose effects of ABA on stomatal aperture of WT, *gad2-1* and *gad1/2/4/5* under constant light conditions. **B.** Comparing stomatal aperture of WT, *gad2-1* and *gad1/2/4/5* after the same concentration of ABA treatment under constant light. In the control group, n = 109 for WT, n = 107 for *gad2-1*, n = 114 for *gad1/2/4/5*; In 2.5μM ABA group, n = 113 for WT, n = 111 for *gad2-1*, n = 110 for *gad1/2/4/5*; In 2.5μM ABA group, n = 122 for WT, n = 120 for *gad2-1*, n = 145 for *gad1/2/4/5*. The box plots indicate median ±data-range. Asterisks indicate significant difference between genotype under same ABA dose (**A**) and between different ABA doses of each genotype (**B**) after Two-way ANOVA. p = 0.005. *, p < 0.05; **, p < 0.01; ***, p < 0.001; ****, p < 0.0001.

When the duration for ABA treatment was increased to 2 hr (Fig. 2), *gad2-1* still showed significantly more open stomata than the other two genotypes regardless of ABA supplement (Fig. 2A). The single mutant had a lower extent of stomatal closing (38.7 ± 0.02% with 2.5 μM ABA, 46.6 ± 0.02% with 5 μM ABA) than that of WT (49.3 ± 0.03% with 2.5 μM ABA, 53.8 ± 0.02% with 5 μM ABA) and *gad1/2/4/5 (*52.7 ± 0.03% with 2.5 μM ABA, 62.3 ± 0.02% with 5 μM ABA) (Suppl. Fig. 2B). Two way ANOVA indicated a correlation effect between genotypes and ABA treatment only with 2 hr ABA treatment, F (4, 1179) = 3.341, p <0.05, η_g^2 = 0.011 for 2 hr treatment; F (4, 1042) = 2.343, p =0.053, η_g^2 = 0.010 (Fig. 1, 2). This was probably due to an increased difference between *gad2-1* to WT and *gad1/2/45 (*Suppl. Fig. 2)*.* Thus, all further experiments were conducted under 2 hr of ABA treatment unless otherwise specified.

Stomatal development on single leaves of plants varies (Geisler and Sack 2002), considering the influence of stomatal length on the pore dimension, stomatal width/length

ratio were also measured. Data representing stomata aperture width or width-to-length ratio gave similar results, suggesting that stomatal morphology and development was probably not altered in any of these mutants (Fig. 1, 2 and Suppl. Fig. 1, 3). Stomatal width thereby is enough to represent an accurate parameter for stomatal opening in our experiments, therefore further experiments use stomatal width only.

A

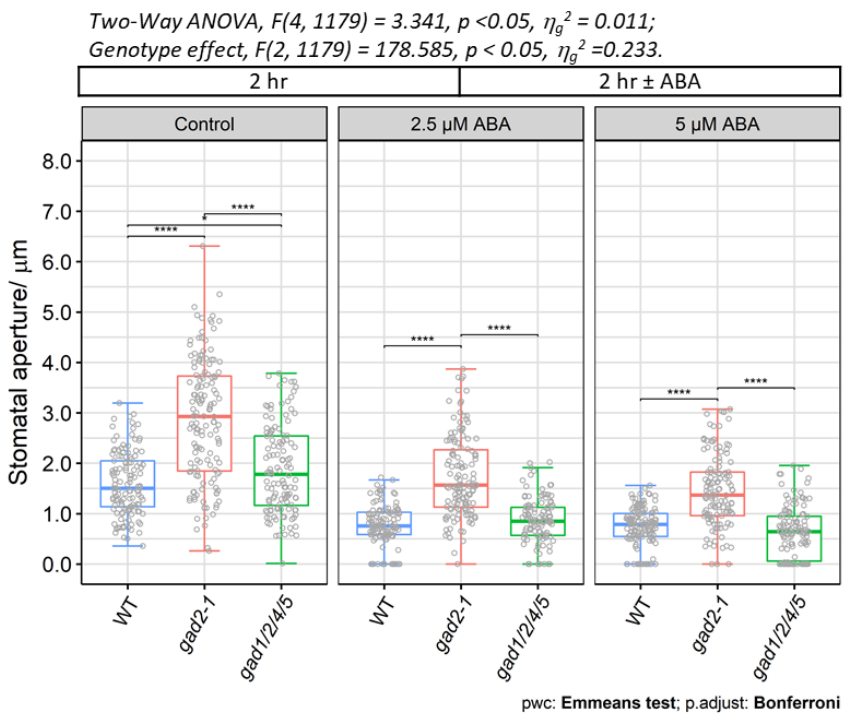
Two-Way ANOVA, F(4, 1179) = 3.341, p <0.05, ηg² = 0.011;
Genotype effect, F(2, 1179) = 178.585, p < 0.05, ηg² =0.233.
2 hr
2 hr ± ABA
Control
2.5 µM ABA
5 µM ABA
Stomatal aperture/ µm
8.0
7.0
6.0
5.0
4.0
3.0
2.0
1.0
0.0
****
WT
gad2-1
gad1/2/4/5
pwc: Emmeans test; p.adjust: Bonferroni

B

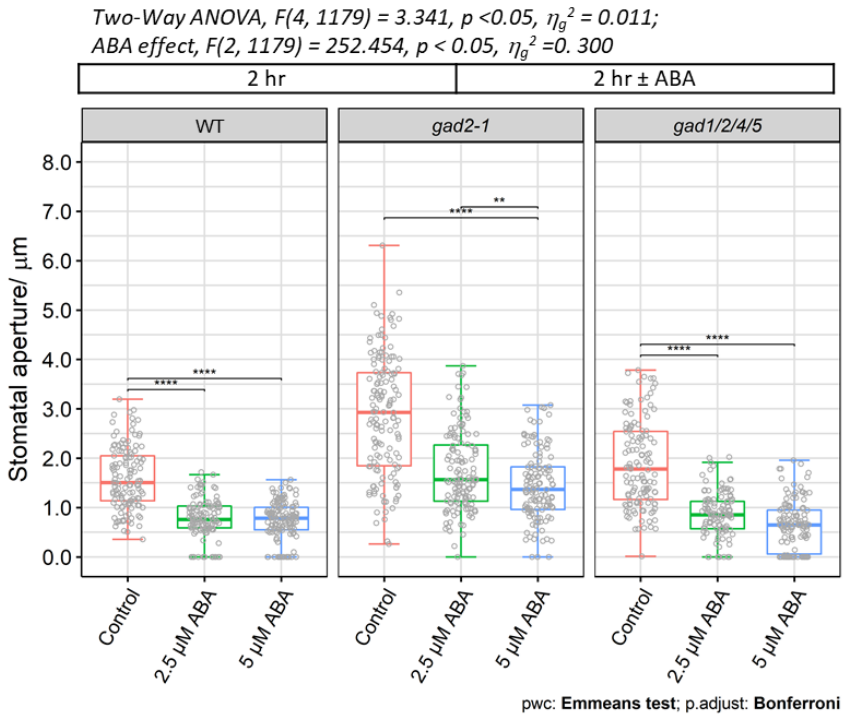
Two-Way ANOVA, F(4, 1179) = 3.341, p <0.05, ηg² = 0.011;
ABA effect, F(2, 1179) = 252.454, p < 0.05, ηg² =0. 300
2 hr
2 hr ± ABA
WT
gad2-1
gad1/2/4/5
Stomatal aperture/ µm
8.0
7.0
6.0
5.0
4.0
3.0
2.0
1.0
0.0
****
**
Control
2.5 µM ABA
5 µM ABA
pwc: Emmeans test; p.adjust: Bonferroni

Figure 2. Stomatal width of WT, *gad2-1* and *gad1/2/4/5* following ABA induced stomatal closing, with 2 hr of ABA treatment.

A. Comparing dose effects of ABA on stomatal aperture of WT, *gad2-1* and *gad1/2/4/5* under constant light. B. Comparing stomatal aperture of WT, *gad2-1* and *gad1/2/4/5* after the same concentration of ABA treatment under constant light. In control group, n = 131 for WT, n = 146 for *gad2-1*, n = 129 for *gad1/2/4/5*; In 2.5 μM ABA group, n = 125 for WT, n = 137 for *gad2-1*, n = 124 for *gad1/2/4/5*; In 5 μM ABA group, n = 133 for WT, n = 134 for *gad2-1*, n = 129 for *gad1/2/4/5*. The box plots indicate median ±data-range. Asterisks indicate significant difference between genotype under same ABA dose (**A**) and between different ABA doses of each genotype (**B**) after Two-way ANOVA. p = 0.005. *, p < 0.05; **, p < 0.01; ***, p < 0.001; ****, p < 0.0001.

Stomatal response of *gad1/2/4/5/GC1:: GAD2Δ* to ABA

Previously, it has shown that guard cell specific complementation of *GAD2Δ* by the *GC1* promoter for *gad2-1* and *gad1/2/4/5 (*respectively designated *gad2-1/GC1:: GAD2Δ* and *gad1/2/4/5/GC1:: GAD2Δ*) led to different outcomes (Chapter IV, Fig. 9). *gad2-1/GC1:: GAD2Δ* restored wildtype-like stomatal aperture, stomatal conductance and water loss (Xu et al. 2021); whilst *gad1/2/4/5/GC1:: GAD2Δ* increased stomatal conductance greater than WT and *gad1/2/4/5*, close to that of *gad2-1 (*Chapter IV, Fig. 9). To examine whether expression of *GAD2* in *gad1/2/4/5* altered stomatal sensitivity to ABA, an epidermal peel assay was conducted on WT, *gad2-1, gad1/2/4/5* and *gad1/2/4/5/GC1:: GAD2Δ*. Two-way ANOVA indicated that stomatal opening in the *gad1/2/4/5/GC1:: GAD2Δ* line was significantly lower than that of *gad2*-1, but greater than WT and *gad1/2/4/5* (Fig. 3A). Differences between stomatal aperture of *gad2-1* and *gad1/2/4/5/GC1:: GAD2Δ* to that of WT and *gad1/2/4/5* showed significance regardless of ABA application (Fig, 3A). As for

stomatal response to serial ABA doses within each genotype (Fig. 3B), 100 nM ABA was effective to trigger stomatal closure; and a 1.5 μM dose further closed stomata to a similar extent with a 2.5 μM dose (Fig. 3B). The effect of ABA across different genotypes were compared using a closing extent, and the result indicated that increasing ABA concentration closed stomata of WT, *gad1/2/4/5* and the complemented line – between 35% to 70%. While *gad2-1* always had a lower stomatal closing percentage than WT and *gad1/2/4/5*, this was not the case when 2.5 μM ABA was applied, where such significance only existed comparing *gad2-1 (*50.4 ± 0.03%) to WT (71.2 ± 0.02%) and *gad1/2/4/5 (*72 ± 0.03%), but not to *gad1/2/4/5/GC1:: GAD2Δ* (62.1 ± 0.03%). The complemented line also had a lower closing extent under 2.5 μM ABA treatment, and there was no significant difference between that in *gad2-1* and *gad1/2/4/5/ GC1:: GAD2Δ* after Two-Way ANOVA, $F(9,1401) = 3.540$, $p < 0.05$, $\eta_g^2 = 0.022$. (Suppl. Fig. 4A).

Given that stomatal aperture of *gad2-1* and *gad1/2/4/5/GC1:: GAD2Δ* was significantly larger under control conditions - when calculating the closing extent - the larger divisor ($\bar{a}_{Ctrl}$) could contribute to the smaller closing extent of these genotypes. Thus, to see how exactly ABA influences stomatal opening across all genotypes, the actual closing extent of stomatal aperture (difference between ABA treated group to the control group) was calculated (Suppl. Fig. 4B). Surprisingly, the ABA triggered stomatal change (in μm) was similar in all genotypes, except when 1 μM ABA was applied, *gad1/2/4/5/GC1:: GAD2Δ* stomata had an average closure of 2.09 ± 0.093 μm, which is significant bigger than that of *gad2-1 (*1.89 μm ± 0.086) (Suppl. Fig. 4B). Further experiments are required to confirm such significance.

A

Two-Way ANOVA, F(9 1401) = 0.937, p <0.05, η_g^2 = 0.006;
Genotype effect, F(3, 1401) = 130.941, p < 0.05, η_g^2 =0.219.

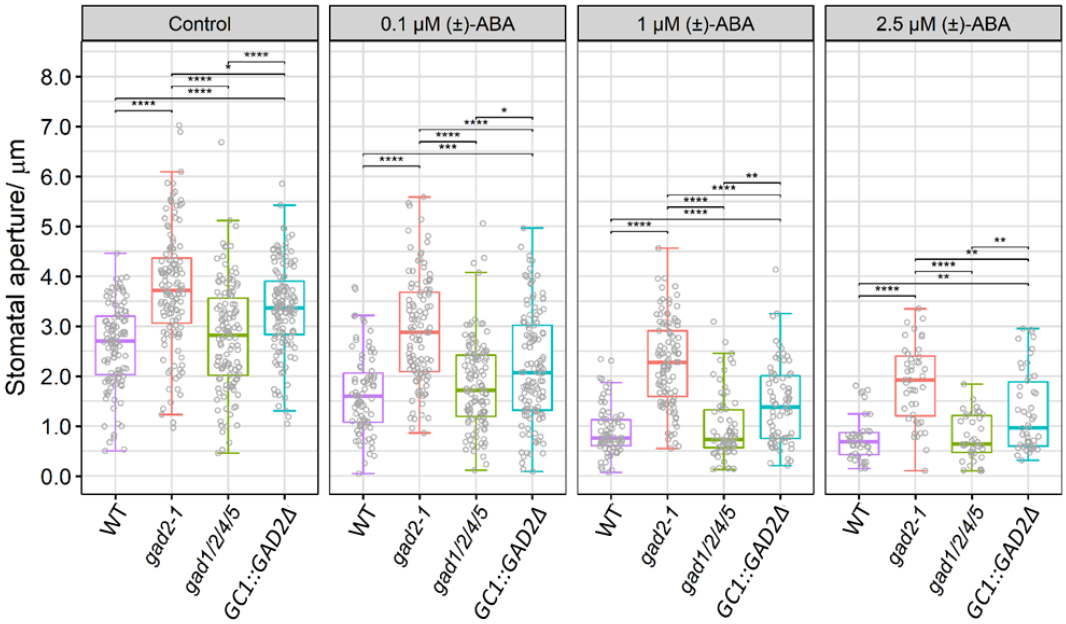

pwc: **Emmeans test**; p.adjust: **Bonferroni**

B

Two-Way ANOVA, F(9 1401) = 0.937, p <0.05, η_g^2 = 0.006;
ABA effect, F(5, 1401) = 326.169, p < 0.05, η_g^2 =0.411.

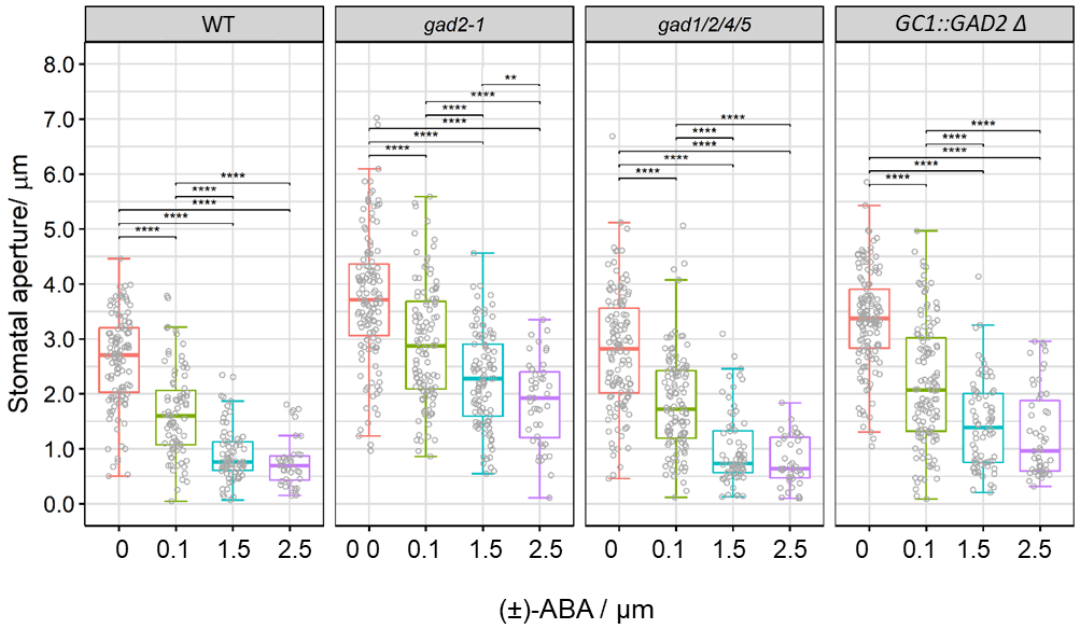

pwc: **Emmeans test**; p.adjust: **Bonferroni**

Figure 3. Dose effect of ABA on stomatal closing of WT, *gad2-1*, *gad1/2/4/5* and *gad1/2/4/5/ GC1:: GAD2Δ*.

Stomatal aperture of plants after 2hr exposure to different doses of ABA under constant light conditions compared among genotypes (**A**) and ABA dose effect is compared within the same genotype (**B**). In the control group, n = 113 for WT, n = 127 for *gad2-1*, n = 126 for *gad1/2/4/5*, n = 133 for *gad1/2/4/5/GC1:: GAD2*Δ; In 0.1 μM ABA group, n = 83 for WT, n = 109 for *gad2-1*, n = 115 for *gad1/2/4/5*, n = 122 for *gad1/2/4/5/GC1:: GAD2*Δ; In 1 μM ABA group, n = 74 for WT, n = 101 for *gad2-1*, n = 68 for *gad1/2/4/5*, n = 74 for *gad1/2/4/5*/ *GC1:: GAD2Δ*; In 2.5 μM ABA group, n = 39 for WT, n = 44 for *gad2-1*, n = 39 for *gad1/2/4/5*, n = 50 for *gad1/2/4/5/GC1:: GAD2*Δ, n = 46 for WT, n = 36 for *gad2-1*, n = 35 for *gad1/2/4/5*, n = 35 for *gad1/2/4/5/GC1:: GAD2Δ* responded to different level of ABA. The box plots indicate median ± min-max. Asterisks indicate significant difference between different pharmacological treatments of each genotype including watered control after Two-way ANOVA. *, $p < 0.05$; **, $p < 0.01$; ***, $p < 0.001$; ****, $p < 0.0001$.

Sensitivity of *gad1/2/4/5* to ABA and its impact on drought tolerance

Previous research on creeping bentgrass (*Agrostis stolonifera*) found that a spray of 0.5 mM GABA mimicked the effect of a (5 μM) ABA spray on improving water availability in leaves under drought stress (Li et al. 2017); similar results were also obtained for *Phaseolus vulgaris* L (Abd El-Gawad et al. 2020). As suggested in chapter II (Suppl. Fig. 3, 11), GABA may interact with ABA signalling during stomatal regulation. Since ABA is a key hormone for plant adaptation to drought stress (McAdam and Brodribb 2018), *gad1/2/4/5* was employed to examine the effect of ABA on stomatal regulation when the capacity of the GABA shunt to produce GABA was abolished. WT and *gad1/2/4/5* plants were sprayed with 0.5 mM GABA (close to the physiological concentration of GABA in

Arabidopsis tissue under normal conditions, i.e. ~0.1-1 mM) (Miyashita and Good 2008, Scholz et al. 2015, Jalil et al. 2019, Xu et al. 2021), ABA or a combination of both treatments during well-watered and drought conditions. Water content was measured after 6-days of continuous treatment to evaluate the pharmacological effect of GABA and ABA and its interaction with knockout of the GABA shunt pathway (Fig. 4). Under well-watered conditions, WT and the quadruple *gad* mutant exposed to all treatments had the same relative water content (Fig. 4A). When withholding water, the application of 0.5 mM GABA itself did not change water content compared to non-GABA treatment within the same genotype; withholding water resulted in a significantly lower leaf water content than a well-watered treatment regardless of GABA application (Fig. 4B). Spraying ABA following drought treatment maintained leaf water content to a similar level compared to leaves under well-watered conditions, which were significantly higher than the drought treatment without ABA spray (Fig. 4B). The quadruple *gad* mutant was somewhat different, where ABA-improved water retention under drought was statistically attenuated when compared to the well-watered condition. This suggests that *gad1/2/4/5* may respond to ABA differently from wildtype seedlings following diurnal cycles and a stress treatment (Fig. 4B). Interestingly, when examining the impact of combined treatment of GABA together with ABA, the WT plants exposed to the combined treatment still had significantly increased water content compared to the drought control, whereas water content of *gad1/2/4/5* plants treated with both GABA and ABA was insignificant from the drought treated control plants (Fig. 4B). However, when directly comparing the effect of spraying GABA, it had no impact on water content in either genotype when compared to the straight ABA treated plants, nor did ABA spray further improve water availability of both the GABA-sprayed WT and *gad1/2/4/5* mutant (Fig. 4B). Collectively these results suggest that GABA has little impact on the ability to retain water when challenged with a simultaneous ABA treatment, at these

concentrations in the experimental system employed, which contrasts with when 2 mM GABA was applied to epidermal peels and inhibited 2.5 μM ABA induced stomatal closure. However, the ABA and GABA sensitivity of plants is subtly altered when plants have the GABA shunt pathway severely impaired in *gad1/2/4/5*. Therefore, the effects of ABA on *gad1/2/4/5* on stomatal opening were examined (Fig.5).

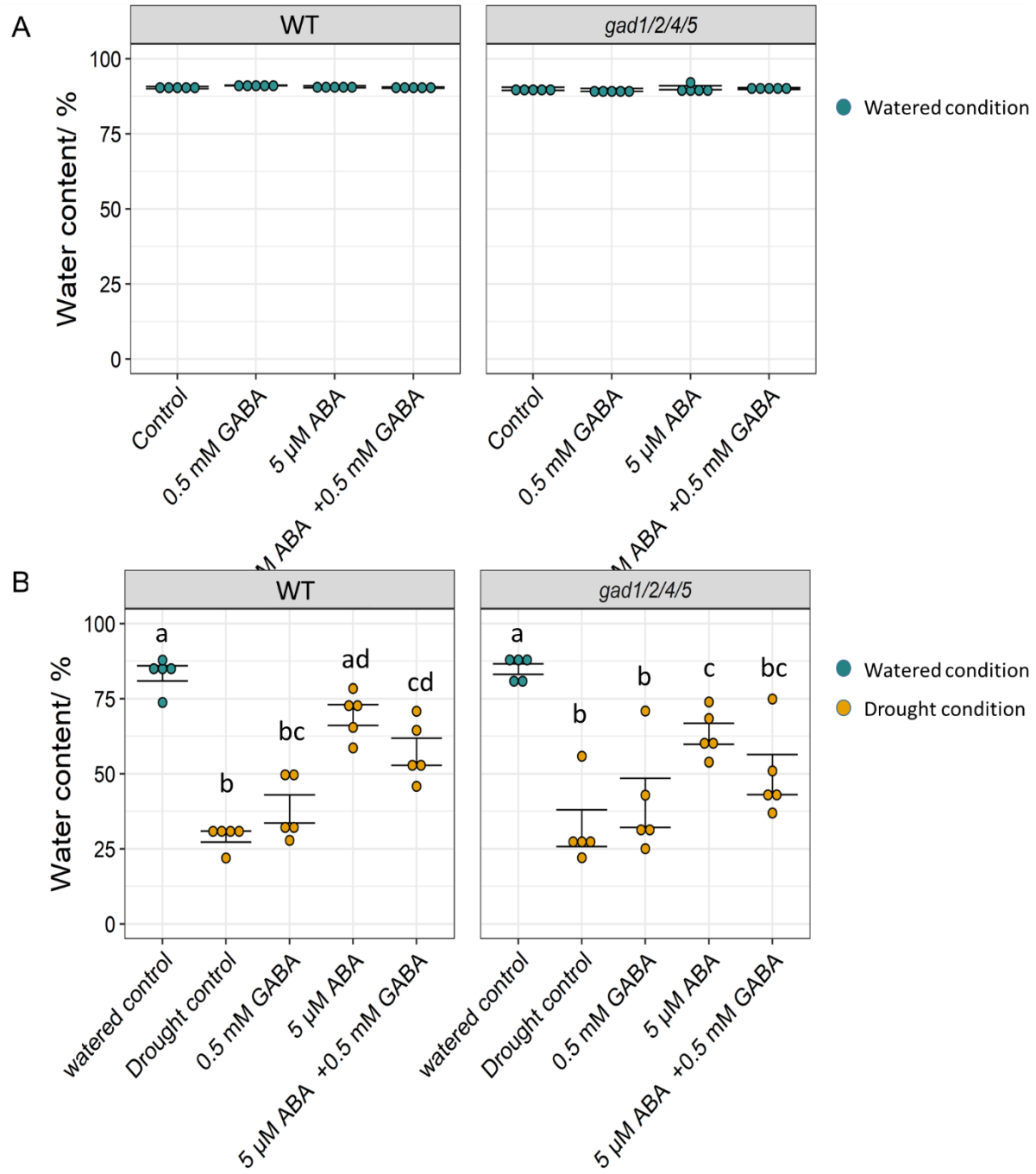

Figure 4. Effect of GABA and ABA on water content of WT and *gad1/2/4/5*.

Water content of WT and *gad1/2/4/5* after 6 days of pharmacological treatment with 0.5 mM GABA and/ or 5 µM ABA under watered (**A**) and drought (**B**) conditions**.** 5 plants of each genotype under

the same treatment were sampled for water content. Asterisks in black indicate significant difference between different pharmacological treatments of each genotype including watered control after Two-way ANOVA, $F_{Interaction}$ (4, 40) = 0.5446, p = 0.7039; $F_{Genotypes}$ (1, 40) = 0.2549, p = 0.6164; $F_{Treatment}$ (4, 40) = 40.17, p < 0.0001. Asterisks in red indicate significant difference between different pharmacological treatments of each genotype excluding watered control after Two-way ANOVA, $F_{Interaction}$ (3, 32) = 0.5401, p = 0.6583; $F_{Genotypes}$ (1, 32) = 0.3731, p = 0.5456; $F_{Treatment}$ (3, 32) = 18.36, p < 0.0001. *, p < 0.05; **, p < 0.01; ***, p < 0.001; ****, p < 0.0001.

Influence of *GADs* on ABA inhibition of stomatal opening

The *gad2-1* mutant altered the extent to which ABA closes stomatal pores compared to wildtype plants; however, such altered sensitivity in *gad1/2/4/5* appeared to be recovered back to wildtype levels (Fig. 1, 2). The use of double and triple *gad* mutants would be expected to inform which of the mutations in *GAD*(s) reverted *gad2* back to a wildtype phenotype. Epidermal strip assays were conducted under a dark to light transition to examine the interaction between GABA and ABA (Fig. 5, 6). Comparing the treatment effect within genotype (Fig. 5A), the dark-to-light transition opening of stomata was significantly inhibited by ABA in all lines. Interestingly, in *gad2/4*, the GABA and ABA co-treatment had significantly more open stomata than that of the ABA treated group (Fig. 5A, first panel at the bottom). When comparing the effect of pharmacological treatments between genotypes (Fig. 5B), *gad2-1* had significantly more opened stomata compared to other genotypes under control conditions. When 0.5 mM GABA was applied, such differences were only the case when comparing stomatal aperture width of *gad2-1* to that of *gad1*, *gad4*, *gad2/4* and *gad1/2/4/5*. Besides, *gad1/2/4* and *gad1/2/5* had more opened stomata than that of *gad4* and *gad1/2/4/5*. As for the ABA-treated group, both *gad2-1* and *gad1/2/4* had more opened

stomata than that of *gad1*, *gad2/4* and *gad1/2/4/5*. When GABA and ABA were treated together, stomatal aperture was larger in WT than that of *gad1* and *gad4 (*Fig. 5B).

Since Two-way ANOVA indicated the pharmacological treatment had a significantly different impact on stomatal aperture (considering statistical variance of both contribution of GABA and ABA to data variance) ($F_{(3,4517)} = 225.285$, $p < 0.001$, $\eta_g^2 = 0.130$), and that the relationship between the treatment and stomatal width depends on the genotypes (Two-Way ANOVA, $F_{(21, 4517)} = 4.113$, $p < 0.001$, $\eta_g^2 = 0.019$), further analysis was conducted using three-way ANOVA to elucidate the effect of ABA and GABA individually to explain the change in significance in Fig. 5B (Fig. 6). The result indicated that both ABA and GABA could significantly influence the stomatal aperture of plants (Three-Way ANOVA, $F_{(7, 4517)} = 4.333$, $p < 0.0001$, $\eta_g^2 = 0.007$). The result confirmed that ABA reduced the stomatal pore width in all genotypes regardless of the presence of GABA (Fig. 6A), whereas GABA's effect on stomatal regulation alone varied in different genotypes and was ABA-dependent. Interestingly, 0.5 mM GABA enhanced stomata opening in WT, *gad1*, *gad1/2/4* and *gad1/2/5* compared to control conditions (by 16.4 ± 0.05%, 20.9 ± 0.05%, 21.4 ± 0.05% and 14.7 ± 0.03% respectively), despite no statistical difference between genotypes within the same treatment (Fig. 6B, upper panel, Suppl. Fig. 7). When ABA was added, such effect was still the case in WT (17.6% increase, GABA + ABA vs. ABA) but not in the three mutants when ABA was added. Furthermore, GABA in addition to ABA could increase stomatal aperture in *gad2/4* and *gad1/2/4/5*, where GABA application reduced the ABA effect by 24.4 ± 0.04% and 17.9 ± 0.04% respectively in the two mutants *(*Fig. 6B, Suppl. Fig. 5).

A

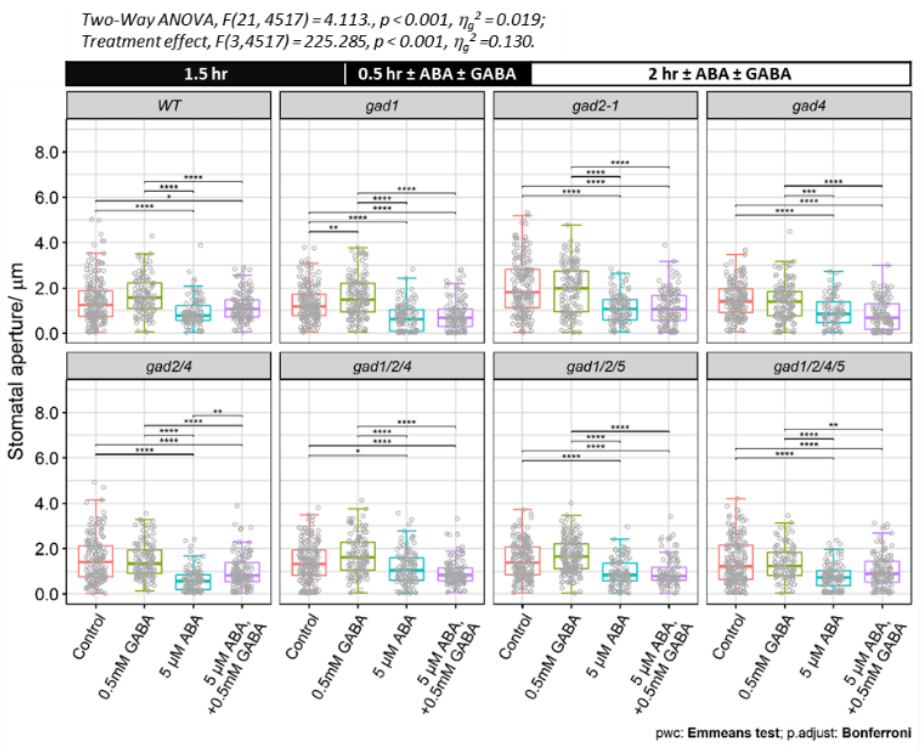
Two-Way ANOVA, F(21, 4517) = 4.113., p < 0.001, η_g^2 = 0.019;
Treatment effect, F(3,4517) = 225.285, p < 0.001, η_g^2 =0.130.
1.5 hr
0.5 hr ± ABA ± GABA
2 hr ± ABA ± GABA
WT
gad1
gad2-1
gad4
gad2/4
gad1/2/4
gad1/2/5
gad1/2/4/5
Stomatal aperture/ µm
Control
0.5mM GABA
5 µM ABA
5 µM ABA, +0.5mM GABA
pwc: Emmeans test; p.adjust: Bonferroni

B

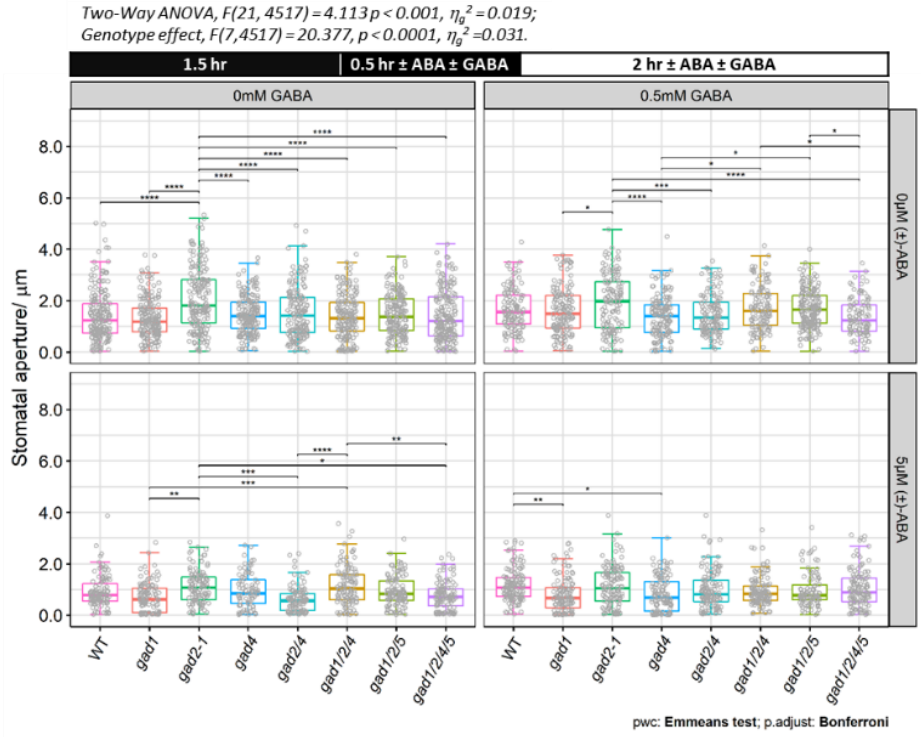
Two-Way ANOVA, F(21, 4517) = 4.113 p < 0.001, η_g^2 = 0.019;
Genotype effect, F(7,4517) = 20.377, p < 0.0001, η_g^2 =0.031.
1.5 hr
0.5 hr ± ABA ± GABA
2 hr ± ABA ± GABA
0mM GABA
0.5mM GABA
0µM (±)-ABA
5µM (±)-ABA
Stomatal aperture/ µm
WT
gad1
gad2-1
gad4
gad2/4
gad1/2/4
gad1/2/5
gad1/2/4/5
pwc: Emmeans test; p.adjust: Bonferroni

Figure 5. Pharmacological effect of GABA and ABA on multiploid mutants of *GAD*s.

Stomatal aperture width of *Arabidopsis* with exogenous GABA and/ or ABA under dark-light transition comparing between treatments for each genotype (**A**) and between genotypes under same treatment (**B**). Asterisks indicated significance after Two-way ANOVA comparing the between genotypes (**A**) or treatments (**B**). For control group, n=210 for WT, n=198 for *gad1*, n=201 for *gad2-1*, n=193 for *gad4*, n=173 for *gad2/4*, n=187 for *gad1/2/4*, n=187 for *gad1/2/5*, n=199 for *gad1/2/4/5*; For 0.5mM GABA group, n=128 for WT, n=153 for *gad1*, n=142 for *gad2-1*, n=150 for *gad4*, n=131 for *gad2/4*, n=129 for *gad1/2/4*, n=186 for *gad1/2/5*, n=104 for *gad1/2/4/5*; For 0.5μM ABA group, n=108 for WT, n=115 for *gad1*, n=117 for *gad2-1*, n=85 for *gad4*, n=108 for *gad2/4*, n=115 for *gad1/2/4*, n=122 for *gad1/2/5*, n=117 for *gad1/2/4/5*; For 0.5mM GABA+ 0.5μM ABA group, n=139 for WT, n=120 for *gad1*, n=133 for *gad2-1*, n=115 for *gad4*, n=130 for *gad2/4*, n=129 for *gad1/2/4*, n=98 for *gad1/2/5*, n=127 for *gad1/2/4/5*. The box plots indicate median ±data-range. Asterisks indicate significant difference between treatments of each genotype (A) and between genotype under treatment (B) after Two-way ANOVA. $p = 0.005$. *, $p < 0.05$; **, $p < 0.01$; ***, $p < 0.001$; ****, $p < 0.0001$.

A

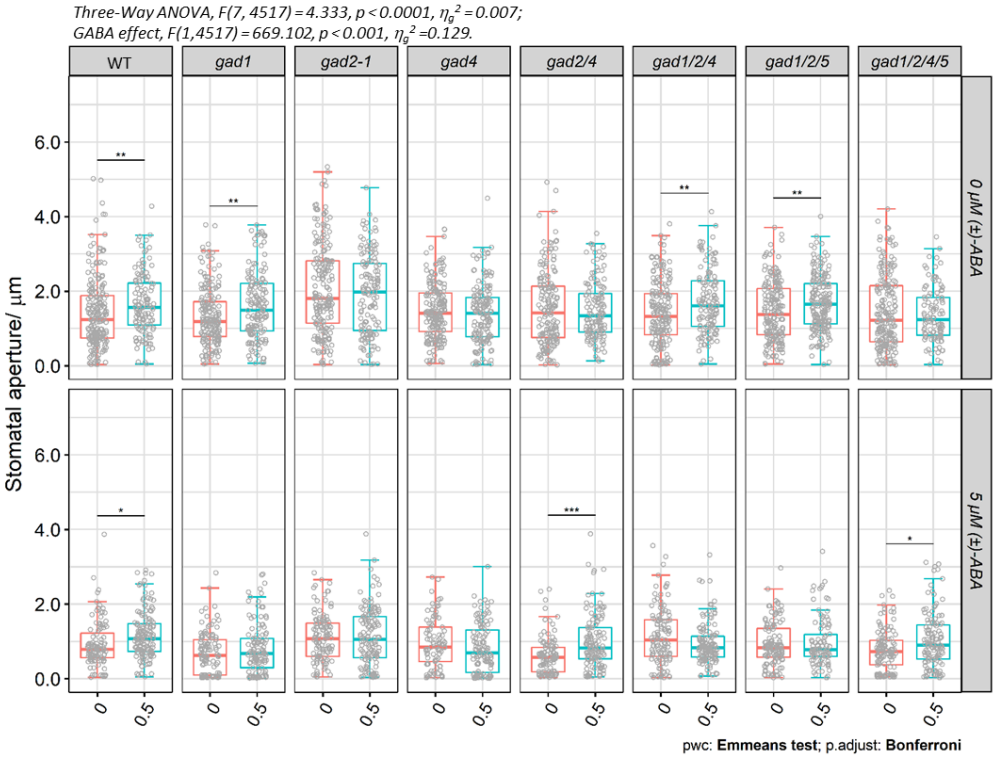
Three-Way ANOVA, F(7, 4517) = 4.333, p < 0.0001, η_g^2 = 0.007;
GABA effect, F(1,4517) = 669.102, p < 0.001, η_g^2 =0.129.
WT
gad1
gad2-1
gad4
gad2/4
gad1/2/4
gad1/2/5
gad1/2/4/5
0 µM (±)-ABA
5 µM (±)-ABA
Stomatal aperture/ µm
0.0
2.0
4.0
6.0
0
0.5
pwc: Emmeans test; p.adjust: Bonferroni

B

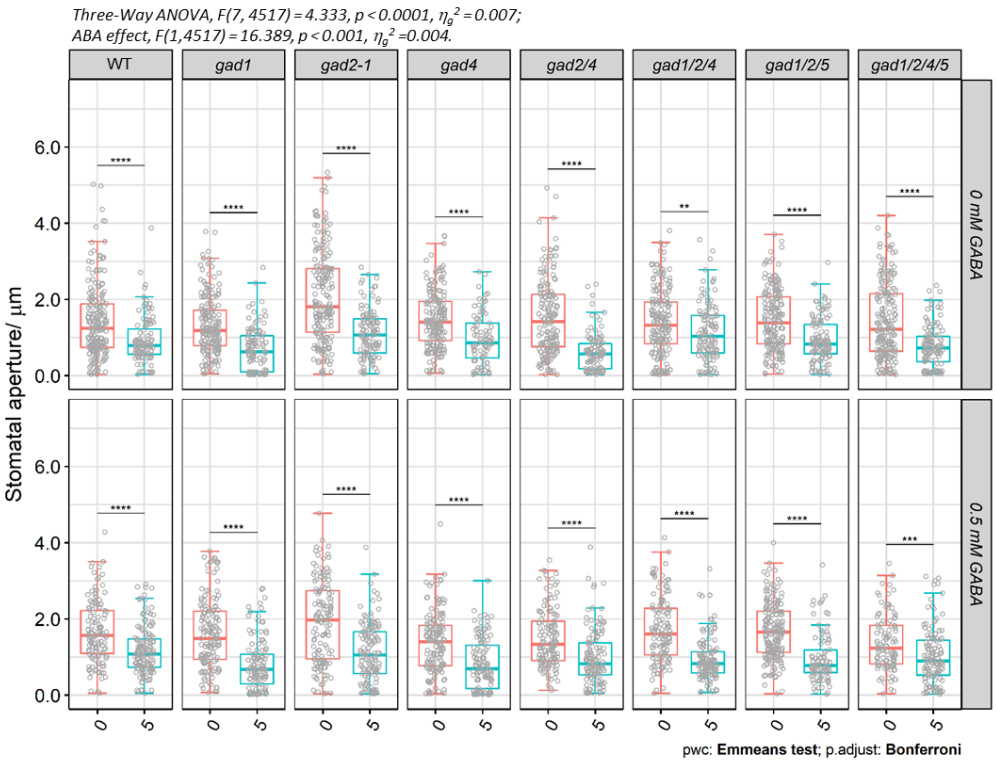
Three-Way ANOVA, F(7, 4517) = 4.333, p < 0.0001, η_g^2 = 0.007;
ABA effect, F(1,4517) = 16.389, p < 0.001, η_g^2 =0.004.
WT
gad1
gad2-1
gad4
gad2/4
gad1/2/4
gad1/2/5
gad1/2/4/5
0 mM GABA
0.5 mM GABA
Stomatal aperture/ µm
0.0
2.0
4.0
6.0
0
5
pwc: Emmeans test; p.adjust: Bonferroni

Figure 6. Effect of GABA and ABA individually on stomatal opening of multiploid mutants of *GAD*s.

Effect of GABA individually on stomatal opening of higher order of mutants of *GAD*s (**A**) and effect of ABA individually on stomatal opening of higher order *GAD* mutants (**B**). Asterisks indicated significance after three-way ANOVA comparing the effect of GABA (A) or ABA (**B**) on each genotype. For control group, n=210 for WT, n=198 for *gad1*, n=201 for *gad2-1*, n=193 for *gad4*, n=173 for *gad2/4*, n=187 for *gad1/2/4*, n=187 for *gad1/2/5*, n=199 for *gad1/2/4/5*; For 0.5mM GABA group, n=128 for WT, n=153 for *gad1*, n=142 for *gad2-1*, n=150 for *gad4*, n=131 for *gad2/4*, n=129 for *gad1/2/4*, n=186 for *gad1/2/5*, n=104 for *gad1/2/4/5*; For 0.5μM ABA group, n=108 for WT, n=115 for *gad1*, n=117 for *gad2-1*, n=85 for *gad4*, n=108 for *gad2/4*, n=115 for *gad1/2/4*, n=122 for *gad1/2/5*, n=117 for *gad1/2/4/5*; For 0.5mM GABA+ 0.5μM ABA group, n=139 for WT, n=120 for *gad1*, n=133 for *gad2-1*, n=115 for *gad4*, n=130 for *gad2/4*, n=129 for *gad1/2/4*, n=98 for *gad1/2/5*, n=127 for *gad1/2/4/5*. The box plots indicate median ±data-range. Asterisks indicate significant effect of 0.5mM GABA on stomatal opening of each genotype (**A**) and effect of 5 μM ABA on stomatal opening of each genotype (**B**) after Two-way ANOVA. $p = 0.005$. *, $p < 0.05$; **, $p < 0.01$; ***, $p < 0.001$; ****, $p < 0.0001$.

Discussion

gad2-1 has a higher ABA threshold for stomatal closure

Previous research indicates that ABA induced stomatal closing was impaired in *gad2* (Chapter II). In this chapter, however, the result indicates that the actual change in stomatal aperture width of *gad2* was similar to the other higher order mutants and WT, to that of WT and *gad1/2/4/5* in response to ABA under constant light (Suppl. Fig. 4B). This suggests the

lesser closing extent of *gad2-1 (*Suppl. Fig. 4A) is likely caused by the elevated base level of stomata opening in *gad2*-1, instead of a lack of ability in closing aperture (Fig. 1-2, Suppl. Fig. 4, 6). This is consistent with the result in chapter II, where higher concentrations of ABA were required to close stomata in *gad2-1* caused by de-regulation of ALMT9-mediated anion uptake into guard cell vacuoles (Chapter II, Suppl. Fig. 14) (Xu et al., 2021). After analysing ABA efficacy on WT, *gad2-1* and *gad1/2/4/5 (*Suppl. Fig 6-8), the result suggested a possible higher EC_{50} of *gad2-1 (*24.72 ± 0.083 μM) than that of WT (8.78 ± 0.087 μM) and *gad1/2/4/5 (*4.29 ± 0.0 μM) after linear scaling (Suppl. Fig. 6A). However, more data replicates at each ABA concentration are required in future experiments to acquire reliable mean ± SD, which will help increase confidence (R square) of the regression analysis and thus given more reliable prediction of EC_{50} of ABA on stomatal closing, especially when comparing WT and *gad1/2/4/5*.

This all said, guard-cell specific complementation of *GAD2Δ*, which also led to higher stomatal conductance and enlarged stomata *of gad1/2/4/5* (Fig. 3), also had similar change in stomatal aperture in response to ABA to that of WT, *gad2-1* and *gad1/2/4/5* (Suppl. Fig. 4A). This suggests that the complementation or disruption of GABA synthesis components do not alter plant response to ABA in closing stomata under constant light, as ABA closes stomata in those mutants and complementation plants (Fig. 1-3). Thus, ABA induced stomatal closing under constant light may not be the optimal condition to explore the cause of variance between the mutants.

Exogenous GABA application impaired stomatal opening differentially across *gad* mutants

The result in Chapter II indicated that GABA (2 mM) impaired induced stomatal opening in *Arabidopsis* WT (Chapter II, Fig. 2A) – 2 mM GABA are stress induced like concentrations of GABA (Xu et al. 2021). In the present study, most of our data compared the stomatal aperture and conductance under a non-stressed condition. Thus, stomatal aperture of WT and mutant lines were measured with application of standard 'resting' concentrations of GABA (0.5 mM) instead (Li, Z. et al. 2016, Wang et al. 2017)(Chapter IV, Fig.1E). In this scenario, 0.5 mM GABA supplement may only cause GABA overaccumulation in WT; instead it may only restore GABA accumulation in *gad1/2/4/5* to resting levels (Scholz et al. 2015, Xu et al. 2021), close to WT under non-stressed conditions.

To our surprise, the data suggested that aside for reducing stomatal opening at stress-induced level, which improves plant acclimation to drought (Chapter II, Fig 4, 5), GABA application at this lower concentration enhanced light-induced stomatal opening in WT, *gad1*, *gad1/2/4* and *gad1/2/5*, which resulted in the stomatal apertures of those genotypes being insignificant from *gad2-1 (*Fig. 6). This type of effect resembles many plant signal molecules, such as ABA and ROS, where varied concentrations of the molecule can either boost or limit plant growth (Huang et al. 2019, Miao et al. 2021). Recently, it was shown in *Arabidopsis* that mutation of the least predominant homologue *GAD3* led to increased sensitivity of plants to combined stress of high light and heat (Balfagón et al. 2021). In WT, plants had higher stomatal conductance, which can help cooling and maintaining plant temperature. While this (higher conductance) possibly may not be the case in *gad3*, and

thus led to increased vulnerability to stress. Repeat experiments are required to confirm enhancing effect of GABA at physiological level in *Arabidopsis*.

GAD mediated GABA homeostasis regulates stomatal movement

In the WT and *gad2-1* backgrounds, increased levels of GABA either by exogenous application or by transgenic manipulation of *GAD2* expression led to reduced stomatal opening (Chapter II, Fig. 4-5). However, complementation of GABA synthesis via *GC1:: GAD2Δ* in *gad1/2/4/5* resulted in an increase in stomatal aperture and stomatal conductance (Fig. 4, Chapter IV, Fig. 9). This suggests that further mutation in *gad2* particularly in *GAD1*, *GAD4* and/or *GAD5* altered stomatal responses in *gad1/2/4/5*, possibly via change in ion (such as, malate^{2-}, Cl^- or K^+) or metabolites (such as proline, dicarboxylates) balance in plants (Mekonnen 2017). Such a hypothesis is also supported by pharmacological treatment during epidermal strip assays (Fig.5,6). In this experiment 0.5 mM GABA promoted light induced stomatal opening of WT regardless of application of ABA, while such an effect on mutant lines varied and is ABA-dependent (Fig. 6A). Recently, it was found in citrus that exogenous application of GABA could lead to increased hormone concentrations in the leaves (Hijaz et al. 2018). The fact that in mutant lines, *gad1*, *gad1/2/4* and *gad1/2/5* respond to GABA without ABA, whereas *gad2/4* and *gad1/2/45* did such with ABA application, indicates there may be an impairment in hormone synthesis/response in mutant plants. On the other hand, daily topical application of 0.5 mM GABA during drought did not suggest that GABA opens stomata (Fig. 4). This is probably due to an accumulated GABA level sprayed daily during the process, or ABA concentrations building up and closing stomata (Jakab et al. 2005, Priya et al. 2019). A

dose-dependent effect analysis of GABA on stomatal movement are required to further verify this hypothesis.

Possible interaction of GABA during ABA inhibited stomatal opening

Although ABA inhibited stomatal opening in all the genotypes, the extent of inhibition differed (Fig. 7). ABA inhibited 59.7 ± 0.03% of stomatal opening in *gad2/4* (showed significance to WT, gad4, *gad1/2/4* and *gad1/2/5*), but only 18.5% ± 0.05% in *gad1/2/4* (showed significance to *gad1*, *gad2-1* and *gad1/2/4/5*). If the effect of GABA and ABA on stomatal movement is independent in those two mutant lines, then GABA (21.4 ± 0.05%) + ABA (-18.5 ± 0.05%) should result in a net change of only a 2.9 % increase in stomatal opening in *gad1/2/4*, while GABA+ABA actually led to a 32.5 ± 0.04% reduction of stomatal opening (Suppl. Fig. 5B). Similarly, a net change between GABA (-2.0 ± 0.04%) + ABA (-59.7 ± 0.03%) for *gad2/4* should result in a net reduction of opening of 61.7%, however, the actual effect of the combined treatment on *gad2/4* led to a 35.3 ± 0.04% reduction of stomatal opening. In the case of *gad1/2/4//*5, a net change between GABA (-3.8 ± 0.05%) + ABA (-46.3 ± 0.04%) should result in a net reduction of opening of 50.1%, while the actual effect of the combined treatment was a 28.4 ± 0.05% reduction of stomatal opening. The difference between net and combined effect GABA + ABA was less different in WT (Fig. 7). This suggests that normal function of *GAD2* and *GAD4* are required in ABA signalling during light induced stomatal opening, and the loss of *GAD1* reversed the ABA efficacy by the loss of *GAD2* and *4*. In this case, GAD1 can alter the contribution of GAD2 and 4, although *GAD1* is predominantly expressed in roots. It may also suggest that the loss of *GAD1* may also shift root sensitivity to ABA-sensitivity. Thereby primary root elongation was measured. Experiments were conducted on WT, *gad1*, *gad2-1*, *gad4* and *gad1/2/4/5*.

No significant difference was detected from these genotypes (Suppl. Fig. 9, 10; Tab. 1-2). Preliminary experiments on seedling developing suggests a delayed influence of ABA on emergence of root hairs (Suppl. Fig.11B), but not on seed germination (Suppl. Fig.11B). Due to time limitation, experiments on *gad2/4* and *gad1/2/4* were not conducted.

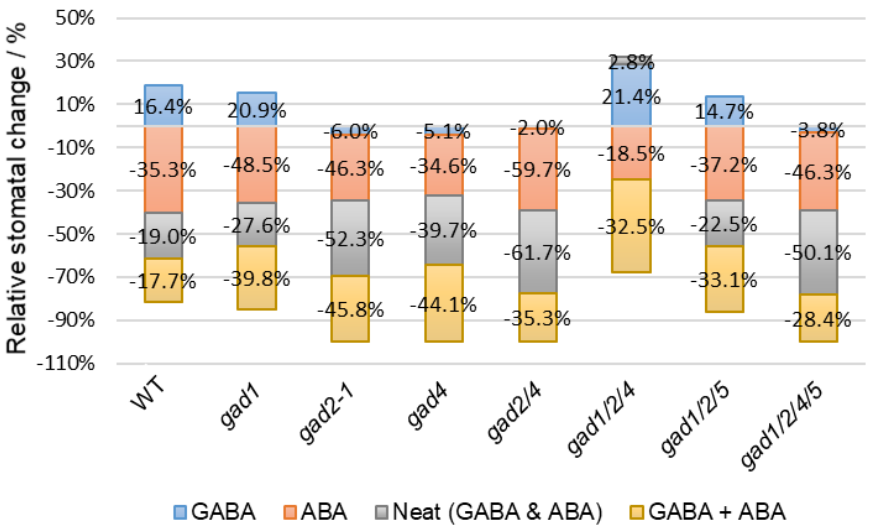

Figure 8. Relative stomatal change of WT and *gads* mutants in stomatal opening.

The bar graph summarises relative stomatal change (with respect to the control condition of each genotype) of plants during light induced stomatal opening in response to pharmacological treatment from Figure 5. Relative stomatal change was calculated relative to stomatal aperture under control condition of each genotype, where positive values indicate more opened stomata than that under control condition, negative values indicate the opposite. Neat (ABA & GABA) represents net effect of ABA and GABA calculated by summation of the mean effect of ABA and GABA on each genotype respectively.

In summary, the different GADs may fulfil particular roles in response to different conditions (Tab.1), which may undergo cross talk with GABA with other signalling networks in guard

cells. For example, *GAD4* might be involved in changing the impact of endogenous ABA concentration (Urano et al. 2009). *GAD1* may be mediating ABA signalling via response to ROS signalling in chloroplast (Maruta et al. 2013). And *GAD2* may maintain GABA level in guard cells, targeting ALMTs in guard cells in buffering stomatal movement in response to changing environment as shown in Chapter II. Repeats in epidermal peel assays would be pertinent to further investigate the promoting effect of the physiological level of GABA on stomatal opening. More information is required to interpret the role of the GAD homologues in altered sensitivity to ABA inhibited stomatal opening and GABA promoted stomatal opening based on the results so far. Certainly, the sensitivity to ABA in serial *gad* mutants will be required to be examined by other techniques, such as real-time recording of stomatal conductance of detached leaves fed by artificial xylem sap solution using infrared gas analyser LiCor LI-6400 (Conn et al. 2013, Xu et al. 2021).

Table 1. **Summary genotypes and stomatal phenotypes of plants with varied *GAD* expression.**

In genotype section, +/- indicate existence or absence of native *GAD* gene (s). In phenotype section relative stomatal aperture and conductance with significant different to WT were indicated. Average change in stomata aperture with significance in response 0.5 mM GABA with or without 2.5 μM ABA was illustrated, ↑ indicates increase in stomatal aperture. "n.s." indicates not significant.

Genotype	contains				Phenotype			
	GAD1	*GAD2*	*GAD4*	*GAD5*	Stomatal aperture/ relative to WT	Stomatal conductance/ relative to WT	Effect of 0.5 mM GABA	Effect of 0.5 mM GABA +2.5 µM ABA
WT	+	+	+	+	1	1	0.23 µm ↑	0.25 µm ↑
gad1	-	+	+	+	n.s.	n.s.	0.28 µm ↑	n.s.
gad2-1	+	-	+	+	1.448	1.499	n.s.	n.s.
gad4	+	+	-	+	n.s.	1.984	n.s.	n.s.
gad1/2	-	-	+	+	not measured	1.659	not measured	not measured
gad2/4	+	-	-	+	n.s.	1.516	n.s.	0.37 µm ↑
gad1/2/4	-	-	-	+	n.s.	n.s.	0.30 µm ↑	n.s.
gad1/2/5	-	-	+	-	n.s.	n.s.	0.21 µm ↑	n.s.
gad1/2/4/5	-	-	-	-	n.s.	n.s.	n.s.	0.26 µm ↑
gad1/2/4/5 /GC:: GAD2Δ	-	GC:: GAD2Δ	-	-	1.177	2.015	not measured	not measured

Material and methods

Epidermal peel assay

For stomatal aperture measurements, epidermal strips were peeled from the abaxial side of mature leaves of 4-6 weeks old plants, and immediately floated on KCl-MES buffer (10

mM MES, 10 mM KCl, 5 mM Malate, pH 6.0 adjusted with Tris base) (Xu et al. 2021). For ABA induced stomatal closing, epidermal peels were incubated in KCl-MES buffer and placed under light (200 µmol µmol photons m^{-2} s^{-1}) for 2 hr to open stomata. Then epidermal strips were transferred into new buffer with or without ABA supplement for another 2 hr before imaging, as indicated in the figure legend. For dark to light transition, epidermal peelings were incubated in KCl-MES buffer and placed under dark for 1.5 hr to close stomata before ABA ((±)-Abscisic acid, Sigma-Aldrich) or GABA (γ-Aminobutyric acid, Sigma-Aldrich) was added into the buffer, and the epidermis was kept under dark for another 0.5 hr, and then 2 hr under light (200 µmol photons m^{-2} s^{-1}) before taking images under a microscope. Stomata status were captured under Zeiss Axiophot Fluorescence Phase Microscope. Stomatal measurement was undertaken by ImageJ. Stomatal width, stomatal width/length ratio and stomatal area was measured in this experiment through ImageJ as described in Suppl. Fig. 3. 2 leaves per plant and 3 plants per genotype were used in each experiment. Stomatal conductance was measured with AP4 porometer (Delta-T Devices Ltd). 4 leaves of each plant from 5-6 biological replicate plants were measured.

Regression analysis

For the best fit of regression of stomata aperture data, both available models, linear and polynomial were used for nonlinear least square regression. The available model was chosen based on the prediction of dose effect of ABA on stomatal closing of *Arabidopsis (*Suppl. Fig. 8-9). This was based on publication and a scatter plot of the data distribution, where there should be two plateau phase at extreme low concentration of ABA (stomata

are still opened) and relative high concentration of ABA (stomata cannot close more with a further increase dose of ABA) (Pantin et al. 2013). Several models were compared, and the best fit model, the sigmoidal dose-response curve (Suppl. Fig. 5A) in our case, was used for further analysis. The model requires containment of maximum and minimum level of the targets, stomatal opening, relative closing extent and change in stomata width. This was done by constrain the parameter based on setting set-off data point, e.g., relative stomatal opening at 0 μM ABA should be 1. For polynomial regression, the order was decided by comparing the p value of coefficients after analysing the data with different order of polynomial. In our case, third polynomial regression provides significance in the coefficients and minimum sum square of error (Ritz and Streibig 2008). Finally, both methods were valued by comparing the sum square of error and R square. Final regression analysis was performed using GraphPad Prism version 8.0.0 for Windows (GraphPad Software, San Diego, California USA).

Regression analysis on primary root elongation and stomatal aperture

For primary root elongation, seeds of each genotypes were sown on ½MS medium (Murashige and Skoog medium, Duchefa-Biochemie; 1% Sucrose, Chem-supply; 0.8% Phytagel, Sigma Aldrich), and stratified at 4°C for 4 days. The petri dishes were then put vertically under short/ long -day conditions with a light intensity of 70 μmol photons m^{-2} s^{-1}. Seedlings aged 2-3 days with similar leaf size and root length were transferred to ½MS medium containing varied concentration of ±-ABA or GABA. For each pharmacological treatment, 12-15 biological replicate plants from 3 petri dishes were used for each genotype. Primary root length was measured every 24 hr on scanned pictures with ImageJ.

For the best fit of regression of primary root elongation data, both linear regressions were attempted (for those with no ABA applied, Suppl. Fig. 9A, E; 10A), and nonlinear least square regression (for those with ABA applied, Suppl. Fig. 9C, G; 10C, E) (Araya et al. 2016). The available model was chosen based on the prediction of dose effect of ABA on stomatal closing of *Arabidopsis (*Suppl. Fig. 9-10). This was based on publication and a scatter plot of the data distribution, where there should be two plateau phase at extreme low concentration of ABA (stomata are still opened) and relative high concentration of ABA (stomata cannot close more with further increase dose of ABA) (Pantin et al. 2013).

Statistical analysis

Statistical analysis was conducted in R. For the dataset with only 2 groups, t-test analysis was applied. For datasets with multiple groups, homogeneity and normal distribution of data in each group are checked. Afterwards, for the dataset with one type of variable, ANOVA test was applied first to test if it has significant difference between groups. Then multiple comparisons were conducted after Tukey post-hoc tests. And for those with two types of variable, ANOVA test was applied first to test if both have significant effects. Then multiple comparisons were conducted after Tukey post-hoc tests. Asterisks represent statistical significance. *, $p < 0.05$; **, $p < 0.01$; ***, $p < 0.001$; ****, $p < 0.0001$.

Supplementary materials

A

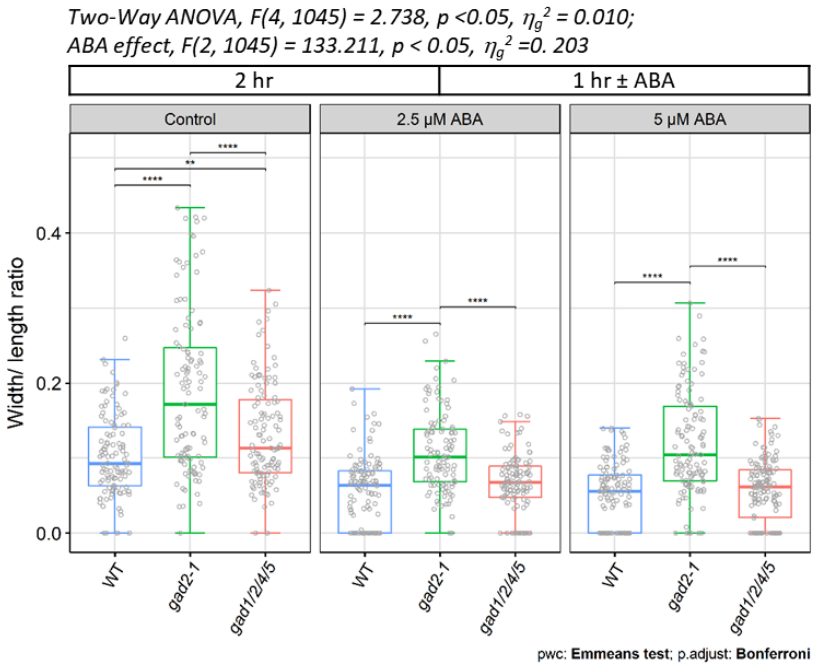

B

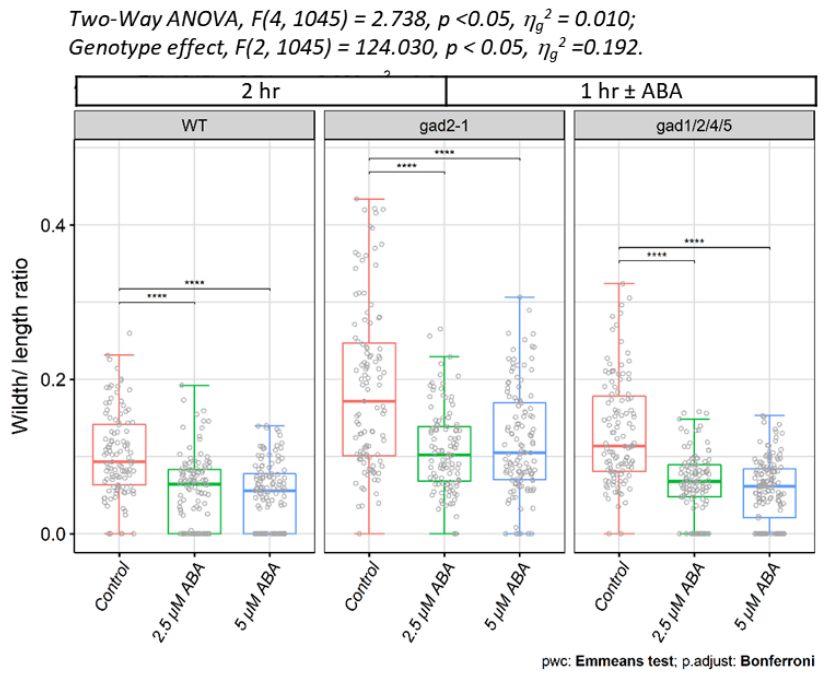

Supplementary Figure 1. Width/length ratio of WT, *gad2-1* and *gad1/2/4/5* following ABA induced stomatal closing after 1 hr of ABA treatment.

A. Dose dependent effects of ABA on stomatal aperture of WT, *gad2-1* and *gad1/2/4/5* under constant light. **B.** Comparing stomatal aperture of WT, *gad2-1* and *gad1/2/4/5* after the same concentration of ABA treatment under constant light. In control group, n = 108 for WT, n = 107 for *gad2-1*, n = 115 for *gad1/2/4/5*; In 2.5 μM ABA group, n = 114 for WT, n = 109 for *gad2-1,* n = 112 for *gad1/2/4/5*; In 5 μM ABA group, n = 122 for WT, n = 121 for *gad2-1*, n = 146 for *gad1/2/4/5*. The box plots indicate median ±data-range. Asterisks indicate significant difference between genotype under same ABA dose (A) and between different ABA doses of each genotype (B) after Two-way ANOVA. p = 0.005. *, $p < 0.05$; **, $p < 0.01$; ***, $p < 0.001$; ****, $p < 0.0001$.

A

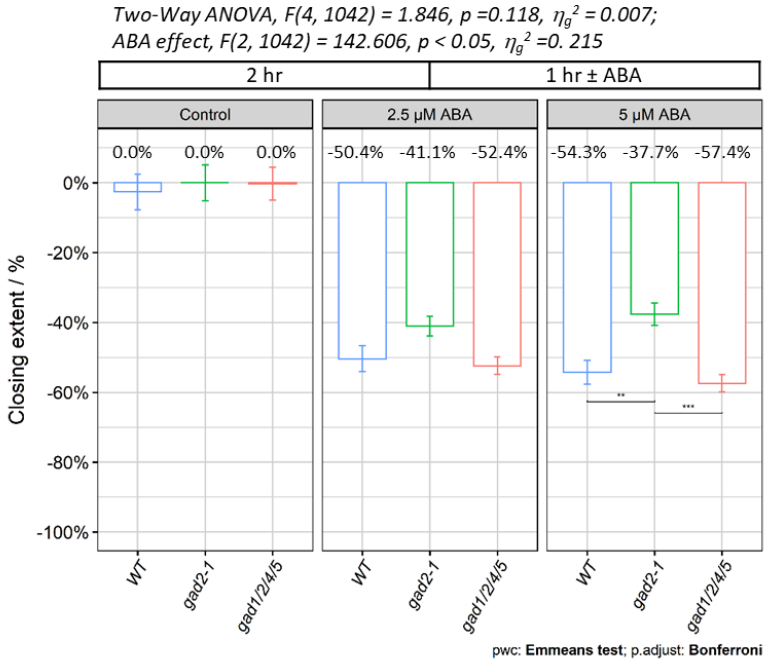

B

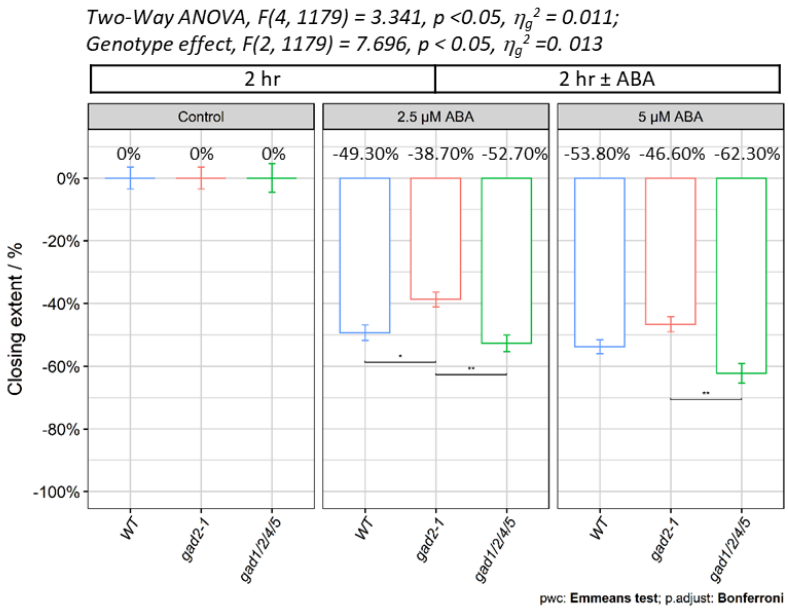

Supplementary Figure 2, Stomatal closing extent of WT, *gad2-1* and *gad1/2/4/5* to ABA induced stomatal closing by ABA treatment.

A. Comparing dose effects of 1 hr ABA treatment on stomatal aperture of WT, *gad2-1* and *gad1/2/4/5* under constant light condition. In control group, n = 109 for WT, n = 107 for *gad2-1* , n

= 114 for *gad1/2/4/5*; In 2.5 μM ABA group, n = 113 for WT, n = 111 for *gad2-1*, n = 110 for *gad1/2/4/5*; In 2.5 μM ABA group, n = 122 for WT, n = 120 for *gad2-1* , n = 145 for *gad1/2/4/5*. **B**. Comparing dose effects of 2 hr ABA treatment on stomatal aperture of WT, *gad2-1* and *gad1/2/4/5* under constant light condition. In control group, n = 131 for WT, n = 146 for *gad2-1*, n = 129 for *gad1/2/4/5*; In 2.5 μM ABA group, n = 125 for WT, n = 137 for *gad2-1* , n = 124 for *gad1/2/4/5*; In 5 μM ABA group, n = 133 for WT, n = 134 for *gad2-1* , n = 129 for *gad1/2/4/5*. The bar plots indicate mean ± SE. Asterisks indicate significant difference between genotype under same ABA dose after Two-way ANOVA. p = 0.005. *, $p < 0.05$; **, $p < 0.01$; ***, $p < 0.001$; ****, $p < 0.0001$.

A

Two-Way ANOVA, F(4, 1748) = 4.519, p <0.05, η_g^2 = 0.010;
Genotype effect, F(2, 1748) = 134.361, p < 0.05, η_g^2 =0.133.

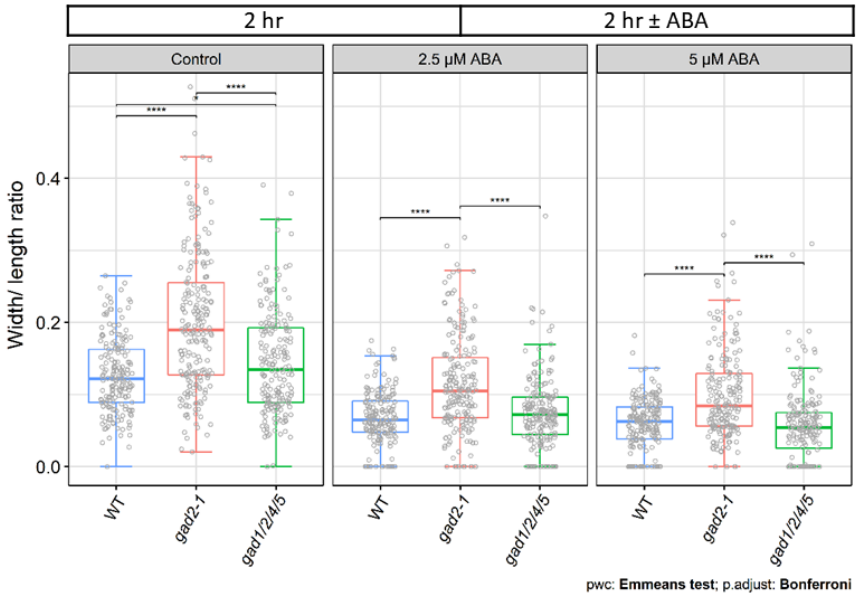

B

Two-Way ANOVA, F(4, 1748) = 4.519, p <0.05, η_g^2 = 0.010;
ABA effect, F(2, 1748) = 341.862, p < 0.05, η_g^2 =0. 281

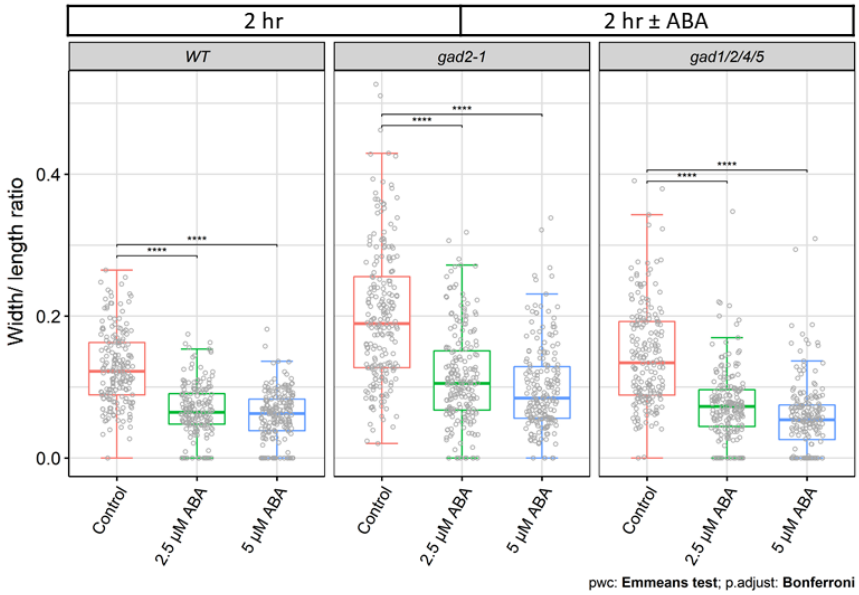

Supplementary Figure 3. Width/length ratio of WT, *gad2-1* and *gad1/2/4/5* to ABA induced stomatal closing under 2 hr of ABA treatment.

A. Comparing dose effects of ABA on stomatal aperture of WT, *gad2-1* and *gad1/2/4/5* under constant light. **B.** Comparing stomatal aperture of WT, *gad2-1* and *gad1/2/4/5* after the same concentration of ABA treatment constant light. In control group, n = 108 for WT, n = 107 for *gad2-1*, n = 115 for *gad1/2/4/5*; In 2.5 μM ABA group, n = 114 for WT, n = 109 for *gad2-1*, n = 112 for *gad1/2/4/5*; In 5 μM ABA group, n = 122 for WT, n = 121 for *gad2-1*, n = 146 for *gad1/2/4/5*. The box plots indicate median ±data-range. Asterisks indicate significant difference between genotype under same ABA dose (**A**) and between different ABA doses of each genotype (**B**) after Two-way ANOVA. p = 0.005. *, p < 0.05; **, p < 0.01; ***, p < 0.001; ****, p < 0.0001.

A

Two-Way ANOVA, F(9 1401) = 3.540, p <0.05, η_g^2 = 0.022;
Genotype effect, F(3, 1401) = 15.554, p < 0.05, η_g^2 =0.032.

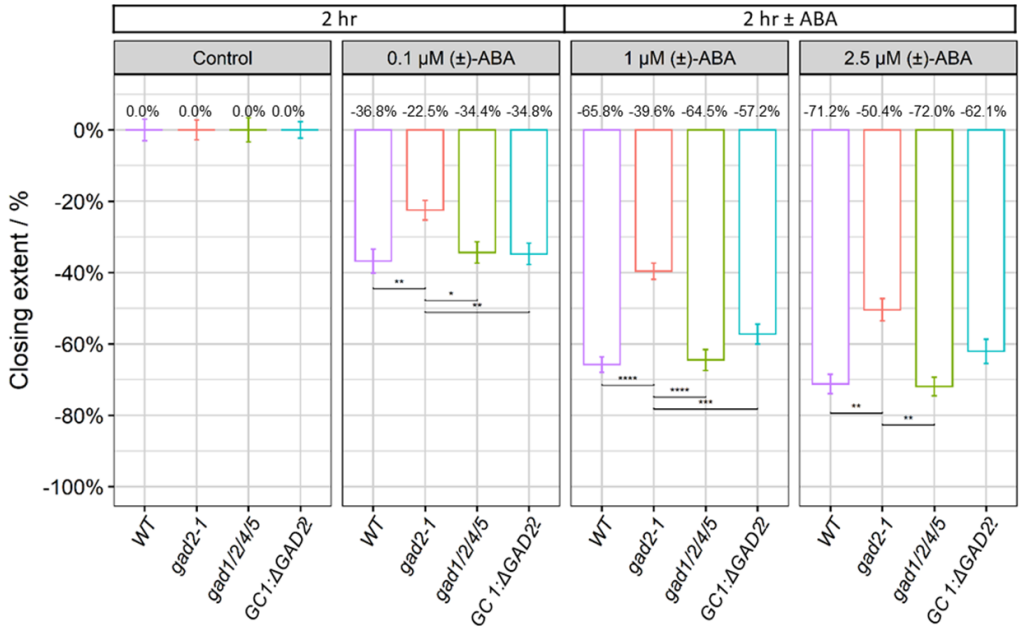

pwc: **Emmeans test**; p.adjust: **Bonferroni**

B

Two-Way ANOVA, F(9 1401) = 3.540, p <0.05, η_g^2 = 0.022;
Genotype effect, F(3, 1401) = 15.554, p < 0.05, η_g^2 =0.032.

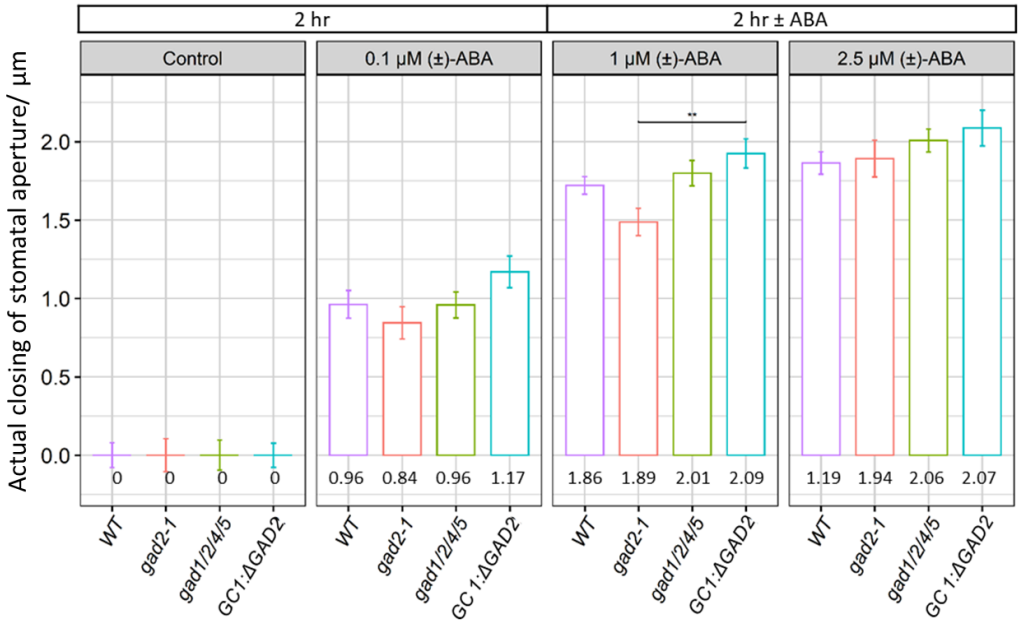

pwc: **T test**; p.adjust: **Bonferroni**

Supplementary Figure 4. Stomatal response of WT, *gad2-1*, *gad1/2/4/5* and *gad1/2/4/5*/*GC1:: GAD2Δ* to ABA induced stomatal closing.

A. Stomatal closing extent. Bar plot indicated the mean value of percentage closing of stomata in each genotype. Asterisks indicate significant difference between genotype under same ABA dose after Two-way ANOVA. p = 0.005. *, p < 0.05; **, p < 0.01; ***, p < 0.001; ****, p < 0.0001. **B**. Actual closing of stomatal aperture by ABA. Bar plot indicated the mean value of μm closing of stomata in each genotype. Asterisks indicate significant difference between genotype under same ABA dose after t-test. p = 0.005. **, p < 0.01. In control group, n = 113 for WT, n = 127 for gad2-1, n = 126 for *gad1/2/4/5*, n = 133 for *gad1/2/4/5/GC1:: GAD2*Δ; In 0.1 μM ABA group, n = 83 for WT, n = 109 for gad2-1, n = 115 for *gad1/2/4/5*, n = 122 for *gad1/2/4/5/GC1:: GAD2*Δ; In 1 μM ABA group, n = 74 for WT, n = 101 for gad2-1, n = 68 for *gad1/2/4/5*, n = 74 for *gad1/2/4/5/GC1:: GAD2*Δ; In 2.5 μM ABA group, n = 39 for WT, n = 44 for gad2-1, n = 39 for *gad1/2/4/5*, n = 50 for *gad1/2/4/5/GC1:: GAD2*Δ, n = 46 for WT, n = 36 for gad2-1, n = 35 for *gad1/2/4/5*, n = 35 for *gad1/2/4/5/GC1:: GAD2Δ* responded to different level of ABA. The bar plots indicate mean ± SE.

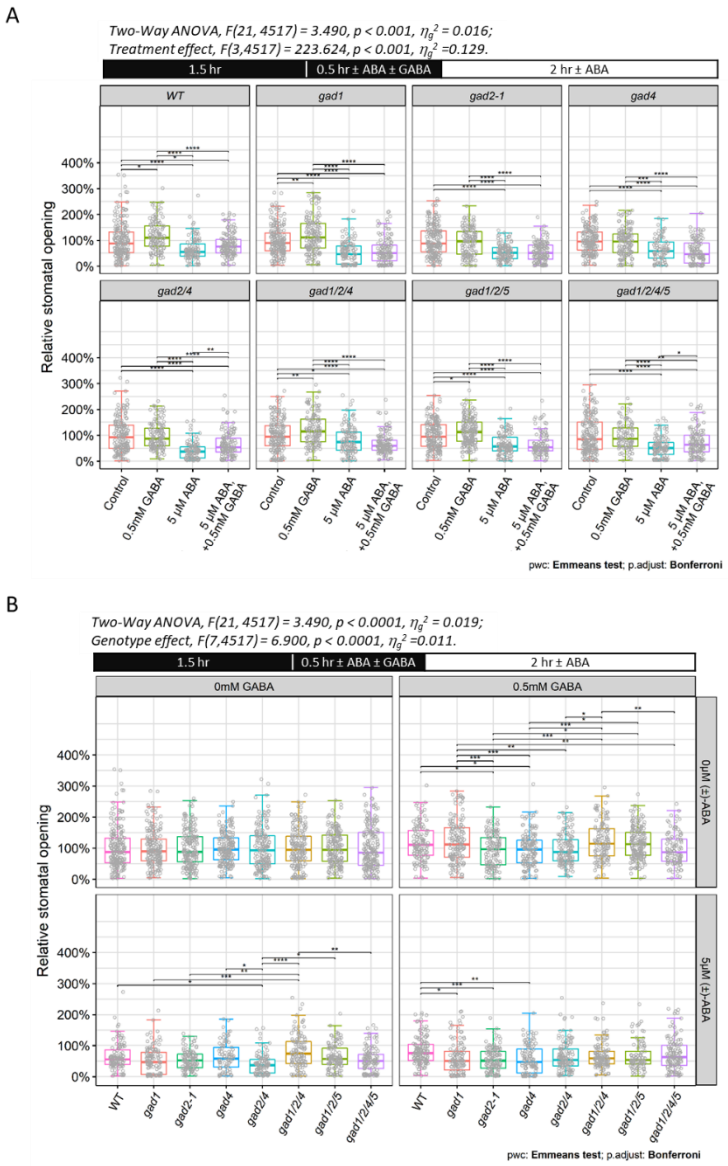

Supplementary Figure 5. Pharmacological effect of GABA and ABA on multiploid mutants of *GAD*s.

A-B. Relative stomatal change in percentage of WT and GABA deficiency mutants with exogenous GABA and/ or ABA under dark-light transition comparing to control group. The bar plot indicates mean ± SE of relative stomatal opening to control group (no GABA or ABA applied). For control group, n=210 for WT, n=198 for *gad1*, n=201 for *gad2-1*, n=193 for *gad4*, n=173 for *gad2/4*, n=187 for *gad1/2/4*, n=187 for *gad1/2/5*, n=199 for *gad1/2/4/5*; For 0.5mM GABA group, n=128 for WT,

n=153 for *gad1*, n=142 for *gad2-1*, n=150 for *gad4*, n=131 for *gad2/4*, n=129 for *gad1/2/4*, n=186 for *gad1/2/5*, n=104 for *gad1/2/4/5*; For 0.5μM ABA group, n=108 for WT, n=115 for *gad1*, n=117 for *gad2-1*, n=85 for *gad4*, n=108 for *gad2/4*, n=115 for *gad1/2/4*, n=122 for *gad1/2/5*, n=117 for *gad1/2/4/5*; For 0.5mM GABA+ 0.5μM ABA group, n=139 for WT, n=120 for *gad1*, n=133 for *gad2-1*, n=115 for *gad4*, n=130 for *gad2/4*, n=129 for *gad1/2/4*, n=98 for *gad1/2/5*, n=127 for *gad1/2/4/5*. Asterisks indicate significant difference between genotype under treatment (**A**) and between treatments of each genotype (**B**) after turkey's pos hoc test of Two-way ANOVA. $p = 0.005$. *, $p < 0.05$; **, $p < 0.01$; ***, $p < 0.001$; ****, $p < 0.0001$.

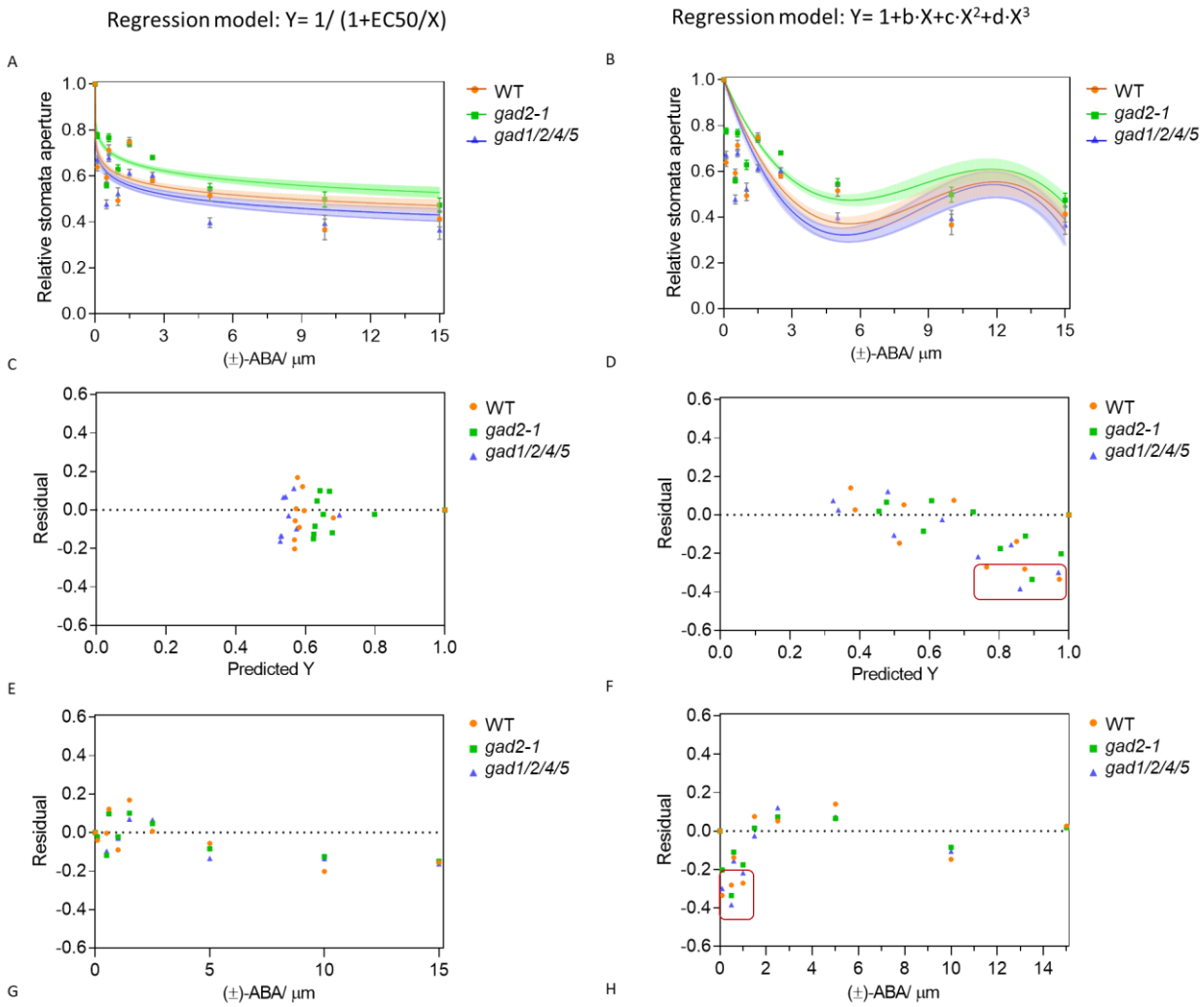

	WT	*gad2-1*	*gad1/2/4/5*
Degrees of Freedom	2197	2397	2414
R squared	0.3447	0.3192	0.3528
Sum of Squares	148.2	127.3	178.2
SE of Residual	0.2596	0.2303	0.2716
EC50/ µM (SE)	8.78 (2.86)	24.72 (8.52)	4.29 (0.94)

	WT	*gad2-1*	*gad1/2/4/5*
Degrees of Freedom	2196	2396	2413
R squared	0.2501	0.2457	0.2541
Sum of Squares	169.6	141.0	205.4
SE of Residual	0.2777	0.2425	0.2916
Coefficient b (SE)	-0.27(1E-2)	0.04(3E-3)	-0.001(1E-4)
Coefficient c (SE)	-0.22(1E-2)	0.03(2E-3)	-0.001(1E-4)
Coefficient d (SE)	-0.3(1E-2)	0.04(03E-3)	-0.002(1E-4)

Supplementary Figure 6, Nonlinear regression analysis of ABA efficacy on relative stomatal opening of WT, *gad2-1* and *gad1/2/4/5*.

A. Sigmoidal regression. The sigmoidal dose-response equation, indicated at the top of the regression plot, was chosen base on the prediction of dose effect of ABA on relative stomatal opening of *Arabidopsis* , where there should be two plateau phase at extreme low concentration of ABA (stomata are still opened) and relative high concentration of ABA (stomata cannot close

more with further increase dose of ABA) (Pantin et al. 2013). Symbols indicated mean ± SE level of relative stomatal opening form based on data of individual stomata, solid lines indicate regression curve, the coloured region around the line indicates error of regression. Residual, the difference between actual and predicted level of relative stomatal opening, was plotted against the predicted level of relative stomatal opening and concentration of ABA (**C**, **E**). These were to help checking fit of regression. **B**. Third order polynomial regression. Residue plot to both predicted relative stomatal opening and concentration of ABA (**D**, **F**). The table (**G**, **H**) is the output of the stats summary of both regressions. Degree of freedom indicates sample size; R square indicates ratio of sum squared of error explained by the regression model; residual mean ± SE is the standard error of residual (the difference between prediction and observation). Sum of square is the sum squared of error of the model, which can be used to compare fit between models.

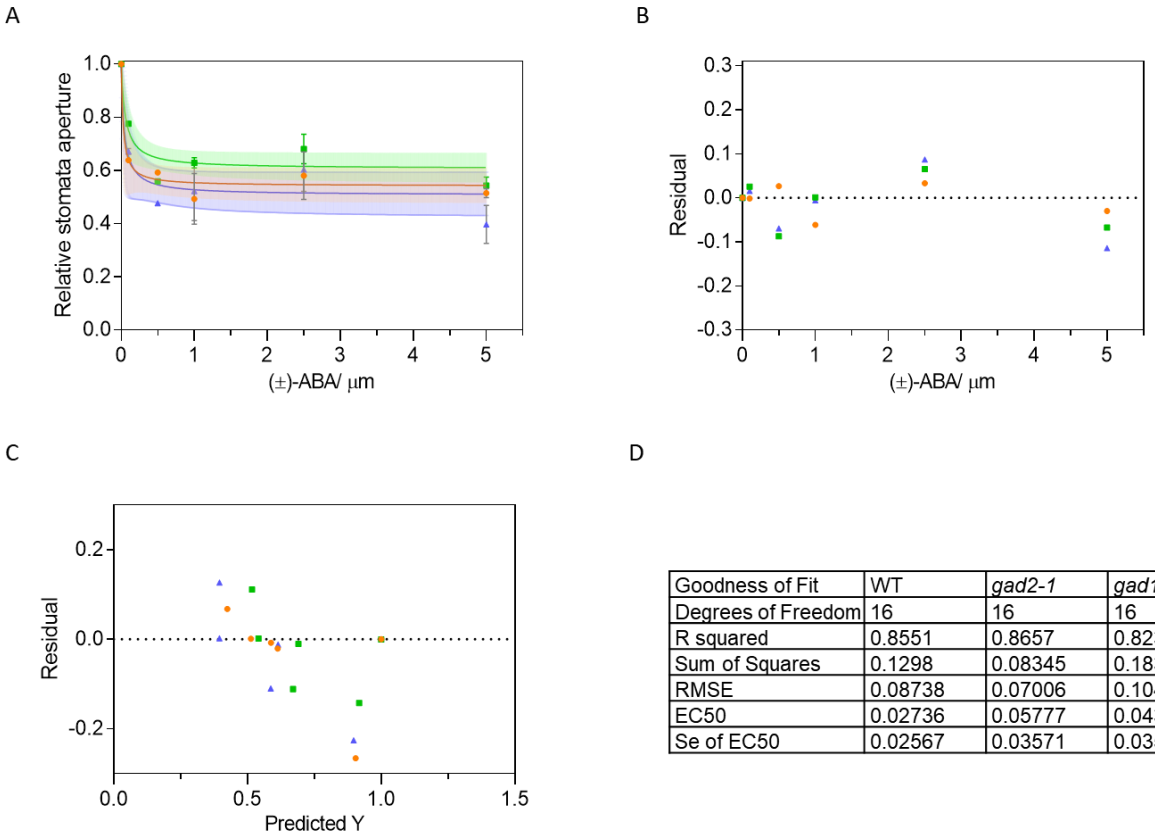

Goodness of Fit	WT	*gad2-1*	*gad1/2/4/5*
Degrees of Freedom	16	16	16
R squared	0.8551	0.8657	0.8238
Sum of Squares	0.1298	0.08345	0.1837
RMSE	0.08738	0.07006	0.1040
EC50	0.02736	0.05777	0.04301
Se of EC50	0.02567	0.03571	0.03529

Supplementary Figure 7. Nonlinear least square regression analysis of ABA efficacy on relative stomatal opening of WT, *gad2-1* and *gad1/2/4/5*.

A. Sigmoidal regression on relative stomatal aperture of WT, *gad2-1* and *gad1/2/4/5* under treatment with varied concentration of ABA. Each data point represents the mean ± SE level of relative stomatal opening of the genotype under single concentration of ABA based on different batch of experiments. **B-C**. Residual plot to concentration of ABA, and to predicted relative stomatal opening level. Each data point represents mean difference between relative stomatal opening and the predicted relative stomatal opening for single ABA concentration. **D**. The table at the bottom is the output of the stat summary of the regression. Degree of freedom indicates sample size (repeat of experiments).

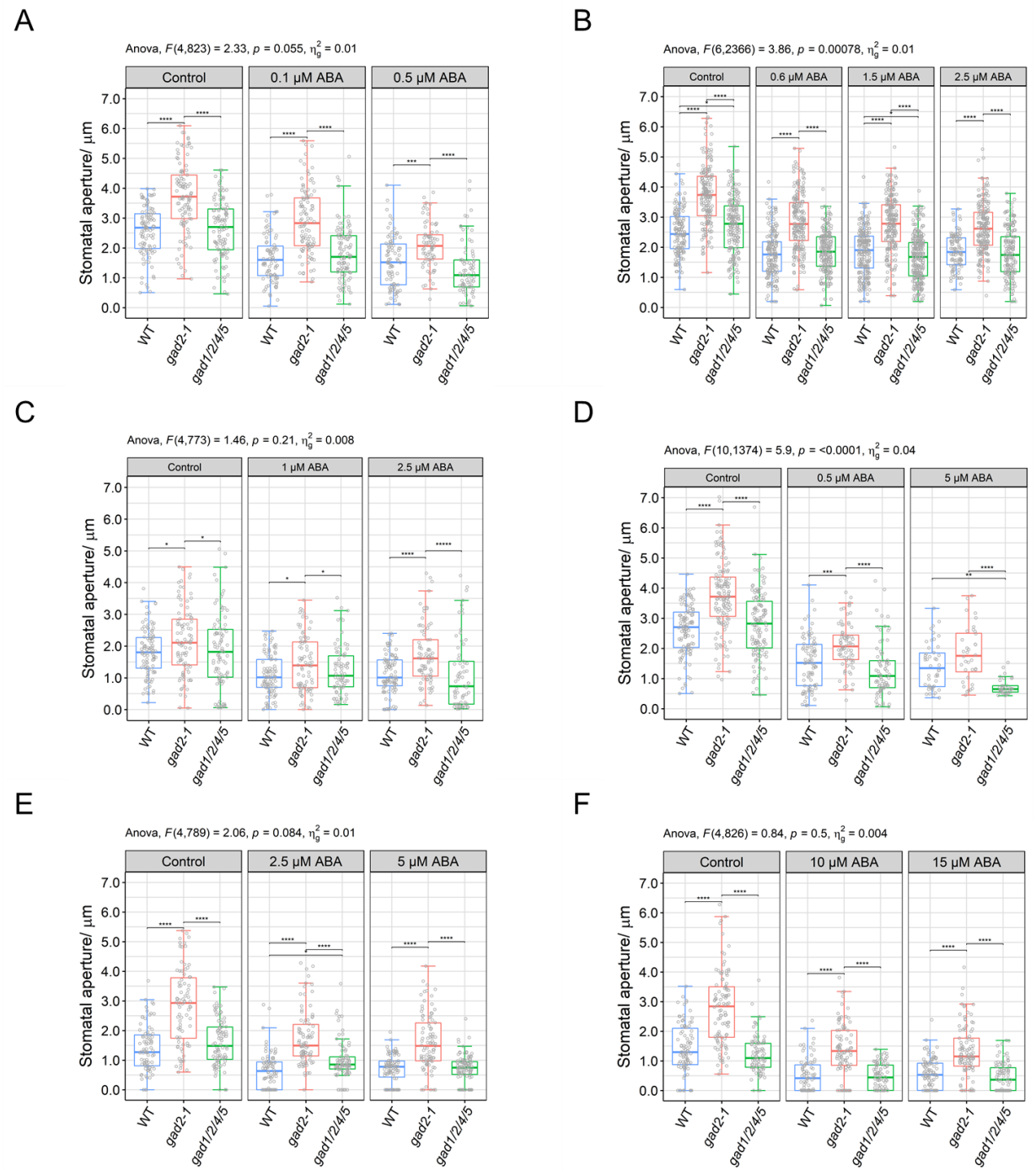

Supplementary Figure 8, Stomatal aperture data of WT, *gad2-1* and *gad1/2/4/5* used in nonlinear regression.

A-E. Stomatal aperture data of WT, *gad2-1* and *gad1/2/4/5* after 2 hr of ABA treatment from different batch of experiments. In control group, n = 646 for WT, n = 684 for *gad2-1*, n = 688 for

gad1/2/4/5; In 0.1 μM ABA group, n = 166 for WT, n = 212 for *gad2-1*, n = 218 for *gad1/2/4/5*; In 0.5 μM ABA group, n = 172 for WT, n = 148 for *gad2-1*, n = 154 for *gad1/2/4/5*; In 0.6 μM ABA group, n = 178 for WT, n = 209 for *gad2-1*, n = 226 for *gad1/2/4/5*; In 1 μM ABA group, n = 170 for WT, n = 183 for gad2, n = 145 for *gad1/2/4/5*; In 1.5 μM ABA group, n = 227 for WT, n = 230 for *gad2-1*, n = 295 for *gad1/2/4/5*; In 2.5 μM ABA group, n = 321 for WT, n = 416 for *gad2-1*, n = 371 for *gad1/2/4/5*; In 5 μM ABA group, n = 141 for WT, n = 127 for *gad2-1*, n = 135 for *gad1/2/4/5*; In 10 μM ABA group, n = 80 for WT, n = 91 for *gad2-1*, n = 94 for *gad1/2/4/5*; In 15 μM ABA group, n = 99 for WT, n = 100 for *gad2-1*, n = 91 for *gad1/2/4/5*.

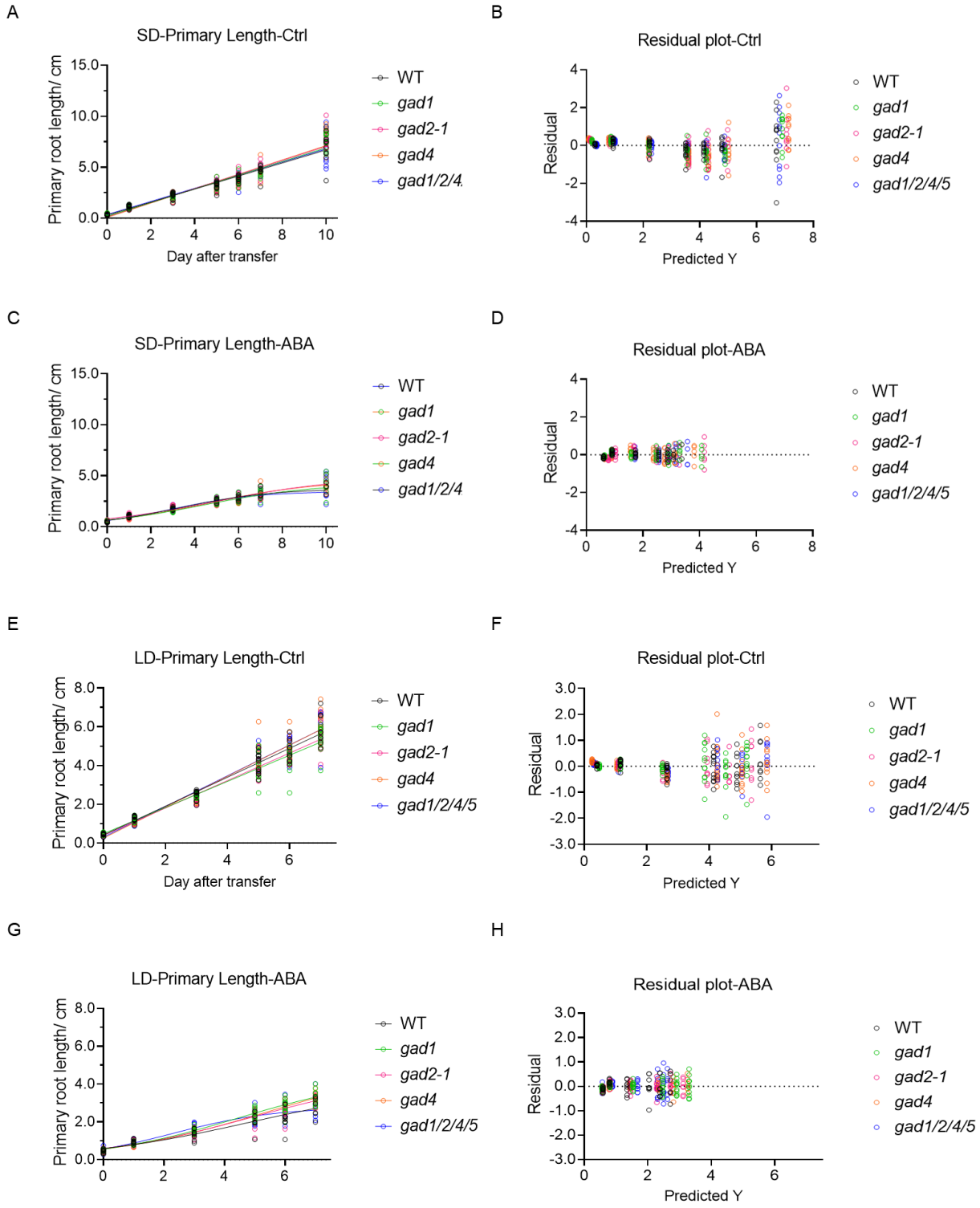
A
SD-Primary Length-Ctrl
Primary root length/ cm
Day after transfer
WT
gad1
gad2-1
gad4
gad1/2/4
B
Residual plot-Ctrl
Residual
Predicted Y
WT
gad1
gad2-1
gad4
gad1/2/4/5
C
SD-Primary Length-ABA
Primary root length/ cm
WT
gad1
gad2-1
gad4
gad1/2/4
D
Residual plot-ABA
Residual
Predicted Y
WT
gad1
gad2-1
gad4
gad1/2/4/5
E
LD-Primary Length-Ctrl
Primary root length/ cm
Day after transfer
WT
gad1
gad2-1
gad4
gad1/2/4/5
F
Residual plot-Ctrl
Residual
Predicted Y
WT
gad1
gad2-1
gad4
gad1/2/4/5
G
LD-Primary Length-ABA
Primary root length/ cm
WT
gad1
gad2-1
gad4
gad1/2/4/5
H
Residual plot-ABA
Residual
Predicted Y
WT
gad1
gad2-1
gad4
gad1/2/4/5

Supplementary Figure 9. Primary root elongation of WT and GABA deficient mutants.

Primary root elongation of plants growing on media containing 0 or 20 μM ABA (**A, C, E, G**). symbols indicate primary root length of individual seedlings, solid line indicate groups without GABA treatment, dash lines indicate groups with GABA treatment. Residues against predicted root length were plotted to check goodness of fit (**B, D, F, H**), details of these fit was explained in Supplementary Table 1 below.

Supplementary Table 1. Summary of regression result in Suppl. Fig. 13.

For linear regression (Suppl. Fig. 9A, C, E, G), linear model was created using Y=a·X+b. Y represents primary root length, X represents days after transfer of seedling to new media. a indicates slope, i.e., growth rate/ cm·day-1. b indicates intercept of the linear regression line on y axis, i.e., initial root length. For nonlinear least square regression (Suppl. Fig. 9B, D, F, H), logistic growth model was choosed. df indicates sample amount. YM indicates predicted max root length (cm). Y0 indicates initial root length. k indicates the velocity of change form Y0 to YM, in our case the velocity indicates how fast primary root elongation stopped after transferring to ABA media. SSE indicates sum square of error of the regression. In both regressions, df indicates sample amount. R2 indicated confidence of prediction.

Light period	Genotype	Linear regression- Ctrl					
		df	Linear model				
Short Day	WT	75	Y= 0.639·X +0.306, R^2= 0.92				
	gad1	79	Y= 0.639·X +0.306, R^2= 0.93				
	gad2-1	58	Y= 0.639·X +0.306, R^2= 0.94				
	gad4	79	Y= 0.639·X +0.306, R^2= 0.95				
	gad1/2/4/5	80	Y= 0.639·X +0.306, R^2= 0.96				
	Genotype	Nonlinea least square regression-logistic- 20 µM ABA					
		df	YM	Y0	k	R^2	SSE
	WT	50	3.462	0.6085	0.5184	0.968	1.743
	gad1	57	4.544	0.6408	0.3973	0.9568	3.631
	gad2-1	43	4.925	0.7779	0.3383	0.9271	5.09
	gad4	56	4.229	0.6448	0.393	0.9442	4.158
	gad1/2/4/5	53	3.72	0.6278	0.4795	0.9411	4.001

Light period	Genotype	Linear regression- Ctrl					
		df	Linear model				
Long Day	WT	68	Y= 0.747·X +0.407, R^2= 0.95				
	gad1	69	Y= 0.676·X +0.478, R^2= 0.93				
	gad2-1	51	Y= 0.709·X +0.387, R^2= 0.93				
	gad4	71	Y= 0.800·X +0.249, R^2= 0.94				
	gad1/2/4/5	67	Y= 0.794·X +0.298, R^2= 0.95				
	Genotype	Nonlinea least square regression-logistic- 20 µM ABA					
		df	YM	Y0	k	R^2	SSE
	WT	44	3.935	0.5908	0.3612	0.8524	5.008
	gad1	67	4.381	0.5622	0.4333	0.9524	3.728
	gad2-1	50	4.557	0.5939	0.381	0.9489	2.43
	gad4	54	4.905	0.5626	0.3894	0.9675	1.937
	gad1/2/4/5	47	2.779	0.5693	0.5912	0.8542	5.365

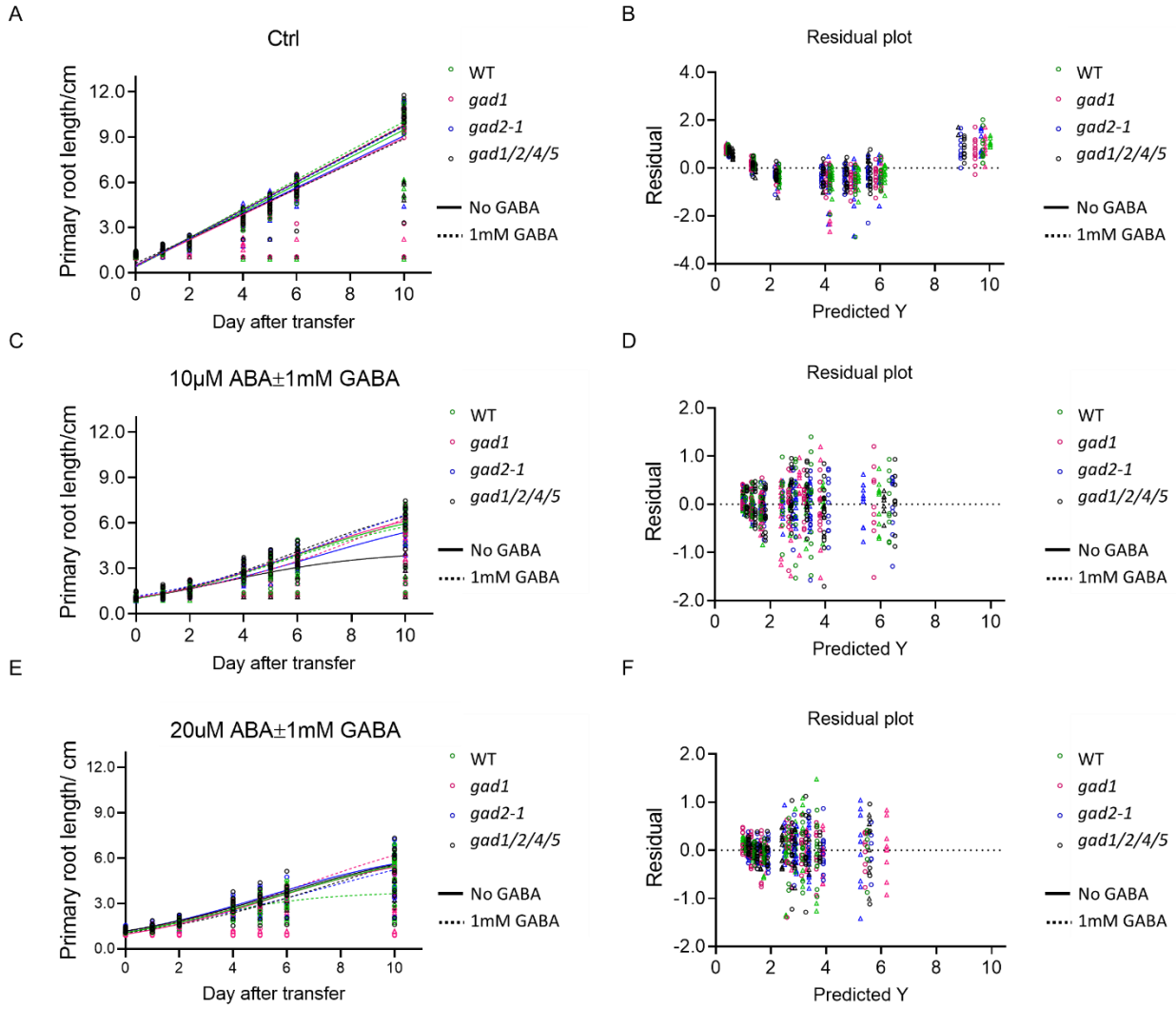

Supplementary Figure 10. Primary root elongation of WT and GABA deficient mutants.

Primary root elongation of plants growing on media containing 0, 10 or 20 μM ABA with or without 1 mM GABA (**A, C, E**). symbols indicate primary root length of individual seedlings, solid line indicate groups without GABA treatment, dash lines indicate groups with GABA treatment. Residues against predicted root length were plotted to check goodness of fit (**B, D, F**).

Supplementary Table 2. Summary of regression result in Suppl. Fig. 10.

For linear regression (Suppl. Fig. 10A, B), linear model were created using Y=a·X+b. Y represents primary root length, X represents days after transfer of seedling to new media. Coefficient indicates slope, i.e., growth rate/ $cm \cdot day^{-1}$. Coefficient b indicates intercept of the linear regression line on y axis, i.e., initial root length. For nonlinear least square regression (Suppl. Fig. 10C-E), logistic growth model was chosen. df indicates sample amount. YM indicates predicted max root length (cm). Y0 indicates initial root length. Coefficient k indicates the velocity of change from Y0 to YM, in our case the velocity indicates how fast primary root elongation stopped after transferring to ABA media. SSE indicates sum square of error of the regression. In both regressions, df indicates sample amount. R^2 indicated confidence of prediction.

Linear regression- without ABA								
Genotype	ABA/ µM	GABA/ mM	df	R				
WT	0	0	80	Y= 0.93*X +0.454, R^2= 0.94				
		1	69	Y= 0.823*X +0.629, R^2= 0.93				
gad1		0	82	Y= 0.908*X +0.396, R^2= 0.96				
		1	73	Y= 0.963*X +0.396, R^= 0.96				
gad2		0	76	Y= 0.847*X +0.48, R^2= 0.95				
		1	70	Y= 0.944*X +0.391, R^2= 0.93				
gad1/2/4/5		0	80	Y= 0.857*X +0.502, R^2= 0.95				
		1	74	Y= 0.929*X +0.401, R^2= 0.92				
Nonlinea least square regression-logistic- with ABA								
Genotype	ABA/ µM	GABA/ mM	df	YM	Y0	k	R^2	SSE
WT	10	0	78	9.763	1.15	0.2715	0.9137	19.93
		1	67	7.787	1.023	0.3197	0.9839	2.691
	20	0	71	7.179	1.184	0.2871	0.8992	12.92
		1	78	8.016	1.184	0.2388	0.9057	12.51
gad1	10	0	77	14.42	1.104	0.224	0.8879	24.01
		1	74	7.387	1.009	0.3264	0.9586	7.827
	20	0	73	7.022	1.093	0.2963	0.9254	9.511
		1	71	3.776	0.9851	0.441	0.7689	16.32
gad2	10	0	77	7.14	1.003	0.3238	0.9262	14.2
		1	73	4.143	1.008	0.3617	0.7503	19.43
	20	0	70	6.602	0.9729	0.3271	0.9283	11.15
		1	76	8.716	1.134	0.2799	0.9593	7.904
gad1/2/4/5	10	0	78	8.188	1.035	0.3235	0.9321	16.7
		1	78	7.548	1.056	0.2723	0.9558	6.324
	20	0	73	6.922	1.174	0.3064	0.9409	7.822
		1	77	8.875	1.058	0.2518	0.9482	7.91

A

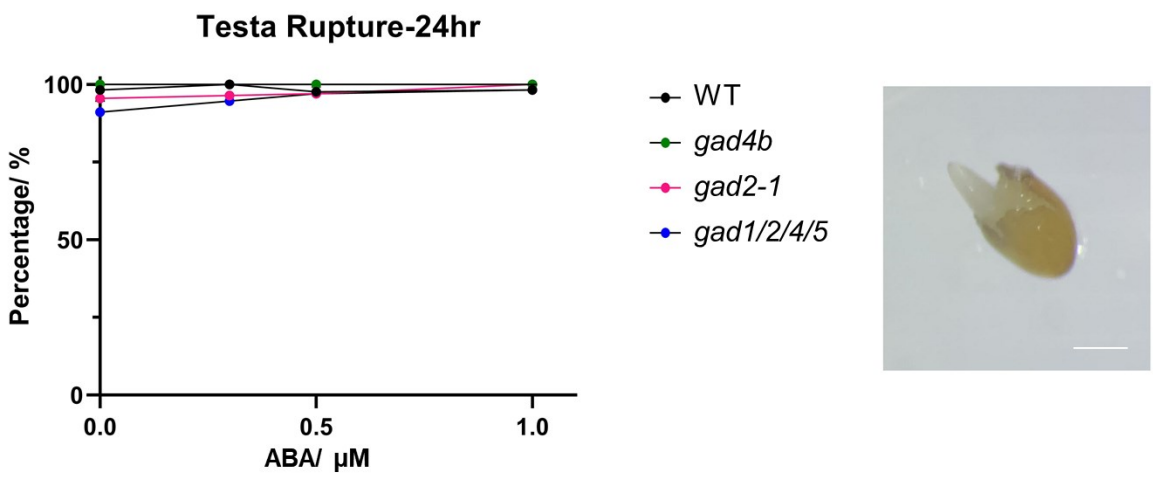
Testa Rupture-24hr
Percentage/ %
100
50
0
0.0
0.5
1.0
ABA/ μM
WT
gad4b
gad2-1
gad1/2/4/5

B

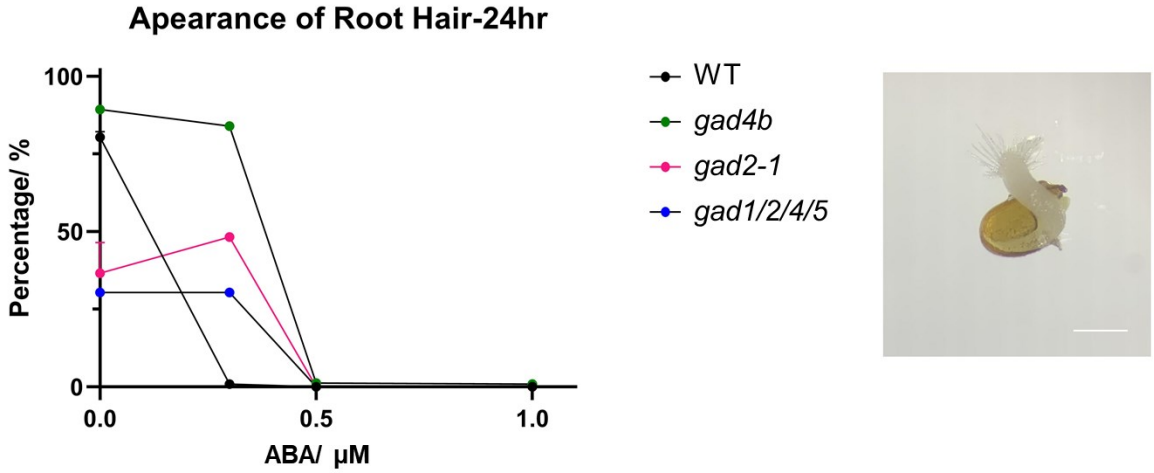
Apearance of Root Hair-24hr
Percentage/ %
100
50
0
0.0
0.5
1.0
ABA/ μM
WT
gad4b
gad2-1
gad1/2/4/5

C

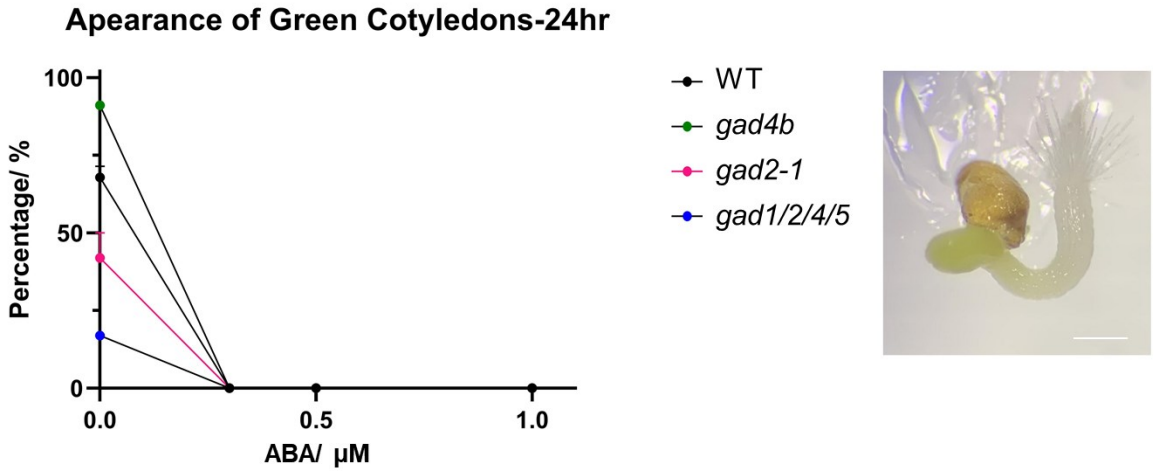
Apearance of Green Cotyledons-24hr
Percentage/ %
100
50
0
0.0
0.5
1.0
ABA/ μM
WT
gad4b
gad2-1
gad1/2/4/5

Supplementary Figure 11. Seed germination and seedling development of WT and GABA deficient mutants.

A. Seed germination was defined as testa rupture at 24h after exposure to the light on half-MS. **B-C**. Seedling development subsequent to seed germination was defined as appearance of root hair and greening cotyledons. Symbols represent for average from 50 seeds/seedlings each genotype on half MS medium from one experiment. Scale bars: 150 μm.

Chapter VI General discussion

GABA as a non-proteinogenic amino acid is metabolised through the GABA shunt (Bown and Shelp 2020). A signalling role of GABA has long been speculated in plants, and it was not until recently that potential mechanism by which the GABA signal can be transduced – in the ALMT family - was discovered in plants (Ramesh et al. 2015, Ramesh et al. 2018). In *Arabidopsis*, approximately 6 (ALMT4, 6, 9, 12, 13 and 14) out 14 of ALMTs are located in guard cells, among which ALMT9 and ALMT12 have well-documented roles in stomatal opening and closure respectively (Meyer et al. 2010, Meyer et al. 2011, De Angeli et al. 2013b, Eisenach et al. 2017). In Chapter II, GABA has been identified as a *bona fide* signal molecule in plants, which modulates stomatal movement in response to stimuli, including ABA, light, and drought. Both ALMT9 and ALMT12 appeared to mediate stomatal opening and closing sensitivity to GABA (Chapter II). And GABA-ALMT9 modulated stomatal opening regulation was further corroborated via site-direct mutagenesis of the putative GABA-binding motif within ALMT9, where GABA-insensitive ALMT9 (*almt9*-2/*35S:: ALMT9*^{F243CY245C}) phenocopied the GABA-deficient mutant (*gad2-1*) with higher stomatal conductance (Chapter III). Previous research suggests that GABA deficiency was correlated with the enlarged stomata of the *gad1/2* double mutant of the most predominant isoforms of *GADs* in *Arabidopsis* (Mekonnen et al. 2016). It was refined that such correlation was contributed by GAD2 (Chapter II). However, further mutation of *GAD4* and *GAD5* (*gad1/2/4/5*) in *gad1/2* decoupled the correlation between GABA concentration and stomatal opening (Chapter IV). The quadruple mutant had a WT stomatal phenotype under constant light, dark-light transition, steady state stomatal conductance and drought response (Chapter IV), suggesting that the nearly complete blockage of the GABA shunt

may alter other physiological parameters, not simply just GABA synthesis, to reverse the effects of the *gad2* single knockout back to a wildtype phenotype. That being said, guard cell specific complementation of *GAD2Δ* reduced stomatal opening of both WT and *gad2* (Chapter II) but elevated that in *gad1/2/4/5* (Chapter IV). The *gad1* mutant did not have visible stomatal phenotype under conditions tested (Chapter IV), nor did the root predominant isoform contribute to varied primary root elongation with or without ABA applied (Chapter V). However, preliminary results on ABA-inhibition of stomatal opening indicated that further mutation of *GAD1* in *gad2/4*, which had hyper-ABA sensitivity compared to that of WT, could significantly reduce ABA sensitivity (Chapter V). These results suggest that GAD1 and GAD4, in addition to GAD2, could work cooperatively in maintaining homeostasis of GABA, which is required in normal function of stomata in response to light and ABA. The following discussion will focus on research gaps which need to be explored based on the current study.

Interaction of GABA with other ALMTs in guard cells

In Chapter III, it was demonstrated that the putative GABA-binding motif is an asset when exploring the GABA-ALMT interaction in regulation of stomatal movement. *GC1:: ALMT12* and *GC1:: ALMT12*^{L203CY205C} have been constructed to further explore the role of GABA in mediating stomatal closing. While it could be more straight forward in the case of ALMT9 and ALMT12, as these mediate anion transport in predominantly a single direction under physiological scenarios (Meyer et al. 2010, De Angeli et al. 2013b), GABA regulation of ALMT4 and ALMT6 could be more complicated. The two transporters mediate bidirectional transport of anions at the tonoplast and are involved in both opening and closure (Meyer et al. 2011, Eisenach et al. 2017). An interesting observation was that stomatal aperture of

WT with 2 mM GABA application and *almt9-2* with or without GABA gradually increased to the similar level of opening with prolonged time of light exposure (Chapter III, Fig. 9; Suppl. Tab. 2). These three groups had larger increase in stomatal aperture of around 0.5 µm, while that was 0.33 µm WT with no GABA applied (Chapter III, Suppl. Tab. 2). Except for Cl^-, ALMT9 can also mediate malate into vacuole (De Angeli et al. 2013b). ALMT9 appears not to be regulated by ABA (De Angeli et al. 2013b). However, ALMT4 is required for ABA-activated anion efflux from guard-cell vacuoles (Eisenach et al. 2017) and as GABA-antagonised ABA-induced stomatal closure and opening (Chapter II, Suppl. Fig. 3; V Fig. 5), ALMT4 may be involved in such GABA-ABA interaction during stomatal regulation. It may also mediate anion influx if the tonoplast is hyperpolarised. To investigate a potential GABA-ALMT6 linkage, *almt6* should be crossed with *gad2* to examine whether the loss of *ALMT6* can compromise the loss of *GAD2* in gas exchange regulation or whether the *gad2/almt6* double mutant can phenocopy the *gad2/almt9* mutant. GABA inhibition of stomatal opening can also be tested on both *almt4* and *almt6* mutants to see whether the mutation can eliminate the gradually increased stomatal opening in WT, which might help explain whether the GABA inhibitory effect takes place in either or both directions of transport activity by ALMT4 and ALMT6. Furthermore, a directed test of whether GABA interacts with ALMTs using electrophysiological assays either in knockout mutants (Meyer et al. 2010) or through heterologous studies (De Angeli et al. 2013b) is warranted.

Elongation of the gamete cell was disrupted when GABA catabolism in the stigma was ablated by mutation of *GABA-T* (Renault et al. 2011). Recently, it was confirmed that a GABA-ALMT12 interaction is involved in anion balance in pollen tubes, which could in turn interact with pH and Ca^{2+} signaling in the cell (Domingos et al. 2019). To further explore the dynamic influence of GABA, future experiments could employ fluorescence sensors for

in vivo GABA signaling monitoring. These include the intensity-based GABA sensing fluorescence reporter (iGABASnFR) for GABA, ClopHensor for cytosol Ca^{2+}, pH, NO_3^-, and Cl^- and CapHensor cytosol Ca^{2+} and pH (Marvin et al. 2019, Demes et al. 2020, Li et al. 2021). The latter two sensors had been tested on pollen tube elongation and guard cells on epidermis , thus both cell type could be employed in future experiments for GABA signaling in plants.

The role of *GAD1*, *GAD2* and *GAD4* in cross talk of GABA and ABA signalling in stomatal regulation

Pharmacological experiments on epidermal strips with GABA and/or ABA indicated differential ABA sensitivity of *gad2/4* and *gad1/2/4*, which was distinct from that of *gad1* and *gad2 (*Chapter V, Fig. 5). This suggests possible involvement of GAD4 in ABA signalling perception in *gad1/2/4.*

Based on the previous research, GABA concentrations diurnally oscillates in plants due to circadian/diel regulation of *GAD* expression (Espinoza et al. 2010). This is also the case genes involved in ABA signalling (Adams et al. 2018). Circadian rhythms are important in many physiological processes in plant, including regulation of stomatal movement (Hassidim et al. 2017). Based on previous published gene profiles in response to diurnal rhythms (Michael et al. 2008a), the expression rhythm of *GAD1* was induced by dark, which is opposite to that of *GAD2* and *GAD4 (*Fig. 1A). Elements of ABA signalling are also controlled by circadian rhythms and vice versa, ABA application and mutation of ABA receptors also perturbs circadian rhythms (Castells et al. 2010). Thus, it is possible that when the three *GAD* homologues were mutated, the disrupted homeostasis regulated or

related to GABA signalling, possible related to circadian rhythms, leads to the discrepancy of *gad1/2/4/5* and *gad2.* Our result from qPCR indicated that the core clock genes, circadian rhythm Late Elongated Hypocotyl *(LHY)*, Circadian Clock Associated-1 (*CCA1*) and Timing of Cab2 Expression1 (*TOC1*) (Fig.1B), were not differently expressed in WT, *gad2-1* and *gad1/2/4/5* at the time when the genes reach the peak and bottom level (Allen et al. 2006) (Fig. 1C). Thus, it is unlikely that the varied phenotype of the *gad* mutants was due to an impairment in core circadian rhythm. For future analysis, stomatal response to dark-to-light and light-to-dark transition could be compared between *gad1*, *gad2* and *gad4* in comparison to WT to see if the varied circadian rhythm could influence stomatal movement in a light-dependent manner.

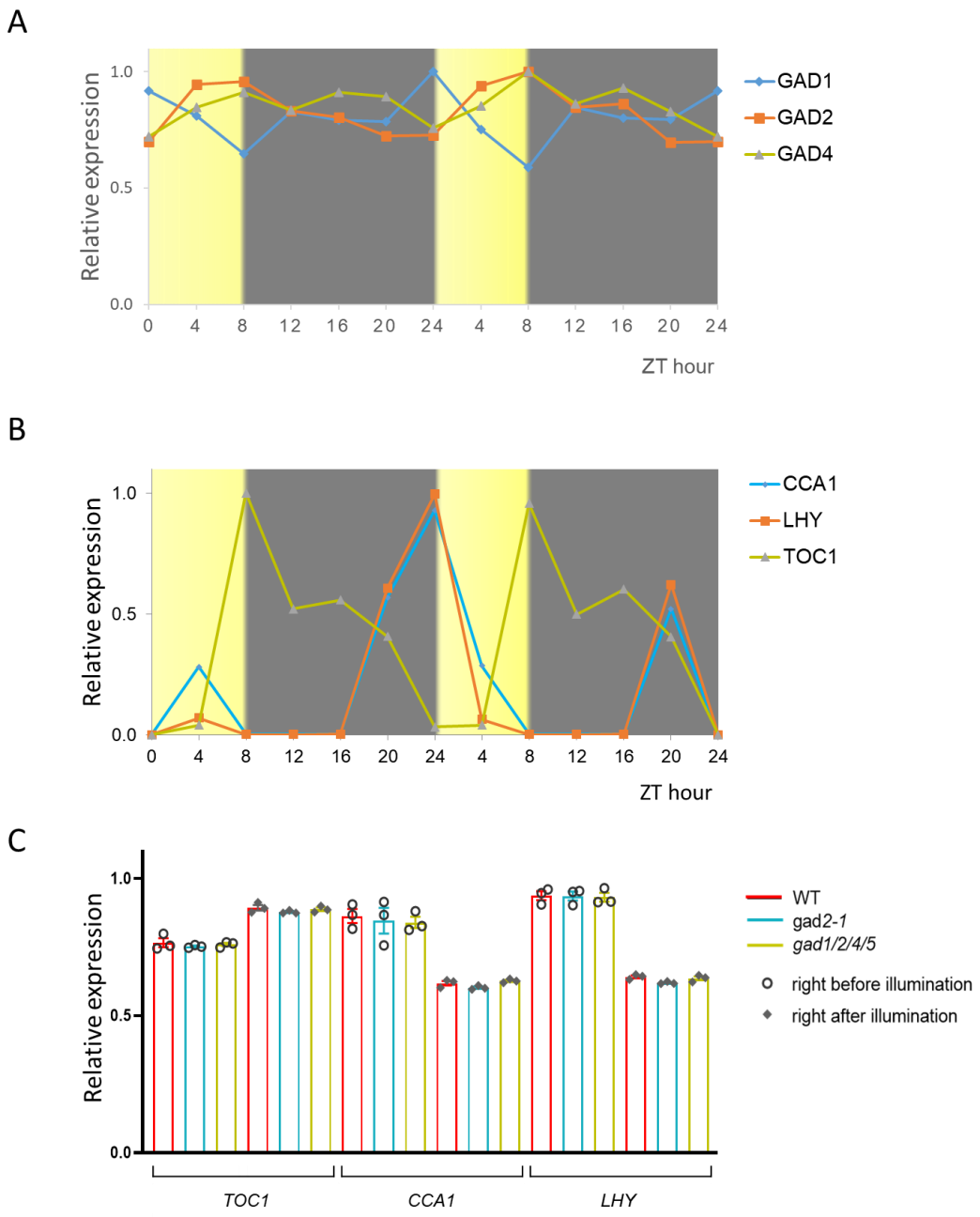

Figure 1. The expression level of core circadian rhythm genes in WT, *gad2-1* and *gad1/2/4/5*.

A. Adapted data of diurnal oscillation of expression of *GAD1, GAD2* and *GAD4* (Michael et al. 2008b). **B**. Adapted data of diurnal oscillation of expression of core element of circadian rhythm *Late Elongated Hypocotyl (LHY), Circadian Clock associated-1 (CCA1)* and *Timing of Cab2*

Expression1 (TOC1) (Michael et al. 2008b). **C.** qPCR analysis of the expression of *LHY, CCA1* and *TOC1* in WT, *gad2-1* and *gad1/2/4/5*. RNA samples were extracted from 4-week-old plants grown under short-lightening period (10 hr light/ 14 hr dark) right before and after light period separately. eIF4a (eukaryotic initiation factor-4A) was used as house-keeping gene for normalization of gene expression. Bar graph indicates mean value of 3 bio-replicates; symbols indicate mean value of 3 technical replicates. The expression pattern of these genes matched the pattern as reported in previous reported (**B)**. There is no significant difference as to expression of these genes comparing mutants to WT.

Contribution of *GAD4* and *GAD5* to WT-like stomatal aperture of *gad1/2/4/5*

Both *gad1/2/4* and *gad1/2/5* showed WT-like stomatal conductance and light-induced stomatal opening, similar to that of *gad1/2/4/5*. Due to relative low expression of *GAD5* in rosette leaves and root, it is hard to interpret how *GAD5* could contribute to WT-like stomatal phenotype in *gad1/2/4/5*. Recent study revealed that the least predominant isoform of *GADs* in these tissues, *GAD3*, was induced under combined stress of high light and heat and is required in plant tolerance to such stress (Balfagón et al. 2021). Except for several exemptions, plant GADs are conserved in activation by Ca^{2+}/CaM at the C-teminus (Akama and Takaiwa 2007). However, enzyme activity of GAD3 and GAD5 might not be regulated by Ca^{2+}/CaM (Shelp and Zarei 2017). Thus, further exploration of contribution of either GAD4 or GAD5 to the prementioned phenotypes might require separate experimental design.

As mentioned in Chapter I, *Arabidopsis* GAD1 shows optimum catalyzing activity when forming a homohexamer under low pH, presence of Ca^{2+}/CaM or increased GAD concentration (Astegno et al. 2015). It is not known whether other homologs also form homo-multimers or whether each monomer acts as a functional decarboxylase, or whether heteromultimeric GADs may form containing different isoforms. An outline of the potential experimental approach to this is outlined below in GADs in ABA inhibited light induced stomatal opening (experimental approach vi). When ABA was applied, different expression of *GAD1*, *GAD4* and *GAD5* could also be detectable in leaves of *Arabidopsis* (Yang et al. 2008, Pandey et al. 2010, Bauer et al. 2013, Dittrich et al. 2019). Thus, an explanation for how the expression of *GC1:: GAD2Δ* had an opposite effect on *gad1/2/4/5* and *gad2-1* could be the lack of interaction of *GAD1*, *GAD4* or *GAD5* in guard cells in modulation of GABA signaling (Chapter IV and V). Complementation or mutation of GADs in a tissue or cell specific manner to see how this will alter plant phenotypes, therefore, is also a practical way to explore synergistic effect between GADs (Yang et al. 2008).

Increasingly research has shown that a consequence of disruption of functional GADs could be far beyond impaired GABA synthesis, where perturbation of many physiological processes could occur (Fig. 2-3), such as photosynthesis, ROS metabolism, respiration, transcriptome and metabolome (Lancien and Roberts 2006, Araújo et al. 2010, Batushansky et al. 2014, Li, W. et al. 2016, Jin et al. 2019, Che-Othman et al. 2020). Perturbed GABA metabolism has been revealed to contribute to altered metabolism of other compounds, such as sucrose, amino acids and phytohormones (Signorelli et al. 2015, Carillo 2018, Hijaz et al. 2018, Priya et al. 2019). These results suggest that GABA could be involved in complex metabolic and signalling pathways. To detangle the key elements

of GABA signalling, future analysis can resort to transcriptome and metabolome analysis. In our case, the inconsistent phenotypes between *gad* single mutants and multiploid mutants may be linked with differential metabolomic changes by the loss of different *GAD* (s). Metabolomic analysis of those mutants could also be an informative way in which to detangle the GABA signalling network. Given that the GAD homologues are differentially expressed in different cell-types and tissues, to identify whether specific metabolic pathways were divergently impaired when certain homologue were mutated, mesophyll cells and guard cell single-cell-type metabolite profiling could be another informative resort in detangling the signalling network of GABA (Misra et al. 2014, Dittrich et al. 2019). Microarray and RNAseq are established techniques employed on analysing signalling pathways (Zimmermann et al. 2004, Zhang et al. 2020). ABA signalling networks has been extensively explored with transcriptome analysis (Liu et al. 2013, Liu et al. 2018). We found GABA could impair ABA signalling in stomatal regulation (Chapter II, Suppl. Fig. 3; Chapter V, Fig. 5,6). Analysing ABA effects on GABA deficit mutants and comparing with available data source may be a promising way, through which genes involved in such interaction and detangling GABA signalling in plants could be revealed, again this could occur using single cell RNAseq as well as whole tissues or cell-type preparations (Misra et al. 2014).

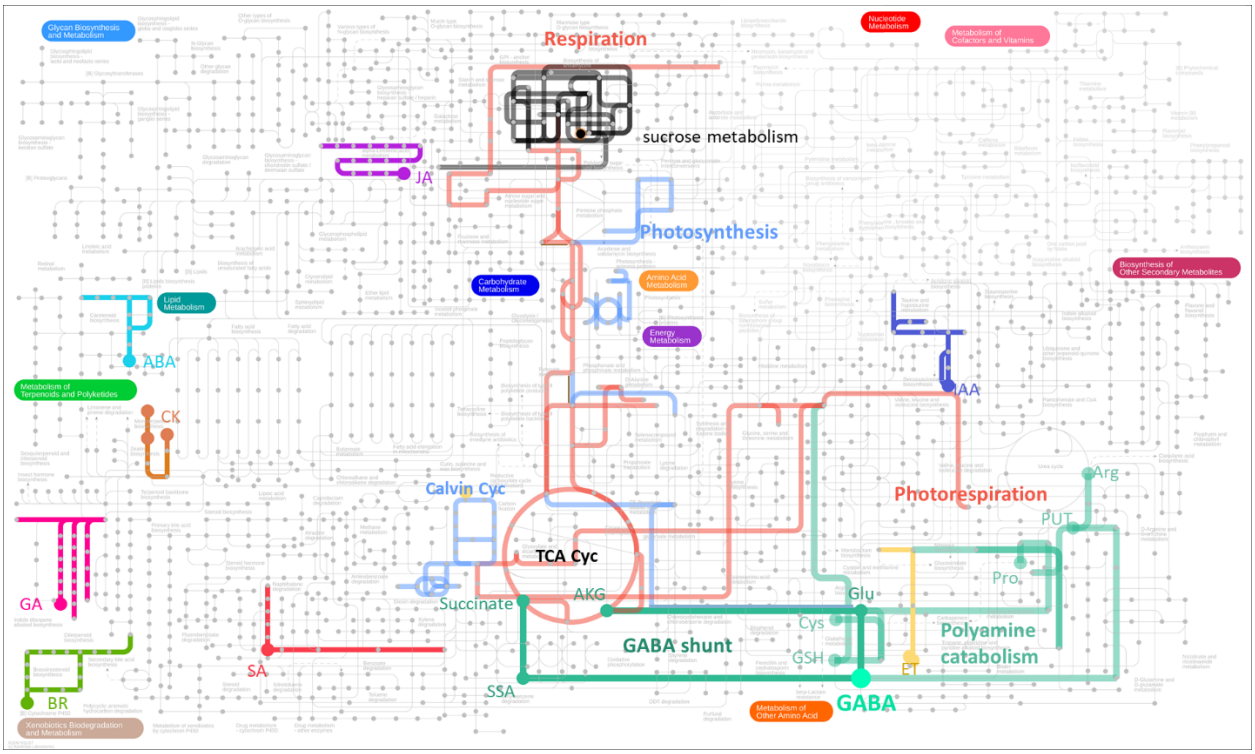

Figure 2. Mapping metabolites impacted by GABA.

The biosynthesis of secondary metabolites maps was adapted from KEGG (Kanehisa and Goto 2000, Kanehisa 2019, Kanehisa et al. 2021). GABA metabolism related metabolism pathway was highlighted in varied colours based on reactions and compounds number from KEGG. GABA synthesis from GABA shunt (bold cyan) and polyamine catabolism (light cyan) were indicated (Bown and Shelp 2020). GABA shunt compounds and polyamines reported in previous publications were labelled with name by circles. Respiration were reported connected to GABA shunt, thus are also indicated (glycolysis, photorespiration and TCA cycle in light red) (Priya et al. 2019, Che-Othman et al. 2020). GABA alleviated stress impaired photosynthesis (Li, W. et al. 2016, Salah et al. 2019). The photosynthesis pathways are marked in light blue. It was reported in citrus that GABA application induced hormone levels, thus key final steps in phytohormones synthesis were marked by colours with hormone compounds labelled by text and circles (Hijaz et al. 2018). GABA could improve sucrose synthesis, the metabolism of which is marked in black (Priya et al. 2019). Key metabolic pathways were automatically labelled in coloured rectangle. JA,

Jasmonic acid; ABA, Abscisic acid; CK, Cytokine; GA, Gibberellin; BR, Brassinolide; SA, Salicylic acid; ET, Ethylene; IAA, Auxin; GABA, γ-Aminobutyric Acid (indicated by green triangles); SSA, Succinic Semi-Aldehyde; AKG, 2-Ketoglutamate; Glu, Glutamate; Cys, Cysteine; Arg, Arginine; PUT, Putrescine; Pro, proline; GSH, Glutathione.

GABA is synthesised mainly in cytosol catalysed by GAD, which is activated by Ca^{2+}/CAM or acid pH (Astegno et al. 2015). In silico analysis suggests possible subcellular location of GADs apart from cytosol, where GAD2 and GAD4 also located in nucleus, GAD3 and GAD4 in mitochondria and GAD5 with plasmodesmata (though mature guard cells lack plasmodesmata) (Oparka and Roberts 2001, Bateman et al. 2020). The extra location could relate to the role of GABA to many physiological processes reported, such as photosynthesis, respiration and ROS synthesis cycle (Li, W. et al. 2016, Li et al. 2019, Thomson et al. 2019). GABA can also be synthesised in the peroxisome and apoplast via polyamine catabolism (Zarei et al. 2016), where ROS synthesis can also take place (Tripathy and Oelmüller 2012). In guard cells, ROS signalling could also acts downstream of ABA signalling by activation of SLAC (SLow Anion Channel) to close stomata (Dreyer et al. 2012). Moreover, ROS synthesis also increases cytosolic Ca^{2+} concentration and vice versa (Görlach et al. 2015). Ca^{2+} can also act down stream of ABA signalling through Calcineurin B-Like protein (CBL) and CBL-Interacting Protein Kinase (CIPK) and calcium-dependent protein kinase (CPK) (Song et al. 2018). GAD enzyme activity is optimised at pH8.5 (Shen et al. 2013). ROS production activated by cytosolic Ca^{2+} contributes to cytosolic acidification (Felle 2001), which could influence GABA synthesis. Mitogen-activated protein kinase (MAPK) signalling, which involved in stomatal regulation and interact with all signalling mentioned above, also contributes to regulation of GABA synthesis (Jammes et al. 2009, Brock et al. 2010, Lv et al. 2018, Deng et al. 2020) (Fig.3).

Future experiments could focus on elucidation of the interaction between GABA and these signaling pathways.

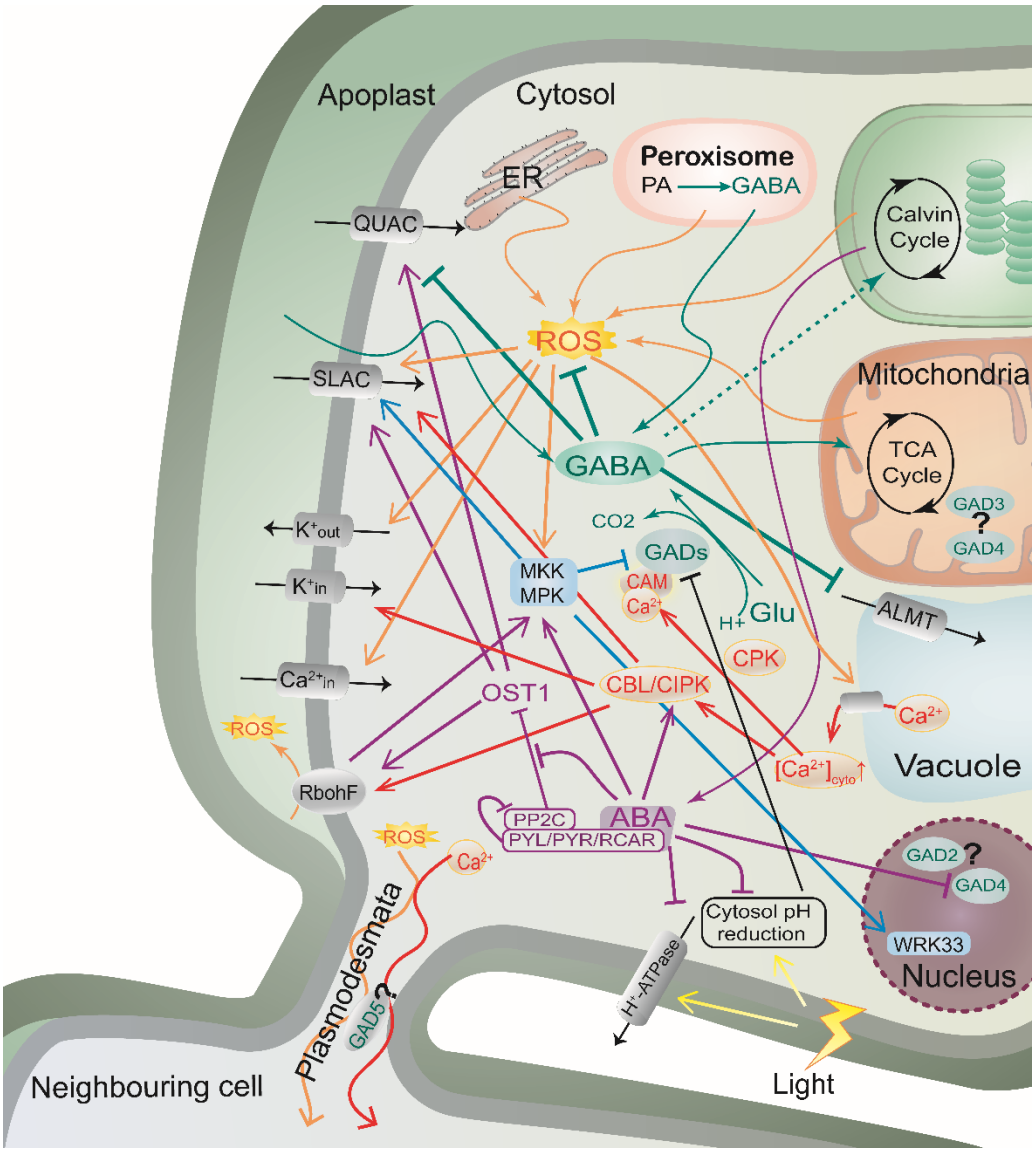

Figure 3. Schematic of established interaction between GABA, ABA, ROS, MPK, pH and Ca^{2+} in plants.

Summary of possible signalling network of cross talk between GABA and other signal compounds focusing on guard cells. Transport of compounds into the cytosol are indicated by narrow lines with

closed arrows. Signal transductions are indicated by bold lines, where open arrows indicate facilitation, blunt arrows indicate inhibition. Different signal pathways are differentiated by colour.

GADs in ABA inhibited light induced stomatal opening

One of the exciting results of this project is the switch in ABA sensitivity in inhibition of light induced stomatal opening of *gad2/4* when *GAD1* was further mutated (Chapter V, Fig.5-6; Suppl. Fig. 5). Thus, the main homologues responsible for ABA hypersensitivity in mutants could be *GAD1*, *GAD2* and *GAD4*. Furthermore, application of 0.5 mM GABA abolished insensitivity of *gad1/2/4*, supporting the conclusion based on the result of guard cell specific complementation of *GAD2Δ* - that GABA concentration in guard cells alone could influence stomatal behaviour. It was observed that there was variance between stomatal opening of *gad4* in whole plants and in epidermis, which indicates possible signalling input of guard cells from mesophyll cells or vasculature; therefore, sensitivity of mutants to ABA in serial *gad* mutants will be required to be examined by other techniques, such as real-time recording of stomatal conductance of detached leaves fed by artificial xylem sap solution using infrared gas analyser LiCor LI-6400 (Conn et al. 2013, Xu et al. 2021). Further experiments are required to delineate the mechanism behind this (Fig. 4). These experiments include:

(i). Investigating the role of the GABA-ALMT/ABA interaction in stomatal regulation. When GABA was applied, the mutant lines had more closing extent in stomata in response to ABA (Chapter V, Suppl. Fig.5), this might be due to impaired GABA-ALMT interaction.

ABA signalling as a stress hormone could induce GABA synthesis in WT, exogenous GABA application was also suggested to induced endogenous GABA synthesis (Scholz et al. 2017, Yong et al. 2017), thus in WT the combined application of GABA and ABA could lead to extra accumulation of GABA, which provides an inhibitory counterbalance to the stimulation of QUAC by ABA and ROS signalling. Meanwhile GABA will inhibit activity of ALMT9 (possibly ALMT4 and 6) to maintain stomatal movement. Such a balancing effect could be dampened in mutant lines. To verify this, GABA concentrations should be measured in plants following by ABA and GABA application.

(ii). Expression of *GAD1* in response to ABA. Transcriptome profiling of ABA responses in *Arabidopsis* indicated that expression of *GAD2* and *GAD4* was reduced by ABA treatment (Yang et al. 2008, Pandey et al. 2010, Bauer et al. 2013, Dittrich et al. 2019). *GAD4* expression was induced in ABA deficient mutants (Urano et al. 2009), so stimulates the expression of this less predominant homologue, but not of *GAD1*. *GAD1* has an opposite circadian/diel response comparing to *GAD2* and *GAD4 (*Fig. 1A). Furthermore, *GAD1*, *GAD2* and *GAD4* responded differently in response to *Pseudomonas syringae* treatment (Deng et al. 2020). Thus, it is possible that it also responds differently to ABA. To test this, expression of *GAD1* could be checked by qPCR in ABA treated plants. Moreover, as mentioned above (Fig. 3), GAD2 and GAD4 could also target nucleus, thus it may also be possible that they can impair ABA regulation of transcription (Fujita et al. 2011). This can be verified by microarray or RNAseq analysis to see whether transcriptome regulation could be differently enriched in mutants comparing to WT in response to ABA.

(iii). Impaired redox balance in mutants. Glutathione, which is a scavenger of ROS, accumulated following exogenous GABA treatment under both control and saline

conditions in muskmelon (*Cucumis melo* L. cv.) (Jia and Davies 2007). Further, exogenous GABA application or perturbed GABA catabolism by mutation of GABA-T reduced ROS concentration in plants including *Arabidopsis*, the legume shrub, *Caragana Intermedia* and tomato (*Solanum lycopersicum L.*) (Shi et al. 2010, Jalil et al. 2017, Wu et al. 2020). ROS signalling could act down stream of ABA signalling in activating transport activity of SLAC1 through Ca^{2+} or Mitogen-activated protein kinase (MPK) signalling (Bai et al. 2014, Medeiros et al. 2020) . Interaction of ROS-GABA signalling has been suggested to improve drought tolerance. In Cucumber plants (*Cucumis sativus cv.*) foliar application of GABA mimics the effect of the reductant Ascorbic Acid during drought stress, in improving water use efficiency (Ghahremani et al. 2021). Thereby, it would be worth monitoring ROS balance in WT and *gad* mutant lines. Plant ROS in plant materials can be quantified by chemical staining, such as Diaminobenzidine tetrahydrochloride (DAB), or by fluorescence using a generic ROS sensor, such as CM 2',7'-dihydrodichlorofluorescein diacetate (DCF-DA) (Halliwell and Whiteman 2004, Ermakova et al. 2014).

(iv) GAD multimer formation. As mentioned in Chapter I, *Arabidopsis* GAD1 shows optimal catalyzing activity when forming a homohexamer under low pH, presence of Ca^{2+}/CAM or increased GAD concentration (Astegno et al. 2015). It is not known whether other homologues also formed homo-mulitmers or whether each homologue acts as a decarboxylase or a cofactor of the enzyme. To further explore this, first, enzyme activity of each GAD could be analyzed on purified protein enriched in *E coli* as previous described (Astegno et al. 2015). For homologue interaction analysis, Yeast Two-Hybrid Assays or bimolecular fluorescence complementation (BiFC) could be employed to see whether there is any conformation interaction between GAD1, GAD2 and GAD4 proteins (Terasaki et al. 2009, Kamigaki et al. 2016).

(iv) Sucrose metabolism. Break down of Sucrose (Fig. 2; Black line) in guard cells is required in light-induced stomatal opening (Renault et al. 2013). Accumulation of GABA increases sucrose concentration by promoting photosynthesis under heat stress in mungbean and in *Arabidopsis* under salt stress (Renault et al. 2013, Jin et al. 2019, Priya et al. 2019). Sucrose can be degrade into Glu, the main precursor of GABA synthesis in cytosol (Daloso et al. 2016). Both these compounds could induce stomatal closing in *Arabidopsis* (Yoshida et al. 2016, Medeiros et al. 2018). Thus, the mutants could have impaired sucrose concentrations, which could also impair effect of both GABA itself and ABA in stomatal regulation. Sucrose concentrations in plants can be measured by Gas Chromatography Mass Spectrometry (GC-MS).

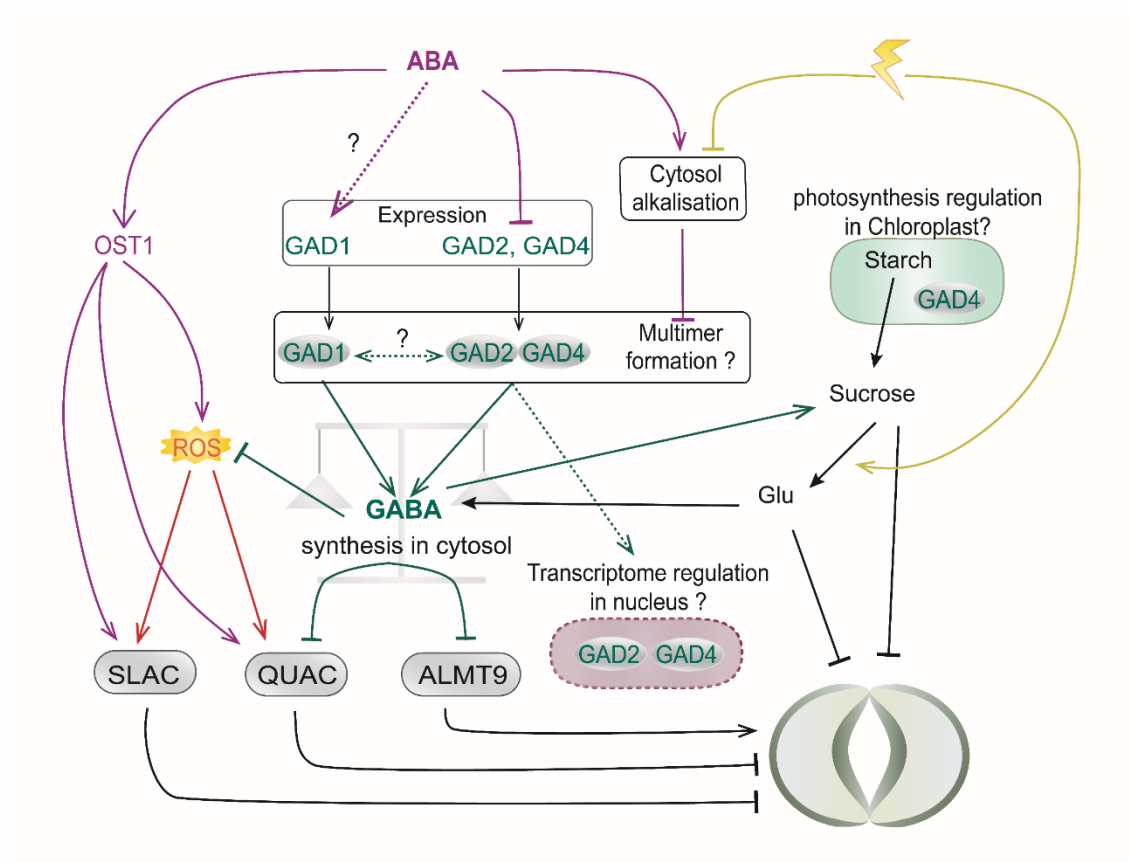

Figure 4. Schematic of possible mechanism of GABA-ABA cross talk.

Putative mechanisms behind reversed ABA sensitivity in *gad2/4* and *gad1/2/4* in light induced stomatal opening. ABA, GABA and possible involvement of ROS signalling are specified in different colours. Possible intersection of signal transduction for such phenotypes were marked by question marks. Open arrows indicate facilitation, blunt arrows indicate inhibition. TF, transcriptome factor; ROS, reactive oxygen species; ALMT, aluminium-activated malate transporter; SLAC, slow anion channel; QUAC, quick anion channel.

Conclusion

This thesis has revealed that GABA is a signal compound modulating stomatal movement. GABA signalling mediated stomatal regulation involves a GABA and ALMT interaction. Such interaction is important for plant acclimation to drought stress since accumulated GABA concentrations in plants improves plant water use efficiency. However, like many signalling molecules, stomatal regulation of GABA is not a simple linear dose-dependent relationship. The fact that GABA concentration is negatively correlated to stomatal aperture in *gad2* and WT, but not in higher order mutants of *GADs* suggests a synergistic contribution and varied function of *GAD* homologues with respect to stomatal movement of *Arabidopsis*. Endogenous GABA concentration determines ABA sensitivity of plants during light induced stomatal opening, this involves *GAD1*, *GAD2* and *GAD4*, where cross talk between GABA and other signal pathways is likely to occur.

References

Abd El-Gawad, H. G., S. Mukherjee, R. Farag, O. H. Abd Elbar, M. Hikal, A. Abou El-Yazied, S. A. Abd Elhady, N. Helal, A. ElKelish and N. El Nahhas. Exogenous γ-aminobutyric acid (GABA)-induced signaling events and field performance associated with mitigation of drought stress in *Phaseolus vulgaris L*. *Plant signaling & behavior*, 1853384 (2020).

Adams, S., J. Grundy, S. R. Veflingstad, N. P. Dyer, M. A. Hannah, S. Ott and I. A. Carré. Circadian control of abscisic acid biosynthesis and signalling pathways revealed by genome‐wide analysis of LHY binding targets. *new phytologist* **220**, 893-907 (2018).

Akama, K. and F. Takaiwa. C-terminal extension of rice glutamate decarboxylase (OsGAD2) functions as an autoinhibitory domain and overexpression of a truncated mutant results in the accumulation of extremely high levels of GABA in plant cells. *Journal of experimental botany* **58**, 2699-2707 (2007).

Al‐Ghussain, L. and S. Energy. Global warming: review on driving forces and mitigation. *Environmental Progress & Sustainable Energy* **38**, 13-21 (2019).

Ali, S., K. Hayat, A. Iqbal and L. Xie. Implications of Abscisic Acid in the Drought Stress Tolerance of Plants. *Agronomy* **10**, 1323 (2020).

Allan, W. L., K. E. Breitkreuz, J. C. Waller, J. P. Simpson, G. J. Hoover, A. Rochon, D. J. Wolyn, D. Rentsch, W. A. Snedden and B. J. Shelp. Detoxification of succinate semialdehyde in *Arabidopsis* glyoxylate reductase and NAD kinase mutants subjected to submergence stress. *Botany* **90**, 51-61 (2011).

Allen, T., A. Koustenis, G. Theodorou, D. E. Somers, S. A. Kay, G. C. Whitelam and P. F. Devlin. *Arabidopsis* FHY3 specifically gates phytochrome signaling to the circadian clock. *The Plant Cell* **18**, 2506-2516 (2006).

Alonso, J. M., A. N. Stepanova, T. J. Leisse, C. J. Kim, H. Chen, P. Shinn, D. K. Stevenson, J. Zimmerman, P. Barajas and R. Cheuk. Genome-wide insertional mutagenesis of *Arabidopsis thaliana*. *Science* **301**, 653-657 (2003).

Araújo, W. L., A. Nunes-Nesi, S. Trenkamp, V. I. Bunik and A. R. Fernie. Inhibition of 2-oxoglutarate dehydrogenase in potato tuber suggests the enzyme is limiting for respiration and confirms its importance in nitrogen assimilation. *Plant Physiology* **148**, 1782-1796 (2008).

Araújo, W. L., K. Ishizaki, A. Nunes-Nesi, T. R. Larson, T. Tohge, I. Krahnert, S. Witt, T. Obata, N. Schauer and I. A. Graham. Identification of the 2-hydroxyglutarate and isovaleryl-CoA dehydrogenases as alternative electron donors linking lysine catabolism to the electron transport chain of *Arabidopsis* mitochondria. *The Plant Cell* **22**, 1549-1563 (2010).

Araya, T., T. Kubo, N. von Wirén and H. Takahashi. Statistical modeling of nitrogen‐dependent modulation of root system architecture in *Arabidopsis thaliana*. *Journal of integrative plant biology* **58**, 254-265 (2016).

Askari-Khorsgani, O., F. Flores and M. Pessarakli. Plant signaling pathways involved in stomatal movement under drought stress conditions. *Advances in Plants & Agriculture Research* **8**, 290-297 (2018).

Astegno, A., G. Capitani and P. Dominici. Functional roles of the hexamer organization of plant glutamate decarboxylase. *Biochimica et Biophysica Acta -Proteins Proteomics* **1854**, 1229-1237 (2015).

Baetz, U., C. Eisenach, T. Tohge, E. Martinoia and A. De Angeli. Vacuolar chloride fluxes impact ion content and distribution during early salinity stress. *Plant Physiology* **172**, 1167-1181 (2016).

Bai, L., P. Wang and C.-P. Song (2014). Reactive oxygen species (ROS) and ABA signalling. Abscisic acid: Metabolism, transport and signaling, Springer**:** 191-223.

Balfagón, D., A. Gómez-Cadenas, J. L. Rambla, A. Granell, C. de Ollas, R. Mittler and S. I. Zandalinas. GABA plays a key role in plant acclimation to a combination of high light and heat stress. *bioRxiv* (2021).

Balzergue, C., T. Dartevelle, C. Godon, E. Laugier, C. Meisrimler, J.-M. Teulon, A. Creff, M. Bissler, C. Brouchoud and A. Hagège. Low phosphate activates STOP1-ALMT1 to rapidly inhibit root cell elongation. *Nature communications* **8**, 1-16 (2017).

Bateman, A., M.-J. Martin, S. Orchard, M. Magrane, R. Agivetova, S. Ahmad, E. Alpi, E. H. Bowler-Barnett, R. Britto and B. Bursteinas. UniProt: the universal protein knowledgebase in 2021. *Nucleic Acids Research* (2020).

Batushansky, A., M. Kirma, N. Grillich, D. Toubiana, P. A. Pham, I. Balbo, H. Fromm, G. Galili, A. R. Fernie and A. Fait. Combined transcriptomics and metabolomics of *Arabidopsis thaliana* seedlings exposed to exogenous GABA suggest its role in plants is predominantly metabolic. *Molecular plant* **7**, 1065-1068 (2014).

Batushansky, A., M. Kirma, N. Grillich, P. A. Pham, D. Rentsch, G. Galili, A. R. Fernie and A. Fait. The transporter GAT1 plays an important role in GABA-mediated carbon-nitrogen interactions in *Arabidopsis*. *Frontiers in plant science* **6** (2015).

Bauer, H., P. Ache, S. Lautner, J. Fromm, W. Hartung, K. A. Al-Rasheid, S. Sonnewald, U. Sonnewald, S. Kneitz and N. Lachmann. The stomatal response to reduced relative humidity requires guard cell-autonomous ABA synthesis. *Current Biology* **23**, 53-57 (2013).

Beerling, D. J. and P. J. Franks. The hidden cost of transpiration. *Nature* **464**, 495-496 (2010).

Bhatti, J. S., G. K. Bhatti and P. H. Reddy. Mitochondrial dysfunction and oxidative stress in metabolic disorders—A step towards mitochondria based therapeutic strategies. *Biochimica et Biophysica Acta -Molecular Basis of Disease*

1863, 1066-1077 (2017).

Bouche, N. and H. Fromm. GABA in plants: just a metabolite? *Trends in plant science* **9**, 110-115, doi:10.1016/j.tplants.2004.01.006 (2004).

Bouché, N., A. Fait, D. Bouchez, S. G. Møller and H. Fromm. Mitochondrial succinic-semialdehyde dehydrogenase of the γ-aminobutyrate shunt is required to restrict levels of reactive oxygen intermediates in plants. *Proceedings of the National Academy of Sciences* **100**, 6843-6848 (2003).

Bouché, N., A. Fait, M. Zik and H. Fromm. The root-specific glutamate decarboxylase (GAD1) is essential for sustaining GABA levels in Arabidopsis. *Plant molecular biology* **55**, 315-325 (2004).

Bown, A. W. and B. J. Shelp. Plant GABA: not just a metabolite. *Trends in plant science* **21**, 811-813 (2016).

Bown, A. W. and B. J. Shelp. Does the GABA Shunt Regulate Cytosolic GABA? *Trends in plant science* (2020).

Breitkreuz, K. E., B. J. Shelp, W. N. Fischer, R. Schwacke and D. Rentsch. Identification and characterization of GABA, proline and quaternary ammonium compound transporters from *Arabidopsis thaliana*. *FEBS letters* **450**, 280-284, doi:Doi 10.1016/S0014-5793(99)00516-5 (1999).

Brock, A. K., R. Willmann, D. Kolb, L. Grefen, H. M. Lajunen, G. Bethke, J. Lee, T. Nürnberger and A. A. Gust. The *Arabidopsis* mitogen-activated protein kinase phosphatase PP2C5 affects seed germination, stomatal aperture, and abscisic acid-inducible gene expression. *Plant Physiology* **153**, 1098-1111 (2010).

Buckley, T. N. How do stomata respond to water status? *new phytologist* **224**, 21-36 (2019).

Carillo, P. GABA shunt in durum wheat. *Frontiers in plant science* **9**, 100 (2018).

Castells, E., S. Portolés, W. Huang, P. Mas and behavior. A functional connection between the clock component TOC1 and abscisic acid signaling pathways. *Plant signaling & behavior* **5**, 409-411 (2010).

Che-Othman, M. H., R. P. Jacoby, A. H. Millar and N. L. Taylor. Wheat mitochondrial respiration shifts from the tricarboxylic acid cycle to the GABA shunt under salt stress. *new phytologist* **225**, 1166-1180 (2020).

Chen, K., G. J. Li, R. A. Bressan, C. P. Song, J. K. Zhu and Y. Zhao. Abscisic acid dynamics, signaling, and functions in plants. *Journal of integrative plant biology* **62**, 25-54 (2020).

Chung, C., S. L. Niemela and R. H. Miller. One-step preparation of competent *Escherichia coli*: transformation and storage of bacterial cells in the same solution. *Proceedings of the National Academy of Sciences* **86**, 2172-2175 (1989).

Cotelle, V. and N. Leonhardt. ABA signaling in guard cells. *Advances in Botanical Research* **92**, 115-170 (2019).

Curtis, M. D. and U. Grossniklaus. A gateway cloning vector set for high-throughput functional analysis of genes in planta. *Plant Physiology* **133**, 462-469 (2003).

Daloso, D. M., L. Dos Anjos and A. R. Fernie. Roles of sucrose in guard cell regulation. *new phytologist* **211**, 809-818 (2016).

Daloso, D. M., D. B. Medeiros, L. Dos Anjos, T. Yoshida, W. L. Araújo and A. R. Fernie. Metabolism within the specialized guard cells of plants. *new phytologist* **216**, 1018-1033 (2017).

De Angeli, A., U. Baetz, R. Francisco, J. Zhang, M. M. Chaves and A. Regalado. The vacuolar channel VvALMT9 mediates malate and tartrate accumulation in berries of *Vitis vinifera*. *Planta* **238**, 283-291 (2013a).

De Angeli, A., J. B. Zhang, S. Meyer and E. Martinoia. AtALMT9 is a malate-activated vacuolar chloride channel required for stomatal opening in *Arabidopsis*. *Nature communications* **4**, doi:Artn 1804

10.1038/Ncomms2815 (2013b).

Demes, E., L. Besse, P. Cubero-Font, B. Satiat-Jeunemaitre, S. Thomine and A. De Angeli. Dynamic measurement of cytosolic pH and [NO_3^-] uncovers the role of the vacuolar transporter AtCLCa in cytosolic pH homeostasis. *Proceedings of the National Academy of Sciences* **117**, 15343-15353 (2020).

Demidchik, V., S. Shabala, S. Isayenkov, T. A. Cuin and I. Pottosin. Calcium transport across plant membranes: mechanisms and functions. *new phytologist* **220**, 49-69 (2018).

Deng, X., X. Xu, Y. Liu, Y. Zhang, L. Yang, S. Zhang and J. Xu. Induction of γ-aminobutyric acid plays a positive role to Arabidopsis resistance against *Pseudomonas* syringae. *Journal of integrative plant biology* (2020).

Dittrich, M., H. M. Mueller, H. Bauer, M. Peirats-Llobet, P. L. Rodriguez, C.-M. Geilfus, S. C. Carpentier, K. A. Al Rasheid, H. Kollist and E. Merilo. The role of *Arabidopsis* ABA receptors from the PYR/PYL/RCAR family in stomatal acclimation and closure signal integration. *Nature plants* **5**, 1002-1011 (2019).

Dodd, A. N., K. Parkinson and A. A. Webb. Independent circadian regulation of assimilation and stomatal conductance in the ztl-1 mutant of *Arabidopsis*. *new phytologist* **162**, 63-70 (2004).

Domingos, P., P. N. Dias, B. Tavares, M. T. Portes, M. M. Wudick, K. R. Konrad, M. Gilliham, A. Bicho and J. A. Feijó. Molecular and electrophysiological characterization of anion transport in *Arabidopsis thaliana* pollen reveals regulatory roles for pH, Ca^{2+} and GABA. *New Phytologist* **223**, 1353-1371 (2019).

Domínguez, E., J. A. Heredia-Guerrero and A. Heredia. The plant cuticle: old challenges, new perspectives. *Journal of experimental botany* **68**, 5251-5255 (2017).

Dreyer, I., J. L. Gomez-Porras, D. M. Riaño Pachón, R. Hedrich and D. Geiger. Molecular evolution of slow and quick anion channels (SLACs and QUACs/ALMTs). *Frontiers in plant science* **3**, 263 (2012).

Driesen, E., W. Van den Ende, M. De Proft and W. Saeys. Influence of Environmental Factors Light, CO_2, Temperature, and Relative Humidity on Stomatal Opening and Development: A Review. *Agronomy* **10**, 1975 (2020).

Du, L., T. Yang, S. V. Puthanveettil and B. Poovaiah (2011). Decoding of calcium signal through calmodulin: calmodulin-binding proteins in plants. Coding and Decoding of Calcium Signals in Plants, Springer**:** 177-233.

Duarte, K. E., W. R. de Souza, T. R. Santiago, B. L. Sampaio, A. P. Ribeiro, M. G. Cotta, B. A. D. B. da Cunha, P. R. R. Marraccini, A. K. Kobayashi and H. B. C. Molinari. Identification and characterization of core abscisic acid (ABA) signaling components and their gene expression profile in response to abiotic stresses in Setaria viridis. *Scientific reports* **9**, 1-16 (2019).

Edwards, K., C. Johnstone and C. Thompson. A simple and rapid method for the preparation of plant genomic DNA for PCR analysis. *Nucleic Acids Research* **19**, 1349 (1991).

Eisenach, C., U. Baetz, N. V. Huck, J. Zhang, A. De Angeli, G. J. Beckers and E. Martinoia. ABA-induced stomatal closure involves ALMT4, a phosphorylation-dependent vacuolar anion channel of *Arabidopsis*. *The Plant Cell* **29**, 2552-2569 (2017).

Elliott, K. and H. H. Jasper. Gamma-aminobutyric acid. *Physiological reviews* **39**, 383-406 (1959).

Ermakova, Y. G., D. S. Bilan, M. E. Matlashov, N. M. Mishina, K. N. Markvicheva, O. M. Subach, F. V. Subach, I. Bogeski, M. Hoth and G. Enikolopov. Red fluorescent genetically encoded indicator for intracellular hydrogen peroxide. *Nature communications* **5**, 1-9 (2014).

Espinoza, C., T. Degenkolbe, C. Caldana, E. Zuther, A. Leisse, L. Willmitzer, D. K. Hincha and M. A. Hannah. Interaction with diurnal and circadian regulation results in dynamic metabolic and transcriptional changes during cold acclimation in *Arabidopsis*. *PLoS One* **5**, e14101 (2010).

Eziz, A., Z. Yan, D. Tian, W. Han, Z. Tang and J. Fang. Drought effect on plant biomass allocation: A meta‐analysis. *Ecology Evolution* **7**, 11002-11010 (2017).

Fàbregas, N. and A. R. Fernie. The metabolic response to drought. *Journal of experimental botany* **70**, 1077-1085 (2019).

Fait, A., H. Fromm, D. Walter, G. Galili and A. R. Fernie. Highway or byway: the metabolic role of the GABA shunt in plants. *Trends in plant science* **13**, 14-19 (2008).

Felle, H. pH: signal and messenger in plant cells. *Plant biology* **3**, 577-591 (2001).

Felle, H. H. pH regulation in anoxic plants. *Annals of Botany* **96**, 519-532 (2005).

Fernando, V. D. and D. F. Schroeder (2016). Role of ABA in Arabidopsis salt, drought, and desiccation tolerance. Abiotic and biotic stress in plants-recent advances and future perspectives, IntechOpen.

Fischer, W. N., D. D. F. Loo, W. Koch, U. Ludewig, K. J. Boorer, M. Tegeder, D. Rentsch, E. M. Wright and W. B. Frommer. Low and high affinity amino acid H^+-cotransporters for cellular import of neutral and charged amino acids. *The Plant Journal* **29**, 717-731, doi:DOI 10.1046/j.1365-313X.2002.01248.x (2002).

Flores, H. E. and P. Filner (1985). Polyamine catabolism in higher plants: characterization of pyrroline dehydrogenase. Polyamines in Plants, Springer**:** 75-89.

Fucile, G., D. Di Biase, H. Nahal, G. La, S. Khodabandeh, Y. Chen, K. Easley, D. Christendat, L. Kelley and N. J. Provart. ePlant and the 3D data display initiative: integrative systems biology on the world wide web. *PLoS One* **6**, e15237 (2011).

Fujita, Y., M. Fujita, K. Shinozaki and K. Yamaguchi-Shinozaki. ABA-mediated transcriptional regulation in response to osmotic stress in plants. *Journal of plant research* **124**, 509-525 (2011).

Geilfus, C.-M. The pH of the apoplast: dynamic factor with functional impact under stress. *Molecular plant* **10**, 1371-1386 (2017).

Geisler, M. J. and F. D. Sack. Variable timing of developmental progression in the stomatal pathway in *Arabidopsis* cotyledons. *new phytologist* **153**, 469-476 (2002).

Ghahremani, Z., M. Mikaealzadeh, T. Barzegar and M. E. Ranjbar. Foliar Application of Ascorbic Acid and Gamma Aminobutyric Acid Can Improve Important Properties of Deficit Irrigated Cucumber Plants (*Cucumis sativus cv. Us*). *Gesunde Pflanzen* **73**, 77-84 (2021).

Gilliham, M. and S. D. Tyerman. Linking Metabolism to Membrane Signaling: The GABA-Malate Connection. *Trends in plant science* **21**, 295-301, doi:10.1016/j.tplants.2015.11.011 (2016).

Gleave, A. P. A versatile binary vector system with a T-DNA organisational structure conducive to efficient integration of cloned DNA into the plant genome. *Plant molecular biology* **20**, 1203-1207 (1992).

Görlach, A., K. Bertram, S. Hudecova and O. Krizanova. Calcium and ROS: a mutual interplay. *Redox Biology* **6**, 260-271 (2015).

Grallath, S., T. Weimar, A. Meyer, C. Gumy, M. Suter-Grotemeyer, J.-M. Neuhaus and D. Rentsch. The AtProT family. Compatible solute transporters with similar substrate specificity but differential expression patterns. *Plant Physiology* **137**, 117-126 (2005).

Gruber, B. D., E. Delhaize, A. E. Richardson, U. Roessner, R. A. James, S. M. Howitt and P. R. Ryan. Characterisation of HvALMT1 function in transgenic barley plants. *Functional Plant Biology* **38**, 163-175 (2011).

Grundy, J., C. Stoker and I. A. Carré. Circadian regulation of abiotic stress tolerance in plants. *Frontiers in plant science* **6**, 648 (2015).

Gutermuth, T., S. Herbell, R. Lassig, M. Brosché, T. Romeis, J. A. Feijó, R. Hedrich and K. R. Konrad. Tip-localized Ca^{2+}-permeable channels control pollen tube growth via kinase-dependent R-and S-type anion channel regulation. *new phytologist* **218**, 1089-1105 (2018).

Halliwell, B. and M. Whiteman. Measuring reactive species and oxidative damage in vivo and in cell culture: how should you do it and what do the results mean? *British Journal of Pharmacology* **142**, 231-255 (2004).

Harrison, S. J., E. K. Mott, K. Parsley, S. Aspinall, J. C. Gray and A. Cottage. A rapid and robust method of identifying transformed *Arabidopsis thaliana* seedlings following floral dip transformation. *Plant Methods* **2**, 1-7 (2006).

Hassidim, M., Y. Dakhiya, A. Turjeman, D. Hussien, E. Shor, A. Anidjar, K. Goldberg and R. M. Green. CIRCADIAN CLOCK ASSOCIATED1 (CCA1) and the circadian control of stomatal aperture. *Plant Physiology* **175**, 1864-1877 (2017).

Henry, L. K., J. Meiler and R. D. Blakely. Bound to be different: Neurotransmitter transporters meet their bacterial cousins. *Molecular Interventions* **7**, 306-309, doi:10.1124/mi.7.6.4 (2007).

Herbell, S., T. Gutermuth and K. R. Konrad. An interconnection between tip-focused Ca^{2+} and anion homeostasis controls pollen tube growth. *Plant signaling & behavior* **13**, e1529521 (2018).

Hijaz, F., Y. Nehela and N. Killiny. Application of gamma-aminobutyric acid increased the level of phytohormones in *Citrus sinensis*. *Planta* **248**, 909-918 (2018).

Hijaz, F. and N. Killiny. Exogenous GABA is quickly metabolized to succinic acid and fed into the plant TCA cycle. *Plant signaling & behavior* **14**, e1573096 (2019).

Hoekenga, O. A., L. G. Maron, M. A. Piñeros, G. M. Cançado, J. Shaff, Y. Kobayashi, P. R. Ryan, B. Dong, E. Delhaize and T. Sasaki. *AtALMT1*, which encodes a malate transporter, is identified as one of several genes critical for aluminum tolerance in Arabidopsis. *Proceedings of the National Academy of Sciences* **103**, 9738-9743 (2006).

Höfgen, R. and L. Willmitzer. Storage of competent cells for *Agrobacterium* transformation. *Nucleic Acids Research* **16**, 9877 (1988).

Hosy, E., A. Vavasseur, K. Mouline, I. Dreyer, F. Gaymard, F. Porée, J. Boucherez, A. Lebaudy, D. Bouchez and A.-A. Véry. The Arabidopsis outward K+ channel GORK is involved in regulation of stomatal movements and plant transpiration. *Proceedings of the National Academy of Sciences* **100**, 5549-5554 (2003).

Hsu, P. K., G. Dubeaux, Y. Takahashi and J. I. Schroeder. Signaling mechanisms in abscisic acid-mediated stomatal closure. *The Plant Journal* **105**, 307-321 (2021).

Huang, H., F. Ullah, D.-X. Zhou, M. Yi and Y. Zhao. Mechanisms of ROS regulation of plant development and stress responses. *Frontiers in plant science* **10**, 800 (2019).

Huang, J., H. Yu, A. Dai, Y. Wei and L. Kang. Drylands face potential threat under 2 C global warming target. *Nature climate change* **7**, 417-422 (2017).

Iqbal, Z., M. S. Iqbal, S. P. Singh and T. Buaboocha. Ca^{2+}/calmodulin complex triggers CAMTA transcriptional machinery under stress in plants: signaling cascade and molecular regulation. *Frontiers in plant science* **11** (2020).

Jakab, G., J. Ton, V. Flors, L. Zimmerli, J.-P. Métraux and B. Mauch-Mani. Enhancing *Arabidopsis* salt and drought stress tolerance by chemical priming for its abscisic acid responses. *Plant Physiology* **139**, 267-274 (2005).

Jalil, S. U., I. Ahmad and M. I. Ansari. Functional loss of GABA transaminase (GABA-T) expressed early leaf senescence under various stress conditions in *Arabidopsis thaliana*. *Current Plant Biology* **9**, 11-22 (2017).

Jalil, S. U., M. I. R. Khan and M. I. Ansari. Role of GABA transaminase in the regulation of development and senescence in *Arabidopsis thaliana*. *Current Plant Biology* **19**, 100119 (2019).

Jammes, F., C. Song, D. Shin, S. Munemasa, K. Takeda, D. Gu, D. Cho, S. Lee, R. Giordo and S. Sritubtim. MAP kinases *MPK9* and *MPK12* are preferentially expressed in guard cells and positively regulate ROS-mediated ABA signaling. *Proceedings of the National Academy of Sciences* **106**, 20520-20525 (2009).

Jezek, M. and M. R. Blatt. The membrane transport system of the guard cell and its integration for stomatal dynamics. *Plant Physiology* **174**, 487-519 (2017).

Jia, W. and W. J. Davies. Modification of leaf apoplastic pH in relation to stomatal sensitivity to root-sourced abscisic acid signals. *Plant Physiology* **143**, 68-77 (2007).

Jin, X., T. Liu, J. Xu, Z. Gao and X. Hu. Exogenous GABA enhances muskmelon tolerance to salinity-alkalinity stress by regulating redox balance and chlorophyll biosynthesis. *BMC Plant Biology* **19**, 1-15 (2019).

Kader, M. A. and S. Lindberg. Cytosolic calcium and pH signaling in plants under salinity stress. *Plant signaling & behavior* **5**, 233-238 (2010).

Kamigaki, A., K. Nito, K. Hikino, S. Goto-Yamada, M. Nishimura, T. Nakagawa and S. Mano. Gateway vectors for simultaneous detection of multiple protein− protein interactions in plant cells using bimolecular fluorescence complementation. *PLoS One* **11**, e0160717 (2016).

Kamran, M., S. A. Ramesh, M. Gilliham, S. D. Tyerman and J. Bose. Role of TaALMT1 malate‐GABA transporter in alkaline pH tolerance of wheat. *Plant, cell & environment* **43**, 2443-2459 (2020).

Kanehisa, M. and S. Goto. KEGG: kyoto encyclopedia of genes and genomes. *Nucleic Acids Research* **28**, 27-30 (2000).

Kanehisa, M. Toward understanding the origin and evolution of cellular organisms. *Protein Science* **28**, 1947-1951 (2019).

Kanehisa, M., M. Furumichi, Y. Sato, M. Ishiguro-Watanabe and M. Tanabe. KEGG: integrating viruses and cellular organisms. *Nucleic Acids Research* **49**, D545-D551 (2021).

Katoh, K. and D. M. Standley. MAFFT multiple sequence alignment software version 7: improvements in performance and usability. *Molecular Biology and Evolution* **30**, 772-780 (2013).

Kaur, G. and B. Asthir. Molecular responses to drought stress in plants. *Biologia Plantarum* **61**, 201-209 (2017).

Kollist, H., M. Nuhkat and M. R. G. Roelfsema. Closing gaps: linking elements that control stomatal movement. *new phytologist* **203**, 44-62, doi:10.1111/nph.12832 (2014).

Kong, D., H.-C. Hu, E. Okuma, Y. Lee, H. S. Lee, S. Munemasa, D. Cho, C. Ju, L. Pedoeim and B. Rodriguez. L-Met activates *Arabidopsis* GLR Ca^{2+} channels upstream of ROS production and regulates stomatal movement. *Cell reports* **17**, 2553-2561 (2016).

Kumar, M., M. S. Kesawat, A. Ali, S.-C. Lee, S. S. Gill and H. U. Kim. Integration of abscisic acid signaling with other signaling pathways in plant stress responses and development. *Plants* **8**, 592 (2019).

Lager, I., O. Andréasson, T. L. Dunbar, E. Andreasson, M. A. Escobar and A. G. Rasmusson. Changes in external pH rapidly alter plant gene expression and modulate auxin and elicitor responses. *Plant, cell & environment* **33**, 1513-1528 (2010).

Lai, A. G., C. J. Doherty, B. Mueller-Roeber, S. A. Kay, J. H. Schippers and P. P. Dijkwel. CIRCADIAN CLOCK-ASSOCIATED 1 regulates ROS homeostasis and oxidative stress responses. *Proceedings of the National Academy of Sciences* **109**, 17129-17134 (2012).

Lancien, M. and M. R. Roberts. Regulation of *Arabidopsis thaliana* 14-3-3 gene expression by gamma-aminobutyric acid. *Plant Cell and Environment* **29**, 1430-1436, doi:DOI 10.1111/j.1365-3040.2006.01526.x (2006).

Lawson, T. and J. Matthews. Guard cell metabolism and stomatal function. *Annual Review of Plant Biology* **71**, 273-302 (2020).

Lee, J., S. Kim, S. Kim and I.-S. Shim. Production of γ-Aminobutyric Acid and Its Supplementary Role in the TCA Cycle in Rice (*Oryza sativa L.*) Seedlings. *Journal of Plant Growth Regulation*, 1-13 (2020).

Lemordant, L., P. Gentine, A. S. Swann, B. I. Cook and J. Scheff. Critical impact of vegetation physiology on the continental hydrologic cycle in response to increasing CO2. *Proceedings of the National Academy of Sciences* **115**, 4093-4098 (2018).

Leonhardt, N., J. M. Kwak, N. Robert, D. Waner, G. Leonhardt and J. I. Schroeder. Microarray expression analyses of *Arabidopsis* guard cells and isolation of a recessive abscisic acid hypersensitive protein phosphatase 2C mutant. *The Plant Cell* **16**, 596-615, doi:10.1105/tpc.019000 (2004).

Li, K., J. Prada, D. S. Damineli, A. Liese, T. Romeis, T. Dandekar, J. A. Feijó, R. Hedrich and K. R. Konrad. An optimized genetically encoded dual reporter for simultaneous ratio imaging of Ca^{2+} and H^{+} reveals new insights into ion signaling in plants. *new phytologist* (2021).

Li, R., R. Li, X. Li, D. Fu, B. Zhu, H. Tian, Y. Luo and H. Zhu. Multiplexed CRISPR/Cas9-mediated metabolic engineering of γ-aminobutyric acid levels in *Solanum lycopersicum*. *Plant Biotechnology Journal* **16**, 415-427 (2018).

Li, W., A. Cowley, M. Uludag, T. Gur, H. McWilliam, S. Squizzato, Y. M. Park, N. Buso and R. Lopez. The EMBL-EBI bioinformatics web and programmatic tools framework. *Nucleic Acids Research* **43**, W580-W584 (2015).

Li, W., J. Liu, U. Ashraf, G. Li, Y. Li, W. Lu, L. Gao, F. Han and J. Hu. Exogenous γ-aminobutyric acid (GABA) application improved early growth, net photosynthesis, and associated physio-biochemical events in maize. *Frontiers in plant science* **7**, 919 (2016).

Li, Z., J. Yu, Y. Peng and B. Huang. Metabolic pathways regulated by γ-aminobutyric acid (GABA) contributing to heat tolerance in creeping bentgrass (*Agrostis stolonifera*). *Scientific reports* **6**, 1-16 (2016).

Li, Z., J. Yu, Y. Peng and B. Huang. Metabolic pathways regulated by abscisic acid, salicylic acid and γ-aminobutyric acid in association with improved drought tolerance in creeping bentgrass (*Agrostis stolonifera*). *Physiologia Plantarum* **159**, 42-58 (2017).

Li, Z., T. Huang, M. Tang, B. Cheng, Y. Peng and X. Zhang. iTRAQ-based proteomics reveals key role of γ-aminobutyric acid (GABA) in regulating drought tolerance in perennial creeping bentgrass (*Agrostis stolonifera*). *Plant Physiology & Biochemistry* **145**, 216-226 (2019).

Li, Z., B. Cheng, W. Zeng, X. Zhang and Y. Peng. Proteomic and metabolomic profilings reveal crucial functions of γ-aminobutyric acid in regulating ionic, water, and metabolic homeostasis in creeping bentgrass under salt stress. *Journal of proteome research* **19**, 769-780 (2020).

Liu, J. and M. Zhou. The *ALMT* gene family performs multiple functions in plants. *Agronomy* **8**, 20 (2018).

Liu, S., Z. Lv, Y. Liu, L. Li and L. Zhang. Network analysis of ABA-dependent and ABA-independent drought responsive genes in *Arabidopsis thaliana*. *Genetics Molecular Biology Reports* **41**, 624-637 (2018).

Liu, Y., X. Ji, L. Zheng, X. Nie and Y. Wang. Microarray analysis of transcriptional responses to abscisic acid and salt stress in *Arabidopsis thaliana*. *International journal of molecular sciences* **14**, 9979-9998 (2013).

Locy, R., S. Wu, J. Bisnette, T. Barger, D. McNabb, M. Zik, H. Fromm, N. Singh and J. Cherry (2000). The regulation of GABA accumulation by heat stress in *Arabidopsis*. Plant tolerance to abiotic stresses in agriculture: Role of genetic engineering, Springer**:** 39-52.

Long, Y., S. D. Tyerman and M. Gilliham. Cytosolic GABA inhibits anion transport by wheat ALMT1. *new phytologist* **225**, 671-678 (2020).

Lu, Y. Extract genomic DNA from *Arabidopsis* leaves (can be used for other tissues as well). *Bio-protocol*, e90-e90 (2011).

Luu, K., N. Rajagopalan, J. C. Ching, M. C. Loewen and M. E. Loewen. The malate-activated ALMT12 anion channel in the grass *Brachypodium distachyon* is co-activated by Ca^{2+}/calmodulin. *Journal of Biological Chemistry* **294**, 6142-6156 (2019).

Lv, X., H. Li, X. Chen, X. Xiang, Z. Guo, J. Yu and Y. Zhou. The role of calcium-dependent protein kinase in hydrogen peroxide, nitric oxide and ABA-dependent cold acclimation. *Journal of experimental botany* **69**, 4127-4139 (2018).

Ma, Y., J. Cao, J. He, Q. Chen, X. Li and Y. Yang. Molecular mechanism for the regulation of ABA homeostasis during plant development and stress responses. *International journal of molecular sciences* **19**, 3643 (2018).

Maia, J., B. J. Dekkers, N. J. Provart, W. Ligterink and H. W. Hilhorst. The re-establishment of desiccation tolerance in germinated *Arabidopsis thaliana* seeds and its associated transcriptome. *PLoS One* **6**, e29123 (2011).

Malcheska, F., A. Ahmad, S. Batool, H. M. Müller, J. Ludwig-Müller, J. Kreuzwieser, D. Randewig, R. Hänsch, R. R. Mendel and R. Hell. Drought-enhanced xylem sap sulfate closes stomata by affecting ALMT12 and guard cell ABA synthesis. *Plant Physiology* **174**, 798-814 (2017).

Mano, H. and M. Hasebe. Rapid movements in plants. *Journal of plant research* **134**, 3-17 (2021).

Martinière, A., R. Gibrat, H. Sentenac, X. Dumont, I. Gaillard and N. Paris. Uncovering pH at both sides of the root plasma membrane interface using noninvasive imaging. *Proceedings of the National Academy of Sciences* **115**, 6488-6493 (2018).

Maruta, T., M. Ojiri, M. Noshi, M. Tamoi, T. Ishikawa and S. Shigeoka. Activation of γ-aminobutyrate production by chloroplastic H_2O_2 is associated with the oxidative stress response. *Bioscience, Biotechnology, and Biochemistry* **77**, 422-425 (2013).

Marvin, J. S., Y. Shimoda, V. Magloire, M. Leite, T. Kawashima, T. P. Jensen, I. Kolb, E. L. Knott, O. Novak and K. Podgorski. A genetically encoded fluorescent sensor for in vivo imaging of GABA. *Nature methods* **16**, 763-770 (2019).

Matthews, J. S., S. R. Vialet-Chabrand and T. Lawson. Diurnal variation in gas exchange: the balance between carbon fixation and water loss. *Plant Physiology* **174**, 614-623 (2017).

Matthews, J. S., S. Vialet-Chabrand and T. Lawson. Role of blue and red light in stomatal dynamic behaviour. *Journal of experimental botany* **71**, 2253-2269 (2020).

McAdam, S. A. and T. J. Brodribb. Mesophyll cells are the main site of abscisic acid biosynthesis in water-stressed leaves. *Plant Physiology* **177**, 911-917 (2018).

McWilliam, H., W. Li, M. Uludag, S. Squizzato, Y. M. Park, N. Buso, A. P. Cowley and R. Lopez. Analysis tool web services from the EMBL-EBI. *Nucleic Acids Research* **41**, W597-W600 (2013).

Medeiros, D. B., L. Perez Souza, W. C. Antunes, W. L. Araújo, D. M. Daloso and A. R. Fernie. Sucrose breakdown within guard cells provides substrates for glycolysis and glutamine biosynthesis during light‐induced stomatal opening. *The Plant Journal* **94**, 583-594 (2018).

Medeiros, D. B., J. A. Barros, A. R. Fernie and W. L. Araújo. Eating away at ROS to regulate stomatal opening. *Trends in plant science* **25**, 220-223 (2020).

Mekonnen, D. W., U.-I. Flügge and F. Ludewig. Gamma-aminobutyric acid depletion affects stomata closure and drought tolerance of *Arabidopsis thaliana*. *Plant Science* **245**, 25-34 (2016).

Mekonnen, D. W. Oversensitivity of *Arabidopsis gad1/2* mutant to NaCl treatment reveals the importance of GABA in salt stress responses. *African Journal of Plant Science* **11**, 252-263 (2017).

Meyer, A., S. Eskandari, S. Grallath and D. Rentsch. AtGAT1, a high affinity transporter for γ-aminobutyric acid in *Arabidopsis thaliana*. *Journal of Biological Chemistry* **281**, 7197-7204 (2006).

Meyer, S., P. Mumm, D. Imes, A. Endler, B. Weder, K. A. S. Al-Rasheid, D. Geiger, I. Marten, E. Martinoia and R. Hedrich. AtALMT12 represents an R-type anion channel required for stomatal movement in *Arabidopsis* guard cells. *The Plant Journal* **63**, 1054-1062, doi:10.1111/j.1365-313X.2010.04302.x (2010).

Meyer, S., J. Scholz-Starke, A. De Angeli, P. Kovermann, B. Burla, F. Gambale and E. Martinoia. Malate transport by the vacuolar AtALMT6 channel in guard cells is subject to multiple regulation. *The Plant Journal* **67**, 247-257, doi:10.1111/j.1365-313X.2011.04587.x (2011).

Miao, R., W. Yuan, Y. Wang, I. Garcia-Maquilon, X. Dang, Y. Li, J. Zhang, Y. Zhu, P. L. Rodriguez and W. Xu. Low ABA concentration promotes root growth and hydrotropism through relief of ABA INSENSITIVE 1-mediated inhibition of plasma membrane H^+-ATPase 2. *Science Advances* **7**, eabd4113 (2021).

Michael, T. P., G. Breton, S. P. Hazen, H. Priest, T. C. Mockler, S. A. Kay and J. Chory. A morning-specific phytohormone gene expression program underlying rhythmic plant growth. *PLoS Biol* **6**, e225 (2008a).

Michael, T. P., T. C. Mockler, G. Breton, C. McEntee, A. Byer, J. D. Trout, S. P. Hazen, R. Shen, H. D. Priest and C. M. Sullivan. Network discovery pipeline elucidates conserved time-of-day–specific cis-regulatory modules. *PLoS Genet* **4**, e14 (2008b).

Michaeli, S., A. Fait, K. Lagor, A. Nunes-Nesi, N. Grillich, A. Yellin, D. Bar, M. Khan, A. R. Fernie and F. J. Turano. A mitochondrial GABA permease connects the GABA shunt and the TCA cycle, and is essential for normal carbon metabolism. *The Plant Journal* **67**, 485-498 (2011).

Misra, B. B., S. M. Assmann and S. Chen. Plant single-cell and single-cell-type metabolomics. *Trends in plant science* **19**, 637-646 (2014).

Missihoun, T. D., E. Willée, J.-P. Guegan, S. Berardocco, M. R. Shafiq, A. Bouchereau and D. Bartels. Overexpression of ALDH10A8 and ALDH10A9 genes provides insight into their role in glycine betaine synthesis and affects primary metabolism in *Arabidopsis thaliana*. *Plant Cell Physiology* **56**, 1798-1807 (2015).

Miura, K., M. Ikeda, A. Matsubara, X.-J. Song, M. Ito, K. Asano, M. Matsuoka, H. Kitano and M. Ashikari. OsSPL14 promotes panicle branching and higher grain productivity in rice. *Nature Genetics* **42**, 545-549 (2010).

Miyashita, Y., R. Dolferus, K. P. Ismond and A. G. Good. Alanine aminotransferase catalyses the breakdown of alanine after hypoxia in *Arabidopsis thaliana*. *The Plant Journal* **49**, 1108-1121 (2007).

Miyashita, Y. and A. G. Good. Contribution of the GABA shunt to hypoxia-induced alanine accumulation in roots of *Arabidopsis thaliana*. *Plant and Cell Physiology* **49**, 92-102, doi:10.1093/pcp/pcm171 (2008).

Nicotra, A. B., O. K. Atkin, S. P. Bonser, A. M. Davidson, E. J. Finnegan, U. Mathesius, P. Poot, M. D. Purugganan, C. L. Richards and F. Valladares. Plant phenotypic plasticity in a changing climate. *Trends in plant science* **15**, 684-692 (2010).

Oparka, K. J. and A. G. Roberts. Plasmodesmata. A not so open-and-shut case. *Plant Physiology* **125**, 123-126 (2001).

Pandey, S., R. S. Wang, L. Wilson, S. Li, Z. Zhao, T. E. Gookin, S. M. Assmann and R. Albert. Boolean modeling of transcriptome data reveals novel modes of heterotrimeric G-protein action. *Molecular systems biology* **6**, 372 (2010).

Pantin, F., J. Renaud, F. Barbier, A. Vavasseur, D. Le Thiec, C. Rose, T. Bariac, S. Casson, D. H. McLachlan and A. M. Hetherington. Developmental priming of stomatal sensitivity to abscisic acid by leaf microclimate. *Current Biology* **23**, 1805-1811 (2013).

Park, D. H., R. Mirabella, P. A. Bronstein, G. M. Preston, M. A. Haring, C. K. Lim, A. Collmer and R. C. Schuurink. Mutations in γ-aminobutyric acid (GABA) transaminase genes in

plants or *Pseudomonas syringae* reduce bacterial virulence. *The Plant Journal* **64**, 318-330 (2010).

Pelvan, A., M. Bor, S. Yolcu, F. Özdemir and I. Türkan. Day and Night Fluctuations in GABA Biosynthesis Contribute to Drought Responses in *Nicotiana tabacum L*. *Plant signaling & behavior*, 1899672 (2021).

Priya, M., L. Sharma, R. Kaur, H. Bindumadhava, R. M. Nair, K. Siddique and H. Nayyar. GABA (γ-aminobutyric acid), as a thermo-protectant, to improve the reproductive function of heat-stressed mungbean plants. *Scientific reports* **9**, 1-14 (2019).

Prokic, L., Z. Jovanovic, M. R. McAinsh, Z. Vucinic and R. Stikic. Species-dependent changes in stomatal sensitivity to abscisic acid mediated by external pH. *Journal of experimental botany* **57**, 675-683 (2006).

Qu, X., B. Cao, J. Kang, X. Wang, X. Han, W. Jiang, X. Shi, L. Zhang, L. Cui and Z. Hu. Fine-tuning stomatal movement through small signaling peptides. *Frontiers in plant science* **10**, 69 (2019).

Ramesh, S. A., S. D. Tyerman, B. Xu, J. Bose, S. Kaur, V. Conn, P. Domingos, S. Ullah, S. Wege, S. Shabala, J. A. Feijo, P. R. Ryan and M. Gilliham. GABA signalling modulates plant growth by directly regulating the activity of plant-specific anion transporters. *Nature communications* **6**, 7879, doi:Artn 8293

10.1038/Ncomms9293 (2015).

Ramesh, S. A., S. D. Tyerman, M. Gilliham and B. Xu. γ-Aminobutyric acid (GABA) signalling in plants. *Cellular Molecular Life Sciences* **74**, 1577-1603 (2017).

Ramesh, S. A., M. Kamran, W. Sullivan, L. Chirkova, M. Okamoto, F. Degryse, M. McLaughlin, M. Gilliham and S. D. Tyerman. Aluminum-activated malate transporters can facilitate GABA transport. *The Plant Cell* **30**, 1147-1164 (2018).

Renault, H., V. Roussel, A. El Amrani, M. Arzel, D. Renault, A. Bouchereau and C. Deleu. The *Arabidopsis* pop2-1 mutant reveals the involvement of GABA transaminase in salt stress tolerance. *BMC Plant Biology* **10**, 20 (2010).

Renault, H., A. El Amrani, R. Palanivelu, E. P. Updegraff, A. Yu, J.-P. Renou, D. Preuss, A. Bouchereau and C. Deleu. GABA accumulation causes cell elongation defects and a decrease in expression of genes encoding secreted and cell wall-related proteins in *Arabidopsis thaliana*. *Plant Cell Physiology* **52**, 894-908 (2011).

Renault, H., A. El Amrani, A. Berger, G. Mouille, L. SOUBIGOU - TACONNAT, A. Bouchereau and C. Deleu. γ-Aminobutyric acid transaminase deficiency impairs central carbon metabolism and leads to cell wall defects during salt stress in *Arabidopsis* roots. *Plant, cell & environment* **36**, 1009-1018 (2013).

Ritz, C. and J. C. Streibig (2008). Nonlinear regression with R, Springer Science & Business Media.

Rivero, L., R. Scholl, N. Holomuzki, D. Crist, E. Grotewold and J. Brkljacic (2014). Handling *Arabidopsis* plants: growth, preservation of seeds, transformation, and genetic crosses. Arabidopsis protocols, Springer**:** 3-25.

Safavi-Rizi, V., M. Herde and C. Stöhr. RNA-Seq reveals novel genes and pathways associated with hypoxia duration and tolerance in tomato root. *Scientific reports* **10**, 1-17 (2020).

Salah, A., M. Zhan, C. Cao, Y. Han, L. Ling, Z. Liu, P. Li, M. Ye and Y. Jiang. γ-Aminobutyric acid promotes chloroplast ultrastructure, antioxidant capacity, and growth of waterlogged maize seedlings. *Scientific reports* **9**, 1-19 (2019).

Santelia, D. and J. E. Lunn. Transitory starch metabolism in guard cells: unique features for a unique function. *Plant Physiology*, pp. 00211.02017 (2017).

Sasaki, T., Y. Yamamoto, B. Ezaki, M. Katsuhara, S. J. Ahn, P. R. Ryan, E. Delhaize and H. Matsumoto. A wheat gene encoding an aluminum-activated malate transporter. *The Plant Journal* **37**, 645-653 (2004).

Sasaki, T., I. C. Mori, T. Furuichi, S. Munemasa, K. Toyooka, K. Matsuoka, Y. Murata and Y. Yamamoto. Closing Plant Stomata Requires a Homolog of an Aluminum-Activated Malate Transporter. *Plant and Cell Physiology* **51**, 354-365, doi:10.1093/pcp/pcq016 (2010).

Sasaki, T., Y. Tsuchiya, M. Ariyoshi, R. Nakano, K. Ushijima, Y. Kubo, I. C. Mori, E. Higashiizumi, I. Galis and Y. Yamamoto. Two members of the aluminum-activated malate transporter family, SlALMT4 and SlALMT5, are expressed during fruit development, and the overexpression of SlALMT5 alters organic acid contents in seeds in tomato (*Solanum lycopersicum*). *Plant Cell Physiology* **57**, 2367-2379 (2016).

Sato, H., H. Takasaki, F. Takahashi, T. Suzuki, S. Iuchi, N. Mitsuda, M. Ohme-Takagi, M. Ikeda, M. Seo and K. Yamaguchi-Shinozaki. *Arabidopsis thaliana* NGATHA1 transcription factor induces ABA biosynthesis by activating NCED3 gene during dehydration stress. *Proceedings of the National Academy of Sciences* **115**, E11178-E11187 (2018).

Scala, A. (2015). The role of E-2-hexenal and γ-amino butyric acid in plant defense responses. Phd, University of Amsterdam.

Schmid, M., T. S. Davison, S. R. Henz, U. J. Pape, M. Demar, M. Vingron, B. Schölkopf, D. Weigel and J. U. Lohmann. A gene expression map of *Arabidopsis thaliana* development. *Nature Genetics* **37**, 501-506 (2005).

Scholz, S. S., M. Reichelt, D. W. Mekonnen, F. Ludewig and A. Mithöfer. Insect herbivory-elicited GABA accumulation in plants is a wound-induced, direct, systemic, and jasmonate-independent defense response. *Frontiers in plant science* **6** (2015).

Scholz, S. S., J. Malabarba, M. Reichelt, M. Heyer, F. Ludewig and A. Mithöfer. Evidence for GABA-induced systemic GABA accumulation in *Arabidopsis* upon wounding. *Frontiers in plant science* **8**, 388 (2017).

Sehgal, A., K. Sita, K. H. Siddique, R. Kumar, S. Bhogireddy, R. K. Varshney, B. HanumanthaRao, R. M. Nair, P. Prasad and H. Nayyar. Drought or/and heat-stress effects on seed filling in food crops: impacts on functional biochemistry, seed yields, and nutritional quality. *Frontiers in plant science* **9**, 1705 (2018).

Sharma, T., I. Dreyer, L. Kochian and M. A. Piñeros. The ALMT family of organic acid transporters in plants and their involvement in detoxification and nutrient security. *Frontiers in plant science* **7**, 1488 (2016).

Shelp, B. J., A. W. Bown and D. Faure. Extracellular γ-aminobutyrate mediates communication between plants and other organisms. *Plant Physiology* **142**, 1350-1352 (2006).

Shelp, B. J., G. G. Bozzo, C. P. Trobacher, A. Zarei, K. L. Deyman and C. J. Brikis. Hypothesis/review: Contribution of putrescine to 4-aminobutyrate (GABA) production in response to abiotic stress. *Plant Science* **193**, 130-135, doi:10.1016/j.plantsci.2012.06.001 (2012).

Shelp, B. J. and A. Zarei. Subcellular compartmentation of 4-aminobutyrate (GABA) metabolism in *Arabidopsis*: An update. *Plant signaling & behavior* **12**, e1322244 (2017).

Shen, J., Y. Zeng, X. Zhuang, L. Sun, X. Yao, P. Pimpl and L. Jiang. Organelle pH in the *Arabidopsis* endomembrane system. *Molecular plant* **6**, 1419-1437 (2013).

Shi, S. Q., Z. Shi, Z. P. JIANG, L. W. QI, X. M. SUN, C. X. LI, J. F. LIU, W. F. XIAO and S. G. ZHANG. Effects of exogenous GABA on gene expression of *Caragana* intermedia roots under NaCl stress: regulatory roles for H2O2 and ethylene production. *Plant, cell & environment* **33**, 149-162 (2010).

Shimono, M., T. Higaki, H. Kaku, N. Shibuya, S. Hasezawa and B. Day. Quantitative evaluation of stomatal cytoskeletal patterns during the activation of immune signaling in *Arabidopsis thaliana*. *PLoS One* **11**, e0159291 (2016).

Signorelli, S., P. D. Dans, E. L. Coitiño, O. Borsani and J. Monza. Connecting proline and γ-aminobutyric acid in stressed plants through non-enzymatic reactions. *PLoS One* **10**, e0115349 (2015).

Singh, R., P. Parihar, S. Singh, R. K. Mishra, V. P. Singh and S. M. Prasad. Reactive oxygen species signaling and stomatal movement: current updates and future perspectives. *Redox Biology* **11**, 213-218 (2017).

Söderman, E. M., I. M. Brocard, T. J. Lynch and R. R. Finkelstein. Regulation and function of the *Arabidopsis* ABA-insensitive4 gene in seed and abscisic acid response signaling networks. *Plant Physiology* **124**, 1752-1765 (2000).

Song, S.-J., Q.-N. Feng, C.-L. Li, E. Li, Q. Liu, H. Kang, W. Zhang, Y. Zhang and S. Li. A tonoplast-associated calcium-signaling module dampens ABA signaling during stomatal movement. *Plant Physiology* **177**, 1666-1678 (2018).

Soon, F.-F., L.-M. Ng, X. E. Zhou, G. M. West, A. Kovach, M. E. Tan, K. M. Suino-Powell, Y. He, Y. Xu and M. J. Chalmers. Molecular mimicry regulates ABA signaling by SnRK2 kinases and PP2C phosphatases. *Science* **335**, 85-88 (2012).

Studart-Guimarães, C., A. Fait, A. Nunes-Nesi, F. Carrari, B. Usadel and A. R. Fernie. Reduced expression of succinyl-coenzyme A ligase can be compensated for by up-regulation of the γ-aminobutyrate shunt in illuminated tomato leaves. *Plant Physiology* **145**, 626-639 (2007).

Su, N., Q. Wu, J. Chen, L. Shabala, A. Mithöfer, H. Wang, M. Qu, M. Yu, J. Cui and S. Shabala. GABA operates upstream of H^+-ATPase and improves salinity tolerance in *Arabidopsis* by enabling cytosolic K^+ retention and Na^+ exclusion. *Journal of experimental botany* **70**, 6349-6361 (2019).

Sussmilch, F. C., J. Schultz, R. Hedrich and M. R. G. Roelfsema. Acquiring control: the evolution of stomatal signalling pathways. *Trends in plant science* **24**, 342-351 (2019).

Takahashi, F., T. Kuromori, K. Urano, K. Yamaguchi-Shinozaki and K. Shinozaki. Drought stress responses and resistance in plants: From cellular responses to long-distance intercellular communication. *Frontiers in plant science* **11**, 1407 (2020).

Terasaki, M., R. Kamata, F. Shiraishi and M. Makino. Evaluation of estrogenic activity of parabens and their chlorinated derivatives by using the yeast two-hybrid assay and the enzyme-linked immunosorbent assay. *Environmental Toxicology Chemistry* **28**, 204-208 (2009).

Thomson, G., J. Taylor and J. Putterill. The transcriptomic response to a short day to long day shift in leaves of the reference legume *Medicago truncatula*. *Peer Journal* **7**, e6626 (2019).

Tokarska, K. B., M. B. Stolpe, S. Sippel, E. M. Fischer, C. J. Smith, F. Lehner and R. Knutti. Past warming trend constrains future warming in CMIP6 models. *Science Advances* **6**, eaaz9549 (2020).

Tripathy, B. C. and R. Oelmüller. Reactive oxygen species generation and signaling in plants. *Plant signaling & behavior* **7**, 1621-1633 (2012).

Trobacher, C. P., A. Zarei, J. Liu, S. M. Clark, G. G. Bozzo and B. J. Shelp. Calmodulin-dependent and calmodulin-independent glutamate decarboxylases in apple fruit. *BMC Plant Biology* **13**, 144 (2013).

Urano, K., K. Maruyama, Y. Ogata, Y. Morishita, M. Takeda, N. Sakurai, H. Suzuki, K. Saito, D. Shibata and M. Kobayashi. Characterization of the ABA-regulated global responses to dehydration in *Arabidopsis* by metabolomics. *The Plant Journal* **57**, 1065-1078 (2009).

Vicente-Serrano, S. M., R. Nieto, L. Gimeno, C. Azorin-Molina, A. Drumond, A. E. Kenawy, F. Dominguez-Castro, M. Tomas-Burguera and M. Peña-Gallardo. Recent changes of

relative humidity: Regional connections with land and ocean processes. *Earth System Dynamics* **9**, 915-937 (2018).

Vishwakarma, K., N. Upadhyay, N. Kumar, G. Yadav, J. Singh, R. K. Mishra, V. Kumar, R. Verma, R. Upadhyay and M. Pandey. Abscisic acid signaling and abiotic stress tolerance in plants: a review on current knowledge and future prospects. *Frontiers in Plant Science*

8, 161 (2017).

Waese, J. and N. J. Provart (2017). The bio-analytic resource for plant biology. Plant Genomics Databases, Springer**:** 119-148.

Wang, Y., W. Gu, Y. Meng, T. Xie, L. Li, J. Li and S. Wei. γ-Aminobutyric acid imparts partial protection from salt stress injury to maize seedlings by improving photosynthesis and upregulating osmoprotectants and antioxidants. *Scientific reports* **7**, 1-13 (2017).

Woody, S. T., S. Austin-Phillips, R. M. Amasino and P. J. Krysan. The WiscDsLox T-DNA collection: an *Arabidopsis* community resource generated by using an improved high-throughput T-DNA sequencing pipeline. *Journal of plant research* **120**, 157-165 (2007).

Wrzaczek, M., M. Brosché and J. Kangasjärvi. ROS signaling loops—production, perception, regulation. *Current opinion in plant biology* **16**, 575-582 (2013).

Wu, X., Q. Jia, S. Ji, B. Gong, J. Li, G. Lü and H. Gao. Gamma-aminobutyric acid (GABA) alleviates salt damage in tomato by modulating Na^+ uptake, the GAD gene, amino acid synthesis and reactive oxygen species metabolism. *BMC plant biology* **20**, 1-21 (2020).

Xiang, Q., A. A. Lott, S. M. Assmann and S. Chen. Advances and perspectives in the metabolomics of stomatal movement and the disease triangle. *Plant Science*, 110697 (2020).

Xiong, L. and J.-K. Zhu. Regulation of abscisic acid biosynthesis. *Plant Physiology* **133**, 29-36 (2003).

Xu, B., Y. Long, X. Feng, X. Zhu, N. Sai, L. Chirkova, J. Herrmann, M. Okamoto, R. Hedrich and M. Gilliham. GABA signalling in guard cells acts as a'stress memory'to optimise plant water loss. *bioRxiv* (2021).

Yang, Y., A. Costa, N. Leonhardt, R. S. Siegel and J. I. Schroeder. Isolation of a strong *Arabidopsis* guard cell promoter and its potential as a research tool. *Plant Methods* **4**, 6 (2008).

Yong, B., H. Xie, Z. Li, Y.-P. Li, Y. Zhang, G. Nie, X.-Q. Zhang, X. Ma, L.-K. Huang and Y.-H. Yan. Exogenous application of GABA improves PEG-induced drought tolerance positively associated with GABA-shunt, polyamines, and proline metabolism in white clover. *Frontiers in physiology* **8**, 1107 (2017).

Yoshida, R., I. C. Mori, N. Kamizono, Y. Shichiri, T. Shimatani, F. Miyata, K. Honda and S. Iwai. Glutamate functions in stomatal closure in *Arabidopsis* and fava bean. *Journal of plant research* **129**, 39-49 (2016).

Zarei, A., C. P. Trobacher and B. J. Shelp. *Arabidopsis* aldehyde dehydrogenase 10 family members confer salt tolerance through putrescine-derived 4-aminobutyrate (GABA) production. *Scientific reports* **6**, 35115 (2016).

Zarei, A., G. Z. Chiu, G. Yu, C. P. Trobacher and B. J. Shelp. Salinity-regulated expression of genes involved in GABA metabolism and signaling. *Botany* **95**, 621-627 (2017).

Zhang, H., F. Zhang, Y. Yu, L. Feng, J. Jia, B. Liu, B. Li, H. Guo and J. Zhai. A Comprehensive Online Database for Exploring∼ 20,000 Public *Arabidopsis* RNA-Seq Libraries. *Molecular plant* **13**, 1231-1233 (2020).

Zhang, J. (2014). Functional and Structural Characterization of the Vacuolar Anion Channels AtALMT9 and AtALMT4 in *Arabidopsis thaliana*. PhD PhD Dissertation, University of Zurich.

Zhang, J., M. T. Hafeez, D. Di, L. Wu and L. Zhang. Precise control of ABA signaling through post-translational protein modification. *Plant Growth Regulation* **88**, 99-111 (2019).

Zhang, X., R. Henriques, S.-S. Lin, Q.-W. Niu and N.-H. Chua. Agrobacterium-mediated transformation of *Arabidopsis thaliana* using the floral dip method. *Nature protocols* **1**, 641 (2006).

Zhang, Y. and A. R. Fernie. On the role of the tricarboxylic acid cycle in plant productivity. *Journal of integrative plant biology* **60**, 1199-1216 (2018).

Zhou, R., A. J. Cutler, S. J. Ambrose, M. M. Galka, K. M. Nelson, T. M. Squires, M. K. Loewen, A. S. Jadhav, A. R. Ross and D. C. Taylor. A new abscisic acid catabolic pathway. *Plant Physiology* **134**, 361-369 (2004).

Zhu, M. and S. M. Assmann. Metabolic signatures in response to abscisic acid (ABA) treatment in *Brassica napus* guard cells revealed by metabolomics. *Scientific reports* **7**, 1-16 (2017).

Zhu, X., J. Liao, X. Xia, F. Xiong, Y. Li, J. Shen, B. Wen, Y. Ma, Y. Wang and W. Fang. Physiological and iTRAQ-based proteomic analyses reveal the function of exogenous γ-aminobutyric acid (GABA) in improving tea plant (*Camellia sinensis L.*) tolerance at cold temperature. *BMC Plant Biology* **19**, 1-20 (2019).

Zhu, Z., S. Piao, R. B. Myneni, M. Huang, Z. Zeng, J. G. Canadell, P. Ciais, S. Sitch, P. Friedlingstein and A. Arneth. Greening of the Earth and its drivers. *Nature climate change* **6**, 791-795 (2016).

Zik, M., T. Arazi, W. A. Snedden and H. Fromm. Two isoforms of glutamate decarboxylase in Arabidopsis are regulated by calcium/calmodulin and differ in organ distribution. *Plant molecular biology* **37**, 967-975 (1998).

Zimmermann, P., M. Hirsch-Hoffmann, L. Hennig and W. Gruissem. GENEVESTIGATOR. *Arabidopsis* microarray database and analysis toolbox. *Plant Physiology* **136**, 2621-2632 (2004).